Applied Optics

WARGA

May
1963

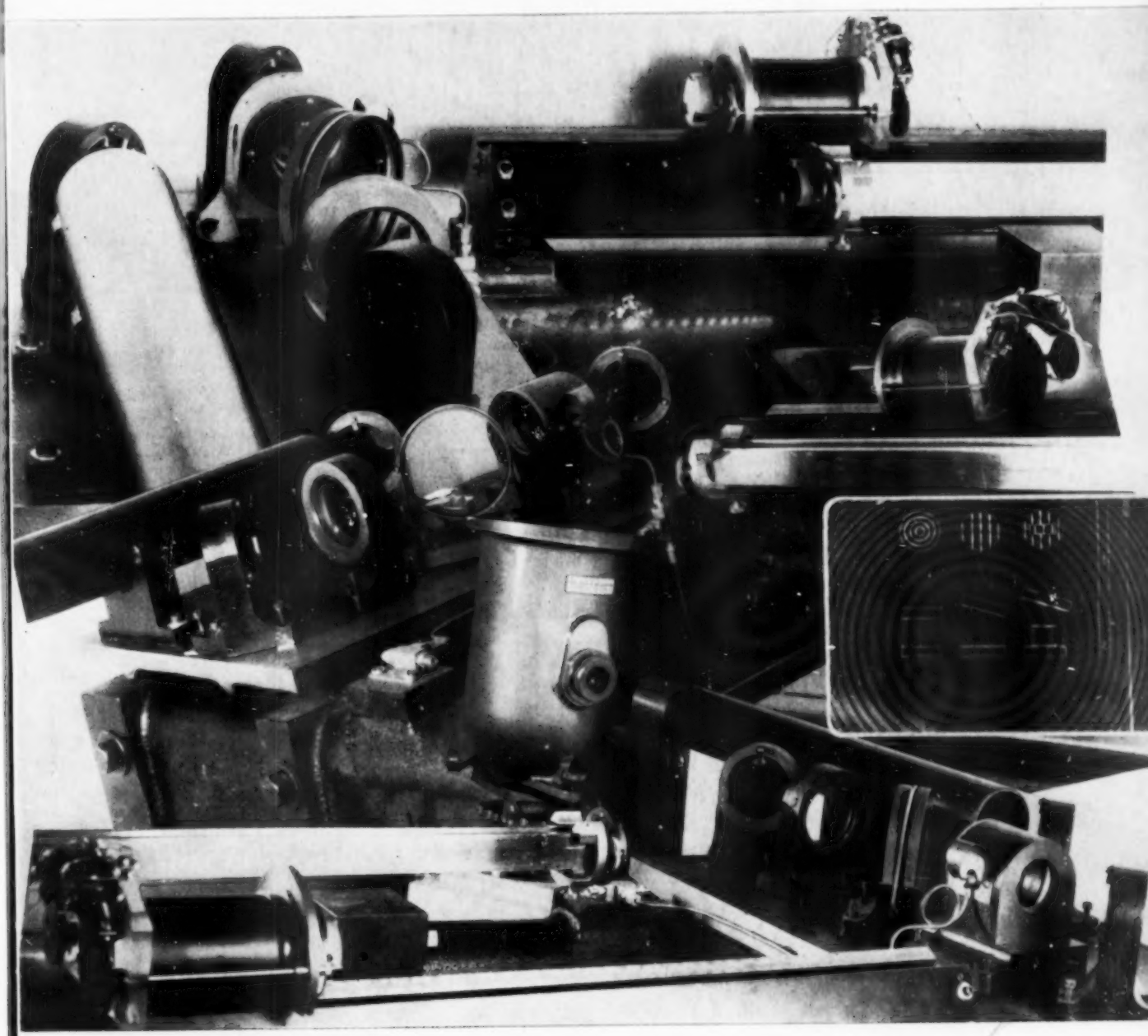

INTERFEROMETRY

OPTICS FOR LASERS
FROM
PERKIN-ELMER

Perkin-Elmer is a convenient, reliable source of precision optics for lasers, in quantities for research or production programs. All are of unexcelled quality. All reflect Perkin-Elmer's years of experience in the design and development of precision optics and optical instrumentation.

INTERFEROMETER FLATS
1.0", 1.5" and 2.0" diameter
Surface: $\frac{\lambda}{10}$ to $\frac{\lambda}{200}$
BK-7 and Quartz

SPHERICAL MIRRORS
1.0", 1.5" and 2.0" diameter
1M, 2M, 3M, 10M, 25M, 50M
radius of curvature
BK-7 and Quartz

WINDOWS
1.0", 1.5" and 2.0" diameter
Standard or Brewster's angle
BK-7 and Quartz

DIELECTRIC COATINGS
Durable, minimum loss,
specified reflectivities
for the full spectrum of laser
research and development

SINGLE CRYSTALS
Tungstate, Molybdate, Sapphire,
Garnet, Emerald

SPECIAL OPTICS
Trihedral and 90° prisms with
deviation within 2 seconds

Perkin-Elmer—a single-source, total capability in optical maser technologies including research, design, material development, fabrication and performance testing, plus development engineering of optical maser systems and applications.

Send today for "Prices and Specifications—Optical Maser Services". Write or phone Perkin-Elmer, Optical Maser Marketing, Norwalk, Conn. Area Code 203-847-0411.

PERKIN-ELMER

Applied Optics

VOLUME 2
NUMBER 5
MAY
1963

A monthly publication of the Optical Society of America

John N. Howard, Editor

R. A. Woodson, Feature Editor

Patricia R. Wakeling, Managing Editor

COVER: Some views are given of the important aspects of interferometry as concerned with precise measurement: from an illustration of some elementary principles (shown in the inset) to the miscellaneous shots of the insides of the NRC (Canada) interference comparator, which was first used in the measurements that confirmed the continuity of the international meter on its redefinition in terms of an optical wavelength.

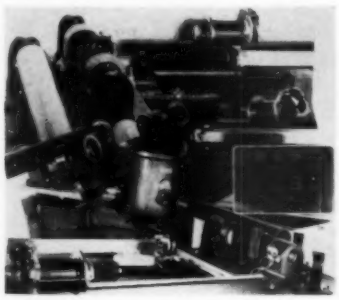

Published monthly by the Optical Society of America, Inc., in cooperation with the American Institute of Physics, at 20th and Northampton Streets, Easton, Pa. Editorial and advertising offices: 1155 16th St. N.W., Washington 6, D.C. 202-Di7-4131 Supported in part by a grant from the National Science Foundation. Subscription rates: $6.00 to OSA members, $8.00 other AIP Societies' members; nonmembers and libraries: $10.00 per year. Single copies $2.00. Second class postage paid at Easton, Pa. © Copyright 1963 by the Optical Society of America.

455 **The International Length Standard**—K. M. Baird and L. E. Howlett

465 **Quantum Limit to Precision of Wavelength Determination**—G. R. Hanes

471 **Interference Comparators for Line Standards**—K. M. Baird

481 **Interferometric Method of Velocity of Light Measurement**—George W. Stroke

487 **The Rapid Measurement of Photographic Records of Interference Fringes**—J. Dyson

491 **On the Correction of Phase Errors in Interferograms**—Ernest V. Loewenstein

495 **Mesure de la Dispersion dans les Raies d'Absorption Infrarouge des Gaz. Appareillage et Corrections Instrumentales**—C. Alamichel, R. Assous, et F. Legay

503 **A Method of Inferring Single-Path Band Transmission Factors from Double-Path Measurements**—M. A. McKiernan and H. W. Wessely

509 **An Analysis of Radiation Transfer by Means of Elliptical Cylinder Reflectors**—S. B. Schuldt and R. L. Aagard

515 **Spectral Band Absorptance for Atmospheric Slant Paths**—Gilbert N. Plass

527 **The Use of Polarized Infrared Radiation in Magneto-Optical Studies of Semiconductors**—E. D. Palik

DEPARTMENTS

539 **Letters to the Editor**

Improved Silver Films for Multiple-Beam Interferometry—D. J. Bradley

Angular Distribution of Light Rays from a Gas Discharge Source—R. L. Aagard, R. A. Dufault, and S. B. Schuldt

Dichroic Multiple Beam Interferometer Microscope—M. J. Irland and E. B. Schermer

An Alignment Interferometer—James B. Saunders

Electric Chopper for Spectral Lamps—R. C. Mackey and S. A. Pollack

On Diffraction Losses in Laser Interferometers—A. G. Fox, Tingye Li, and S. P. Morgan; **Author's Reply**—C. L. Tang

Practical Aspects of Aerial Photographic Targets—Milton D. Rosenau, Jr.

Observation of Ionization of Gases by a Ruby Laser—E. K. Damon and R. G. Tomlinson

463 **From the Editor**

470 **Books**

501 **Meeting Reports**

547 **Patents**

NOW!

10 LASER PULSES PER SECOND

Model 325 Power Supply available for:

- Up to 10 Laser pulses per second
- Higher average powers
- Greater average Laser output
- Fast cycling for tracking purposes and product research
- Up to 20,000 joules of energy storage
- Individual capacitor fusing, safety interlocks and automatic discharge

NOW!

A 100,000 JOULE POWER SUPPLY

Model 350 Power Supply available for:

■ 100,000 joules of energy storage ■ Choice of operating voltages: 5,000, 10,000 or 20,000 ■ Average powers to 5KW ■ Forced air circulation ■ Maximum safety: individually fused capacitors, safety interlocks and automatic discharge

NEW!

ARC QUENCH AT 50 MICROSECONDS

Model 3C-4000 Rotary Arc Quench Variable trigger makes it possible to shorten flash duration to as little as 50 microseconds yet retain maximum peak light. This provides:

- Reduced flash tube heat
- Higher repetition rates
- Faster re-cycling
- Greater Laser output with less average pump power

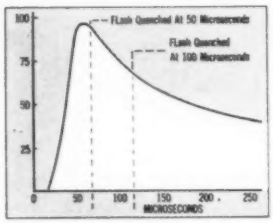

Other Accessories include: ■ Solid State Laser Mounts — air cooled or liquid nitrogen cooled — for rods of all sizes ■ Q Spoiling ■ Peak Power Meter ■ Optical Bench

Technical questions? Phone or write our engineering staff.

ELECTRO POWERPACS, INC.

Manufacturers of Power Supplies, Laser Mounts and Accessories .

A SUBSIDIARY OF HYDRA-POWER CORPORATION

6 Hadley Street, Cambridge 40, Mass., Phone: 617-876-9220

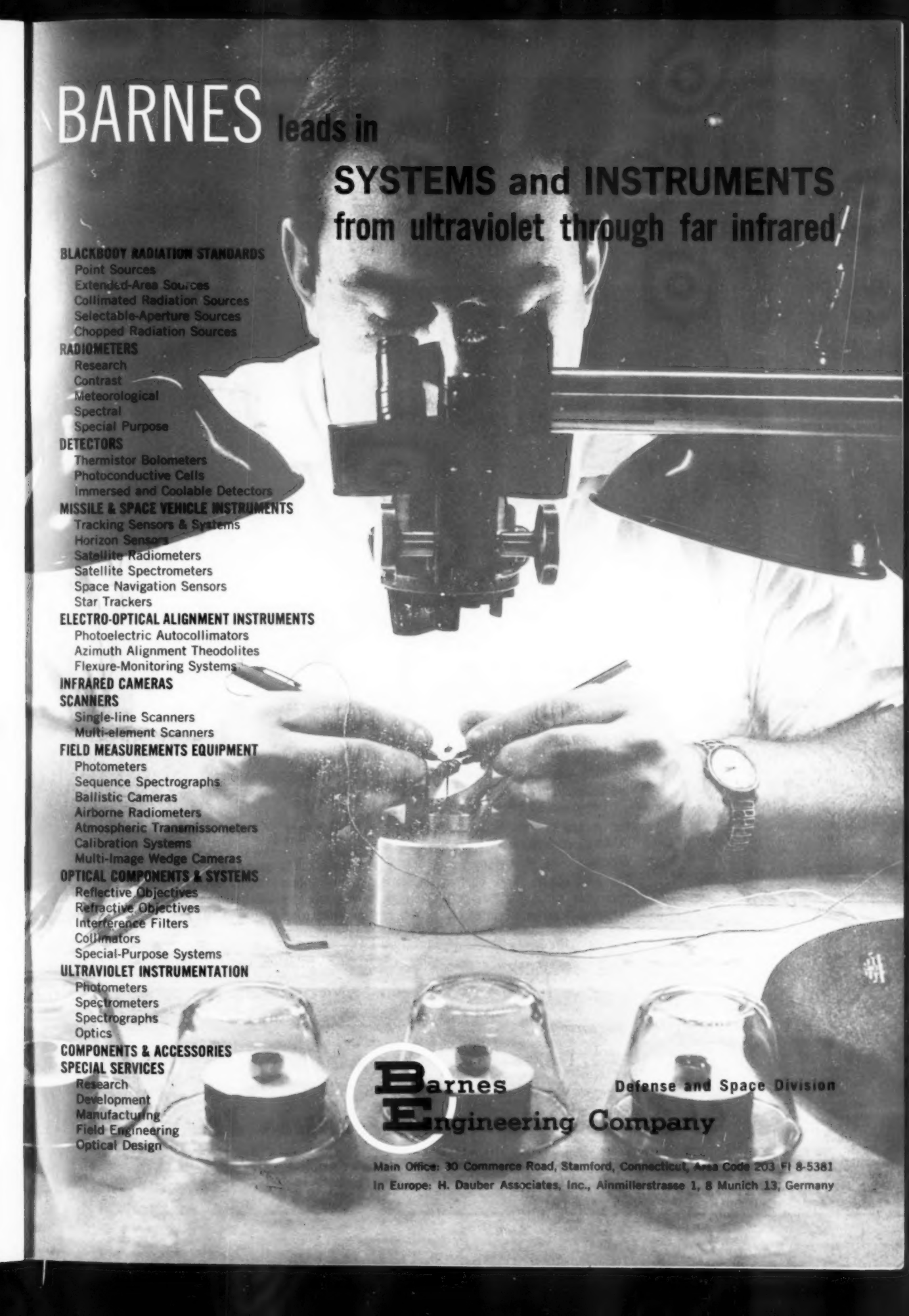

BARNES leads in

SYSTEMS and INSTRUMENTS from ultraviolet through far infrared

BLACKBODY RADIATION STANDARDS
- Point Sources
- Extended-Area Sources
- Collimated Radiation Sources
- Selectable-Aperture Sources
- Chopped Radiation Sources

RADIOMETERS
- Research
- Contrast
- Meteorological
- Spectral
- Special Purpose

DETECTORS
- Thermistor Bolometers
- Photoconductive Cells
- Immersed and Coolable Detectors

MISSILE & SPACE VEHICLE INSTRUMENTS
- Tracking Sensors & Systems
- Horizon Sensors
- Satellite Radiometers
- Satellite Spectrometers
- Space Navigation Sensors
- Star Trackers

ELECTRO-OPTICAL ALIGNMENT INSTRUMENTS
- Photoelectric Autocollimators
- Azimuth Alignment Theodolites
- Flexure-Monitoring Systems

INFRARED CAMERAS

SCANNERS
- Single-line Scanners
- Multi-element Scanners

FIELD MEASUREMENTS EQUIPMENT
- Photometers
- Sequence Spectrographs
- Ballistic Cameras
- Airborne Radiometers
- Atmospheric Transmissometers
- Calibration Systems
- Multi-Image Wedge Cameras

OPTICAL COMPONENTS & SYSTEMS
- Reflective Objectives
- Refractive Objectives
- Interference Filters
- Collimators
- Special-Purpose Systems

ULTRAVIOLET INSTRUMENTATION
- Photometers
- Spectrometers
- Spectrographs
- Optics

COMPONENTS & ACCESSORIES

SPECIAL SERVICES
- Research
- Development
- Manufacturing
- Field Engineering
- Optical Design

Barnes Engineering Company

Defense and Space Division

Main Office: 30 Commerce Road, Stamford, Connecticut, Area Code 203 FI 8-5381

In Europe: H. Dauber Associates, Inc., Ainmillerstrasse 1, 8 Munich 13, Germany

OPTO mechanisms' / OPTO WAVE DIGITIZER

automatic measuring interferometer for distances and angles

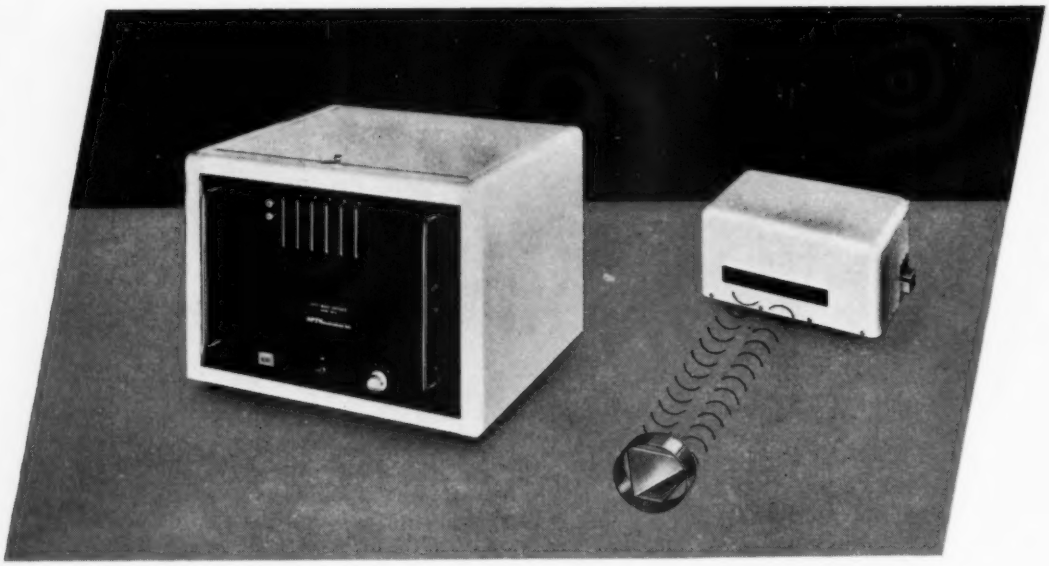

The OPTO WAVE DIGITIZER is an automatic measuring interferometer . . . a device utilizing light waves as a standard of measurement. The instrument is capable of measuring angles to 0.05 seconds and distances to one micron. The simplicity of its automated visual digital readout when used with machine tools, measuring tables, and inspection-test equipment, will reduce measuring time to fractions of conventional methods.

In Photographic Interpretation on film for data reduction to computers, the automatic readout may be recorded on hard copy . . . punched tape . . . or punched card.

The measuring interferometer generates optical fringes . . . the number of which determines distance travelled.

A unique method of mounting the optics assures stability of measurement. The split phase, three photomultiplier detection produces highly accurate reversible sensing of fringes. The light waves are counted between the tetrahedral prism, mounted on the moving body whose location it is desired to determine, and the sensor. This exciting development opens the door to new concepts of measurement and unprecedented accuracy of angular and linear measurement.

OPTO mechanisms Inc.

ENGINEERS HILL, PLAINVIEW, L. I., N. Y. GE 3-8100
TWX: CODE 516 433 9690

Introducing... B/A ELECTRO-OPTIC
light modulator

The B/A Electro-Optic Light Modulator, a solid state device, provides a practical source of light pulses in the micro-second range and serves as a light beam modulator at frequencies from D.C. through the video region. Numerous applications have been found for these units in the fields of laser modulation, communications, polarimetry, densitometry, photography, photometry, interferometry and the measurement of semiconductor parameters.

B/A now has a series of standard models, each bridging a specific range of operations. For example, types are available for applications that require large linear aperature with no obstructions. These units are manufactured with transparent electrodes. A model is also made giving maximum contrast ratio with low driving voltage achieved through the use of double crystal construction.

If your application involves modulation at high frequencies, thick single crystal units are available from stock that can be operated continuously up to 5 megacycles.

Continuing research by Baird-Atomic scientists has demonstrated that the crystals used in these modulators can be operated at frequencies of 80 megacycles and pulse times of 20-30 nanoseconds. Others have operated similar crystal units at frequencies as high as 25 Kilomegacycles.

Baird-Atomic engineers invite you to submit your modulation specifications.

Write Adv. Dept. today for current brochure.

Engineers and scientists: *Investigate challenging opportunities with B/A. Write Industrial Relations Director. An equal opportunity employer.*

B/A BAIRD-ATOMIC, INC.
33 University Road · Cambridge 38, Mass.

ADVANCED OPTICS AND ELECTRONICS...SERVING SCIENCE

infrared specialist

Outstanding Infrared Specialist sought for lead and/or research position in a research and development orientated organization.

Work covers optics, detection, radiometry, information processing, systems electronics, simulation techniques and instrumentation development. Applied work primarily directed toward weapons guidance, sparo seeker systems and surveillance systems. Liberal funds available for more basic research. A complete laboratory is at the disposal of the IR personnel (optics, radiometry, spectrophotometry, electronics, cryogenics and detector analysis). An excellent solid-state laboratory is also available for materials and device research. Candidates should hold a doctorate and possess recognized qualifications, based on demonstrated achievements in one or more of the applicable fields. Professional status will be considered in lieu of doctorate requirement.

The excellent Southern California location of General Dynamics | Pomona offers unsurpassed living conditions. Suburban Pomona is only thirty minutes from Los Angeles and Hollywood and in close proximity to many recreational centers; the mountains, the desert, the ocean and is within America's finest year-round living climate.

Please address your resume to:
Mr. O. C. Byrd, Engineering Personnel Administrator
General Dynamics | Pomona, P.O. Box 1011
Pomona, California

U. S. Citizenship Required

An Equal Opportunity Employer

GENERAL DYNAMICS | POMONA GD

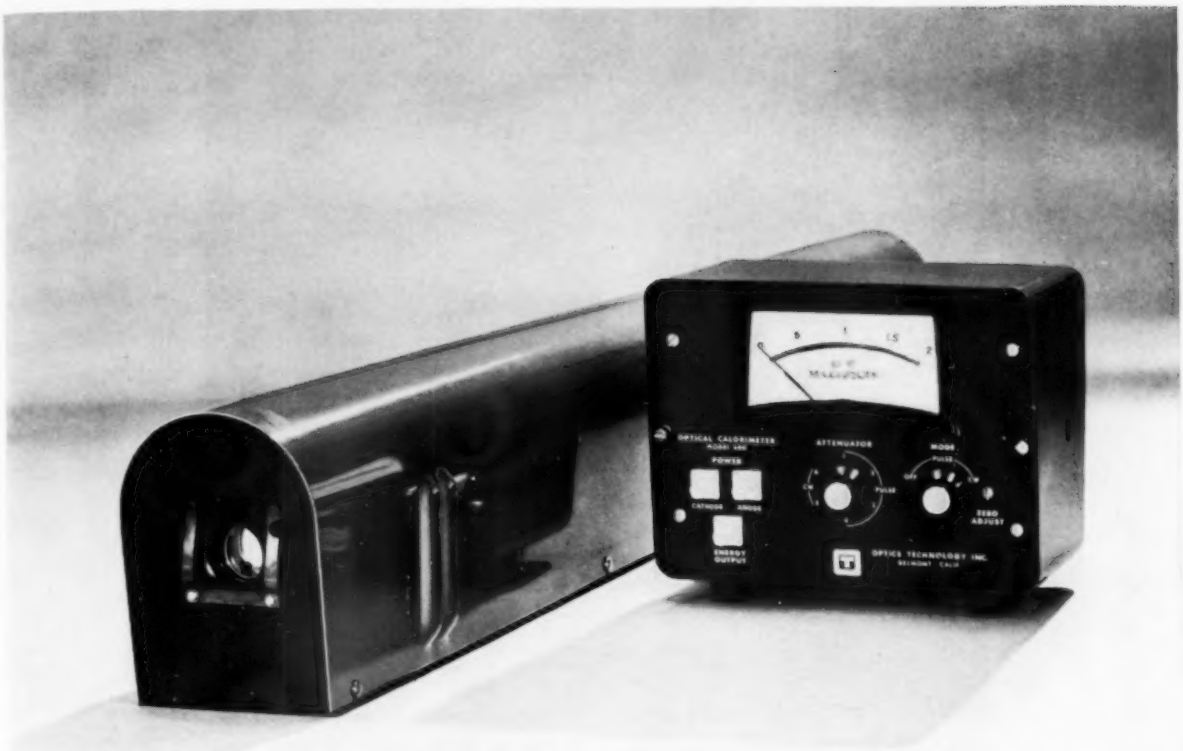

VISIBLE & INFRARED CW LASER

Model 150 is complete with precision multi-layer mirrors in differential thread interferometer assembly and power supply. Gas tube produces continuous coherent output at 6,328 Å and 11,530 Å. Mirrors are available for either wavelength, or for both at once.

Also available:

***Model 120 Pulsed Laboratory LASER**, with power supply, ruby and other LASER crystals, cryogenic cooling and self-contained interferometer accessories.*

***Model 50A Interference Filter Set** provides low absorption attenuators and beam splitters for ruby LASER research.*

OPTICAL CALORIMETER

Model 600 calorimeter measures optical energy, power and peak power. It may be used with either pulsed or CW sources. Range: 312 joules (watts CW) to .037 joules (watts CW). From 20,000 Å to 4,000 Å. Absolute accuracy ±10%. New design eliminates error-producing wedge cavities and simplifies alignment. It incorporates highly sensitive calorimeter cell, phototube, amplifier, meter, and broad band attenuators.

Our high-efficiency multi-layer LASER mirrors can be deposited on your own substrates. Contact us for full details.

OPTICS TECHNOLOGY, INC

248 Harbor Boulevard
Belmont, California
LYtell 1-0358 (Area Code 415)

Research and development positions available for scientists and engineers in Fiber Optics. Contact Personnel Department.

For additional information, write OTI or your nearest OTI representative: New England: H. J. Schuft Co.; New York, Metropolitan: E. C. Smith and Assoc.; New York, Upstate: E. W. Stone Co.; Mid-Atlantic: C. E. Snow Co.; So. California: Abbott Instrument & Engineering; Southwest & Mountain States: Southwestern Engineering & Equipment Co.; Europe: HVL, Brussels; Other export: Henley and Co., New York, N. Y.

Diffraction pattern produced by monochromatic laser beam illuminating a pinhole of approximately 500 microns diameter.

SPECTRA-PHYSICS
- a leader in CW Gas Laser technology

In January of 1963, a scientist at Spectra-Physics' laboratories in Mountain View pushed a button and turned on a light. It was no ordinary light; the yellow-orange beam was the first 6118Å continuous-wave gas laser transition ever seen by human eye.

In producing this transition, the shortest laser wavelength yet observed, Spectra-Physics employed a novel technique — use of an intra-cavity prism to remove all competing wavelengths from the cavity resonator except for the one of interest.[1]

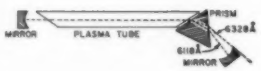

By demonstrated ability to conceive and carry through advanced ideas in laser technology, Spectra-Physics has become identified as a leader in bringing the laser to practical reality. Further evidence of Spectra-Physics' leadership in gas laser technology includes many more original contributions, such as:

discovery of the first high-gain CW gas laser transition — 3.39 microns, helium-neon;[2]

achievement of the highest power CW gas laser output yet observed — over 0.1 watt

Over 70% of all commercial CW gas lasers in use today were developed and produced by Spectra-Physics

Spectra-Physics offers, in addition to its off-the-shelf gas laser product line, competent application-oriented research services for systems developers interested in the exploration and application of laser techniques. Write for details.

1. A. L. Bloom, "Observation of new visible gas laser transitions by removal of dominance," Applied Physics Letters, Vol. 2, No. 5, pp 101, March 1, 1963.
2. A. L. Bloom, W. E. Bell, and R. C. Rempel, "Laser operation at 3.39 microns in a helium-neon mixture," Applied Optics, Vol. 2, No. 3, pp 317, March 1963.

SPECTRA-PHYSICS INC.
738 Terra Bella/Mountain View 5/California
(415) 968-4467

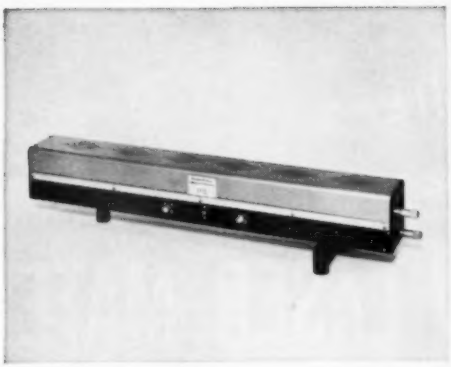

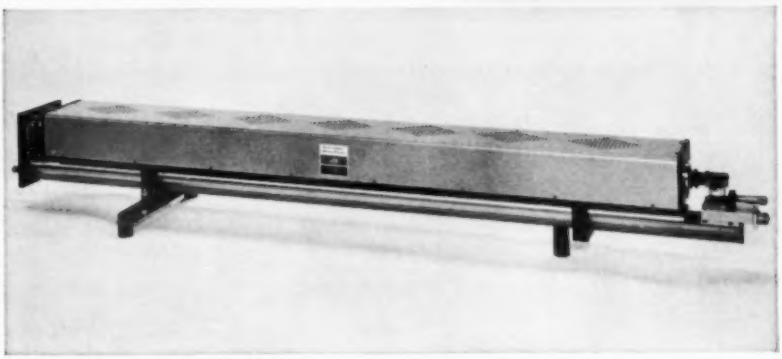

SPECTRA-PHYSICS
-leading producer of CW Gas Lasers

Throughout the scientific disciplines, continuous-wave gas lasers built by Spectra-Physics have achieved acceptance as primary equipment for every use from simple demonstration to the most sophisticated research. They are in use in many leading universities, aerospace laboratories, government and military research centers, and industrial facilities.

The availability of these highly practical, reliable, and thoroughly proven CW gas lasers — built by Spectra-Physics, sold and fully guaranteed by Perkin-Elmer/Spectra-Physics — has been the key to success in a number of significant advances in laser application.

Current production models of high-precision laboratory gas lasers include:

Model 115 (upper photo) — lightweight (8 lbs.) source of continuous-wave, highly monochromatic light from a helium-neon plasma; visible and infra-red; 6328Å, 11,523Å, and 33,912Å; interchangeable confocal and hemispherical resonators; plane-parallel resonator option.

Model 112 — advanced research model; provides, in addition to capabilities of Model 115, stable operation in plane-parallel resonator configuration; capacity for precision experiments such as optical heterodyning.

An unmatched continuity of experience and user-proven performance stand behind every Perkin-Elmer/Spectra-Physics CW gas laser.

Would you like to receive bulletins bringing you application information and describing how others employ laser technology? A current bulletin explores properties of coherent light as compared to those of incoherent radiation.

Send your name today to receive this bulletin, subsequent application information, and our newest product brochure.

SPECTRA-PHYSICS
INC.
738 Terra Bella/Mountain View 5/California
(415) 968-4467

Announcing

HARSHAW LASER MATERIALS

Calcium Fluoride with various activators

★ Available from stock
★ Available as polished LASER rods
★ Proven LASER action

The Harshaw Chemical Company's entry to the LASER field is based on established excellence in crystal growth supplemented by a competent Research and Development team of chemists and physicists in their Crystal-Solid State Division. Proven crystal production know-how is now backed up by theoretical studies and careful experimental measurements of LASER materials. Additional LASER materials (tungstates, molybdates, etc.) and electro-optical materials suitable for modulation of LASER beams will be announced as they become available.

FEATURES:

- Specified activator type and concentration
- Specified activator valence state
- Charge compensation
- Measured absorption spectrum
- Measured fluorescence emission spectrum

SERVICE: Harshaw will grow experimental LASER and optical crystals to customer specification.

ADDRESS INQUIRIES TO: The Crystal-Solid State Division
The Harshaw Chemical Company
1945 East 97th Street, Cleveland 6, Ohio

HARSHAW

The International Length Standard

K. M. Baird and L. E. Howlett

This paper describes the characteristics of the $2p_{10}$-$5d_5$ radiation of Kr-86 which was adopted in 1960 as the primary standard of length. After a brief history of the developments leading to the adoption of this spectral line, its physical characteristics are discussed with a view to showing its merits as a standard. The relative merits of possible alternatives are also considered. It is concluded that the $2p_{10}$-$5d_5$ radiation is superior to any available alternative.

Introduction

Although measurement of the things in the world about man has been a problem for him since his earliest times, it was only in 1954 that world acceptance was formally given to a system of units for measurement. In this year the Tenth International Conference of Weights and Measures adopted the International System of Units which established the dimensions: length, mass, time, electric current, temperature, and luminous intensity as the fundamental ones on which the system should rest.[1] At the same time the Conference approved as units for these dimensions the meter, the kilogram, the second, the ampere, the thermodynamic degree, and the candela. The reasons and the thinking that led to this decision are extensively set forth in other places and will not be dealt with here.[2] It will suffice to say that it is not by any means to be assumed that this system is an absolute one in the sense that it is based on dimensions that have an intrinsic fundamental importance in the physical world or that it will have validity into the indefinite future. Already changes in the basic dimensions have been proposed and are being actively studied. The International System of Units is simply, on the basis of our present knowledge of experimental techniques, the most practical, convenient, precise, and rational system of measurement to meet current needs of both science and industry.

To have established a system in this way is only the beginning of meeting practical needs. Before any measurements can be made, reproducible standards must be set up for each unit to which reference can be conveniently and precisely made in order to relate all scientific and industrial measurement. The realization of these objectives is a continuing responsibility of the International Bureau of Weights and Measures, the national physical laboratories and, indeed, of all science. It is one of science's most difficult and challenging tasks and one which must continually draw on the very latest discoveries with a view to continual improvement and refinement. In this article we are going to concern ourselves with the unit of length which owes its present satisfactory status to the advanced techniques of interferometry and our knowledge of spectroscopy.

However, before proceeding to our main theme there are several questions which should be rendered unambiguous since they concern meanings of words or concepts on which there is sometimes unjustifiable confusion.

We must make quite clear what we shall mean by "precision" and "accuracy". "Precision" refers to the reproducibility of a measurement or an average of a series of measurements. If the number of separate values obtained is sufficiently large and their distribution is found to satisfy certain criteria, well-known statistical methods can be applied in order to calculate the contribution of the observed scatter to the final error; one can then also express the precision in some conventional form, such as standard deviation, in order to indicate the reproducibility of that particular measurement.

"Accuracy" refers to the relation of the observed result to some "absolute" correct value. Usually in the measurement of physical magnitudes, the correct value is unknown, so the accuracy is often judged by guessing the likely limits of systematic errors (usually optimistically!) or by the "precision" of the measurements based on consideration of the values obtained from laboratory to laboratory and from time to time.

The authors are in the Division of Applied Physics, National Research Council, Ottawa, Canada. L. E. Howlett is Vice-President, International Committee of Weights and Measures and President, Advisory Committee for the Definition of the Meter.

Received 10 November 1962.

The use of these terms with respect to standards is now clear. The "precision" of a standard is the degree to which it can be reproduced at various times or places. If some natural phenomenon is used as a standard, one may refer to the "*accuracy*" of the standard as indicating how closely this natural phenomenon can be measured or realized by some practical means. In this connection it should perhaps be noted that some natural phenomena have inherent limitations on their precision which are quite apart from the influence of perturbations on their apparent or observed value. We believe the velocity of light in free space would not, however, be subject to these additional limitations whereas the determination of an atomic wavelength will be ultimately limited by the line-width or intensity.

We must establish at this time what characteristics are required to make a standard both acceptable and desirable. These are simple to state but not so easy to realize:

(1) A standard must be capable of being established with a precision at least equal to and preferably considerably better than the precision with which comparative measurements can be made on the same or related phenomena.

(2) A standard that is universally available and immune to secular change, damage, or destruction, has its attractiveness considerably increased.

To meet our requirements we have two general sorts of standards—arbitrary and natural. The arbitrary standard is a specific piece of apparatus. Its character does not necessarily limit in any way its precision but such a standard can never have the desirable second requirement. The natural standard depends on the association of a number with a natural phenomenon that is considered constant everywhere and for all time. It can possess both the characteristics noted above if chosen with sufficient knowledge of the workings of the physical world. The philosophical attractiveness of such standards has always appealed to scientists generally. Unfortunately all too often a choice of a natural standard has involved the acceptance of one that has not been sufficiently studied to ensure that it can fulfill the first and absolutely essential requirement for a certain minimum precision. The original standard of length for the metric system, based on the length of the meridian, and the present standard for the candela are two natural standards that have failed in this respect. On the other hand, length and mass, both of which have in practice always depended on arbitrary physical standards until 1960, have had an excellent record for meeting the demands made on them for precision at the various periods of their history. The need for very profound knowledge of a natural phenomenon before it can be accepted as having sufficient precision for use as a standard should always lead to extreme caution in a final decision to adopt it. Even with very thorough study a natural standard always runs the risk of later knowledge showing it incapable of the increased precision that the future will almost certainly demand of it.

It will be seen from the description of the present primary standard that in going from an arbitrary standard of length—a metal bar—to a natural one—the wavelength of a particular radiation—a sufficiently comprehensive study was made of all phenomena which might be expected to be relevant to its precision of realization and that the resulting data was considered with sufficient prudence in order to avoid the unfortunate impreciseness which has often followed other passages from an arbitrary to a natural standard.

Arbitrary Standards of Length Until 1960

The history of standards of length up to 1960 is one of using various materials for making bars of various designs to establish an arbitrary unit of length as the distance between two lines ruled on a bar or as the distance between its ends. Progress was entirely confined to a better choice of materials and improvements in the technique of making the lines. Most of this improvement took place in the last two hundred years with a preponderance of it in the last century. To replace a welter of arbitrary standards of length in Europe the Mètre des Archives emerged from the confusion of the French Revolution to constitute with the Kilogramme des Archives the standards of the Metric System which eventually, after important extensions, was to become the International System of Units adopted in 1954. In passing, it may be regretted that the English scientists of the Royal Society in the late 18th century and early 19th, who, in spite of the political climate, worked closely with French scientists to develop a universal measuring system, were so preoccupied by the second-pendulum as a standard of length that they eventually exhausted the patience of their French colleagues who went on to make their own decisions. As a result, the Anglo-Saxon world has ever since been plagued by the English system of measurement.

Unfortunately, the Mètre des Archives, and its copies throughout Europe, did not prove a satisfactory standard. In 1870 the French government called an international conference (Commission Internationale du Mètre) in Paris to study the situation, this initiative led to the signing of a treaty, the Convention du Mètre, by seventeen countries on 20 May 1875. Under the aegis of this treaty progress was rapid and in 1889 the First General Conference of Weights and Measures (operating under the Convention) was able to give the world the first truly international standard of length which defined the meter as the distance between two lines engraved on a bar of platinum–iridium.[3] This

bar has been kept ever since at the International Bureau of Weights and Measures at Sèvres, near Paris, France. National copies of the international standard were distributed among the member countries and these have been regularly calibrated against the primary standard at Sèvres.

An extensive and very painstaking series of measurements (in 1890) showed that the definition of the meter which had been established was significant to about $\pm 0.2\ \mu$ or two parts in ten million. As a consequence of very competent work done at that time, and particularly the happy choice of a very stable alloy for the standard, the latter did indeed prove significant to such precision during the seventy years until its recent replacement. In all the varied and numerous measurements for which it has been used there has been no evidence of any errors larger than $0.2\ \mu$ that could be ascribed to lack of precision of the primary standard. It therefore served well its function of providing during this time an excellent (the most precise possible) representation of the unit of length.

The Natural Standard of Length 1960

As early as 1827 Babinet suggested the wavelength of light for the standard of length. Again in 1890 the yellow line emitted by sodium was suggested but was wisely rejected as being insufficiently precise.[4] The first serious competition to the prototype meter standard came in 1893 when Michelson showed that length could be measured to a high precision in terms of the red line emitted by Cd and demonstrated the latter's characteristics of stability and precision.[5] During the next forty years the relation between the Cd red line and the meter was measured several times and the results were often used to argue the desirability of redefining the meter. In this period, as a consequence of the development of the technique of measuring end standards (such as Johannson gauge blocks) by interferometry, and as a consequence of the requirements of spectroscopists for accurate wavelength tables, there arose a considerable body of opinion that favored a wavelength definition of the standard of length. A number of happenings gave impetus to the movement. In 1907 spectroscopists adopted the angstrom unit based on the Cd red line (but very nearly equal to 10^{-10} m).[6] In 1927 the relation between the Cd red line and the meter was sanctioned by the Seventh General Conference of Weights and Measures.[7] The Eighth General Conference in 1933 recommended the study of the definition of the meter as a function of light waves. The greatly increased availability during the 1940's of pure isotopes which emitted spectral lines that were sharper and more precise than the red line of natural Cd was perhaps the final factor necessary. In any case the Ninth General Conference in 1948 issued a very specific resolution inviting the national laboratories to study seriously the problem of basing the meter on a particular wavelength. In 1952 the Advisory Committee for the Definition of the Metre was set up to coordinate research to this end and prepare specific recommendations for action.

This committee met for the first time in 1953. Its principal decisions were on the procedure to be followed in making a transition from the meter bar to a wavelength standard. It decided to work from the relationship between the Cd red line and the meter bar already sanctioned in 1927 and thus implicitly accepted the accuracy of the mean of earlier comparisons. It was further agreed that the meter should be defined in terms of the vacuum wavelength of whatever spectral wavelength was chosen. Since the relationship between the Cd red line and the meter had been established for standard air, a means for reduction to vacuum was required, and to this end the Edlén formula for the refractive index of air, approved by the Joint Commission for Spectroscopy in 1952, was accepted. To ensure the clarity and permanence of the new standard it was agreed to define the meter in terms of a radiation corresponding to a transition between the unperturbed atomic levels involved and not in terms of a radiation emitted by a particular source. Recommendations on the best current method of realizing the ideal standard were to be issued from time to time by the International Committee of Weights and Measures.

Following this meeting of the Advisory Committee a great deal of research was done, mostly in national laboratories and at the International Bureau of Weights and Measures, in order to choose the best wavelength, compare its wavelength with that of the red line of cadmium and then to redefine the meter in terms of it. Spectral lines emitted by Cd-114, Hg-198, and Kr-86 were the ones most seriously considered although other proposals such as a Ca atomic beam source also received consideration. Most of the scientific work is described in the Proceedings of the Advisory Committee.[8,9]

A second meeting of the Advisory Committee was held in 1957 to consider the results available. The scientific case was overwhelmingly in favor of the $0.606\ \mu$ orange line of Kr-86 and the committee unanimously recommended its adoption. The relation between this line and the Cd red line had been measured by five different laboratories to within a spread of 6 parts in 10^8 or $0.06\ \mu$ in the meter. The mean value was used in determining the number of wavelengths to equal 1 meter.

The culmination of all this activity and study, lasting over a century, came at 6 p.m. on 14 October, 1960, when the Eleventh General Conference of Weights and Measures adopted unanimously the following resolution[10]:

1. Le Mètre est la longueur égale à 1 650 763, 73 longueurs d'onde dans le vide de la radiation correspondant à la transition entre les niveaux $2p_{10}$ et $5d_5$ de l'atome de krypton, 86. 2. La définition du Mètre en vigueur depuis 1889, fondée sur le Prototype International en platine iridié, est abrogée. 3. Le Prototype International de Mètre sanctionné par la Première Conférence Générale des Poids et Mesures de 1889 sera conservé au Bureau International des Poids et Mesures dans les mêmes conditions que celles qui ont été fixées en 1889.

The picture is made complete by adding the first recommendation for realizing the new standard which was made by the International Committee at its October session, 1960.[11]

Conformément au paragraphe 1 de la Resolution 2 adoptée par la Onzième Conférence Générale des Poids et Mesures (octobre 1960), le Comité International des Poids et Mesures recommande que la radiation du krypton 86 adoptée comme étalon fondamental de longueur soit réalisée au moyen d'une lampe à décharge à cathode chaude contenant du krypton 86 d'une pureté non inférieure à 99 pour cent, en quantité suffisante pour assurer la presence de krypton solide à la temperature de 64°K, cette lampe étant munie d'un capillaire ayant les caracteristiques suivantes: diamètre intérieur 2 à 4 millimètres, épaisseur des parois 1 millimètre environ.

On estime que la longueur d'onde de la radiation émise par la colonne positive est égale, à 1 centmillionième (10^{-8}) près, à la longueur d'onde correspondant à la transition entre les niveaux non perturbés, lorsque les conditions suivantes sont satisfaites: (1) le capillaire est observé en bout de façon que les rayons lumineux utilisés cheminent du côté cathodique vers le côté anodique; (2) la partie inférieure de la lampe, y compris le capillaire, est immergée dans un bain réfrigérant maintenu a la température du point triple de l'azote, à 1 degre près; (3) la densité du courant dans le capillaire est 0,3 ± 0,1 ampère par centimètre carré.

The degree to which the continuity of the meter has been conserved is a point of great importance and the Eleventh General Conference received satisfactory experimental reassurance on it. Four well-known copies of the meter had already been measured (at the National Research Council of Canada) directly in terms of the new standard by an interference comparator.[10,12] The results indicated that the meter, according to the new definition, is shorter than the meter as formerly defined by 0.2 to ±0.2 μ. The amount of this discontinuity is barely significant in relation to past calibrations of individual meter bars in terms of the prototype meter. Certainly it is not important with respect to scientific or industrial measurements done before 1960.

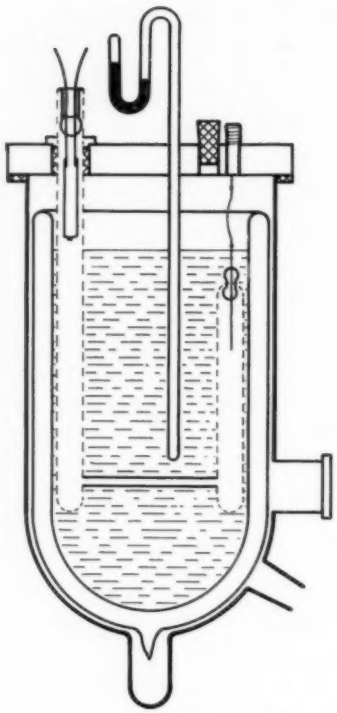

Fig. 1. Recommended source for the primary standard radiation. The hot cathode lamp is immersed in a bath of N_2 at its triple point contained by the dewar inside a vacuum vessel. A nitrogen vapor pressure thermometer is also shown. The light from the horizontal capillary emitted from the anode end is viewed through the window at the right.

In 1961 the International Astronomical Union ratified a new definition of the angstrom unit making it exactly equal to 10^{-10} m so that the former may well go out of use without loss.[13]

Discussion of the Natural Standard

Having discussed the characteristics desired in a primary standard and having briefly reviewed the history leading to the present definition of the meter, it is our intention to review now the essential properties of the 0.606 μ line of Kr-86 to show how well it fulfills the requirements of a primary standard of length.

It will be seen from this review that the historic 1960 decision was founded on an adequate knowledge of the physical factors that might affect the precision of realization of the ideal wavelength and that the results gave all reasonable assurance in the light of current

knowledge that it would be unreasonable to suspect that unknown perturbations will turn up later to cause a discontinuity or an unforeseen inaccuracy in our measurements. It will further be seen that the results of work done since the decision was taken justifies the expectation that in the near future a method of realization can be recommended that will substantially improve the precision and accuracy of the realization of the standard.

Characteristics of Recommended Source

In redefining the meter on the basis of a spectral line it was essential to choose one that was *known* to be capable of actually being produced with the smallest possible ambiguity in the wavelength due to conditions of production, the nature of its profile, etc. The 0.606 μ line of Kr-86, in addition to having desirable physical characteristics, was known to be reproducible in a lamp which, by chance circumstances, fulfills the requirements of a standard particularly well. This lamp, originally developed by the Physikalisch Technische Bundesanstalt in Germany, is illustrated schematically in Fig. 1.

According to the recommended means of operation already given the lamp ought to be operated at the temperature of N_2 at its triple point. This is done simply by having the lower part of the lamp immersed in a dewar of liquid nitrogen having a clear window opposite the end of the capillary which carries the discharge; the whole is contained in a vacuum tank as illustrated in the figure. A pumping capacity of about 25 liters/min will cool 2 liters of N_2 to its triple point in about twenty minutes, and pumping at the rate of 5 liters/min will hold the temperature while the lamp is run at the specified current; an initial charge of 2 liters of nitrogen will last about 4 hours.

The electrical supply for the lamp consists of a low wattage filament source and less than 40 mA at 100 to 150 V dc to maintain the discharge; a higher voltage or a tesla coil is often needed for starting.

The production of the radiation providing the primary standard of length is thus seen to be extremely simple; its cost is negligible compared with equipment involved in any measurements which come close to taking advantage of its great precision.

At the triple point of nitrogen the vapor pressure of Kr is about 0.032 torr: since the lamps are filled with an excess of Kr, the pressure is, during use, accurately and automatically regulated at a fixed value throughout the life of the lamp (which is very long). At this pressure the intensity of the 0.606-μ line is near a maximum and there is no temptation to run the lamp at other than the correct conditions in order to improve the brightness. Moreover, at this pressure, which is relatively low for a discharge lamp, the wavelength shift due to nearby atoms and ions is only about one part in 10^8 at the recommended current; furthermore it is almost exactly compensated by a shift in the opposite direction due to a Doppler effect, if the lamp is viewed from the anode end as specified.[11]

Although the lamp is viewed from the end, there is no measurable broadening of the line (which would suggest self-reversal) as compared with the line-width when the lamp is viewed from the side. Because there is no carrier gas (unlike the case of most metallic vapor lamps) there are no other significant perturbing effects to the emitted wavelengths.

By comparing the radiation emitted from the side of the lamp (to eliminate Doppler effect) and by measurements over a range of currents and Kr pressures and temperatures to very low values, a measure of the differences between the emitted radiation and the defined unperturbed radiation has been made. Among the five laboratories who made the measurements, the largest value reported for this difference was less than five parts in 10^9 (see Table I).

Precision Possibilities

During the studies of the 0.606-μ line which have been made already, a great deal has been learned about its spectroscopic characteristics, such as the symmetry of the line profile and the effects on the emitted wavelength due to excitation current, temperature, pressure, lamp geometry, etc. In making these investigations various laboratories have developed photoelectric fringe scanning apparatus which enabled settings sufficiently sensitive to measure shifts of a few parts in 10^{10} in single settings. By measurement over a range of pressure down to 0.005 torr and currents down to 0.03 A/cm^2 and by studying the effects of direction of viewing, temperature, isotope impurities, capillary diameter, etc., it has been possible to obtain, with a high degree of assurance, the difference between the radiation

Table I. Reported Wavenumber Differences Between the Primary Standard as Defined and the Line Produced as Recommended

Laboratory	Net difference
Physikalisch Technische Bundesanstalt (Germany) 1959[14]	-0.003 m^{-1}
Physikalisch Technische Bundesanstalt (Germany) and International Bureau of Weights and Measures (1960)[15]	-0.001
National Standards Laboratory (Australia) 1960[16]	-0.001
National Physical Laboratory (Great Britain) 1961[17]	-0.007
National Research Council (Canada) 1961[18]	$+0.002$

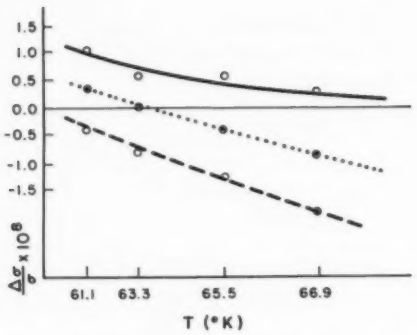

Fig. 2. Curves indicating the magnitude of the perturbations to the primary standard radiation when it is emitted by the recommended source. The solid curve indicates the proportional wavenumber shift due to a Doppler shift when the radiation is observed from the anode end of the capillary; the dashed curve indicates the shift due to a pressure-current effect at a current density of 0.3 A/cm.^{2} It will be noted that the net shift, given by the dotted line, is near zero at 63.3°K which is the recommended temperature of operation.

excited under some given conditions and that which would be observed under the ideal conditions specified in the definition.[16,18,19]

Some unpredictable (though not entirely unexpected) effects were turned up during the course of the investigations. One such effect is the fact that the interatomic Stark shift could not be specified solely in terms of the total current divided by the capillary cross section because wall effects influence the distribution of ions in the tube. Another such effect is due to the relation of the mean free path to the capillary diameter and the influence of this relation on ion drift velocity and on the pressure differences which result from the dc discharge. Still another is the apparent very slight asymmetry which likely accounts for an apparent slight dependence of the wavelength on the method by which the spectral line is observed.

The details of the physical characteristics of the 0.606 μ line are of course best appreciated by consulting the references cited. However, it is of interest to note here the order of magnitude of the perturbations to the line under practical conditions. This is indicated in Fig. 2 which shows the effect of current density, pressure, and direction of viewing on the wave number of the radiation emitted by the lamp recommended at present.

A possible result of the detailed knowledge of the perturbations described above is that one might get the impression that the new standard is particularly susceptible to them. A recent paper reporting precise wavelength determinations referred to the doubt in the corrections to the standard line which had been variously reported at -8×10^{-6} Å to $+3 \times 10^{-6}$ Å. To the casual reader this suggests a rather unsatisfactory standard! However, when one realizes that the doubt amounted to $\pm 10^{-9}$ λ and that it was only very recently that the relation of any two spectral wavelengths to one another was known to better than 100×10^{-6} Å, the uncertainty is put in its proper perspective.

Another important consequence of the studies of the new standard has been the realization of the factors which limit the precision with which one can point on a spectral line. A quantitative study of these factors has not only shown how to obtain the best precision in practice, but also the *limiting precision*, which is determined by the maximum signal-to-noise ratio inherent in the finite number of photoelectrons per unit time which can be produced by real sources and receivers.[20,21] Where this limitation is realized, i.e., if equipment is not imposing unnecessary limitations, the highest precision to which a spectral line defines a length is determined only by the intensity at the peak of the profile (for a given time constant). That is, apart from considerations such as symmetry and perturbations, a sharp line is not inherently more precise than a broad one and the practical advantages of the sharpness may indeed not compensate a lower inherent precision, if the sharp line should happen to be *significantly* less intense than the broader line. (A similar situation holds in the case of photoelectric setting on engraved lines on meter bars, where broad lines with good edges are preferable to narrower lines with equally good edges, though with crude apparatus, such as the naked eye, the sharper lines may appear to define the distance more precisely.)

Summary of the Present Situation

The quality of the newly defined standard may now be summed up as follows:

(1) It has been established that the 0.606-μ emission line of Kr-86 can be produced relatively free of perturbations, yet having an intensity and sharpness enabling visual setting to one part in 10^8 and photoelectric setting sensitive to two or three parts in 10^{10}.

(2) A simple practical source will produce the radiation with a net perturbation of under one part in 10^8, i.e., it provides a simple working standard which can be used to reproduce the *same* length to this precision at different times or in different laboratories.

(3) The knowledge already obtained gives the possibility of a somewhat more difficult lamp of more stringent specifications which would realize the defined standard to the order of one part in 10^9.

(4) If an experiment should merit it, one can determine by extrapolation the difference between the radiation from one's own source (under given conditions of excitation and observation) and the defined standard, to a precision of one in 10^9 or better; the scatter in

the values given in Table I is largely due to differences in operating conditions which are inadequately specified by current density, etc., and which are imperfectly reproduced.

The foregoing considerations indicate that replacement of the newly adopted primary standard of length could not be advantageous until an alternative is found which is precise to considerably better than one part in 10^9, or is this precise but with considerable advantages in convenience.

It must be emphasized that it is extremely difficult to take advantage of even an accuracy of one part in 10^8 in physical measurement; the limit in most cases will be imposed by faults in the technique of comparison or by the dependence on environment of the physical length being determined.

Other Possible Standards

Having considered the characteristics of the natural constant now chosen for defining the meter, it is in order to consider the relative merits of some alternative possibilities. The important ones are as follows:

(1) The wavelengths of other optical spectral lines emitted in an ordinary electrical discharge or absorbed in a cell containing atoms having the normal gas distribution of velocities;

(2) the wavelengths of optical radiations emitted or absorbed by atoms in an atomic beam;

(3) the wavelengths of optical radiations emitted by a laser;

(4) the wavelengths of γ-radiations emitted under the conditions of the Mössbauer effect;

(5) the use of an atomic frequency standard and some agreed arbitrary value for the velocity of light.

These alternatives will be considered in the above order.

(1) The only absorption line seriously advocated was an iodine absorption line; however, this particular line was found to be less precise than the present Kr-86 standard line. Other *emission* lines which might reasonably be considered have been shown to be definitely inferior because of imprecision resulting from the effects of environment on the emitted wavelength. The possible exceptions are other Kr-86 lines which, however, are unlikely to be significantly more precise and have not been nearly so thoroughly studied. These lines are now being studied, for use as secondary standards, by the Advisory Committee on the Definition of the Metre.[22]

(2) If radiation is observed (in emission or absorption) from a highly collimated beam of atoms traveling at right angles to the direction of observation, the broadening due to Doppler effect can be reduced by a factor of ten or so. In addition, the very low density of atoms under the usual conditions of a beam would lead one to expect the perturbing effect of neighboring atoms to be very small. These factors suggest that the atomic beam technique would have very great advantages in providing a standard. However, there are also two important disadvantages.

One disadvantage is that the wavelength of the observed radiation is sensitive to the geometry relating the direction of all the atoms in the beam and the direction of observation; although means for reducing these effects have been described,[23] many second-order effects have not been taken into account, and the technique has far to go before there is any assurance that the precision significantly exceeds one part in 10^9.

The other disadvantage is that the intensity of the radiation is very low, with a consequent loss in precision for the reason mentioned earlier. Attempts to produce the 0.606-μ line of Kr-86 and the 0.546-μ line of Hg-198 in a beam have not succeeded in obtaining enough intensity for any precise measurement of a wavelength, let alone to provide a useful standard. The 0.254-μ resonance line for Hg-198 has been produced with a good intensity but still not sufficient to be inherently more precise than the 0.606-μ line emitted by the lamp recommended for the present standard.[24] A comparison of the precision of these two lines made in the reference just cited is not a valid comparison of their inherent respective precisions because it was influenced by the authors' conventional method of setting and their exposure times, both of which favored the beam emitted line.

Although the atomic beam may eventually provide a much improved standard, it is as yet far from having been demonstrated.

(3) Lasers have been demonstrated to yield optical radiations of extreme sharpness, such that the linewidth at half intensity is as little as $10^{-14}\ \lambda$.[25] However, the wavelength of the emitted radiation is primarily determined by the length of the etalon (or resonant cavity), within the Doppler width of the spectral line being stimulated; it is, therefore, subject to all the perturbations and instabilities which are characteristic of material standards, such as meter bars. One suggested prospect of lasers as standards is to relate their frequency to known frequency standards by frequency dividing; from the point of view of the present this appears to be fraught with great difficulties, theoretical as well as practical! Another prospect is to use laser light, with all its power and sharpness, to determine the value of some atomic transition. It has already been demonstrated that the He–Ne gas laser line at 1.153 μ can be controlled to about one part in 10^8 with respect to the center of the Ne line[25]; this system is not yet very attractive because the Ne line, which is the control, is subject to conditions of perturbing influences very much greater than that of the

present Kr-86 standard line at 0.606 μ. A laser line, in conjunction with absorption, either in a beam or otherwise, would seem attractive, but a suitable line has yet to be found. Thus, while the laser technique holds promise, a serious specific example has yet to be discovered.

(4) Radiations emitted under the conditions of the Mössbauer effect also yield lines of extreme sharpness, comparable to that of the laser. However, the difficulty of relating its wavelength to physical lengths and lack of information on the constancy within different environments or samples rule it out for consideration as an absolute standard for the present.

(5) The use of atomic frequency standards to define the standard of length by ascribing an arbitrary value to the velocity of light has been proposed as attractive philosophically. However, as experiments to relate the velocity of light, atomic frequency standards, and physical lengths are at present accurate only to one part in 10^6, it will be some time before this method poses a serious challenge for practical consideration.

Conclusion

In basing the international standard of length on an optical radiation the world has gained the advantage of a natural constant, of a greatly enhanced precision, and of the convenience of modern interferometric techniques for length measurements. One can now measure equally readily, in terms of the primary standard, wavelengths, the most important types of secondary length standards (represented by gauge blocks and scales, respectively) or any displacements which can be related to optical surfaces. Although maximum lengths of only about 1 meter are conveniently compared directly to the primary standard, techniques for measuring much greater lengths by optical multiplication are well established.

The optical radiation chosen has been clearly shown to be the best one on the basis of the extensive investigations cited in the references, most of which are documented in the *Proceedings of the International Committee of Weights and Measures*. Indeed, the Advisory Committee, in October 1962, having considered all research to date, unanimously agreed as to the continued superiority of the Kr radiation as the primary standard in comparison with all other known sources. This point cannot be too strongly emphasized because the impression has been widespread in the United States that better alternatives are available, particularly in regard to Hg-198 radiations; the latter have been sometimes advocated with an enthusiasm that appeared to be based as much on chauvinism as on objective scientific considerations.

This paper is appropriately concluded by drawing attention to evidence that the conservative point of view has always proved correct on the question of replacing standards, particularly when an international standard is involved. In looking back, the replacing of the old meter prototype standard was not delayed one day too long. Although enthusiasts had been proposing the red line of Cd as a substitute for sixty years, uncertainty in its reproducibility has only recently been shown to be as great as the uncertainty in the length of the old prototype meter bar. Measurement techniques being what they were, no advantage would have resulted from an earlier change. On the other hand, in the case of the standards of luminous intensity and of electrical units, over-enthusiastic hurry resulted in the setting up of "natural" primary standards which are less precise than the secondary standards which are calibrated in terms of them.

If the new primary standard of length fulfills its requirements as well as the former one, it will have performed well. It should satisfy all needs for some time to come.

In conclusion, it ought to be mentioned that the work leading to the new definition of the meter was done by a very large number of workers at the International Bureau and at various national laboratories. No names have been mentioned in the preceding text but it would be inappropriate not to acknowledge the work of three men whose contributions were outstanding: W. Kösters and E. Engelhard of the Physikalisch Technische Bundesanstalt, who were responsible for the development of the Kr-86 lamp, and J. Terrien, Director of the International Bureau of Weights and Measures, who contributed very important personal research as well as doing much to coordinate the work in other laboratories.

References

1. Tenth General Conference of Weights and Measures, Sèvres, France, October, 1954.
2. Compt. rend., Eleventh General Conference of Weights and Measures, Paris, p. 134, (1960).
3. First General Conference of Weights and Measures, Paris (1890).
4. Procès Verbaux du C.I.P.M., p. 30, (1890).
5. A. A. Michelson and J. R. Benoit, Trav. et Mem. du B.I.P.M. **11**, 3, 85 (1895).
6. Trans. Intern. Union for Solar Research **2**, 28 (1907).
7. Seventh General Conference on Weights and Measures, Sèvres, France, October, 1927.
8. Procès Verbaux du C.I.P.M. **24** (1954).
9. Procès Verbaux du C.I.P.M. **26** (1958).
10. Eleventh General Conference of Weights and Measures, Sèvres, France, October, 1960.
11. Procès Verbaux du C.I.P.M. **28**, 71 (1960).
12. K. H. Hart and K. M. Baird, Can. J. Phys. **39**, 781 (1961).
13. Eleventh General Assembly, I.A.U., Berkeley, California (1961).
14. E. Engelhard, *Proc. Symposium on Interferometry at the National Physical Laboratory*, June, 1959, p. 34.
15. E. Engelhard and J. Terrien, Rev. opt. **39**, 11 (1960).

16. C. F. Bruce and R. M. Hill, Australian J. Phys. **14**, 64 (1961).
17. W. R. C. Rowley, Trans. I.A.U. **XIA**, 98 (1961).
18. K. M. Baird and D. S. Smith, J. Opt. Soc. Am. **52**, 507 (1961).
19. J. Terrien and J. Hamon, Compt. rend. **243**, 740 (1956).
20. G. R. Hanes, Can. J. Phys. **37**, 1283 (1959).
21. D. S. Smith, Can. J. Phys. **38**, 983 (1960).
22. Meeting of the Advisory Committee on the Definition of the Metre, Sèvres, France (October, 1962).
23. R. L. Barger and K. G. Kessler, J. Opt. Soc. Am. **50**, 352 (1960).
24. R. L. Barger and K. G. Kessler, J. Opt. Soc. Am. **51**, 827 (1961).
25. A. Javan, E. A. Ballik, and W. L. Bond, J. Opt. Soc. Am. **52**, 96 (1962).

From the Editor

We continue our discussion of the format and content of this journal, quoting from our complaint department. First, a few items on the mechanics of journals: "A good journal should reach the readers on the day designated on the cover, my July ('62) issue arrived on 14 July." *Applied Optics*, believe it or not, is much more prompt in its appearance than most of the other physics journals. Our mailing date from the printer is five days *before* the first of the month; therefore most of you should receive the journal close to the first of the month, even in California. For reasons of economy, however, the journal is sent second class, and some delays in delivery may be due to your local post office. It is also true that in July the printer ran out of those little yellow postcard inserts inviting people to subscribe and waited a week or so for a reorder. (Several of you have said you dislike these inserts, and so does your Editor, but they do appear to produce subscriptions, so for the present we must tolerate them.)

"I received only the front cover of the March 1962 number." We had a number of these complaints, and we have taken two steps to cure this: We have changed the gluing process of attaching the cover; and we now mail in a paper wrapper, which costs more, but which has greatly reduced the number of defective and lost copies. Your Editor, by the way, would appreciate a postcard complaint about any faulty mailings: some copies intended for Miss. went to Mass. and for N.H. to N.D. We cannot correct these failings if we do not know about them.

"I will not submit papers to you unless I can see the galley proof." We have not enforced the no-galley rule as rigorously as some of you suspect. After a very short time, we found that we could not adhere to this practice, and galleys of all papers and Letters are now sent to all authors. We included such a statement in the early *Information for Contributors* to discourage those authors who send in a preliminary version of their results with the thought that later data or even drastic changes in the conclusions might be inserted in galley. This practice is time consuming and expensive, can disrupt the mock-up of an issue, and can even delay the appearance of the entire issue. Even two or three galleys returned to authors who neglect to return them promptly can delay an issue. Our hope was and is that a rule such as this might make the author prepare his manuscript more carefully. As it is, it appears that a distressing proportion of our authors do not heed the *Information for Contributors*.

We have had several complaints about authors' abstracts: they are not sufficiently informative; they are simply rewrites of the title or the introduction. This problem is not peculiar to *Applied Optics;* the AIP Publications Board has also given thought to this matter. There are now several scientific journals devoted to abstracting the literature: *Physics Abstracts*, *Chemical Abstracts*, *Meteorological Abstracts*, and many others. In about 9 of every 10 abstracts used in these abstract journals, the one originally prepared by the author is selected. Having to rewrite an abstract delays the time between the appearance of the original article in print and the publication of the abstract journal and, in addition, requires a larger technical staff to scan the article and write the abstract. We are attempting to improve the quality of our abstracts. Our reviewers and referees are now asked specifically to consider the quality of the abstract of papers under review, and each author is now reminded that his abstract may appear verbatim: does it contain the essence of the article? While we speak of abstracts, we should mention those authors who practice the art of Abstractsmanship, the ability to write an abstract that is better than the paper itself. This sort of abstract is ordinarily sent to program committees to assure the author a place on the program. There is an interesting discussion of this art in Proc. Inst. Radio Engrs. **51**, 241 (1963), in which two authors relate how they submitted to a nationally sponsored meeting an elaborate abstract describing "the Linotron, a practical solid-state device for the implementation of majority logic." (It was simply a flowery description of a resistor.) The paper was promptly accepted. This, we hasten to add, could not happen in our journal, as every paper is reviewed prior to acceptance by at least two readers.

Let us turn to another topic: the pros and cons of featuring a specific topic or technical area in each issue. While this practice appears to be popular with our readers, it has caused more editorial difficulties and headaches than all other problems combined. One must remember that more than two years of editorial planning and discussion preceded the appearance of our first issue. (This is indeed the case with each issue.) Some of these discussions concerned the question of how such a new journal without a solid reputation could attract readers or even papers and in particular, how we could do this without treading on the toes of *J. Opt. Soc. Am.* We early resolved that we should concentrate on bringing back to the Society those groups who were tending more and more to split into subdisciplines (such as the UV or IR) and on offering a haven to the optical pumping papers. The next problem was practical: optical applications are so varied that no single editor could possibly be knowledgeable in the entire field. We were therefore led almost inevitably to designate Feature Editors, each responsible for a given area of optics. They, in turn, would draw on close knowledge of specialized topics to stimulate or elicit papers for issues featuring those topics.

Our problems began when our Feature Editors went to work with such enthusiasm that each of them received many more papers than we could include in his issue. (Remember that we do operate on a budget, and we were intended as a 100-page per issue journal.) With this surplus began the complex problem of spill-over of papers into later issues that were also already crowded. As the first few issues appeared and were favorably received, we also began to receive contributed manuscripts in many areas other than those announced as features. And there is no one so impatient as an impatient author. He has invested years in his research study and agony in the writing; having finally sent the paper to the journal, he is properly eager to see it in print. The world has been waiting since before Newton for this paper on the optical anisotropy of infrared laser beams from

spacecraft: what should we do if the manuscript arrives just after our Laser, Space, or Infrared issue?

At our early editorial meetings, some people argued against featured topics: if an issue is devoted to a feature we are either encouraging a paper before it has ripened naturally or else we are delaying reportable research to a later suitable feature. In either case, they argued, we are introducing an unnatural order. The progress of human history has been chiefly motivated to dethroning the privileged, and there is nothing so democratic as the queue: get in line; wait your turn; first come, first served. We should print papers strictly in the order received. On the other hand, some have said that a featured topic inconveniences the authors in order to accommodate the readers: if many papers on ultraviolet are gathered together, they have more impact on the reader than the same papers strewn through several issues. There is some hope here that the whole becomes greater than the sum of the parts. Take, for example, the papers of our January 1963 issue featuring astrometric astronomy. In one paper, we learn that 25 of the 48 stars nearest the sun are members of visual binaries or triples, but that we cannot yet distinguish whether the displacement is due to a planetary system of negligible luminosity or to a luminous stellar companion. Other papers discuss improvements of telescope-image quality; improvement of seeing characteristics by balloon astronomy or space telescopes; still other papers describe techniques for substantial improvements in the luminosity of spectrometers. Putting all of these discussions together might stimulate someone to the next step in answering this intriguing question.

Now that we are a monthly, some have suggested alternating featured topics with issues devoted simply to contributed papers. Perhaps this will not be necessary; as a monthly we may be able to keep up with our influx of papers. Your Editor does not mean to imply that he does not appreciate enthusiastic Feature Editors; indeed our success is largely due to them: crown them with daphne. But the contributed papers demonstrate that this journal was needed, features or no, and we must also strive to serve this need.

JOHN N. HOWARD

Meetings Calendar

May

2–7 7th Internatl. Color Mtg., Florence *Centre c'-Information de la Couleur, 23, rue Nôtre-Dame-des-Victoires, Paris 2, France*

6–10 2nd Hungarian Optical Conf., Budapest *Soc. of Optics, Acoustics and Film Technics, Szabadság-tér 17, Budapest 5, Hungary*

6–10 Internatl. Conf. on Atmospheric and Space Electricity, Montreux, Switz. *H. R. Byers, Dept. of Geophys. Sciences, U. of Chicago, Chicago 37, Ill.*

6–11 14th Natl. Science Fair-Internatl., Albuquerque, N.M. *Science Service, 1719 N St. N.W., Wash. 6, D.C.*

6–17 Quantum Electronics Course, UCLA *Engr. Ext., Engr. Bldg., U. of Calif., Los Angeles 24, Calif.*

2nd week French Soc. of Ophthalmology, 70th Cong., Paris *M.-A. Dollfus, Soc. Française d'Ophtalmologie, 27, rue du Faubourg-St.-Jacques, Paris 16, France*

14 SAS New York and Delaware Valley Sects., Forrestal Res. Center, Princeton U., Princeton, N.J.

16–17 Soc. of Technical Writers and Publishers, 10th Ann. Conv., Boston, Mass.

20–23 14th Ann. Mid-America Spectroscopy Symp., Sheraton-Chicago Hotel, Chicago *J. E. Forrette, Borg-Warner Corp., Wolf and Algonquin Rds., Des Plaines, Ill.*

21–23 Am. Federation of Information Processing Societies, Spring Joint Computer Conf., Detroit, Mich.

22 OSA Natl. Capital Sect. *H. K. Hammond III, Rm. 316, East Bldg., NBS, Wash. 25, D.C.*

June

— APS, summer mtg., Buffalo, N.Y. *K. K. Darrow, 538 W. 120 St., New York 27, N.Y.*

4–7 German Soc. for Applied Optics, Ann. Mtg., Braunschweig *H. Volkmann, Deutsche Gesells. für Angewante Optik Schriftfuhrer, Zeppelinstr. 23, 792 Heidenheim, Germany*

4–8 Soc. of Phys. Chem., ann. mtg., Paris *G. Emschwiller, Soc. de Chimie Physique, 10, rue Vauquelin, Paris 5, France*

6–8 Chem. Inst. of Canada, 46th Natl. Conf., Toronto, Ont. *CIC, 48 Rideau St., Ottawa 2, Ont., Canada*

6–9 Canadian Assoc. of Physicists, Laval U., Quebec City *L. Katz, U. of Saskatchewan, Saskatoon, Canada*

7–13 European Ophthalmological Soc. 2nd Cong., Vienna *J. François, 15, pl. de Smet de Naeyer, Ghent, Belgium*

10–14 Triple Commission on Spectroscopy, Columbus *H. H. Nielsen, Ohio State U., Columbus, Ohio*

10–14 Molecular Structure and Spectroscopy, 18th symp., Columbus *H. H. Nielsen, Ohio State U., 174 W. 18 Ave., Columbus 10, Ohio*

10–21 Industrial Use of the Polarizing Microscope, McCrone Res. Inst. *J. A. Reffner, McCrone Res. Inst., 451 E. 31 St., Chicago 16, Ill.*

13–Aug. 9 Geometric Optics Summer Course, Indiana U. *R. W. Everson, Div. of Optometry, Indiana U., Bloomington, Ind.*

17–21 Carbon Conf., U. of Pittsburgh *R. A. Friedel, U.S. Bureau of Mines, 4800 Forbes Ave., Pittsburgh 13, Pa.*

17–24 CIE, Hofburg Palace, Vienna, Austria

17–28 AFOSR Summer Scientific Seminar on Topics in Optics, Cloudcroft, N.M. *AFOSR Seminar, P.O. Box 1053, Holloman AFB, N.M.*

18–26 Internatl. Comm. on Illumination, 15th Cong., Vienna, Austria

23–28 ASTM Ann. Mtg., Chalfonte-Haddon Hall, Atlantic City, N.J. *ASTM, 1916 Race St., Philadelphia 3, Pa.*

24–26 APS, Buffalo *K. K. Darrow, 538 W. 120 St., New York 27, N.Y.*

24–26 Internatl. Astrophysics Symp., Liège *M. Migeotte, Inst. d'Astrophysique, Cointe-Sclessin, Belgium*

24–27 Groupement pour l'Avancement des Methodes Spectrographiques, 25th Cong., Paris *GAMS, 1, rue Gaston Boissier, Paris 15, France*

24–28 Gordon Conf. on Magnetic Resonance, Tilton School, Tilton, N.H.

25–29 Oil and Colour Chemists' Assoc., biennial conf., Scarborough, England

July

1–5 IUPAC Internatl. Symp. on Macromolecular Chem., Paris *Symp. Sec., Lab. de Chimie Physique, 11, rue Pierre Curie, Paris 5, France*

1–5 Gordon Conf. on Chemistry and Physics of Space, Tilton School, Tilton, N.H.

1–14 Applications of Quantum Mechanical Methods to the Study of Molecular Properties, Menton *R. Daudel, Centre de Mechanique Ondulatoire Appliquee, 23, rue du Maroc, Paris 19, France*

2–5 Internatl. Symp. on Free Radicals, 6th, Cambridge *A. B. Collear, U. of Cambridge, Lensfield Rd., Cambridge, England*

5–9 IUPAC Conf., London *Sec., IUPAC Conf., 47 Belgrave Sq., London, SW1, England*

8–13 Ionization Phenomena in Gases, Orsay *P. Hubert, CENFAR, B. P. No. 6, Fontenay-aux-Roses, Seine, France*

8–19 Industrial Use of the Polarizing Microscope, McCrone Res. Inst. *J. A. Reffner, McCrone Res. Inst., 451 E. 31 St., Chicago 16, Ill.*

8–27 Summer Course in Modern Optics, Inst. of Optics, U. of Rochester *Inst. of Optics Summer Course, U. of Rochester, River Campus Station, Rochester 20, N. Y.*

10–17 IUPAC Congress, London *Sec., IUPAC Congress, 47 Belgrave Sq., London, SW1, England*

15–19 IUPAP, 2nd Internatl. Conf. of Nuclidic Masses, Vienna, Austria

15–26 Optical Physics and Its Applications Course, UCLA *Engr. Ext., Engr. Bldg., U. of Calif., Los Angeles 24, Calif.*

18–23 IUPAC Symp. on Thermodynamics and Thermochemistry, Lund *S. Sunner, Thermochem. Lab., Lund U., Lund, Sweden*

22–26 Physics of Electronic and Atomic Collisions, London *Conf. Sec., Physics Dept., University Col., Gower St., London, W.C. 1, England*

Quantum Limit to Precision of Wavelength Determination

G. R. Hanes

The precision of wavelength determination is ultimately limited by noise arising from the quantum nature of light and light detection. Expressions are derived for the limiting precision attainable by various interferometers and conventional spectrometers in terms of parameters characterizing the instruments, the source, and the detector. A comparison of five different instruments shows the superiority of the interferometers and indicates that they are divided into three classes, according to the role played by the half-width of the radiation from the source.

I. Introduction

In this article we shall consider the application of various types of interferometers and conventional spectrometers to high-precision measurements of wavelength and wavelength shifts. Work of this nature has been very important in the redefinition of the meter in terms of the 6056 Å line of Kr^{86} and is being actively pursued in the establishment of accurate secondary wavelength standards. In particular, we wish to examine the limit to the precision of such measurements imposed by the quantum nature of light and light detection. This limit is fundamental. It arises because an experiment of finite duration must be performed with a finite number of photons. The number arriving at the detector in successive equal time intervals will fluctuate, and this fluctuation or noise will prevent us from detecting arbitrarily small signals. Other noise sources, which are of practical importance but which in principle can be eliminated with sufficient effort, will not be considered. In practice, these other noise sources can be reduced sufficiently, so that the fundamental limit is approached. An investigation of this limit will thus provide us with a useful standard against which to compare observed performance. It will also show what characteristics of a source and detector are valuable in attaining high precision and how to use a particular instrument to best advantage.

Theories of the quantum limit to precision have been considered by a number of authors for the Michelson and Fabry-Perot interferometers. Before discussing their contributions, it is proposed to develop a rather general treatment of five types of spectrometers: conventional prism and grating instruments, the Fabry-Perot and Michelson interferometers, and the recently invented spherical Fabry-Perot of Connes.[1] These various instruments are treated on an approximately equal footing, so that their relative merits may be examined. The contributions to the theory made by previous authors will then be reviewed to show the origin of the basic ideas and to indicate where they have gone beyond the somewhat simplified theory presented here.

The author is with the Division of Applied Physics, National Research Council, Ottawa, Canada.

Received 15 November 1962.

II. Theory

A. The Concept of Precision

In the determination of wavelength by a spectroscopic instrument, the essential measurement on any one line is made by exploring the profile of the light emerging from the dispersing element with an aperture. This is to be done in a manner that will determine as accurately as possible the position of the center of the profile, which we assume to be symmetric, in terms of some variable of the instrument which is at our disposal and whose relation to a wavelength or wavenumber scale is known. With a prism or grating, the variable is an angle of refraction or diffraction. With an interferometer, we could use the off-axis angle, but for most efficient use of these instruments we must observe on axis[2] and use as the variable the optical spacing between the plates. Now the dispersion of the instrument will be known, so that when the measurement is repeated and the inevitable statistical spread in the results appears, the fluctuations can be translated into apparent fluctuations in wavenumber. The root-mean-square fluctuation in wavenumber we shall call $\delta\sigma$, and the precision of a single measurement will be defined as

$$\mathcal{P} = \sigma/\delta\sigma, \tag{1}$$

where σ is the wavenumber of the radiation being measured. We might point out the analogy with resolving

power or resolvance

$$\mathcal{R} = \sigma/s, \tag{2}$$

where s is the smallest resolvable wavenumber separation. For our purposes, s may be taken to be the half-width of the instrumental profile. $\mathcal{P}$, of course, refers to a complete measurement, whereas $\mathcal{R}$ is a characteristic of the spectrometer only. $\mathcal{P}$ will be much larger than $\mathcal{R}$, since the position of the center of a profile can be established to within a small fraction of the half-width in normal circumstances.

B. Pointing

We now wish to discover what the maximum value of $\mathcal{P}$ will be if we eliminate all the nonessential sources of noise, leaving only the statistical fluctuations in the number of photons arriving at the detector in successive time intervals. To do this, we must first examine more closely the details of the operation of setting on the center of the profile, an operation that metrologists refer to as "pointing". Any method of pointing involves the comparison of the flux received from points on opposite sides of the peak; that is, we observe the difference in the response of our detector for two positions of the exploring aperture, and when this difference is zero the two positions are symmetrically disposed with respect to the center of the profile. This concept of the mechanism of pointing is quite general and can be applied, with varying degrees of complication, to such procedures as setting bifilar crosshairs on an engraved line on a meter bar, setting a crosshair on a photographic record of the profile of a line from a spectrograph, or locating a null in the "derivative" of the profile obtained by scanning the detector over it. The simple method of pointing considered here, that of photoelectric observation of the flux at two positions only, is probably capable of the highest precision, because the detector spends all its time observing at positions of high sensitivity and because photoelectric detectors have a higher quantum efficiency than other types and, therefore, use the available flux to greater advantage.

How large should the viewing aperture be, and what should be the separation between the two positions, to achieve the maximum precision? Instead of making a detailed calculation of these values, which depend in a complicated way on the exact shape of the profile being examined, we shall choose values that are convenient, in the sense that they make the calculations much simpler and yet are sufficiently close to the optimum that the final results will be reasonably accurate. More appropriate choices of the aperture size and spacing would gain a numerical increase in the estimated precision, but this gain would be fairly well compensated by the inclusion of instrumental transmission losses, which we shall neglect here. The resulting expressions for $\mathcal{P}$ will be algebraically correct, and the numerical coefficient will be seen to be in error by not more than a small factor in those cases where comparison can be made with more detailed calculations.

The aperture size will be taken to be equal to the half-width of the profile, and its two positions will be taken to be contiguous. The dividing line will be on the center of the profile when the pointing is done. We also assume that the intensity of the profile at the outer edge of the aperture can be neglected. These assumptions will allow us to discuss prism and grating spectrometers and Fabry-Perot interferometers of high finesse. Some modifications will be necessary when we come to the other two instruments.

C. Calculation of Precision

Let us now suppose that in an observing time τ, one-half of which is spent on each side of the profile, an average of N photons falls on the detector, assumed for the moment to be a perfect quantum detector. We can now show that $\delta\sigma$, the root-mean-square fluctuation of the apparent wave number in a series of pointings is of the order of $N^{-1/2}$ of the half-width v of the profile presented to the exploring aperture, i.e., $\delta\sigma \sim v/N^{1/2}$. We receive $N/2$ photons from each side of the profile. Since the photons arrive effectively at random, the fluctuation in this number in successive pointings will be $(N/2)^{1/2}$, and the fluctuation in the difference that we are trying to make zero will be $N^{1/2}$. This assumption of randomness is not strictly true, since photons are bosons and show a tendency to be correlated and thus give rise to an additional fluctuation over and above that estimated here. Brown and Twiss[3] have investigated this subject in their discussions of intensity interferometry, with the conclusion that with conventional light sources " the excess photon noise is too small to be detected . . . with one photocathode."

To translate these signal fluctuations into equivalent fluctuations in wave number we need to know what difference signal δN is produced by a given offset $\delta\sigma$. Such an offset will add to the observation on one side, and subtract from the other side, a narrow strip of width $\delta\sigma$ from the center of the profile. Near the center of the profile, the photon flux per unit wave number per $\tau/2$ is approximately N/v, and so $\delta N = 2(N/v)\delta\sigma$. Thus the wavenumber fluctuation corresponding to fluctuations of $N^{1/2}$ in the difference signal is $\delta\sigma = v/2N^{1/2}$, and the precision of a single setting is given by

$$\mathcal{P} = 2N^{1/2}\sigma/v. \tag{3}$$

Now, N and v are not independent variables, for if we try to make v smaller by increasing the resolvance of the instrument (e.g., by using smaller slits), N will also decrease. To examine this relationship we note that

$$N = \left(\frac{P}{hc\sigma}\right)\left(\frac{\mathcal{E}}{2}\right)\tau, \tag{4}$$

where P is the radiance of the source for the line we are studying [$(P/hc\sigma)$ is thus the photon flux per unit area, solid angle, and time], $\mathfrak{L}$ is the luminosity of the instrument defined as the ratio of the transmitted flux to the radiance of the source, and the 2 under the $\mathfrak{L}$ accounts for the fact that we observe only one-half of the profile. Jacquinot[2] has shown that the luminosity of a spectrometer is related to the resolvance by the relation

$$\mathfrak{L}\mathcal{R} = ZA, \tag{5}$$

where A is a characteristic area of the dispersing element (area of the base of a prism, projected area of a grating, area of Fabry-Perot plates) and Z is a constant (at least for the Fabry-Perot; for the prism and grating it is related to the angular height of the slits and the derivative of the angle of the exit beam with wavelength). Combining Eqs. (2)–(5) we have

$$\mathcal{P} = \left[\frac{2Z}{hc}\, A\tau P\, \frac{S}{v^2}\right]^{1/2}.$$

Thus far, we have assumed a perfect quantum detector. The modification for actual detectors is easily made by introducing the detective quantum efficiency of Jones,[4] defined as the square of the ratio of the signal to noise at the output of the detector to that at the input. For a photomultiplier, which is probably the most common detector used, the detective quantum efficiency θ is about two-thirds of the quantum efficiency of the photocathode, the reduction being caused by noise introduced in the multiplier. If the noise in the dark current is not negligible, θ may become much smaller. Our actual detector, therefore, uses effectively only a fraction θ of the incident photons, which is equivalent to having a source θ times as radiant. The modified equation for $\mathcal{P}$ is

$$\mathcal{P} = \left[\frac{2Z}{hc}\, A\tau\theta P\, \frac{S}{v^2}\right]^{1/2}.$$

Finally, we shall express v in terms of s and w, the half-width of the line profile, as $v = s \oplus w$, where the symbol $\oplus$ indicates that v is the half-width of the convolution of the instrumental and line profiles. The expression for the precision of a single pointing that we can apply to some of our instruments is

$$\mathcal{P} = \left[\frac{2Z}{hc}\, A\tau\theta P\, \frac{s}{(s \oplus w)^2}\right]^{1/2}. \tag{6}$$

III. Application of the Theory

A. Prism Spectrometers

For a prism instrument, s will be large compared to the w of lines used for high-precision measurements (e.g., Kr^{86} and Hg^{198} sources have $w \sim 10^{-6}\sigma$). Therefore, $s \oplus w$ will be essentially equal to s, and the precision will vary as $s^{-1/2}$. This relation will fail when the slit-widths become so narrow that diffraction losses increase catastrophically. Let us assume that we can get to within a factor of two of the theoretical resolving power without serious loss. To calculate Z and the minimum s, we assume also the following values for certain parameters of the instrument: the angular height of the slits as seen from the prism, 3×10^{-2} rd; $\lambda d\mu/d\lambda$, where μ is the refractive index of the prism material, 10^{-1}; we let the thickness of the prism at the base be T. Using the expressions in ref. 2, we have

$$\mathcal{P} = 3.9 \times 10^{10}\, [AT\tau\theta P]^{1/2}.$$

To arrive at a numerical value, we choose the primary standard Kr^{86} line for which $P = 3 \times 10^{-1}$ W m^{-2} sr^{-1}, a detector with $\theta = 5 \times 10^{-2}$ at this wavelength (a trialkali photocathode) and an observing time of 1 sec. These values will be used for all the instruments. For the prism spectrometer under consideration here, we assume a prism base 20-cm square and arrive at a value of

$$\mathcal{P} = 4.2 \times 10^{8}.$$

B. Grating Spectrometers

Grating spectrometer instruments are capable of achieving much higher resolvance than prism spectrometers, but a value of $\mathcal{R} = 10^6$ is not readily obtained, and the arguments given above concerning $s \oplus w$ will apply here. Making the same assumptions about the minimum s and the angular height of the slits, assuming a 30° diffracting angle, and letting the grating width be W, we have

$$\mathcal{P} = 39 \times 10^{10}\, [AW\tau\theta P]^{1/2}.$$

For a 20-cm square grating and the same source and detector, the numerical value of $\mathcal{P}$ is

$$\mathcal{P} = 4.0 \times 10^{9}.$$

C. Fabry-Perot Interferometer

The restrictions on s encountered above do not apply to the Fabry-Perot, for we can make s as small as we like by increasing the thickness of the spacer. An examination of the ratio $s/(s \oplus w)^2$ shows that it has a maximum value $\simeq 1/(2w)$ when $s \simeq w$. For larger values of s, $\mathcal{P} \sim s^{-1/2}$, as with the first two instruments; for smaller values, $\mathcal{P} \sim s^{1/2}$. Using the value of $Z = 3.4$ from ref. 2, we have for the Fabry-Perot of high finesse,

$$\mathcal{P} = 410 \times 10^{10} \left[A\tau\theta\, \frac{P}{w}\right]. \tag{7}$$

Using the same source, detector, and observing time as above, with $w = 1.4$ m^{-1}, and assuming 4-cm diameter plates, the value of the precision becomes

$$\mathcal{P} = 1.5 \times 10^{10}.$$

Within the approximations of the theory outlined above, the precision attainable by a Fabry-Perot is

power or resolvance

$$\mathcal{R} = \sigma/s, \tag{2}$$

where s is the smallest resolvable wavenumber separation. For our purposes, s may be taken to be the half-width of the instrumental profile. $\mathcal{P}$, of course, refers to a complete measurement, whereas $\mathcal{R}$ is a characteristic of the spectrometer only. $\mathcal{P}$ will be much larger than $\mathcal{R}$, since the position of the center of a profile can be established to within a small fraction of the half-width in normal circumstances.

B. Pointing

We now wish to discover what the maximum value of $\mathcal{P}$ will be if we eliminate all the nonessential sources of noise, leaving only the statistical fluctuations in the number of photons arriving at the detector in successive time intervals. To do this, we must first examine more closely the details of the operation of setting on the center of the profile, an operation that metrologists refer to as "pointing". Any method of pointing involves the comparison of the flux received from points on opposite sides of the peak; that is, we observe the difference in the response of our detector for two positions of the exploring aperture, and when this difference is zero the two positions are symmetrically disposed with respect to the center of the profile. This concept of the mechanism of pointing is quite general and can be applied, with varying degrees of complication, to such procedures as setting bifilar crosshairs on an engraved line on a meter bar, setting a crosshair on a photographic record of the profile of a line from a spectrograph, or locating a null in the "derivative" of the profile obtained by scanning the detector over it. The simple method of pointing considered here, that of photoelectric observation of the flux at two positions only, is probably capable of the highest precision, because the detector spends all its time observing at positions of high sensitivity and because photoelectric detectors have a higher quantum efficiency than other types and, therefore, use the available flux to greater advantage.

How large should the viewing aperture be, and what should be the separation between the two positions, to achieve the maximum precision? Instead of making a detailed calculation of these values, which depend in a complicated way on the exact shape of the profile being examined, we shall choose values that are convenient, in the sense that they make the calculations much simpler and yet are sufficiently close to the optimum that the final results will be reasonably accurate. More appropriate choices of the aperture size and spacing would gain a numerical increase in the estimated precision, but this gain would be fairly well compensated by the inclusion of instrumental transmission losses, which we shall neglect here. The resulting expressions for $\mathcal{P}$ will be algebraically correct, and the numerical coefficient will be seen to be in error by not more than a small factor in those cases where comparison can be made with more detailed calculations.

The aperture size will be taken to be equal to the half-width of the profile, and its two positions will be taken to be contiguous. The dividing line will be on the center of the profile when the pointing is done. We also assume that the intensity of the profile at the outer edge of the aperture can be neglected. These assumptions will allow us to discuss prism and grating spectrometers and Fabry-Perot interferometers of high finesse. Some modifications will be necessary when we come to the other two instruments.

C. Calculation of Precision

Let us now suppose that in an observing time τ, one-half of which is spent on each side of the profile, an average of N photons falls on the detector, assumed for the moment to be a perfect quantum detector. We can now show that $\delta\sigma$, the root-mean-square fluctuation of the apparent wave number in a series of pointings is of the order of $N^{-1/2}$ of the half-width v of the profile presented to the exploring aperture, i.e., $\delta\sigma \sim v/N^{1/2}$. We receive $N/2$ photons from each side of the profile. Since the photons arrive effectively at random, the fluctuation in this number in successive pointings will be $(N/2)^{1/2}$, and the fluctuation in the difference that we are trying to make zero will be $N^{1/2}$. This assumption of randomness is not strictly true, since photons are bosons and show a tendency to be correlated and thus give rise to an additional fluctuation over and above that estimated here. Brown and Twiss[3] have investigated this subject in their discussions of intensity interferometry, with the conclusion that with conventional light sources " the excess photon noise is too small to be detected . . . with one photocathode."

To translate these signal fluctuations into equivalent fluctuations in wave number we need to know what difference signal δN is produced by a given offset $\delta\sigma$. Such an offset will add to the observation on one side, and subtract from the other side, a narrow strip of width $\delta\sigma$ from the center of the profile. Near the center of the profile, the photon flux per unit wave number per $\tau/2$ is approximately N/v, and so $\delta N = 2(N/v)\delta\sigma$. Thus the wavenumber fluctuation corresponding to fluctuations of $N^{1/2}$ in the difference signal is $\delta\sigma = v/2N^{1/2}$, and the precision of a single setting is given by

$$\mathcal{P} = 2N^{1/2}\sigma/v. \tag{3}$$

Now, N and v are not independent variables, for if we try to make v smaller by increasing the resolvance of the instrument (e.g., by using smaller slits), N will also decrease. To examine this relationship we note that

$$N = \left(\frac{P}{hc\sigma}\right)\left(\frac{\mathcal{L}}{2}\right)\tau, \tag{4}$$

where P is the radiance of the source for the line we are studying [$(P/hc\sigma)$ is thus the photon flux per unit area, solid angle, and time], $\mathfrak{L}$ is the luminosity of the instrument defined as the ratio of the transmitted flux to the radiance of the source, and the 2 under the $\mathfrak{L}$ accounts for the fact that we observe only one-half of the profile. Jacquinot[2] has shown that the luminosity of a spectrometer is related to the resolvance by the relation

$$\mathfrak{L}\mathfrak{R} = ZA, \tag{5}$$

where A is a characteristic area of the dispersing element (area of the base of a prism, projected area of a grating, area of Fabry-Perot plates) and Z is a constant (at least for the Fabry-Perot; for the prism and grating it is related to the angular height of the slits and the derivative of the angle of the exit beam with wavelength). Combining Eqs. (2)–(5) we have

$$\mathcal{P} = \left[\frac{2Z}{hc} A\tau P \frac{S}{v^2}\right]^{1/2}.$$

Thus far, we have assumed a perfect quantum detector. The modification for actual detectors is easily made by introducing the detective quantum efficiency of Jones,[4] defined as the square of the ratio of the signal to noise at the output of the detector to that at the input. For a photomultiplier, which is probably the most common detector used, the detective quantum efficiency θ is about two-thirds of the quantum efficiency of the photocathode, the reduction being caused by noise introduced in the multiplier. If the noise in the dark current is not negligible, θ may become much smaller. Our actual detector, therefore, uses effectively only a fraction θ of the incident photons, which is equivalent to having a source θ times as radiant. The modified equation for $\mathcal{P}$ is

$$\mathcal{P} = \left[\frac{2Z}{hc} A\tau\theta P \frac{S}{v^2}\right]^{1/2}.$$

Finally, we shall express v in terms of s and w, the half-width of the line profile, as $v = s \oplus w$, where the symbol $\oplus$ indicates that v is the half-width of the convolution of the instrumental and line profiles. The expression for the precision of a single pointing that we can apply to some of our instruments is

$$\mathcal{P} = \left[\frac{2Z}{hc} A\tau\theta P \frac{s}{(s \oplus w)^2}\right]^{1/2}. \tag{6}$$

III. Application of the Theory

A. Prism Spectrometers

For a prism instrument, s will be large compared to the w of lines used for high-precision measurements (e.g., Kr^{86} and Hg^{198} sources have $w \sim 10^{-6}\sigma$). Therefore, $s \oplus w$ will be essentially equal to s, and the precision will vary as $s^{-1/2}$. This relation will fail when the slit-widths become so narrow that diffraction losses increase catastrophically. Let us assume that we can get to within a factor of two of the theoretical resolving power without serious loss. To calculate Z and the minimum s, we assume also the following values for certain parameters of the instrument: the angular height of the slits as seen from the prism, 3×10^{-2} rd; $\lambda d\mu/d\lambda$, where μ is the refractive index of the prism material, 10^{-1}; we let the thickness of the prism at the base be T. Using the expressions in ref. 2, we have

$$\mathcal{P} = 3.9 \times 10^{10} [AT\tau\theta P]^{1/2}.$$

To arrive at a numerical value, we choose the primary standard Kr^{86} line for which $P = \frac{4}{3} \times 10^{-1}$ W m^{-2} sr^{-1}, a detector with $\theta = 5 \times 10^{-2}$ at this wavelength (a trialkali photocathode) and an observing time of 1 sec. These values will be used for all the instruments. For the prism spectrometer under consideration here, we assume a prism base 20-cm square and arrive at a value of

$$\mathcal{P} = 4.2 \times 10^{8}.$$

B. Grating Spectrometers

Grating spectrometer instruments are capable of achieving much higher resolvance than prism spectrometers, but a value of $\mathfrak{R} = 10^6$ is not readily obtained, and the arguments given above concerning $s \oplus w$ will apply here. Making the same assumptions about the minimum s and the angular height of the slits, assuming a 30° diffracting angle, and letting the grating width be W, we have

$$\mathcal{P} = 39 \times 10^{10} [AW\tau\theta P]^{1/2}.$$

For a 20-cm square grating and the same source and detector, the numerical value of $\mathcal{P}$ is

$$\mathcal{P} = 4.0 \times 10^{9}.$$

C. Fabry-Perot Interferometer

The restrictions on s encountered above do not apply to the Fabry-Perot, for we can make s as small as we like by increasing the thickness of the spacer. An examination of the ratio $s/(s \oplus w)^2$ shows that it has a maximum value $\simeq 1/(2w)$ when $s \simeq w$. For larger values of s, $\mathcal{P} \sim s^{-1/2}$, as with the first two instruments; for smaller values, $\mathcal{P} \sim s^{1/2}$. Using the value of $Z = 3.4$ from ref. 2, we have for the Fabry-Perot of high finesse,

$$\mathcal{P} = 410 \times 10^{10} \left[A\tau\theta \frac{P}{w}\right]. \tag{7}$$

Using the same source, detector, and observing time as above, with $w = 1.4$ m^{-1}, and assuming 4-cm diameter plates, the value of the precision becomes

$$\mathcal{P} = 1.5 \times 10^{10}.$$

Within the approximations of the theory outlined above, the precision attainable by a Fabry-Perot is

independent of finesse, providing we adjust the etalon length so that the instrumental width is approximately equal to the line-width. The theory overestimates the precision for very high finesse; first, because the reflection coatings become inefficient at very high reflectance, and, second, because of the effects of surface imperfections. It also overestimates at low finesse, because the overlapping of adjacent orders invalidates the assumption of negligible intensity at the outer edge of the exploring aperture. This loss of contrast results in a reduction in sensitivity and an increase in the noise because of higher average flux. A rather flat maximum of precision is found at a reflection coefficient of about 70–80% for dielectric films and at somewhat lower values for aluminum films. The optimum path difference for the primary standard is about 10 cm (i.e., 5-cm spacer).

D. Michelson Interferometer

Some changes in the arguments of Section II will be required to calculate the precision for the Michelson interferometer, because of the sinusoidal fringe shape obtained with this instrument. A convenient size for the exploring aperture is one-half of a fringe, in which case the luminosity to be used in Eq. (4) is readily shown to be

$$\mathfrak{L} = \frac{\pi A}{p\sigma},$$

where p is the path difference. In calculating the equivalent wavenumber fluctuations $\delta\sigma$, we must now take explicit account of the loss of contrast. The relative intensities at the edges of the aperture are $1 + V$ and $1 - V$, where V is the visibility of the fringes. The expression for δN becomes $4NpV\delta\sigma$ and for the precision the analog of Eq. (3) is

$$\mathcal{P} = 4N^{1/2}\sigma\, p\, V. \tag{8}$$

Substituting for N and introducing θ, we have

$$\mathcal{P} = \left[\frac{8\pi}{hc} A\tau\theta P p V^2\right]^{1/2}. \tag{9}$$

If we assume the line to have a Doppler-broadened profile of half-width w, the visibility is $V = \exp(-\pi^2 p^2 w^2/4 \ln 2)$, and the maximum value of pV^2 of $0.16/w$ occurs at $p = 0.27/w$ and $V = 0.78$. Substituting in Eq. (9), we obtain finally for the Michelson interferometer

$$\mathcal{P} = 450 \times 10^{10}\left[A\tau\theta\frac{P}{w}\right], \tag{10}$$

which is identical with Eq. (7) for the Fabry-Perot, within the approximations of our calculations. The optimum path difference for the primary standard is about 19 cm.

E. Spherical Fabry-Perot Interferometer

The spherical Fabry-Perot has the remarkable property that its luminosity increases with path difference for a given finesse. In comparison with the plane Fabry-Perot, it is evidently advantageous for use at large path differences. As with the Michelson interferometer, the luminosity gain will eventually be offset by loss of contrast in the fringes. An exact calculation of the precision to be expected with the spherical Fabry-Perot would be very difficult; for example, the instrumental profile due to the apertures is not rectangular as it is with all the other instruments considered above. However, we shall sketch an approximate theory which should have the correct functional form, although the numerical coefficient may not be very accurate. The effort seems justified, since the precision attainable by this instrument has not been discussed previously, and it does show some noteworthy distinctions from the other instruments.

We start with Eq. (9) of ref. 1, which gives the gain in luminosity of the spherical over the plane Fabry-Perot. We assume that the finesse due to the reflectance of the films and that due to the apertures are equal and together give an instrumental width of one-half of a fringe. Taking these values and the known luminosity of the plane Fabry-Perot, we arrive at a luminosity of the spherical interferometer under the conditions of our experiment of

$$\mathfrak{L} = \frac{\pi^2/p}{32\sqrt{2}\,\sigma},$$

where the path difference p is four times the etalon length. The precision in terms of the number of photons received will be given approximately by Eq. (8), since at large path difference and with low reflectance films the fringes become sinusoidal. Substituting for N, using the above luminosity, and introducing θ, we have

$$\mathcal{P} = \left[\frac{\pi^2}{4\sqrt{2}\,hc}\tau\theta P p^3 V^2\right]^{1/2}.$$

For a Doppler-broadened line of half-width w, the maximum of p^3V^2 is $0.022/w^3$ for $p = 0.46/w$, and the precision becomes

$$\mathcal{P} = 78 \times 10^{10}\left[\tau\theta\frac{P}{w^3}\right]^{1/2}.$$

The notable feature of this expression, in comparison with Eq. (7) and Eq. (10) for the other interferometers, is the replacement of the area A by $1/w^2$, where w is the line-width. We may express this distinction by noting that the precision attainable with a spherical Fabry-Perot is the same as that for a plane interferometer having reflecting surfaces of diameter equal to

$^1/_5$ of the coherence length $L = 1/w$ of the radiation being measured. For the primary standard, which has $w = 1.4\ \mathrm{m}^{-1}$ ($L = 70$ cm), this equivalent diameter is about 15 cm.

The optimum path difference for the spherical interferometer using the primary standard is about 32 cm (i.e., 8-cm spacer), and the diameter of the apertures at the reflectors is about 8 mm. The precision is

$$\mathcal{P} = 5.8 \times 10^{10}.$$

If sharper lines were available, the gain over conventional interferometers would be larger. Alternatively, sharper lines with a smaller radiance, such as those produced by an atomic-beam source, might be measured with the same precision.

IV. Review of Earlier Work

Terrien[5] was the first to explore for his Michelson interferometer the limit to precision caused by noise. He considered a photoelectric method of pointing on the fringes essentially the same as that used here and established the dependence of the precision on the exit aperture size and on the path difference in terms of the line-width (i.e., optimum visibility equal to 0.78). He also examined the effect of intensity fluctuations of the source, which we have ignored, and showed that when this was the dominant noise source the optimum visibility was 0.61. Both the Fabry-Perot and Michelson interferometers were considered by Hanes,[6] again using essentially the same pointing procedure, but with aperture size and spacing somewhat closer to the optimum. A derivation was given of the dependence of the precision on the path difference in terms of the line-width, the finesse and efficiency of the Fabry-Perot reflectors, the area of the plates, the detective quantum efficiency of the detector, and the radiance of the source divided by its half-width. The expression for the precision was essentially the same as Eq. (7) and Eq. (10); the numerical coefficients were within 20% of those obtained here, which confirms that the choice of convenient aperture sizes made here did not unduly compromise the accuracy of the calculation. Hanes also discussed a number of practical problems involved in the attainment of the theoretical precision.

Smith[7] began his discussion of the Fabry-Perot by noting that the optimum reflectance was relatively low, so that the fringe profile could be considered to be sinusoidal with a fair degree of accuracy. He then investigated different methods of pointing: (1) by switching the aperture between the two viewing positions on the profile and (2) by oscillating sinusoidally over the peak. His expressions for the smallest detectable fringe fraction showed the dependence on the aperture sizes and the separation of the aperture positions (or the scan amplitude) and were given in terms of currents observed with the photomultiplier rather than source radiance, plate area, and quantum efficiency. The scanning method, which is preferable in practice, was shown to give a precision about 40% less than the switching method. Smith's experimental precision was within a factor of five of that predicted from theory. Very recently, Hill and Bruce[8] gave an analysis of the precision attainable with Fabry-Perot and Michelson interferometers, using the oscillating method of pointing, and presented experimental results. In the theory, they considered the detailed shape of the profile and used a computer to find the effect of various interferometer films, path differences, scanning apertures, and amplitudes. There are two basic points in their theoretical treatment with which the present author disagrees: they obtain a value of the order of 50% for the excess photon noise, whereas the author's estimate would be about 0.1%; a comparison of their expression for the transmission of a Fabry-Perot interferometer with that given in ref. 6 shows that theirs is greater by a factor $(1 + R)/(1 - R)$. These points are under discussion at the time of writing.*

Table I. Relative Precision Capabilities of Various Spectrometers[a]

Dispersing element	$\mathcal{P}/10^{10}[\tau\theta P]^{1/2}$
Prism	$3.9\ [AT]^{1/2}$
Grating	$39\ [AW]^{1/2}$
Fabry-Perot	$410\ [AL]^{1/2}$
Michelson	$450\ [AL]^{1/2}$
Spherical Fabry-Perot	$78\ [L^3]^{1/2}$

[a] A is the area of the dispersing element, T is the prism base thickness, W is the grating width, and L is the coherence length, (half-width)$^{-1}$, of the radiation being studied. All units MKS.

V. Summary and Discussion

A survey has been given of the theoretical precision capabilities of various spectroscopic instruments. We have attempted to treat them on a uniform basis so that their performances may be intercompared. Numerical examples have been given for the precision that should be attainable for the primary standard line of Kr^{86} with instruments of reasonable dimensions.

Prism and grating spectrometers are outclassed by interferometers because of relatively lower luminosity and limited resolvance. The spherical Fabry-Perot is in a special class because its transverse dimensions are controlled by the characteristics of the line being studied rather than by practical limitations. We can make an interesting comparison of the various instruments by tabulating $\mathcal{P}/10^{10}[\tau\theta P]^{1/2}$, as in Table I. This ratio depends only on the parameters of the spectrometers; the appearance of the coherence length of the radiation expresses the fact that certain dimensions

* Hill and Bruce have since informed the author that they are publishing a correction note concerning this paper.

in the interferometers can be chosen to be optimum for theoretical reasons rather than being limited by practical consideration. When we note that L, for spectral lines used as wavelength standards, is of the order of 50 cm, the superiority of the interferometers is quite apparent.

For all the instruments, the precision can be made arbitrarily large in principle by increasing the observing time. In practice, a large gain cannot be realized by this method because of time variations of critical dimensions of the apparatus, particularly with temperature. A precision of 10^{10} already requires a temperature stability approaching 10^{-4} °C during the observing time. Closer temperature control for long times becomes very difficult.

Concerning desirable source characteristics, the instruments fall into three classes: prism and grating spectrometers, because they are unable to resolve the line-width of sources that have the requisite wavelength stability to be used as standards, require only that the source radiance be as high as possible. For conventional Fabry-Perot and Michelson interferometers, the parameter of the source to be maximized is the radiance divided by the line-width, i.e., a high peak radiance or high equivalent blackbody temperature. For the spherical Fabry-Perot, the radiance divided by the cube of the line-width is to be made large for best results.

References

1. P. Connes, J. Phys. Radium **19,** 262 (1958).
2. P. Jacquinot, J. Opt. Soc. Am. **44,** 761 (1954).
3. R. Hanbury Brown and R. Q. Twiss, Proc. Roy. Soc. (London) **243,** 291 (1957–58).
4. R. C. Jones, Phot. Sci. Eng. **2,** 57 (1958).
5. J. Terrien, J. Phys. Radium **19,** 390 (1958).
6. G. R. Hanes, Can. J. Phys. **37,** 1283 (1959).
7. D. S. Smith, Can. J. Phys. **38,** 983 (1960).
8. R. M. Hill and C. F. Bruce, Australian J. Phys. **15,** 194 (1962).

Applied Optics BOOKS

Books for review should be submitted to the Managing Editor, APPLIED OPTICS, 1155 16th St., N.W., Washington 6, D.C.

Studies in Optics. By A. A. MICHELSON. Phoenix Science Series, The University of Chicago Press, Chicago, Illinois. Published in 1927, First Phoenix Edition, 1962. $1.75.

Rarely does a reviewer have the pleasure of reviewing a book which he has cherished as a rare gem for many years before. Indeed it was in 1927 that A. A. Michelson completed his book *Studies in Optics* which has now been reprinted as a paperback by the University of Chicago Press, the original publisher. In this time of ours when the vast amount of new literature makes it increasingly difficult to explore important scientific achievements of only yesterday in their author's original description, and results in much misunderstanding and even some inaccurate legends, it is refreshing to have available from Michelson himself this admirably concise yet complete résumé of his monumental scientific achievements, covering some 53 years of a career which came to an end at the age of 79 only four years after the publication of this work.

If the titles of the fifteen chapters in this work sound as if they were taken out of last year's issue of the *Journal of the Optical Society of America* or of *Applied Optics*, then we may undoubtedly find there some insight into the remarkable fruitfulness of Michelson's investigations which, it is well known, also brought him the Nobel Prize in Physics in 1907, as the first American of many to be so honored. In his preface, preceding the table of contents, Michelson describes, in admirable modesty, the general character of his work:

> The following pages are intended to give a résumé of my own investigations, somewhat after the manner of the treatment given *Light Waves and Their Uses* [*reviewer's note:* also recently republished in the Phoenix Science Series], from which booklet many of the illustrations are taken, but with more attention to the theoretical side, and covering a number of investigations in which I have been occupied since the appearance of that publication. While much of the work is of a nature which involves a general acquaintance with the method of calculus, it is hoped that a fair idea of the experimental method and results may be presented to those who may be interested in the subject, but who lack the necessary mathematical equipment.
>
> In order to give the subject a semblance of continuity, it will be desirable to introduce considerable matter which will be found in any of the standard works on optics—but even here it may be of interest to present these investigations from my own point of view and to convey my own impressions in such a way as to emphasize the ideas of the founders of the science which have made the deepest impression on my own mind.
>
> In the chapter on "Diffraction" I have selected freely from the scientific papers of Lord Rayleigh.

The fifteen chapters of Michelson's book could each be the subject of a full review in their own right: theory and application of interference of light waves; interference of light waves; the interferometer; light-wave analysis; measurement of standard meter in light waves; diffraction; testing of optical surfaces; diffraction gratings; the ruling of diffraction gratings; the echelon grating; application of interference to astronomical investigation; velocity of light; effects of motion of the medium on velocity of light; relativity; metallic colors in birds and insects. Clearly most of these areas still form the subject of contemporary work in one form or another. It is one of the great lessons in science which may be read in this book of Michelson's that, had it not been for the great technological advances since his time, many of the dramatic improvements in modern grating ruling, interferometric spectroscopy, velocity of light measurements, and relativity experiments might have already been attained by him at his time. Even so, the remarkable precisions obtained by Michelson in his diffraction gratings, velocity of light, and double-star measurements, as well as in his interferometric spectral analysis are truly legendary indeed. They are all reported in this book, as is the famous Michelson–Morley ether-drift experiment, and several other experiments in relativity. Of course, there has also been much theoretical progress in several

continued on page 479

Interference Comparators for Line Standards

K. M. Baird

This paper reviews progress in the techniques of calibration of scales and line standards by interferometry, techniques that have been under very active development since the redefinition of the meter in terms of an optical wavelength. After a study of some general considerations, specific examples of interference comparators are described, and, finally, the effect of the development of these techniques on the usefulness of scales as secondary standards is discussed.

From 1889, the date of the first General Conference of Weights and Measures, until 1960, the primary standard for the metric unit of length was a line standard, that is, a standard whose length was given by the distance between two lines that were engraved near its ends. Naturally enough, other line standards and length scales, being of the same nature, were calibrated by direct comparison with it or with other line standards which had been. Subdivisions were determined by a rather lengthy procedure which also involved the comparison of two intervals, defined by lines, with one another. The techniques involved the use of the Abbe and the transverse forms of comparator which are well known.

From time to time, line standards were compared with wavelengths, notably in the seven classical determinations of the relation between the international meter and the wavelength of the Cd red line.[1] However, these were elaborate and difficult experiments, and the techniques did not lend themselves readily to routine or even semiroutine measurements. There has been no long development of interference comparators for the calibration of line standards by direct comparison with wavelengths.

The situation is in marked contrast to that of end standards, which indicate a length by the distance between optically flat, parallel ends. These, by their very nature, lend themselves readily to techniques of interferometry and, indeed, it is in great part due to the convenience of precise calibration by interferometry that this type of standard has come into such wide use. Interferometers for the calibration of gauge blocks have been in use for 60 years, and the technique has reached a high degree of development.[2]

The author is with the Division of Applied Physics, National Research Council, Ottawa, Canada.

Received 18 December 1962.

With the adoption in 1960 of an optical wavelength for the definition of the international meter, there immediately was created a strong reason for the development of interference comparators for the measurement of line standards directly in terms of wavelengths. As a result, many of the national standards laboratories already have such comparators either completed or in an advanced state of construction. The following sections will treat some of the problems and limitations associated with the new techniques; examples of the designs of comparators will be briefly described; and, finally, it will be shown that an interesting consequence of the new definition of the meter based on an optical wavelength has enhanced usefulness of line standards, rather than the contrary, as might have been expected.

General Considerations

In order to fulfill the requirements of legal, industrial, and scientific metrology, calibrations of line standards may be required to have an accuracy of as great as 1 part in 10^7, i.e., 0.1 μ in 1 m, or, in special cases, even better. This is very near the practical limit to which material lengths and wavelengths can be compared and therefore the demands on interference comparators will be very great.

The reproduction of the primary standard does not impose an important limitation. It has been demonstrated that the 0.606-μ line of Kr-86 can be reproduced to an accuracy approaching 1 part in 10^9, if certain fairly difficult precautions are taken; it is quite readily reproduced to an accuracy of 1 part in 10^8 by the use of a lamp specified by the International Committee of Weights and Measures.[3] Neither is there a serious limitation imposed by the pointing on the interference fringes; this is quite readily done either visually or photoelectrically, to about 1 part in 10^8, in distances greater than one decimeter, or 0.002 μ in shorter distances.

The difficulty in approaching or exceeding 1 part in 10^7 accuracy in practical comparison is connected, first with the nature of the material standard; second, with the problem of having an adequate knowledge of the parameters that define the environment and affect the length of the standard; and, third, it is connected with the technique of comparison, that is, with assuring that the separation or displacement of optical surfaces, indicated by the primary standard, truly corresponds with the separation of the lines that define the interval to be calibrated.

It is possible to control individual sources of errors, such as those due to temperature effects, random errors of pointing, etc., so that they are individually of the order of 1 part in 10^8. However, there are certain practical limitations that make it unlikely that any material secondary standards, such as are known today, can be calibrated to such accuracy in the final result. This is certainly the case if the calibration is to be made on a semiroutine basis and if the standard is to have ascribed to it a length that does not involve too stringent requirements as to the method of observation. It is clear that, where very great precision is concerned, the length of an interval defined by the separation of two lines can depend on the method of pointing; though any given method may be used with precise significance to define a length, the method of pointing may have to be included in the specification of the length. There can be cases for which the lines are effectively of perfect form and the surround symmetrical; then different methods of pointing will likely give the same result. Such is the case where, with modern rulings, the sought-for precision is 0.1 μ. But there will also be cases for which the results will be different, and the differences will be more important and occur more frequently in proportion to the degree of precision sought. Such arguments are, of course, not peculiar to line standards. The significant length of a given end standard also depends on how it is used—whether it is the optical length that is involved or the amount by which it will hold apart the anvils of a comparator or other gauge blocks wrung to it, and so on.

The determination and control of temperature is one of the most difficult of the problems associated with the conditions of environment, but it is one which has been very much studied. One can follow well-established practice regarding the provision of adequate shields against radiation as well as conduction and the use of massive parts in order to be able to determine the value of the temperature to about 0.001°C; this corresponds to a length uncertainty of about 10^{-8} for most materials from which standards are made. It is worth pointing out that it is very advantageous to circulate the air within the interferometer enclosure. This would ordinarily produce an undesirable steady rise in the temperature inside a heavily insulated chamber, due to the accumulation of heat arising from the energy imparted to the air. The difficulty is easily avoided, however, by the use of a small air turbine to supply power to the blower, which stirs the air; if the exhaust of the turbine is conducted through a copper coil within the chamber, refrigeration is provided, which compensates the heating due to the stirring.

The control and knowledge of refractive index is a second important requirement regarding the environment, in this case concerning the reproduction of the wavelength standard. In measurements of gauges longer than one decimeter, it is done best by reference to an interference path in vacuum during the course of the measurement, following the practice of Kösters.[4] In effect, the method yields results in terms of vacuum wavelengths, but at the same time has the advantage of having an atmosphere in the interferometer.

From the point of view of refractive index of air also, it is advisable to stir the air in the interferometer enclosure for very accurate interferometric calibration of standards. Otherwise, there can occur striae of differing refractive index, due either to convection currents or vapors, which cause apparent differences in the optical path amounting to 2 to 3 parts in 10^8 from one part of the interferometer to another close by.

Although it is almost essential to measure or control the refractive index for the most precise measurements, it has been the author's experience that errors are unlikely to be greater than 5×10^{-8} in the refractive index given by the Edlén formula[5], with corrections only for temperature, pressure, and humidity; precautions must be taken against the presence of unusual vapors, but, otherwise, no special control of the composition of the air is required for this accuracy.

A practical point in connection with refractive index concerns the question of whether the interferometer enclosure ought to be pressure tight. There is certainly much to be said for this method for the elimination of the effect of atmospheric pressure changes. On the other hand, in the use of the microscope which is required for pointing on the lines, and in cases where the measurement involves the displacement of the standard, there is considerable advantage of convenience in not having to seal the enclosure, even though small variations of barometric pressure may affect the observations on the interference fringes. The latter can be taken into account by the use of a recording microbarometer, sensitive to about 0.01 torr, on which is recorded the time of making each interferometric observation. Such a record will show at a glance whether corrections ought to be made, and how great they ought to be, for any change in pressure during the time of measurement.

The technique for the measurement of line standards by interferometry differs significantly from usual interferometer techniques in that the scale or the microscope usually must be displaced accurately along some speci-

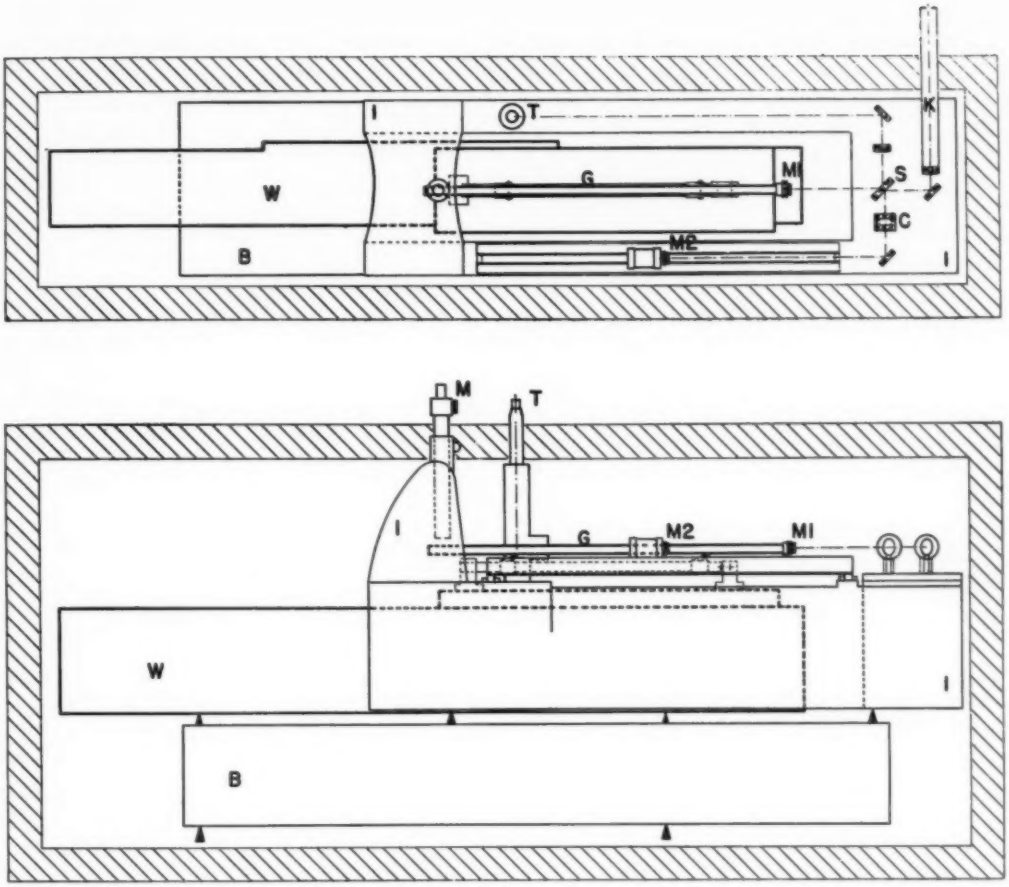

Fig. 1. NRC interference comparator. The scale G is mounted under a micrometer microscope M and has attached to it a mirror M_1, which forms part of an interferometer system whose other parts are seen at K, S, C, M_2, and T. A large base B supports the interferometer-microscope system I-I and accurate ways W along which traverses a table that carries the scale.

fied direction by as much as one meter, and, during this displacement, there must be no change in the relative positions of the microscope and the interferometer components. This requirement demands extra attention to the kinematic design and the provision of an extremely rigid and stable structure which is best if simple and symmetrical. In the comparators that are described in the next section, the errors due to bending of the structure are designed to be less than 0.01 μ.

In order to reduce errors due to obliquity effects to less than 10^{-8} times the length measured, the following directions must be parallel to better than 10^{-4} rad: the direction of the vector which defines the interval (usually indicated on precise scales by a longitudinal pair of lines); the direction of translation to which the change in relative positions of the scale and the microscopes correspond; and the central direction of the collimated interferometer beam. An additional effect due to obliquity is due to the fact that the collimated interferometer beam consists of a finite cone of light whose mean direction is oblique with respect to the central direction. However, this effect can be accurately taken into account.[6] Care must also be taken to ensure the uniform distribution of light with respect both to the angular distribution of this cone and the flooding of the interferometer plates.

For precise comparison of physical lengths with wavelengths, care must be taken to avoid certain effects due to parasitic fringes arising from scattered coherent light, due to polarization, or the like. These effects have been treated by Terrien.[7]

Generally speaking, direct observation with the interferometer yields only the amount by which the length to be measured exceeds some unknown whole number of orders of interference or fringes; this amount, expressed as a fraction of a whole order is usually referred to as the excess fraction. The total number of orders can be obtained in three ways:

One way is to determine the length to within one order by means of some technique of comparison with

another secondary material standard. This method has practical advantages where a large number of standards of similar lengths are calibrated and is the method most used up to the present at the U.S. Bureau of Standards and the German Physikalisch-Technische Bundesanstalt.

A second method is to determine the excess fractions for a number of wavelengths, from which the total order can be inferred by the "method of exact fractions".[8] This method is advantageous where unusual lengths often have to be measured. If the technique of measurement yields accurate values of the excess fractions, and if several accurately known wavelengths are available, such as the new values given by the CCDM for the Kr-86 lamp,[9] the method of exact fractions can be made very convenient by the use of a special slide rule or suitably prepared tables. This method is in use at the National Physical Laboratory of Great Britain and other laboratories and is generally preferred by the author. Unknown intervals up to 50 cm can be conveniently measured solely by the use of a micrometer device and by observations with three different wavelengths.

A third method to obtain the total order is to use the technique of photoelectric counting of all the fringes passed as the optical surface is moved from one end of the interval to the other.[10] This method has been developed recently at several laboratories and in principle has obvious advantages in routine or automatic measurements of large numbers of intervals in succession, such as in the calibration of all the millimeter divisions of a meter scale. There have been certain practical difficulties in the technique, so that, for the very precise measurement of relatively few single intervals, such as in the calibration of meter standards or of other special intervals for certain specific experiments, the method of exact fractions usually has been found preferable. Even for the routine application mentioned above, conventional sources did not yield spectacular success because of problems of a low signal-to-noise ratio at path differences greater than about 10 cm. However, the advent of laser sources changes that picture completely, and the use of its powerful, sharp, and relatively long wavelength radiations appears very promising for use in automatic techniques involving fringe counting.

The radiations emitted by lasers will make possible the measurement by direct interferometry of lengths much greater than the order of 1 m, which has been the limit with discharge lamps. It should be remarked however that methods of optical multiplication, such as that due to Professor Väisälä or that making use of Brewster's fringes, are also practical for distances of the order of at least 100 m.[11,12]

Some Specific Examples of Comparators

Having briefly considered the general aspects of interference comparators for line standards, examples of specific designs will be described; some of them are shown in Figs. 1–4. The instruments are nearly all newly constructed or in the final stages of construction at national laboratories. Some have already been used for the measurement of meter bars.

1. Figure 1 shows the design of the interference comparator developed at the National Research Council of Canada.[13] This instrument is a simple, straightforward design, specifically for the calibration of line standards. The microscope M for sighting on the lines of the scale G is mounted in a heavy yoke rigidly attached to a Michelson interferometer; the combined structure is kinematically mounted on a heavy casting, which also supports accurate ways, on which moves a table carrying the line standard or scale in such a way that the latter can be moved under the microscope. The scale has attached to its end a very light mirror M_1, which constitutes one of the back mirrors of the interferometer system. When the scale is displaced so that successive lines are nearly on the axis of the microscope, observations by means of the micrometer microscope and the interferometer give directly the scale intervals in terms of wavelengths. These can be referred to vacuum wavelengths by means of a vacuum-control interferometer path (not shown in Fig. 1). Settings or pointings on the lines of the scale are made by means of a photoelectric microscope, which reads the offset to an accuracy of a few thousandths of a micron. Settings on the interference fringes are made visually to about the same accuracy by means of a half-shade technique in conjunction with a system whereby the fringes can be displaced small amounts by a change in the pressure in an air cell C in one of the interferometer arms. A maximum length of only somewhat greater than 50 cm can be measured in one step because of the limit imposed by the coherence length of Kr-86 radiations; in order to calibrate an interval of one meter, it is necessary to have a line near the center of the bar and measure the two intervals separately. This instrument was used in 1960 for the measurement of four copies of the meter in order to give assurance that the new definition of the meter did not cause a significant discontinuity in the length of the unit.

The interferometer is in a heavily insulated chamber, which, however, is not sealed against the atmosphere. The order of interference is determined by the method of exact fractions in conjunction with the use of a micrometer drum on the lead screw that moves the scale.

2. The interference comparator built at the Australian National Standards Laboratory is shown schematically in Fig. 2.[14] In this design, also, the scale has a mirror attached to its end and is transported under

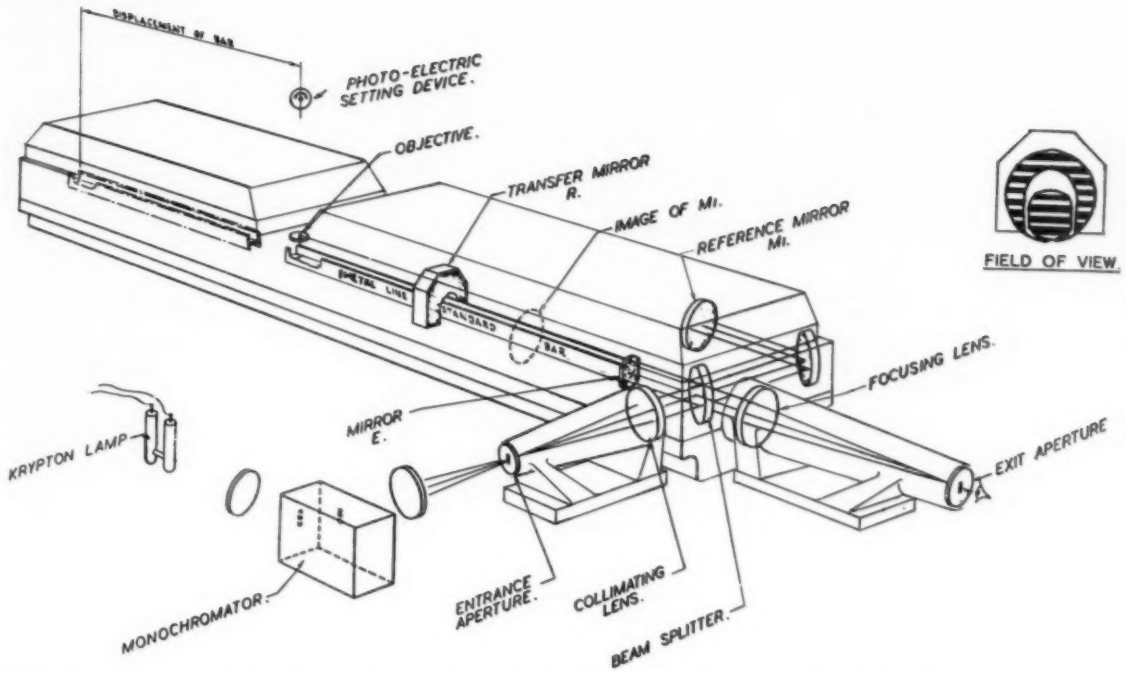

Fig. 2. NSL interference comparator. Displacements of the meter line standard under the photoelectric setting device are measured by observation of the change in order of interference due to the corresponding displacements of the small attached interferometer mirror. The transfer mirror R makes possible measurements of 1m without an intermediate setting of the meter bar, even though the maximum path difference used is only 50 cm.

the microscope; observations of the order of interference and pointings on the lines at each end of the displacement yield a direct calibration of the interval in terms of wavelengths. The total order of interference is determined by the method of exact fractions.

An interesting feature of the interferometer is the transfer mirror R, which eliminates the need for a central line in the measurement of a one meter interval. At the first position, the reference mirror M is as shown in the figure; in the second position the meter bar is transported one meter, and the reference mirror is transported about 50 cm, so that fringes can be observed in each position with a path difference of only 50 cm. Observation of the displacements of the fringes on mirror E with respect to those on R at the two positions indicates the distances of the plane of E from the plane of R at the two positions; the sum gives the total displacement of the scale. At present the excess fractions are read by measuring the displacements of the line indicated by the photoelectric microscope when the two sets of fringes in the field of view are made to coincide, separately for each color, by adjustment of the position of the bar.

The apparatus is enclosed in a metal chamber that can be sealed against the atmosphere and whose temperature is regulated by a circulating thermostatted liquid.

3. The well-engineered interference comparator built at the National Research Laboratory of Metrology in Japan is illustrated schematically in Fig. 3.[15] The interferometer consists of a Kösters double prism, seen at F in the Fig. 3, and two cube-corner reflectors at H and G. There are two especially interesting features of this instrument: first is that the order of interference corresponding to displacements of the interferometer reflector is measured by photoelectric counting. The second is the use of Eppenstein's principle for relating the mirror displacement to the scale intervals, as follows: A part O of the microscope optical system, a mirror U, and one of the cube corners G, are rigidly attached to the movable carriage R; the scale (near the position indicated by R in the figure) is at the focal plane of O, and the distance of the vertex of the cube corner from the plane of the scale is made equal to the focal length of the lens O. As a consequence, any tilt of the carriage R causes an offset in the scale position, relative to the axis of the photoelectric microscope system, which is very nearly equal to the resultant movement of the vertex of the cube corner. Thus, errors due to inaccurate ways are, in the first order, eliminated. The advantage of this system over the Abbe system is that the comparator can be much shorter. This instrument is stated to be accurate to $\pm 0.05\ \mu$ in measurements of lengths of one meter.

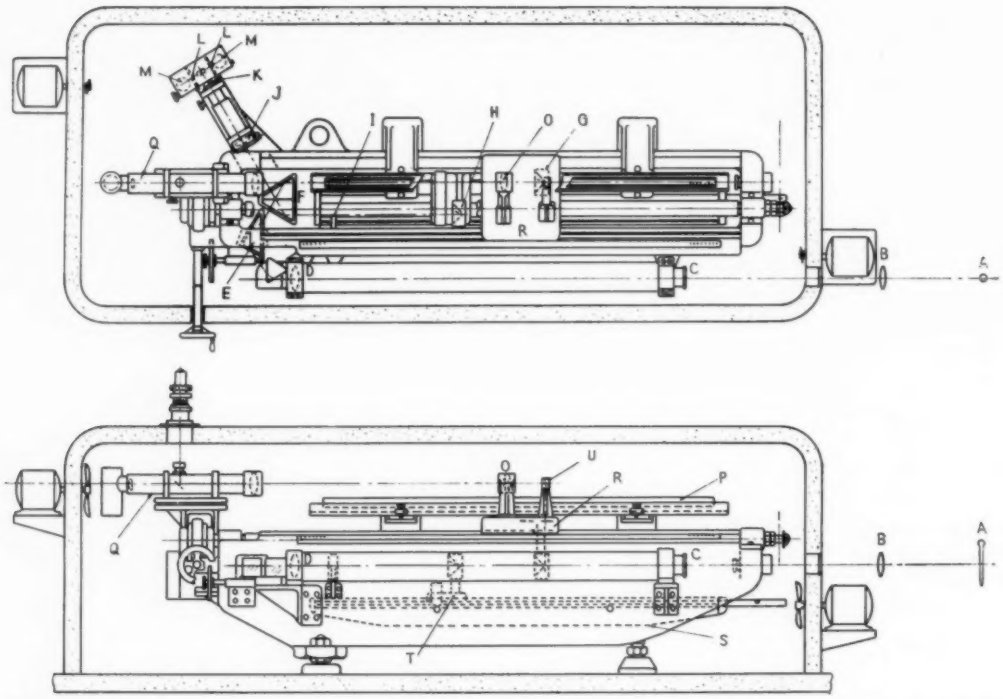

Fig. 3. CIIWM interference comparator. Collimated monochromatic light falls on the Kösters beam splitter F; one beam goes to the reference cube corner reflector T, the other to a cube corner reflector attached to a movable carriage R, which also carries parts O and U of the photoelectric system for pointing on the lines of the scale P. Fringes are counted reversibly by means of the photocells at M.

A second type of interference comparator has just been constructed at the Government Mechanical Laboratory in Japan for the rapid calibration of scales.[16] It employs "fringe counting" technique with a Twyman interferometer in conjunction with six photoelectric microscopes that read simultaneously on different portions of the scale while the latter is moved. All the lines at millimeter intervals in a 1-m bar will be calibrated in 40 min to an accuracy of $\pm 0.1\ \mu$.

4. At the Central Institute of Metrology in Leningrad, a rather complicated universal-interference comparator is used for the comparison of line standards and end standards with one another, or directly with wavelengths, or with multiples of the length of a Fabry-Perot etalon.[17] It is illustrated in Fig. 4. Intervals on the line standard are measured by observing the displacement of the microscope 19 as it is moved from one line to the next by the movable support 10; the displacement in terms of wavelengths is given through the interferometer mirror 9. Small displacements of the carriage can be measured either by the interferential indicator B or by an autocollimation device C. This instrument does not appear as suitable for the calibration of long-line standards directly in terms of wavelengths as do instruments designed specifically for this purpose.

5. An interference comparator for line standards was built at the German Physikalisch-Technische Bundesanstalt (PTB) in 1956 by modification of a large displacement comparator.[18,19] In this instrument, a microscope and an interferometer mirror are mounted on a carriage, which is transported along the length of a line standard in a line that is controlled by an autocollimation technique so that it is straight to ± 0.5 sec arc. A two-beam interferometer that utilizes a Kösters double prism gives the displacement of the carriage in terms of wavelengths. For the measurements of long intervals, up to 1 m, the usual single mirror in the reference arm of the interferometer is replaced by a 50-cm end standard having a flat wrung to its rear surface. Readings of the order of interference are taken at the positions corresponding to 0, 50, and 100 cm. The first and last readings are taken to determine the position of the carriage mirror with respect to the image of the front and back of the end standard, respectively; the reading at 50 cm gives the distance between the surfaces of the end standard. The sum of the three observed orders of interference gives the total displacement of the carriage and, hence, of the microscope that is used to point on the lines of the meter bar. Thus, no line is required at an intermediate position on the bar, even though a maximum path difference of

only 50 cm is used in order to measure a 1-m interval. The instrument is equipped with a photoelectric microscope. Readings of the excess fractions of the order of interference are measured by means of the microscope in the same manner as that described for the Australian comparator.

An improved instrument, specifically designed for the interferometric calibration of line standards, is now being built for the PTB by the Johannes Haidenhain Co. The improvements for the most part have to do with the provisions for mechanical and thermal stability.

6. A comparator design of considerable importance is that developed by cooperation of the International Bureau of Weights and Measures (BIPM) and the Société Génevoise d'Instruments de Physique (SIP).[20,21] The mechanical parts of the comparator and the photoelectric microscopes have been designed and constructed by SIP, the interferometer by BIPM. Several of these comparators are being constructed, one for BIPM, others for SIP itself and for several government laboratories, including that of Switzerland.

The comparator, which is massive, consists of a longitudinal comparator (Abbe type) with provision for moving a scale or meter under the microscopes in such a way that its displacements may be measured in terms of wavelengths, by means of a Michelson interferometer; the beam splitter of the latter is mounted at the Brewster angle in order to eliminate unwanted light. The comparator is mounted in a hermetically sealed, insulating chamber about 4 m long by about 2 m diam. Adjustments and photoelectric observations are made from a remote position. The comparator can be used to intercompare line standards directly with one another as well as to calibrate them in terms of wavelengths, and it will therefore be useful in the testing of techniques for the calibration of line standards by interferometry. These instruments are in final stages of construction.

A technique closely associated with interferometric calibration of scales is that whereby interferometry is used to control the ruling of scales. It is not intended to discuss this subject in any detail here, but it is worth noting that such techniques are now under active development and are likely to come into wide use, paralleling the development of interferometric calibration.

Interferometric control of the ruling of scales is not new; as early as 1947, C. G. Peters of the National Bureau of Standards had ruled a meter bar, using the Cd red line as a control. The technique was not attractive at that time from a practical point of view, but has since been given a new stimulus by the development of single isotope sources and the development of photoelectric fringe counting. An early result of this stimulus was the notable work of Harrison and Stroke on interferometrically controlled ruling of diffraction gratings.

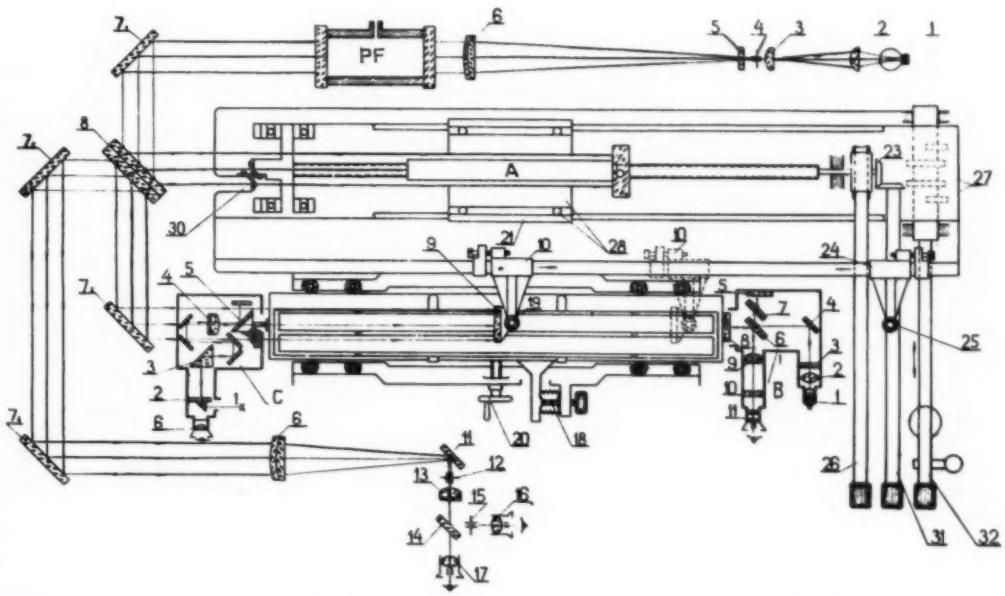

Fig. 4. IMM interference comparator. The line standard is mounted on a movable carriage 20, small displacements of which are observed by means of an autocollimation indicator C or a small interferometer B; another movable carriage 10 carries a microscope 19, having fixed to it one mirror 9 of an interferometer whose beam splitter is at 8. Scale intervals can be calibrated by measuring displacements of the pointing microscope 19, either directly in terms of wavelengths, by comparison with the length of an end gauge at A, or by comparison with a Fabry-Perot etalon PF; end gauges can also be calibrated in terms of wavelengths.

At the present time, interferometric machines for the automatic routine ruling of precise scales are under construction at Bausch & Lomb Inc. in the United States and at the National Research Laboratory of Metrology in Japan. An interesting system is being used at the latter laboratory, whereby the atmosphere in the chamber that contains the interferometer is automatically controlled to make a whole number of fringes of the Kr-86 0.565 μ line equal 1 mm, exact to 1 part in 10^8; thus, an integral number of fringes is counted between rulings, thereby simplifying the programming procedure.

Discussion

It has been seen that the technique of measurement of line standards and scales on a routine basis by interferometry is very new. The comparators described above are still under construction or have been completed very recently. Consequently, it is still too early to have sufficient evidence to make specific judgments about accuracy.

It was noted at the beginning of this article that the individual sources of error that can now be taken into account can likely be controlled to the order of 1 part in 10^8, but that the limitations of the material secondary standards themselves may prevent such accuracy in the final result. It must also be expected that future experience may turn up additional sources of error or that known sources of errors will be less well controlled than we expect. A knowledge of the accuracy in practice will only be acquired by experience and best by an exchange and comparison of line standards among various laboratories equipped to measure them. Such a program is planned by the International Advisory Committee for the Definition of the Meter and will be undertaken under the auspices of the International Bureau of Weights and Measures when the various national laboratories have time to develop their techniques of interferometric calibration.

A conclusion that can be drawn even after the limited experience that has been acquired so far is that the precise measurement of line standards directly in terms of optical wavelengths by interferometry is extremely practical and convenient; in fact, a given number of intervals can be calibrated more easily and in shorter time than the same number of end standards. Furthermore, the naturally subdivided scale provided by interference fringes makes it easy to measure any length, whether it be an even decimeter, a millimeter or not, unlike the case formerly when the subdivision of a meter interval defined by lines required a long and laborious procedure.

Now that both line standards and end standards will be calibrated by interferometry, it is of interest to note briefly some of the relative merits of these two types. From the point of view of convenience, line standards have some obvious advantages in the ease of interpolation between lines, in their application to the automatic control of the movement of machine tool parts, and the like; and they no longer suffer the disadvantage compared to end gauges as regards calibration. On the other hand, end gauges have obvious advantages where the distance to be measured is also determined by opposed surfaces, such as in the measurement of diameters, the calibration of micrometer calipers, etc.

From the point of view of ultimate accuracy, there are two important considerations in comparing the two types of standards. First, an end standard has an advantage in that the length can be determined by simultaneous observation of the two ends so that the observed separation of the optical surfaces is effected by the environment only to the same extent as the length of the standard itself. On the other hand, we have seen that line standards are best measured by techniques that involve a mechanical displacement between the observations at the two ends of the interval; changes due to the environment can occur between the observations in either the interferometer structure or the standard and will give rise to errors which are generally greater than in the case of end standards; the importance of this source of error will be known only after considerable experience.

The second consideration concerns differences between the calibrated length and the length that is effective when the standard is used in secondary measurement. In this case, the advantage is with the line standard because, first, for calibration and for use the lines are observed in similar fashion and, second, the length of an interval is defined by what corresponds to a pure translation so that end effects tend to be eliminated. On the other hand, an end standard defines a length by flat end surfaces that are opposed, so that different manifestations of the surface (optical, mechanical, etc.) result in lengths that differ in the first order with end effects. Such effects arise from wedged wringing films, lack of flatness of the surfaces, surface roughness, optical phase change of the bulk material, and the nature and magnitude of the pressure on the end surface in mechanical application. The effects can be very complex; for example, the last named must include, in addition to externally applied loads, the cohesive force of wringing contact and the forces due to surface-free energy similar to those that tend to close microcracks in bulk materials.

Whichever type of secondary standard turns out to be capable of the highest ultimate precision, it does seem clear that the development of interferometric techniques for the calibration of line standards will very much enhance their usefulness compared to what it has been in the past.

References *overleaf*

References

1. Cf. K. H. Hart and K. M. Baird, Can. J. Phys. **39,** 782 (1961).
2. Cf. *Metrology of Gage Blocks,* NBS Circular 581 (Government Printing Office, Washington, D.C., 1957).
3. Procès Verbaux du CIPM **28,** 71 (1961).
4. Cf. ref. 2, p. 6.
5. Cf. B. Edlén, J. Opt. Soc. Am. **43,** 339 (1953).
6. C. F. Bruce, Opt. Acta **4,** 127 (1957).
7. J. Terrien, Procès Verbaux du CIPM **26b,** M162–M67 (1958).
8. Cf. C. Candler, *Modern Interferometers* (Hilger & Watts, London, 1951), p. 202.
9. Procès Verbaux du CIPM (Oct. 1962).
10. E. R. Peck and S. W. Obetz, J. Opt. Soc. Am. **43,** 505 (1953).
11. Y. Väisälä, Procès Verbaux du CIPM **25,** M60 (1954).
12. Cf. ref. 8, pp. 64, 225.
13. K. M. Baird, Rev. Sci. Instr. **32,** 549 (1961).
14. C. F. Bruce, P. E. Ciddor, and H. J. Ritter, submitted to the Adv. Comm. Defn. Meter, cf. ref. 9.
15. Y. Sakurai, S. Takahashi, and K. Ota, Nat. Res. Lab. Metrology (Sept. 1962).
16. Y. Doi, K. Shimizu, T. Teiichi, and T. Kono, J. Mech. Lab., Japan **16,** 121 (1962).
17. M. L. Brjezinski and N. Trofirnova, Procès Verbaux du CIPM **26B,** M95 (1958).
18. C. Hoffrogge, Microtecnic **6,** 244 (1956).
19. C. Hoffrogge, *Amtsblatt der PTB* (Braunschweig, 1961), p. 192.
20. J. Pettavel, Microtecnic **14,** 6 (1960).
21. A. W. Ostrop, Machinery **99,** 944 (1961).

Books *continued from page 470*

of these fields since 1927, perhaps as important in the eyes of the new contributors as the effects of technology. Whatever the case may be, *Studies in Optics* is, as Michelson put it, a résumé of his *own* investigations, which he had also published in some 78-odd papers throughout his career. In that sense the book forms the kind of monograph which only a rare few can write without drawing upon themselves any stigma of insufficient reference to the literature or to related work.

It is interesting to observe that two of the most talked about and fruitful advances in the field of contemporary optics in the last decade or two were clearly already in Michelson's mind, as a result probably also of his rather close contact with Lord Rayleigh: the principle of the Fourier-transform description of the relation between wavefronts and diffraction images seems to be stated with little doubt on page 58, and the need for determining not only the visibility curve but also the "phase curve" in interferometric spectroscopy is explicitly stated on page 39, thus clearing up one of the frequent criticisms of this aspect of Michelson's work. That many modern versions of Michelson's relativity experiments are very much at the forefront of present-day investigations is another recognition of Michelson's genius in his choice of experiments.

Michelson's *Studies in Optics* is warmly recommended for reading, not only for its basic beauty and wealth of material, but also for its historical importance. Excellent biographies of Michelson's life and career have been previously given in book form by Bernard Jaffe in *Men of Science in America* (1958) as well as in his more recent paperback *Michelson and the Speed of Light* (1960). The present book includes a fascinating foreword with biographical material by Harvey Brace Lemon, as a somewhat abridged reprint of his 1936 article in *The American Physics Teacher,* as well as a brief note on the relativity experiments by S. Chandrasekhar. Any of the modern books on relativity will place Michelson's pace-setting experiments into their full perspective; Panofsky and Phillips' *Classical Electricity and Magnetism* presents a particularly well-documented study of these experiments. The books on interferometry by W. E. Williams (*Interferometry*) and by C. Candler (*Modern Interferometers*), the article by M. Françon in the *Handbuch der Physik* ("Grundlagen der Optik"), edited by S. Flügge as well as several modern textbooks on optics, such as R. W. Ditchburn's *Light,* John Strong's *Concepts of Classical Optics,* and Born and Wolf's *Principles of Optics* should provide the interested reader with an additional excellent complement on literature references and more particularly with the development of the many fields in optics described so excitingly by A. A. Michelson in his *Studies in Optics.*

GEORGE W. STROKE

Masers and Lasers. By C. A. HOGG and L. G. SUCSY. Maser/Laser Associates, Cambridge, Massachusetts, 1962. 226 pp. $18.75.

This report, prepared by ten graduates of the Harvard Graduate School of Business Administration, is described as "a comprehensive study of the field . . . designed to provide a clear and simplified technical review, to relate the history of development and to act as a guide to the future." This courageous undertaking has resulted in a volume which is, on the whole, a successful and useful contribution to the field made in an area (namely, that which is accessible in every sense to nontechnical or semitechnical managements) which is all too rarely provided for in many technical fields. The book is perhaps at its weakest as a "guide to the future" although this is hardly surprising. The orders of magnitude of many of the quantities associated with optical masers have changed so dramatically in the short life of two years that forecasting must necessarily be heavily speculative.

The first two chapters give the background of the necessary ideas from atomic physics and an outline of the basis of the operation of the maser. These sections are designed to be understood by anyone who has taken college physics; the level appears to be admirably pitched. In spite of the fact that the chapters occupy only sixty-five pages, the coverage is remarkably good and the material well presented. The few minor defects appear to arise mainly from the extreme condensation. Thus the remarks on page 32 appear to imply that the lower level of a maser transition is necessarily the ground state, although the three-level maser is adequately discussed in the following chapter. The paragraph on the 180° pulse method of inversion is probably too brief to be understandable. The applications of masers (as distinct from lasers) is well covered in Chapter 3, which contains a brief but valuable section on the maser in relation to other amplifiers. The development of lasers is discussed and the properties of most solid and gas systems developed up to the time of writing (mid-1962) are included. The 26 observed transitions are usefully summarized in a table which, however, uses the abbreviation M/W both for megawatt and milliwatt. It is of interest to note that the total of 26 transitions has, by the end of the year, increased *threefold.*

After a useful *caveat* regarding the misleading use to which big numbers are put—one recalls the effusions of the popular press at the time of laser announcements—a long section is devoted to possible laser applications. The possibilities considered are those which are either within present reach or which do not call for outrageous extrapolations in laser development. The potentialities and limitations of the laser in the wide range of fields discussed, which includes: communications, defense,

radar, biological, and various technological applications, as well as those for the physics laboratory, are considered in a sober and reasonable way. A number of imaginative, but at the same time feasible, applications are discussed in a section marred only by a raggedness of style which was absent in the first part of the book.

In the account of the present position regarding the number of organizations engaged in maser and, more especially laser activities the suspicion seems to be confirmed that there is a substantial "band wagon" effect. The authors' general conclusions—expressing doubts that laser devices will provide a market large enough to support the large number of organizations at present involved—will probably be supported by many in the field and may induce a useful amount of heart-searching.

The field covered by this report, of which the length is modest but not the price, is extensive so that matters cannot be dealt with at any depth. In a field which is developing as rapidly as is the laser field, this cursoriness is hardly a disadvantage. Many of the present aspects which cause intense excitement at this moment may well be of no more than historical interest in a year or two. The aim of the book, to provide an account of the work in this field for the nonspecialist reader, appears to have been well met.

O. S. Heavens

Investigations of Infra-Red Spectra. By William W. Coblentz. Coblentz Society and Perkin-Elmer Corporation, Norwalk, Conn., 1962. 183 pages. $3.50.

The early works of Coblentz which were originally in three volumes have now been reproduced under a single cover, the subject matter being divided into seven sections.

Part I deals with infrared absorption spectra and contains 132 figures showing the transmission curves of various materials, nearly all of them in a highly purified state. The spectra were measured by the point-by-point method, and the individual determinations are shown on the curves. These spectrograms were standard in the literature for many years, but it was over 20 years before industry found that this was a very rapid and accurate method of analysis and made important use of these spectra. This part of Coblentz's work is the best known to spectroscopists and has been a guide to many in their researches. When in 1929 Raman discovered his effect of characteristic scattering by monochromatic light, he referred to the infrared frequencies of several molecules as measured by Coblentz and reported in this book. In addition to spectra, Part I has a chapter on previous work in infrared spectroscopy and another on apparatus and methods used in the measurement of the spectra.

Part II deals with the infrared emission spectra of metals. The first part of this section shows the relative sensitivity of various kinds of detectors, such as the Boys and Nichols radiometers and those made by Coblentz. The emission spectrum of a carbon arc is studied, and the spectra of several compounds placed in the arc are recorded.

Part III shows results of work by Coblentz on the infrared transmission of crystals. Minerals containing water of crystallization are treated at length. Coblentz also studied a number of crystals containing water of constitution. This section is an interesting application of infrared methods to crystal structure.

The results of measurements on the infrared reflection of various substances are given in Part IV. The measurements include the reflection spectra of alums, quartz, nitrates, and mica. The reflection measurements are continued in the next part.

Part V continues with infrared reflection spectra and shows the characteristic maxima from various molecular groups. Some of the materials measured are carbonates, sulfides, and oxides.

Parts VI and VII include the results of a number of studies on different subjects. Among the more interesting studies at the present time are those on the radiation from a Nernst glower and the reflection and radiation from the moon.

This book is of great historical value and includes many subjects that are of interest today. Considering that the treatise was written many years ago, it is quite modern; it has pointed the way for the great development in infrared research in the last 50 years. It will be a valuable addition to the library of all infrared spectroscopists. This republication was carried out under the joint sponsorship of the Coblentz Society and the Perkin-Elmer Corporation.

Copies may be obtained from H. B. Kessler, Perkin-Elmer Corporation, Norwalk, Conn., for $3.50 postpaid.

Earle K. Plyler*

* Dr. Plyler is the feature editor for the Coblentz Commemoration issue to be published in November 1963.

Classical Electrodynamics. By John David Jackson. John Wiley & Sons, Inc., New York, 1962. 641 pp. $13.00.

The author asserts that this book is a text for a two-semester course in electromagnetic theory given to beginning graduate students. I assert that it is an excellent and comprehensive treatise on electromagnetic theory such as I would be proud to have written myself. But if I had been writing it as a textbook, I should have put in a great many more words of explanation concerning what I was up to in my analysis and, hence, I would either have made the book longer or have covered fewer topics. The terse manner of presentation of the analysis will, without a great deal of classroom explanation and assistance, defy any but the brilliant theoretical student possessing a high degree of mathematical sophistication. As an example, at the beginning of Chapter 9, the fields and radiation of a localized oscillating source are derived from the vector potential alone, with no hint of explanation to the puzzled student as to why the scalar potential is not also being computed in the symmetrical fashion in which the scalar and vector potentials had been handled in previous chapters (the explanation is, however, nicely presented much later in Chapter 16). Considered inexcusable in a book at any level is the unusual shortage of back references to previous sections and equations in the book, to guide the reader who may not have a perfect memory of everything that has appeared earlier.

This book is surprisingly comprehensive in the topics treated, which include waveguides and resonant cavities; diffraction; magnetohydrodynamics and plasma physics; collisions and scattering of charged particles; bremsstrahlung; Cerenkov radiation; radiation damping; and an excellent discussion of multipole fields, including those that result from the intrinsic magnetization of electrons and nuclei. While the discussion of each topic may not be exhaustive, each chapter gives an extensive annotated set of "references and suggested reading." These references alone would make the book a must in every physicist's reference library.

The author has made one commendable innovation in terminology (or at least one that the reviewer has not seen previously). He uses the term *magnetostatics* to refer to the study of magnetic fields resulting from static *currents*, whereas historically this term has been reserved for use in connection with magnetic poles. The reviewer promises that in the next editions of his own introductory physics texts this sensible terminology will also be employed. On the other hand, this reviewer suggests adoption of

continued on page 489

NEW SUBSCRIPTION ORDER

APPLIED OPTICS

Please enter my/our subscription* and continue until countermanded:

- ☐ OSA member rate $6.00 per year
- ☐ Other AIP Societies' rate $8.00 per year
- ☐ Regular rate $10.00 per year
- ☐ Please send OSA membership information
- ☐ check enclosed ☐ bill me
- ☐ Single copy of issue $2.00
- ☐ **MASERS Supplement** published December 1962 .. $5.00

Name ..... Membership No. .....

Address .....

.....

*Subscriptions entered for calendar year only.

NEW SUBSCRIPTION ORDER

APPLIED OPTICS

Please enter my/our subscription* and continue until countermanded:

- ☐ OSA member rate $6.00 per year
- ☐ Other AIP Societies' rate $8.00 per year
- ☐ Regular rate $10.00 per year
- ☐ Please send OSA membership information
- ☐ check enclosed ☐ bill me
- ☐ Single copy of issue $2.00
- ☐ **MASERS Supplement** published December 1962 .. $5.00

Name ..... Membership No. .....

Address .....

.....

*Subscriptions entered for calendar year only.

FIRST CLASS
Permit No. 18297
New York, N. Y.

BUSINESS REPLY MAIL
No postage stamp necessary if mailed in the U. S. A.

POSTAGE WILL BE PAID BY

APPLIED OPTICS
American Institute of Physics
335 E. 45th Street
New York 17, N. Y.

Attention Miss J. Raimondi, Circulation

FIRST CLASS
Permit No. 18297
New York, N. Y.

BUSINESS REPLY MAIL
No postage stamp necessary if mailed in the U. S. A.

POSTAGE WILL BE PAID BY

APPLIED OPTICS
American Institute of Physics
335 E. 45th Street
New York 17, N. Y.

Attention Miss J. Raimondi, Circulation

Interferometric Method of Velocity of Light Measurement

George W. Stroke

An association of interferometric methods in the 3.2-cm microwave and visible-light optical domains is now being used for the measurement of the velocity of light in terms of primary atomic constants, an atomic clock for the frequency and a light source (Hg 198, Kr 86, optical maser) for the length. The microwave interferometry is carried out by hydraulically and continuously moving a piston in a perfect, silver-plated, optically polished, fused-quartz, cylindrical resonant cavity. The optical and mechanical systems involve several novel features extending the interferometric servo-control method using photoelectric detection successfully applied by the author to the ruling of high-resolution gratings. With precisions as good or better than those obtained in any previous measurement of c, an increase in accuracy by one to three orders of magnitude results from the use of primary standards for the frequency and length rather than the unreliable secondary standards used heretofore. This fact applies to other velocity-of-light measurements as well and should help in reducing the rather disturbing dispersion in the values of c, which heretofore considerably exceeded the precisions obtained in the measurements.

Critical reviews of velocity of light measurements carried out in the past have been given by several authors[1] and will not be repeated here. The need for measuring the velocity of light in terms of primary atomic constants was stimulated by Zacharias and Harrison, and was first proposed by them with Searle and Mason and the author.[2] The construction of an apparatus for carrying out such a measurement has been under way since 1956,[3–5] principally at Massachusetts Institute of Technology. A highly precise microwave resonant cavity has been obtained by optically polishing a fused-quartz cylinder at the Optical Shop of Boston University, where the author spent the year from 1956 to 1957. The mechanical, optical, interferometric, and electronic parts for the experiment have just been completed at MIT, and experiments with all the equipment operating have demonstrated the satisfactory operation of the principal components of the apparatus. Initial measurements have shown that the proper order of magnitude of c is indeed being obtained.

It is the purpose of this paper to give a brief description of the principle of the experiment, of the apparatus, and of the operation of its principal components, inasmuch as they involve many novel features of interest in the field of optical and microwave techniques. A critical discussion of the experiment and of the manner of suppressing various sources of error has been given by the author and associates in a series of progress reports[3–5] and will be amplified when the results of measurements are published by Stroke, Searle, and Zacharias. The progress of the work has been much assisted by the work of assistants, associates, and students, in particular by Melvin A. Yaffee as well as by Vincent Bates and Arthur Funkhouser. The optical work on the microwave cavity was carried out under the direction of George Random, and the optical work on the glass part of the hydraulic piston by Arthur Hall.

The Principle of Experiment

The method used for measuring the velocity of light c is based on the equation

$$c = f\lambda_f, \tag{1}$$

where λ_f is the free-space wavelength of an electromagnetic radiation at the frequency f. With atomic clocks as the source of radiation, f is very conveniently obtained in the microwave domain. For example, with a Cs-133 atomic clock, such as that designed by Zacharias *et al.*,[6] a suitable transition is found at 9192.632 Mc/sec. In fact, f is taken as the unit of frequency in Eq. (1). For the computation of c according to Eq. (1), we require a measurement of λ_f in terms of an appropriate unit of length; a vacuum wavelength λ of an optical radiation such as emitted by an optical maser; Hg-198 or Kr-86 light sources are equally suit-

The author is with the Department of Electrical Engineering and the Research Laboratory of Electronics, Massachusetts Institute of Technology, Cambridge, Massachusetts.

This work was supported in part by the U. S. Army, the Air Force Office of Scientific Research, and the Office of Naval Research.

Received 10 December 1962.

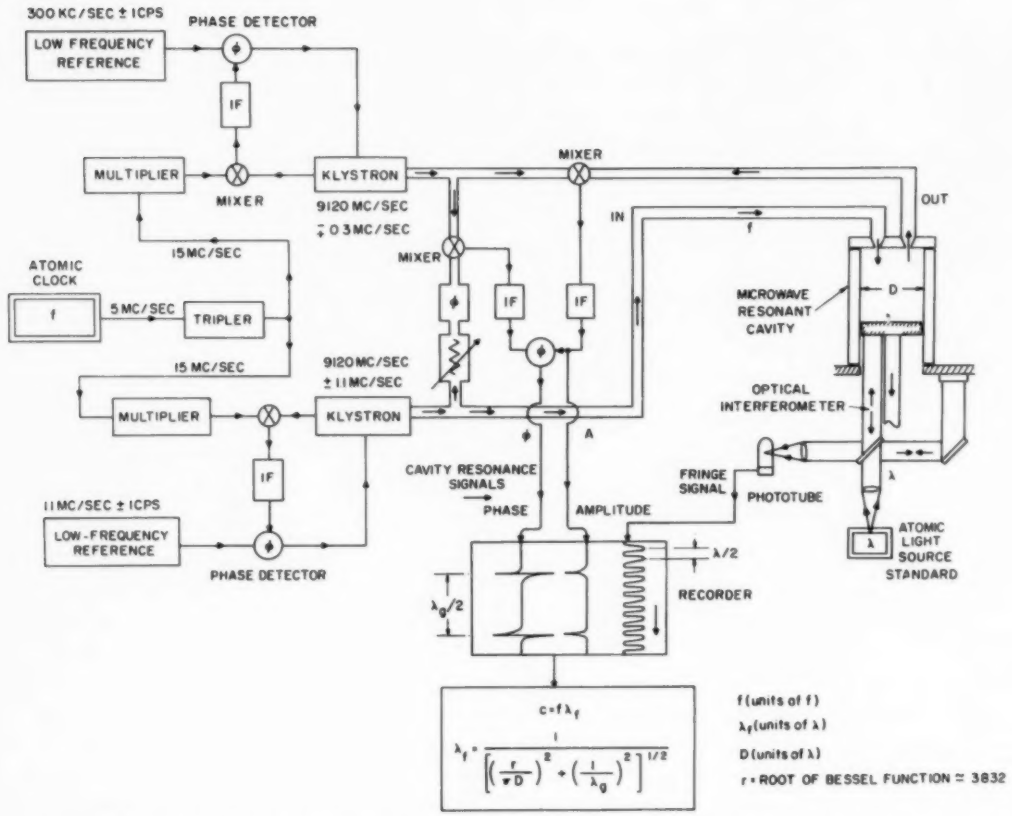

Fig. 1. Schematic diagram of velocity of light-measurement method in terms of primary atomic standards described in text. Phase-lock control is used for the klystrons in a system using Varactor multipliers.

able. Our initial experiments used a Hg-198 source for reasons of convenience. The measurement of λ_f, in terms of λ, is easily carried out with the help of a photoelectric interferometer, as previously described by the author and successfully used by him and others in the interferometric control of grating ruling.[7,8]

The choice of a suitably well-behaved electromagnetic field at the microwave frequency f is crucial in a velocity of light experiment. If plane waves in free space could be easily generated with the help of microwave lenses or similar radiating horns or systems, one would choose this approach in preference to resonance methods. In particular, one would wish to use Fabry-Perot-like systems in order to obtain sharply defined microwave interference fringes, as was first suggested by Culshaw[9]: the problems associated with these methods have been under study for many years by Culshaw *et al.*[10] at the National Bureau of Standards in Boulder, Colorado, as well as by Froome[11] at the National Physical Laboratory in Teddington, Middlesex. We have preferred to use a microwave cavity in which the field is considerably better behaved than in free space, provided that one succeeds in producing a cylindrical cavity and end plates of adequate precision. We have previously reported[3–5] that measurements indicate our cavity to have its surface contained between two truly geometrical circular cylinders less than ± 2 optical fringes apart (i.e., ± 0.5 μ apart) for a diameter of 16.119 cm. We force the cavity to oscillate at the frequency f determined by an atomic clock.

The measurement of c consists in measuring the distance between resonance positions of a moving piston in our cylindrical cavity at the frequency f: the so-called guide wavelength λ_g thus obtained is simply related to the free-space wavelength λ_f by the equation

$$\lambda_f = \frac{1}{\left[\left(\frac{r}{\pi D}\right)^2 + \left(\frac{1}{\lambda_g}\right)^2\right]^{1/2}}, \tag{2}$$

obtained by solving Maxwell's equations with the appropriate boundary conditions, in case of a perfect cavity. Here, D is the diameter of the cavity, and $r \cong 3.832$, a root of a Bessel function. Detailed examination of the requirements on perfection in the geometry of the cavity and conductivity of the silver

film for a given precision of the measurement of c are given elsewhere[3–5]; their proper evaluation is as important in this measurement as is the evaluation of the requirements on interferometer alignment and of the effects of finite-source hole apertures in the measurement of the guide wavelength.[12] It is essential to observe that the choice of the microwave resonance measurement described here was made after prior studies had made clear that many of the so-called perturbations could be either ignored or made negligibly small by judicious choice of cavity dimensions, resonant modes, and very careful manufacture of the crucial components. For instance, with an X-band frequency around 9000 Mc/sec and a guide wavelength of about 3.2 cm, one can easily see from Eq. (2) that $\partial c/c \simeq \partial\lambda_g/\lambda_g$, but $\partial c/c \simeq (1/16)(\partial D/D)$ only. (One says that the diameter is "suppressed.") In other words, if a precision of 1.5×10^{-7} in c is to result from a precision of 1.5×10^{-7} in the measurement of λ_g, i.e., about 0.02 fringes in visible light per λ_g, then a precision of only 2.4×10^{-6} is required on the measurement of D, i.e., about 1.4 fringes, or 0.38 μ, or about 1.5×10^{-5} in. Precision achieved in the manufacture of the cavity is quite remarkable and indeed adequate. We recall that the accuracy of the measurements is that of the standards in terms of which the precision is obtained:

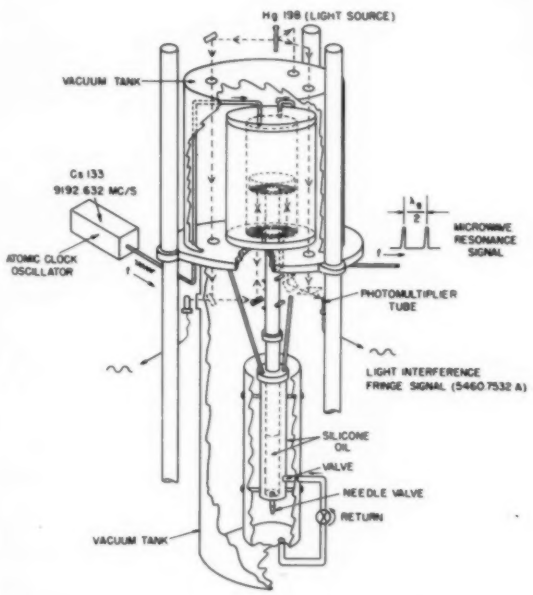

Fig. 2. Schematic diagram showing principal elements of velocity-of-light measurement apparatus. A TE_{01n} mode is excited in the cavity through a 3-mm diameter iris in the top plate, and detection of the transmission resonance is obtained through a similar iris at 90°, both irises being centered at about 0.48 a from the cylinder axis (a = radius of cavity). Successful detection of resonances shown in Fig. 7 is obtained with an insertion loss as great as 80 dB. Inner diameter of cavity about 161.1 mm, length about 290 mm, outer diameter about 240 mm.

Fig. 3. Photograph of the hydraulic system used in moving the tuning piston for the purpose of going through successive resonances in the cavity. The piston rests on a hypodermic syringe containing silicone oil. The method used for avoiding the introduction of air bubbles clearly appears in the photograph. The tangential brass cylinders which serve to guide the optically polished glass piston without any stick-slip appear in the top of the photograph. The straightness of travel of this piston has been measured with the help of the alignment interferometer described by the author[16] and found to be good to ±0.3 sec of arc over a 15-cm traverse.

reproducible accuracies of at least 10^{-9} for the length and frequency standards used are representative orders of magnitude. For a measurement precision of 1×10^{-6} in c, the requirements are only 0.13 fringes per λ_g and 9.4 fringes on the diameter. In reality, by forcing the cavity to oscillate successively at two different frequencies f_1 and f_2, one can eliminate the need for measuring D, inasmuch as the same microwave diameter is obtained at two neighboring frequencies. (The optical diameter D is smaller than the microwave diameter by twice the skin depth, i.e., by 2 μ or so, and can easily be separately measured, if required, as a check, by comparing the diameter to a Fabry-Perot etalon in a null measurement using air-gauge methods.

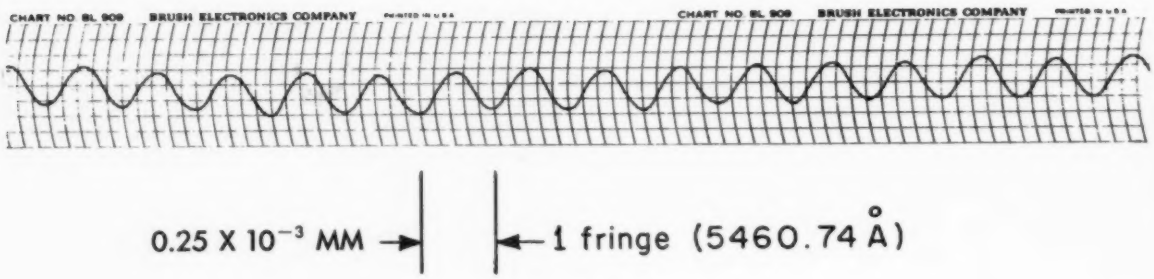

Fig. 4. Early photoelectric recording of interferometric fringe signal obtained with hydraulic motion produced by system of Fig. 3. Note the regularity of motion in the fraction of a fringe range; this regularity is maintained over the entire available traverse of approximately 150 mm.

At any rate, any error that could be made on estimating the skin depth is seen to be certainly much smaller than any error on D that would affect the precision required in giving c.) Clearly, also, the resonance in the cavity is measured over several λ_g, and the tolerances are correspondingly more favorable.

In summary, it is seen that two remarkable features distinguish our method of measuring c from past methods:

1. The measurement of the velocity of light is being carried out directly in terms of primary atomic standards for the frequency and the wavelength. A very considerable increase of accuracy is thus obtained, even if there were no increase in precision compared to past experiments that were performed in terms of uncertain and generally irreproducible standards.

2. The apparatus has been designed to require no corrections for effects of apparatus errors to an order of accuracy that exceeds the present dispersions in the values given for c by at least one, if not two or three, orders of magnitude.

We may also note that the cavity-resonance methods used previously did not have the advantages of the availability of such a precise cavity. Moreover, interferometric measurements with a continuously moving piston and primary atomic constants have not been used. We have the pleasure of acknowledging here the significant encouragement and advice received from L. Essen of the National Physical Laboratory in Teddington who was the first, with Gordon Smith, to use cavity resonance methods in the determination of c.[13] The work of the late W. W. Hansen at Stanford University had gone a long way in the direction of achieving results comparable to those that we have now obtained.[14]

Apparatus

Figure 1 shows a block diagram of the principle of the experiment, and Fig. 2 gives a more detailed schematic description of the mechanical and optical features. Perhaps the most important element in the interferometric system is the continuously hydraulically moved piston, shown in Fig. 3. The moving piston consists of an optically polished 50-cm long, 5-cm diam glass tube guided by tangential brass cylinders in a kinematical mount. The piston

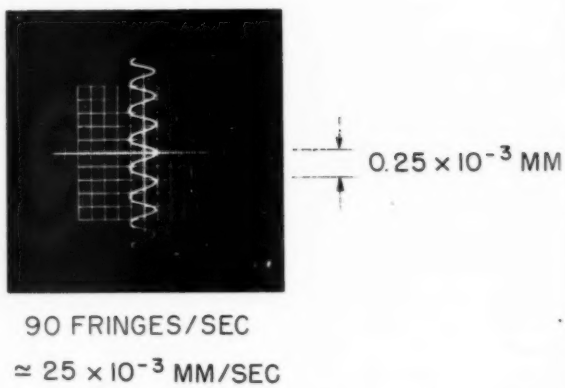

Fig. 5. Oscilloscope display of early magnetic-tape recording of photoelectric interference fringe signal obtained with hydraulically moved piston at 90 fringes per second. Note regularity in motion and very high signal-to-noise ratio in signal.

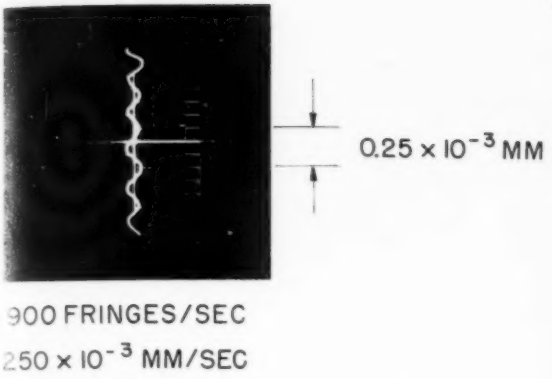

Fig. 6. Oscilloscope display of early magnetic tape recording of photoelectric interference fringe signal obtained with hydraulically moved piston at 900 fringes per second. Improvements in the appearance of the signal are obtained by avoiding irregularities in the recording, as present here.

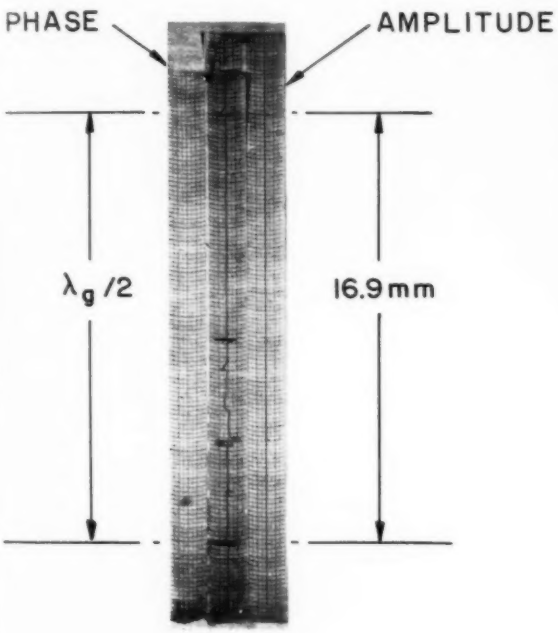

Fig. 7. One of the first phase and amplitude resonance recordings obtained at 9121 Mc/sec by transmission through the microwave cavity and with the help of the phase-locked klystron system shown in Fig. 1. Note the remarkable sharpness of the phase resonance. (Q's on the order of 10^8 were measured in our experimental silver-plated 10.16-cm diameter pyrex cavity, see ref. 4, and were shown to depend critically on the perpendicularity of the tuning piston and end plate to the cavity axis, a 3% decrease in Q resulting from a 1 min of arc tilt. A Q exceeding 2×10^8 can be obtained under similar conditions in the present cavity.) Also note the absence of all but a very small number of other excited modes and their large separation from the desired forced resonance at the extremities of $\lambda_g/2$.

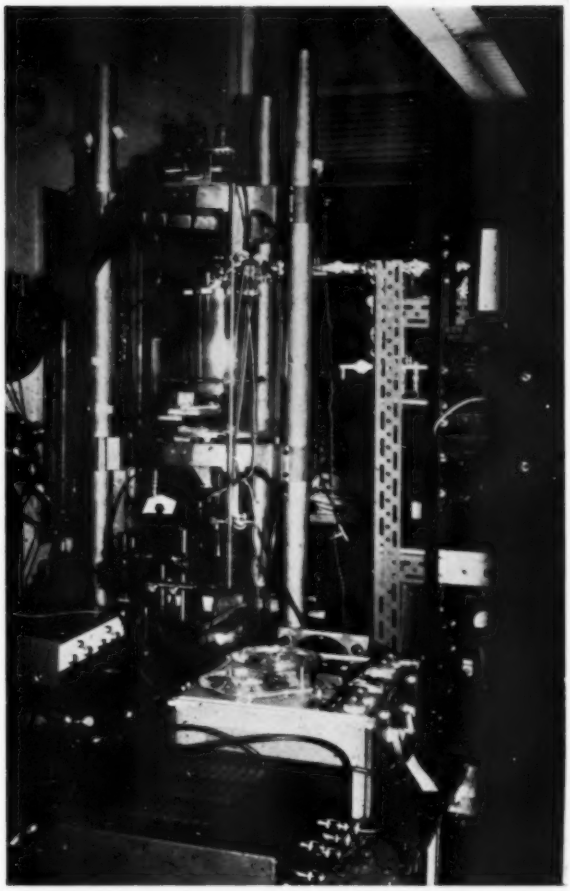

Fig. 8. Photograph of velocity of light apparatus used for experiments described in text and figures. Note silver-plated optically polished fused-quartz microwave-resonance cavity, excitation and resonance detecting electronics on the right, part of magnetic tape-recording equipment in foreground, Hg 198 light source excited by rf oscillator in an electrodeless discharge on top of apparatus, and photoelectric interferometer in a layout generally following the schematic layout of Fig. 2. Measurements of c are carried out with the cavity and interferometers in vacuo.

tube rests on top of a hypodermic syringe, and the rate of advance is simply controlled with an appropriate needle. Extremely uniform motion is obtained as seen by the recording of the photoelectric fringe signal in Fig. 4. Piston advance rates up to 100 and even 1000 fringes per second have been obtained with this system (see Figs. 5 and 6), and these rates are 25 to 50 times greater than those obtained on grating ruling engines driven by screws. In fact, the possibility of obtaining such great piston speeds, and of reducing the duration of the measurement from days to just minutes, was an important factor in designing a special apparatus for this measurement instead of using the MIT ruling engine, as was originally contemplated.

Fig. 9. Fused quartz cylinder in process of optical grinding. A similar arrangement was used for polishing. About one year's work was involved in attaining the optical perfection described in text.

(Of course, we have simultaneously devoted our attention to so improving the MIT ruling engine as to increase the spectral quality of the gratings ruled by a factor of about 10, as already reported[7].) It is significant to note that the delicate microwave and interferometric measurements described here have all been performed with the apparatus mounted in a room four floors above ground in a modern steel and cement building (the K. T. Compton Laboratory at MIT); the success in preventing any mechanical vibrations from disturbing the apparatus is largely due to the mounting of the critical parts from the rather massive central plate shown in Figs. 2 and 8 and to a judicious elimination of any high-frequency resonance elements in the interferometric and hydraulic mounts. The entire apparatus is mounted on three brass-tube columns, which are isolated from the floor by 5-cm thick balsa-wood blocks. Typical early-phase and amplitude recordings obtained in the cavity are shown in Fig. 7; a complete view of the principal elements of the apparatus is shown in Fig. 8. A photograph of the cavity in the process of optical grinding is shown in Fig. 9. Even the first measurements performed in air just before the writing of this paper have given a value of c of the proper order of magnitude, namely, 3.00×10^5 km/sec. The final measurements will be carried out with the apparatus in vacuo, and c will be given in units of (Cs 133 frequency) $\times$ (Hg 198 wavelengths) or in equivalent units using other atomic or molecular clocks and light standards.

References

1. E. Bergstrand, "Determination of the Velocity of Light" in *Handbuch der Physik*, S. Flügge ed. (Springer, Berlin, 1956), Vol. 24; R. Dupeyrat, J. Phys. Radium **19,** 557 (1958); P. Grivet, Rev. Gen. Elec. **67,** 285 (1958); G. W. Stroke, "Velocity of Light" in *American Institute of Physics Handbook*, D. E. Gray ed. (McGraw-Hill, New York, 1962), 2nd ed.
2. J. R. Zacharias, G. R. Harrison, G. W. Stroke, S. J. Mason, and C. L. Searle, Quart. Prog. Rpt., MIT Res. Lab. Electronics (Jan. 15, 1956), p. 59.
3. J. R. Zacharias, G. W. Stroke, C. L. Searle, and S. J. Mason, Quart. Prog. Rpt., MIT Res. Lab. Electronics (Apr. 15, 1956), p. 31.
4. G. W. Stroke and C. L. Searle, Quart. Prog. Rpt., MIT Res. Lab. Electronics (July 15, 1956), p. 27.
5. G. W. Stroke, Quart. Prog. Rpt., MIT Res. Lab. Electronics (Oct. 15, 1956), p. 46; J. R. Zacharias and G. W. Stroke, Quart. Prog. Rpt., MIT Res. Lab. Electronics (Jan. 15, 1958), p. 57; G. W. Stroke and J. R. Zacharias, Quart. Prog. Rpt., MIT Res. Lab. Electronics (Oct. 15, 1958), p. 69; G. W. Stroke, Quart. Prog. Rpt., MIT Res. Lab. Electronics (Oct. 15, 1961), p. 105; G. W. Stroke and A. Funkhouser, *ibid.*, p. 107; G. W. Stroke, J. G. King, D. C. Papa, and A. Funkhouser, *ibid.*, p. 109; G. W. Stroke, M. A. Yaffee, and A. Funkhouser, Quart. Prog. Rpt., MIT Res. Lab. Electronics (July 15, 1962), p. 42.
6. J. R. Zacharias and J. G. Yates, Quart. Prog. Rpt., MIT Res. Lab. Electronics (Oct. 15, 1954), p. 30.
7. G. R. Harrison and G. W. Stroke, J. Opt. Soc. Am. **45,** 112 (1955); G. W. Stroke, J. Opt. Soc. Am. **51,** 1321 (1961). R. F. Jarrell, G. W. Stroke, D. K. Rice, and G. Sintiris, paper No. 35, Tenth Colloq. Spectroscopicum Internatl., U. of Md., June 1962.
8. H. W. Babcock, Appl. Opt. **1,** 415 (1962).
9. W. Culshaw, Proc. Phys. Soc. (London) **B66,** 597 (1953).
10. W. Culshaw, J. M. Richardson, and D. M. Kerns, *Interferometry*, Paper No. 4-3, Symp. No. 11, Natl. Phys. Lab., June 1959 (Her Majesty's Stationary Office, London, 1960), p. 329.
11. K. D. Froome, *Interferometry*, Paper No. 4-2, Symp. No. 11, Natl. Phys. Lab., June 1959 (Her Majesty's Stationary Office, London, 1960), p. 309.
12. G. W. Stroke, J. Opt. Soc. Am. **47,** 1097 (1957); *ibid.* **48,** 276 (1958); J. Phys. Radium **19,** 415 (1958).
13. L. Essen, Proc. Roy. Soc. (London) **A204,** 260 (1950); L. Essen and A. C. Gordon-Smith, Proc. Roy. Soc. (London) **A194,** 348 (1948).
14. K. Bol, Phys. Rev. **80,** 298 (1950); also Ph.D. thesis, Stanford U. (1950). See also D. H. Janney, M. L. Report No. 343 (Oct. 1956), Air Force Office of Scientific Research.
15. G. W. Stroke, J. Opt. Soc. Am. **51,** 1340 (1961).

Erich Marchand and John Simons *Eastman Kodak*, Robert A. Woodson *General Precision-Link*, William Woodbury *Eastman Kodak*, Harold Edgerton *MIT*, Edwin J. Breneman *Eastman Kodak* and Rodger P. Loveland during the OSA Rochester Fall 1962 Meeting.

photo D. L. MacAdam

The Rapid Measurement of Photographic Records of Interference Fringes

J. Dyson

The measurement of photographs of interference fringes can be a lengthy and tedious process. Some types of record, however, exemplified by streak photographs, offer the possibility of more rapid methods of measurement than the usual microdensitometer trace. A new instrument for effecting this measurement is described, with a discussion of its errors.

Introduction

Many optical instruments, such as interference microscopes, optics-testing interferometers, and the like, present their output information in the form of a photographic plate bearing a record of a field of interference fringes. The information is contained in the positions of these fringes and can only be extracted by accurate measurement of their position.

This process is a time-consuming one, especially if the record is essentially two-dimensional, i.e., if measurements of many points along the length of each of many fringes are required.

If, however, the fringes are essentially parallel and equidistant, the information appearing as small shifts of portions of each fringe, the measurement can be accelerated considerably by the use of a device described in this paper.

Nature of the Problem

Photographic records of this type are generated by "streak photography," in which the image of a narrow slit is swept rapidly by a rotating-mirror camera across the photographic plate in a direction at right angles to the length of the slit. An interferometer produces fringes that are seen through the slit and are at right angles to its length. As the slit is narrow, the light emerging from it can be regarded as giving a close approximation to a linear section through the fringe field. If the fringes are stationary, the plate will record a number of parallel fringes. Any movement of the fringes falling on the slit will be recorded as a displacement of the fringes on the plate.

The problem of measuring a record of this kind arose recently in connection with the development of a method for time-resolved measurement of the electron density in a pinched toroidal gas discharge.[1] The electron density was calculated from its effect on the optical path length through the discharge, this being revealed by displacement of the fringes formed in an interferometer of the "common-path" type.[2] The slit image on the plate was approximately 1-mm wide and 24-mm long, being formed on a standard 8.25 cm × 10.8 cm plate and swept along its length. A typical (negative) record is shown in Fig. 1. The slit is interrupted by two opaque bars for electrical reasons. The narrow strips above and below the main image are due to two evacuated tubes, which were used as reference paths free from discharge. The plate used was Ilford HPS, developed in PQ developer diluted 1:9, the wavelength band being centered on 6200 Å. Only a portion of the record is shown here.

This particular discharge was made at a relatively high pressure, and the fringe shifts are, in places, easily visible to the eye. It was desired to measure the fringe displacement to an accuracy of at least $^1/_{100}$ fringes.

The first measurements were made by taking a microdensitometer tracing across the fringes and ascertaining the points at which the trace passed through a suitably chosen reference density. Since, however, it is necessary to make such a tracing for every 2 mm of length of the fringes over a length of several centimeters, each tracing taking about 20 min to obtain, the time and cost of this process proved prohibitive. The situation is made worse by the grain of this very fast plate, which is too large to be ignored, necessitating the use of an inconveniently wide slit and the performance of a calculation to ascertain each of the points of crossing the reference density.

A well-known method of Rymer and Halliday[3] was

The author is with Research Laboratory, Associated Electrical Industries, Aldermaston Court, Aldermaston, Berkshire, England.
Received 30 November 1962.

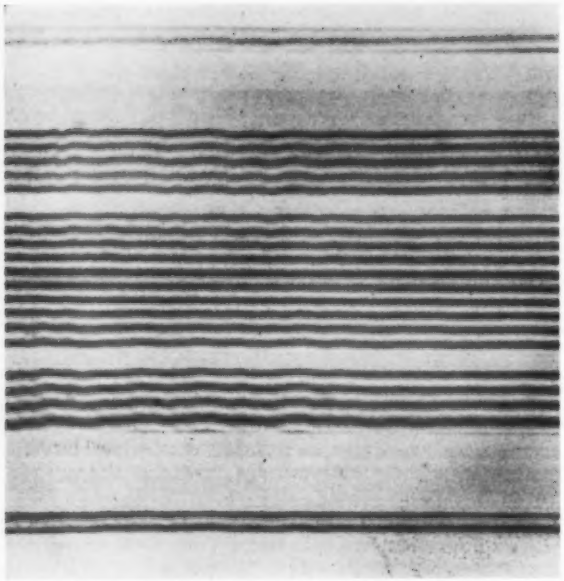

Fig. 1. Streak photograph of interference fringes.

explored, but time did not allow the setting up of the special mechanics and electronics required.

Experimental Apparatus

The measurements were finally made by means of the apparatus shown diagrammatically in Fig. 2. A slit illuminated by a microscope lamp, operated from dc to avoid ripple, is imaged by a condenser, at suitable magnification, on to the emulsion of the plate. This is mounted on a carriage which can be translated, with micrometer control, in two mutually perpendicular directions in its own plane. A rhomb of Iceland spar (a natural crystal with two faces ground and polished to remove imperfections) is placed in the light beam. This doubles the image on the plate, each slit being approximately 1 mm × 0.25 mm and separated by about 0.25 mm, with the long dimension parallel to the fringes.

The emulsion, illuminated by the two slit images, is viewed by a low-power microscope objective and eyepiece. Light reaches the eyepiece via a 45° mirror which can be swung out (as indicated in dotted lines) to allow the light to be received by a photomultiplier. Before reaching the position of this mirror, the light traverses an analyzer that consists of a sheet of Polaroid fixed to a flywheel mounted on a hollow shaft that can be rotated at about 2000 rpm. A quarter-wave plate is fixed to the back of the Polaroid so that the light reaching the photomultiplier is circularly polarized. This is a well-known precaution to avoid variation of electron emission as the plane of polarization rotates. The output from the photomultiplier is displayed on an oscilloscope.

The apparatus is so adjusted that, when seen through a clear part of the plate, the two slit images are of equal brightness. Both images are polarized, the planes of polarization in each image being mutually perpendicular. The rotating analyzer will, therefore, cause the brightness of each image to vary cyclically with time, the variations of the two images being in antiphase. Consequently, the output of the photomultiplier will contain no ac component. The initial setting to equality of brightness is conveniently made by angular adjustment of a polarizer before the Iceland spar crystal.

When the slit images fall on a part of the plate containing the fringe record, it is evident that the ac output will only be zero when the mean absorptions for the two images are equal, i.e., when the images are symmetrically disposed with respect to the peak or the trough of the fringe, if the latter is symmetrical. Accordingly, if the plate be moved in a direction normal to the fringes until the ac output is seen to be zero on the oscilloscope and the micrometer read, this reading will correspond to the peak or trough (whichever lies between the two images) of the fringe in question.

This setting is made very quickly, and a complete traverse across a record such as is shown in Fig. 1, giving two readings per fringe, can be made in about 2 min.

Setting Accuracy and Accuracy of Measurement

The setting accuracy was more than was required for this application; it was not difficult to obtain readings repeatable on the same portion of a given fringe to $^1/_{500}$ of the fringe separation. However, this does not represent a corresponding accuracy of measurement for, owing to the plate grain, the fringe position is not defined over 1-mm length to this degree of accuracy.

To minimize errors due to grain, the area of each slit image was made as large as possible and the separation chosen to give the greatest sensitivity. It is seen easily that the greatest signal for a given small setting error is obtained when the center of each slit image falls on the point of maximum rate of change of density of the fringe, i.e., when the centers of the images are separated by one-half the separation of adjacent fringes. Further, since the rate of change of density is small near the peak or trough of a fringe, there is little to be gained by making each slit image wider than one-quarter of the fringe separation. With a fringe separation of 1.10 mm, the figures given above for the dimensions of the slit images are near optimum. For other fringe widths,

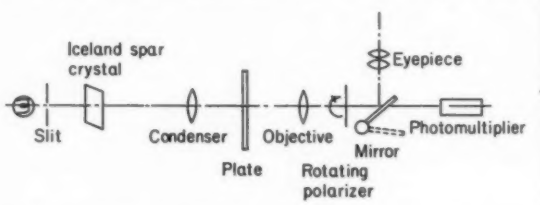

Fig. 2. Diagrammatic optical system of fringe-measuring instrument.

the dimensions of the slit images and their separation may be varied, while keeping the proportions constant, by varying the magnification of the condenser lens.

To ascertain the true accuracy of measurement, a plate was taken with no gas in the discharge tube. There was, therefore, no perturbation of the fringes. A series of measurements was taken at 2-mm intervals along the plate on the central fringe (which does not move even if gas is present) and the results processed to remove the effect of general fringe curvature due to distortion in the rotating-mirror camera. Variation in the resulting figures gave the uncertainty of setting due to plate grain and imperfections (chiefly mechanical) of the instrument.

A series of 38 readings gave a maximum variation from the mean of 11 μ and a standard deviation of 5.6 μ corresponding to 0.011 and 0.0051 fringe widths, respectively. It could thus be assumed that the required accuracy of 0.01 fringe width was reached in the great majority of the measurements.

Variation of Fringe Width

In all the above, it has been assumed that the fringe separation remains constant. However, the existence of the perturbations to be measured shows that it varies. To estimate the magnitude of the resulting error, a distribution of transmission of the form

$$T = 1 + \cos(x + Ax^2)$$

may be assumed, where A expresses the local departure from constancy of fringe separation. The effect of this on the setting obtained by the above method near the zero of x can readily be calculated, and the error introduced is given to the first order by

$$\text{error} \approx -2.65\,A.$$

As an extreme case, the width of the first fringe on one side of the zero of x may be taken to be twice the width of that on the other side, corresponding to a value of 0.0382 for A. This gives an error of 0.0096 of the mean widths of the two fringes. As, in fact, no variation in fringe width approaching 2:1 was observed in this series of experiments, it was taken that variation in fringe width was not a serious source of error.

Conclusions

Under certain conditions, i.e., where interference fringes approximate to straight parallel bands, the measurement of their position is greatly facilitated by means of the instrument described above. The method is impersonal and not fatiguing, and its errors can be measured or calculated to be of reasonable magnitude.

In cases where the plate noise is reduced by using wider fringes or finer-grain emulsions, better setting accuracy may be required. This can easily be obtained by the use of a phase-conscious rectifier with a center-zero meter in place of the oscilloscope as the indicating device.

This work was supported in part by a UKAEA contract.

The author wishes to express his thanks to K. M. Young for conducting a long series of measurements with this instrument, both while proving it and in use, and to T. E. Allibone, CBE, FRS, Director of the Laboratory, for permission to publish this work.

References

1. J. Dyson, R. V. Williams, and K. M. Young, Nature **195**, 1291 (1962).
2. J. Dyson, J. Opt. Soc. Am. **47**, 386 (1957).
3. T. B. Rymer and J. S. Halliday, J. Sci. Instr. **27**, 50 (1953).

Books *continued from page 480*

other terminology that the author is using in place of some that should become obsolescent. The author refers to the vector **E** at a point as the *electric field*, which it is not, and uses the clumsy terms *magnetic flux density* and *magnetic induction* for **B**. The reviewer prefers the perfectly correct but not yet commonly used terms *electric intensity* and *magnetic intensity* (of the field at a point).

I should like to introduce one gratuitous observation: the exposition of electromagnetism has certainly come far since Frenkel wrote his outstanding *Electrodynamik* in 1928 and decided that, since everyone thought of **H** as the fundamental magnetic vector (whereas it was really **B**) he would interchange **H** and **B** so that **H** could really be fundamental. No one appreciated this confusion, and, to my knowledge, no one has followed Frenkel's usage, but at least the younger generation got the idea, and no longer does a student have my own experience of learning **H** and **B** one way as a sophomore and having to interchange the concepts as a junior!

To summarize: this book is highly recommended as a reference volume, but I raise serious questions as to its suitability as a *beginning* graduate text.

GEORGE SHORTLEY

Japanese Journal of Applied Physics. Publication Office, Faculty of Science, University of Tokyo, Bunkyo-ku, Tokyo, Japan. $10.00 per annum, single copy $1.00.

This new publication, issued monthly under the auspices of the Physical Society of Japan and the Japan Society of Applied Physics, would seem to supplement the monthly journal in this field, written in Japanese, which was formerly known as the *Journal of Applied Physics, (Japan)*. This will continue to be published; but the new journal will clearly be of help to western physicists: papers will be published in English, French, or German.

The first two numbers carried articles on topics having to do with crystal vibrations, crystal growth, piezoelectricity, photoconductivity, transistors and other semiconductor studies, masers (both gas phase and crystal), physical properties of polymers, optics, and field-emission studies. Lacking competence in all these fields, the reviewer sampled and can report—what will surprise no one—that the quality of the published material will stand comparison with that found in the comparable journals of the American Institute of Physics.

The reviewer found interest also in the publication charge of this new journal. It is not a page charge, proportional to the number of pages; it is a publication charge given by a quadratic expression which should operate to curtail excessive length of

papers. The average length of the papers in the first issue was eight pages; that in a recent issue of *Applied Optics* was seven pages. It would be interesting, after sufficient data have accumulated, to compare the distribution of lengths of papers published under the linear and the quadratic systems.*

BRYCE CRAWFORD, JR.

Wave Mechanics of Crystalline Solids. By R. A. SMITH, Wiley, New York, 1961. 473 pp. $13.00

The author, who was Professor of Physics at the University of Sheffield (now at MIT), gives as the purpose of the book "to treat the fundamental theory of wave motion in solids, both that of the lattice, and of the electrons, in as elementary a way as possible". An elementary knowledge of quantum mechanics is taken for granted but the author develops all the concepts of wave motion; the book should be readily understandable to a first-year American graduate physics student. Two chapters are taken up with the properties of a one-dimensional crystal and consider the concepts of normal modes of vibration, lattice waves, and the motion of an electron in a lattice in the simplest possible form. This is followed by two chapters on three-dimensional lattices and their vibrations in which the treatment is straightforward and the concept of a phonon is introduced in a natural way. The six remaining chapter titles will give an idea of the solid-state phenomena which are then treated with this foundation: 8. Motion of Electrons in a Perfect Crystal; 9. Distribution of Electrons between the Allowed Energy Levels in a Crystal (Mean Free Path Scattering, Electrical Conduction, Heat Conduction, Thermoelectric effect, Hall effect, etc.); 10. Electrical and Thermal Transport Phenomena in Crystalline Solids (Conductors, Semiconductors, Influence of Impurities and Discussion of the Properties as Determined by the Energy Band Structure); 11. The Effective-mass Approximation; 12. Magnetic Phenomena Due to Free Electrons and Holes in Crystals; and 13. Interaction of Electrons with Photons and Phonons.

The book is certainly not intended as a handbook of solid-state physics, as important fields like paramagnetism not due to free electrons, superconductivity and the particular phenomena occurring in salts of the transition elements and the rare earths are left out entirely. It gives an introduction into the simpler phenomena found in conductors and semiconductors. A person who does not have the basic knowledge which can be acquired by a study of this book would have a hard time understanding the more specialized and advanced literature. The author has taken a great deal of trouble to make the presentation with simple mathematical tools, and he stresses the physical principles involved. Mathematical rigor is often lost, and here and there inaccuracies slip in, not enough, however, to spoil the value of the book, which is to introduce the beginner into the theory of the electron in a vibrating crystal lattice.

A reader of *Applied Optics* might justifiably ask what this book has to do with optics of the solid state and the answer is: very little. In the last chapter a paragraph deals with the optical absorption in semiconductors due to direct electron transitions between two bands and another one to transitions where one or more phonons are involved. Compared to the great variety of optical properties that have now been studied, for instance those on which a crystalline laser depends, the optical properties found in this book form only a very meager selection. Again it may be said that the person interested in the more specialized literature on optical solid-state properties or the optical investigator who needs to know the basic properties of the solid state will find the basic facts in an easily accessible form in this book.

G. H. DIFKE

* There is no page charge for publication in *Applied Optics*.

Flammenphotometrie (2nd Revised Edition). By R. HERRMANN AND C. TH. J. ALKEMADE. Springer-Verlag, Berlin, 1960. 394 pp. DM 88.

This book discusses the methods and data of spectrochemical analysis using flames as sources of excitation. Not a theoretical book, its purpose is to describe in detail the apparatus and instruments used in flame spectrochemical analysis and to discuss the advantages and disadvantages of the many available methods and experimental procedures. Coverage of the pertinent literature is comprehensive. Most of the 766 references cited are referred to in the text. A vast amount of labor was obviously involved in evaluating and organizing the results of so many individual documents, and it is not surprising that some inaccuracies in the authors' interpretation of the literature occurred as noted below. These however are occasional rather than chronic.

Material is presented in five sections: Fundamentals, Instruments, Analytical Methods, Determination and Elimination of Errors, and Applications: "Fundamentals" describes briefly the nature of flames, dissociation and ionization, and flame radiation. Relevant physical facts are briefly mentioned. It is desirable that one who practices flame photometry be conversant with self-absorption, self-reversal, the influence of Doppler and collision broadening on emission line growth curves, the theoretical reasons for calibration curves deviating from ideality, and the reasons for mutual interactions of spectral lines. Subjects such as these are not treated here from the fundamental standpoint, and the analyst will need to acquire this knowledge from other sources. The section on "Instruments" is good and will be of great help to any analyst confronted with the tasks of designing his own apparatus and of selecting equipment to be bought. Subjects such as type of flame to be used, atomization, optical arrangements, filters, monochromators, and spectrographs are discussed. "Analytical Methods" will be equally helpful to the practicing analyst in organizing his procedure. The most useful spectral lines and bands are tabulated, and many methods suggested for specific determinations. It is here that errors sometimes occur with regard to determination of nonmetals that do not have spectral lines which can be excited in flames. For example the *CN* bands are recommended for determination of organic nitrogen, and the green *NO* bands, for nitrogen generally. In the former case, it is not adequately pointed out that the intensity will depend upon the particular compound being analyzed and is not a function only of the amount of organic nitrogen present. In the latter case, the spectrum is due to the $NO + O$ continuum and not to *NO* bands; the reviewer is not sure whether T. M. Sugden, who is quoted as a reference on the $NO + O$ spectrum, would agree that this is a general test for nitrogen instead of for atomic oxygen. Similar reservations are held relating to the determination of carbon through observation of the C_2, *HCO*, and H_2CO bands. It is clear that on these items re-examination of the pertinent literature is in order. "Determination and Elimination of Errors" treats many interesting details of practical importance, such as the mutual influence of one line on the intensity of another. "Applications" presents in great detail the use of flame photometry in many disciplines including medicine and biology.

As a general matter, this reviewer takes exception to the use in this book of the terms "kation" and "anion" for the Na and Cl that are formed in the flame from, for example, NaCl. Those terms are proper only for electrolytic solutions and do not describe the species that are found in the flame.

In brief, *Flammenphotometrie* is of practical use through its near-encyclopedic review of data and techniques, although at times nonrigorous in its interpretation of spectral features and their application to flame photometry.

H. G. WOLFHARD

On the Correction of Phase Errors in Interferograms

Ernest V. Loewenstein

When an interferogram is an even function of path difference, it suffices to compute the cosine Fourier transform of the interferogram from zero to D, the maximum path difference, to produce the spectrum. If the computation does not start from exactly zero path difference, there is a phase error, which leads to asymmetry of the scanning function and, in the case of continuous spectra, distortion of the base line. The phase error may best be corrected by introducing a corresponding phase correction into the transforming cosine function. Taking the total transform, $T = \sqrt{C^2 + S^2}$ leads to a symmetric scanning function which has rather broad wings.

I. Introduction

In recent years there has been increased interest in interferometric spectroscopy, sometimes referred to as Fourier transform spectroscopy. Workers both in the United States and abroad have built two-beam interferometers for the near and far infrared.[1-7] Some interest has even been shown by microwave people, as the extension of microwave techniques into the submillimeter region has not proceeded as rapidly as some had hoped.

A Fourier transform of the interferogram, either by digital or analog means is required to produce a spectrum, and this is the principal drawback of the method. In many cases the interferogram is an even function of path difference x as is shown in Fig. 1. In such cases the cosine Fourier transform may be used, since

$$\int_{-\infty}^{\infty} f(x)e^{i\omega x}dx = 2\int_{0}^{\infty} f(x)\cos\omega x dx \quad [\text{if } f(x) = f(-x)].$$

(A common feature of all interferograms, which are really auto-correlation functions, is a peak at zero path difference, called the central maximum. There can be no peak anywhere in the interferogram greater than the central maximum, as it represents the total energy in the spectrum.) The advantages gained are a reduction in the amount of data to be gathered and processed, and a consequent reduction in the processing time. Since computer time is expensive, and storage space in any computer has its limitations, these are important considerations. In addition, in balloon or satellite-borne systems, the information storage or transmitting capacity is always limited, and a factor of two in the amount of information to be handled may be of overriding importance.

In order to take advantage of the evenness of the interferogram function, it is necessary to start the Fourier transform at exactly zero path difference. In the case of a sampled system, errors in finding the exact zero may arise, and the abscissa of the data point closest to the central maximum may be displaced by an amount δ (see Fig. 1). This is what gives rise to a phase error. In the case of a spectrum with only a single spectral line, the phase error is $2\pi\delta/\lambda$. For a heterochromatic spectrum we simply characterize the phase error by the offset δ.

In an analog system, the interferogram function is multiplied by a cosine wave and integrated. A phase error arises when the cosine function is not a maximum at the peak of the central maximum of the interferogram.

II. Scanning Function

The instrument function of an interferometer, corresponding to the slit function of a conventional spectrometer, is called the scanning function. It is defined as the spectrum produced by the instrument for a narrow, monochromatic line input (delta function input). Its importance lies in the fact that the observed spectrum is the true spectrum convolved with the instrument function.

If an interferometer is illuminated with monochromatic light, the resulting interferogram is a pure cosine wave. Cutting off the interferogram at some finite path difference D gives width to the scanning function:

The author is in the Optical Physics Laboratory, AFCRL, Bedford, Massachusetts.

Received 17 January 1963.

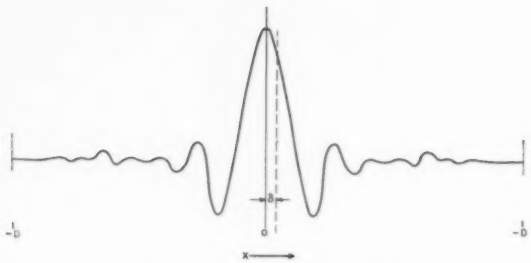

Fig. 1. Example of an interferogram which is an even function of path difference. δ represents the phase error.

$$C(\omega) = \int_0^D \cos\omega_0 x \cos\omega x dx$$

$$= \frac{D}{2}\frac{\sin(\omega-\omega_0)D}{(\omega-\omega_0)D} + \frac{D}{2}\frac{\sin(\omega+\omega_0)D}{(\omega+\omega_0)D}. \quad (1)$$

The second term, involving $(\omega + \omega_0)$, corresponds to a spectral line at $-\omega_0$. Since negative frequencies are not computed, terms involving $(\omega + \omega_0)$ will be dropped in all further calculations. When investigating spectra close to $\omega = 0$, both terms must be used. Otherwise one will suffice, as the other will always be smaller by a factor of $1/(2\omega_0)$.

The scanning function of Eq. (1) is of the form $\sin x/x$, and has rather large side lobes. In order to suppress them, we "apodize" the interferogram,[8] multiplying it by a slowly varying function of path difference which is unity at $x = 0$ and zero at $x = D$. In a recent paper Vanasse[9] has shown that "triangular" apodization is in a certain sense optimum; we therefore use $(1 - x/D)$ as the apodizing function:

$$C_A(\omega) = \int_0^D (1 - x/D)\cos\omega_0 x \cos\omega x dx$$

$$= \frac{D}{4}\frac{\sin^2[\frac{1}{2}(\omega-\omega_0)D]}{[\frac{1}{2}(\omega-\omega_0)D]^2}. \quad (2)$$

This is the same function as the diffraction limited grating slit function. It has much lower side lobes, but a main peak 50% wider at half maximum than that of the unapodized scanning function. Thus we see that the wings of the scanning function can be adjusted, at a cost of some resolution.

Since the scanning function enters the spectrum directly, it is pertinent to inquire: (1) what changes take place in the scanning function and spectrum when there is a phase error in the interferogram, and (2) how can these changes, or errors, be corrected?

III. Phase Errors and Their Effects

Consider the scanning function for the apodized case, where there is an error δ in finding the position of the central maximum. We will put a quantity ϵ into the transform which we may adjust later:

$$C'_A(\omega) = \int_0^D [1 - (x/D)]\cos\omega_0(x+\delta)\cos\omega(x+\epsilon)dx. \quad (3)$$

This yields for the scanning function [ignoring terms in $(\omega + \omega_0)$]:

$$C'_A(\omega) = \frac{D}{4}\frac{\sin^2[\frac{1}{2}(\omega-\omega_0)D]}{[\frac{1}{2}(\omega-\omega_0)D]^2}\cos(\omega\epsilon - \omega_0\delta)$$

$$- \delta\left[1 - \frac{\sin(\omega-\omega_0)D}{(\omega-\omega_0)D}\right]\frac{\sin(\omega\epsilon - \omega_0\delta)}{\omega-\omega_0}. \quad (4)$$

For $\epsilon = \delta = 0$, this reduces to the expression of Eq. (2). There is no problem of the second term on the right becoming infinite as $\omega \to \omega_0$, for the term in square brackets goes to zero as $(\omega - \omega_0)^2$.

If $\epsilon \neq \delta$, and neither vanishes, $C'_A(\omega)$ is neither symmetric nor antisymmetric about ω_0. If $\epsilon = 0$,

$$C'_A(\omega) = \frac{D}{4}\frac{\sin^2[\frac{1}{2}(\omega-\omega_0)D]}{[\frac{1}{2}(\omega-\omega_0)D]^2}\cos\omega_0\delta$$

$$- \delta\left[1 - \frac{\sin(\omega-\omega_0)D}{(\omega-\omega_0)D}\right]\frac{\sin\omega_0\delta}{\delta}. \quad (5)$$

In this case, the first term is symmetric about ω_0, the second term antisymmetric; their sum gives rise to a lopsided scanning function, as shown in Fig. 2. This is substantially the result which has been presented by Connes.[10]

It may be seen from Eq. (5) that the magnitude of the asymmetry depends on the ratio δ/λ_0, for

$$\sin\omega_0\delta \cong \omega_0\delta = 2\pi\delta/\lambda_0.$$

For the case illustrated in Fig. 2, $\delta/\lambda_0 = 0.015$.

In addition to producing asymmetric spectral lines, the asymmetric scanning function, when convolved with a continuous spectrum, distorts the amplitude of the spectrum, or, equivalently, distorts the baseline. Fig-

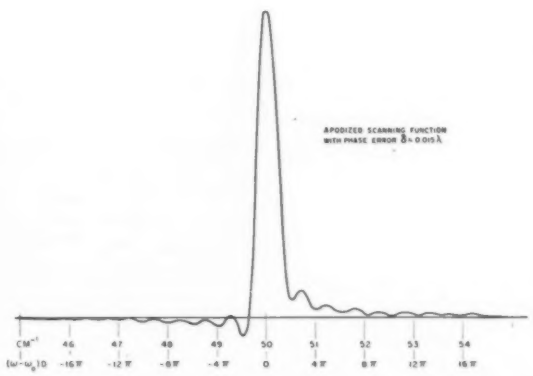

Fig. 2. Scanning function resulting from an interferogram with triangular apodization and a phase error $\delta/\lambda = 0.15$.

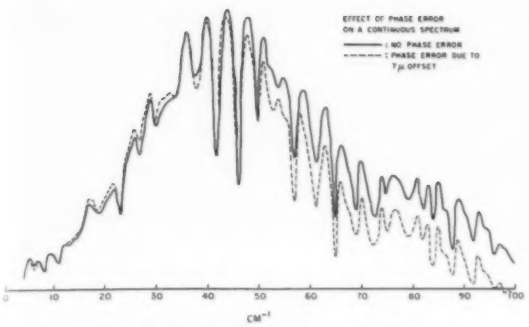

Fig. 3. An example of a spectrum with and without phase error. Solid curve: no phase error; broken curve: $\delta = 7\ \mu$.

ure 3 shows a spectrum computed from an interferogram with no phase error. There is provision in the transformation program for putting in a factor ϵ just as it appears in Eq. (3). The solid curve in Fig. 3 was computed with $\epsilon = 0$, the dotted one with $\epsilon = 7\ \mu$. Triangular apodization was used in both cases.

It is seen that the level of the spectrum is raised slightly on the low frequency side and lowered on the high frequency end. This is the effect to be expected if the function illustrated in Fig. 2 is scanned across the correct spectrum of Fig. 3.

IV. Correction of the Phase Error

The symmetry can be restored to the scanning function in one of two ways. Either we may compute the sine transform, $S(\omega)$, and use $T = (C^2 + S^2)^{1/2}$ for the spectrum, or we may set $\epsilon = \delta$.

The first method is the less desirable, because it yields a scanning function which drops off only as $(\omega - \omega_0)^{-1}$, and also has shoulders. The sine transform is:

$$S'_A(\omega) = \int_0^D (1 - x/D)\cos\omega_0(x + \delta)\sin\omega(x + \epsilon)dx$$

$$= \frac{D}{4}\frac{\sin^2[1/2(\omega - \omega_0)D]}{[1/2(\omega - \omega_0)D]^2}\sin(\omega\epsilon - \omega_0\delta)$$

$$+ \delta\left[1 - \frac{\sin(\omega - \omega_0)D}{(\omega - \omega_0)D}\right]\frac{\cos(\omega\epsilon - \omega_0\delta)}{(\omega - \omega_0)\delta}. \quad (6)$$

Combining, we have for the total Fourier transform:

$$T^2{}_A(\omega) = \left[\frac{D}{4}\frac{\sin^2[1/2(\omega - \omega_0)D]}{(1/2(\omega - \omega_0)D)^2}\right]^2$$

$$+ \frac{1}{(\omega - \omega_0)^2}\left[1 - \frac{\sin(\omega - \omega_0)D}{(\omega - \omega_0)D}\right]^2. \quad (7)$$

There is no longer any reference to ϵ and δ, and the function is symmetric about ω_0. However, the second term determines the rate of decline of T_A, and it drops only as $1/(\omega - \omega_0)$ (after the square root is taken).

Figure 4 illustrates two cases of cosine scanning functions and total scanning functions superimposed: one apodized with $(1 - x/D)$, the other unapodized. In the apodized case, it is clear that $T_A(\omega)$ has no zeros. This is a disadvantage from the point of view of information theory, for when points are computed according to the sampling theorem, the peak of the scanning function for any one sampling point is made to fall on a zero of the scanning function for neighboring points. Thus at any sampling point, the contribution from all other sampling points is zero. This situation does not obtain for $T_A(\omega)$.

The preferable method of restoring symmetry to the scanning function is to set $\epsilon = \delta$. Then

$$C'_A(\omega) = \frac{D}{4}\frac{\sin^2[1/2(\omega - \omega_0)D]}{[1/2(\omega - \omega_0)D]^2}\cos\delta(\omega - \omega_0)$$

$$- \delta\left[1 - \frac{\sin(\omega - \omega_0)D}{(\omega - \omega_0)D}\right]\frac{\sin\delta(\omega - \omega_0)}{\delta(\omega - \omega_0)}. \quad (8)$$

There remains a small error term of the order of δ/D compared to the peak of the principal term. It is

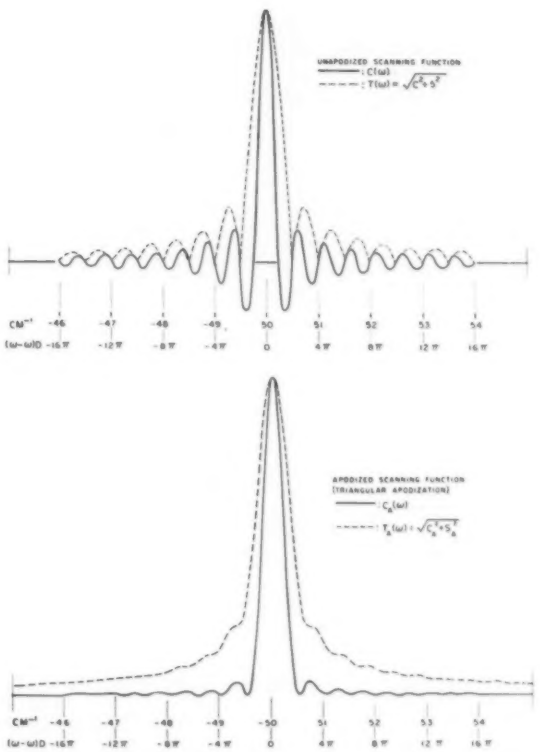
UNAPODIZED SCANNING FUNCTION
: C(ω)
: T(ω) = √(C²+S²)
CM⁻¹ -46 -47 -48 -49 50 51 52 53 54
(ω-ω)D -16π -12π -8π -4π 0 4π 8π 12π 16π
APODIZED SCANNING FUNCTION
(TRIANGULAR APODIZATION)
: C_A(ω)
: T_A(ω) = √(C_A²+S_A²)
CM⁻¹ -46 -47 -48 -49 50 51 52 53 54
(ω-ω)D -16π -12π -8π -4π 0 4π 8π 12π 16π

Fig. 4. Superimposed scanning functions, with no phase error. Solid curves represent cosine transform and broken curves are $T = (C^2 + S^2)^{1/2}$. Upper, unapodized; lower, triangular apodization. All computed scanning functions used a cosine function of 100 cycles, with ten points per cycle. The parameters to the computer were arranged to simulate a monochromatic line at 50 cm^{-1}, and a maximum path difference of 1 cm.

negative, and so tends to bring the scanning function down a little more rapidly. It will not give any appreciable negative values, if δ/D is sufficiently small (see Appendix).

Finally, we should remark on two things which do not work. First, it might appear attractive to set $\epsilon = (\omega_0\delta/\omega)$, for each value of ω computed, thus making the correction identically zero. However, this works only for a truly monochromatic spectrum. If there is as little as one more line in the spectrum, then there is no way of making the correction identically zero. To illustrate, suppose we have a transform with two frequencies ω_0 and ω_1:

$$G(\omega) = \int_0^D [\cos\omega_1(x+\delta) + \cos\omega_0(x+\delta)]\cos\omega(x+\epsilon)dx$$
$$= {}^1/_2\int_0^D \cos[(\omega-\omega_1)x + \omega\epsilon - \omega_1\delta]dx$$
$$+ {}^1/_2\int_0^D \cos[(\omega-\omega_0)x + \omega\epsilon - \omega_0\delta]dx. \quad (9)$$

Now regardless of what value of ϵ is chosen, there will be a term left over in one of the integrands.

Second, while it might be desirable from the point of view of mathematical symmetry to correct the apodizing function, by using $[1 - (x + \delta/D)]$, the effect is just to add some more small terms to the scanning function (of order δ/D^2 and smaller), no further correction of the scanning function is effected.

V. Conclusion

We have considered interferograms which are even functions of path difference, so that the cosine Fourier transform of one side is equal to half the Fourier transform of the entire interferogram. Then a phase error results in asymmetry of the scanning function, and distortion of the base line. The amount of asymmetry is proportional to the ratio δ/λ, where δ is the error in finding the position of zero path difference, and λ the wavelength under consideration.

The asymmetry may be removed either by taking the entire Fourier transform or, preferably, by entering a correction factor into the argument of the cosine function in the transformation. The former method gives rise to a scanning function with rather broad wings, while the latter restores the scanning function to its previous shape with a residual error of the order of δ/D, where D is the maximum path difference.

The writer is indebted to G. A. Vanasse and R. G. Walker of the Optical Physics Laboratory, AFCRL, for numerous discussions which helped to clarify the matters set forth above. Much of the graphical and numerical work was done by Laurence Rothman.

Appendix

To determine whether the negative values of the error term in Eq. (8) are important, we must calculate the point at which the main term and error term become equal. This is done by solving the transcendental equation:

$$\frac{\cos\delta(\omega-\omega_0)}{2(\omega-\omega_0)^2D} = \frac{\sin\delta(\omega-\omega_0)}{\omega-\omega_0}. \quad (10)$$

(Terms of modulus 1 are omitted.) Setting $(\omega - \omega_0) = x$, the equation may be reduced to

$$\cos^2 x\delta = \frac{x^2}{1/(4D^2) + x^2}. \quad (11)$$

Equation (11) may be solved graphically, but if $\delta \ll 1$, it may be reduced to a biquadratic:

$$[1 - (x\delta)^2]^2 = \frac{x^2}{1/(4D^2) + x^2} \quad (12)$$

yielding

$$x^2 = -\frac{1}{8D^2} \pm \frac{1}{4D\delta}\left[\frac{1}{4}(\delta/D)^2 + 2\right]^{1/2}. \quad (13)$$

In this writer's experience, D is usually of the order of 1 cm and values of $\delta \approx 10^{-3}$ are easy to obtain, and we have, for the point of equality

$$x = \omega - \omega_0 \cong 19/D,$$

for $D = 1$ cm, $\omega - \omega_0 \cong 19 \cong 6\pi$. As will be seen from Fig. 3, the value of $C_A(\omega)$ is negligible at this distance from ω_0, and it is immaterial whether the function from there on declines as $(\omega - \omega_0)^{-1}$ or $(\omega - \omega_c)^{-2}$.

References

1. P. Fellgett, Seminar talk, Johns Hopkins University, 1954; J. Phys. Radium **19,** 187 (1958).
2. H. A. Gebbie and G. A. Vanasse, Nature **178,** 432 (1956).
3. J. Connes and H. P. Gush, J. Phys. Radium **20,** 915 (1959).
4. L. Mertz, J. Opt. Soc. Am. **46,** 548 (1956).
5. J. Strong and G. A. Vanasse, J. Opt. Soc. Am. **49,** 844 (1959); **50,** 113 (1960).
6. H. A. Gebbie, L. Delbouille, and G. Roland, "Emission Spectra in the Infrared by Interference Spectroscopy," Xth Colloq. Spect. Internatl., U. of Maryland, June 1962.
7. P. L. Richards, Bell Telephone Laboratories, private communication.
8. P. Jacquinot, Appendix E in *Concepts of Classical Optics*, by John Strong (Freeman, San Francisco, 1958).
9. G. A. Vanasse, J. Opt. Soc. Am. **52,** 472 (1962).
10. J. Connes, Rev. Opt. **40,** 45, 101, 157, 213 (1961).

Have you read the Russian maser papers in Optics and Spectroscopy?–see p. 551

Mesure de la Dispersion dans les Raies d'Absorption Infrarouge des Gaz. Appareillage et Corrections Instrumentales

C. Alamichel, R. Assous, et F. Legay

An apparatus consisting of a Michelson interferometer and a high-resolution grating spectrometer has been set up in order to measure the dispersion in the vibration-rotation bands of gases. The influence of the imperfections of the interferometer and the slit-width is discussed. The instrumental corrections in a single line with Lorentz shape have been calculated for the case of a triangular "slit function" for certain values of specific parameters, and the best experimental conditions have been determined. The first experimental results are given for the $R(2)$ line of the first harmonic of HCl^{37}.

Introduction

Les mesures de dispersion en infrarouge fournissent un moyen précis de détermination des intensités et des largeurs de raie. Peu de mesures ont jusqu'ici été faites dans les raies de vibration-rotation des gaz, et en dehors du montage décrit ici, le seul réfractomètre fonctionnant actuellement à notre connaissance est celui de Jaffe.[1]

Le dispositif expérimental s'inspire directement d'un montage utilisé il y a quelques années (Legay[2, 3]). Ce montage, bien que réalisé avec des moyens relativement simples, avait donné d'excellents résultats, au moins aussi précis que ceux obtenus par les méthodes directes de mesure des intensités. L'utilisation d'un nouvel interféromètre et d'un monochromateur beaucoup plus résolutif a permis d'améliorer considérablement les performances du dispositif.

Dispositif Expérimental

Le schéma de l'appareillage est montré sur la Fig. 1. Il s'agit essentiellement d'un spectromètre à réseau servant de monochromateur à un interféromètre de Michelson utilisé comme réfractomètre.

Le spectromètre est du type Czerny de 180 cm de distance focale et a été construit suivant un modèle mis au point par Cornet *et al.*[4] Il est équipé d'un système optique constitué par deux miroirs faisant entre eux un petit angle et montés sur un chariot qui se déplace suivant l'axe du spectromètre. Ce dispositif bien connu permet d'explorer une petite région du spectre avec une grande précision.[5]

The authors are with the Laboratoire d'Infrarouge, Chimie-Physique, Faculté des Sciences à Orsay (Seine-et-Oise), France.

Received 9 November 1962.

Le réseau utilisé est un réseau échelette Bausch & Lomb de 20 cm de largeur et de 600 traits/mm qui a permis d'atteindre un pouvoir de résolution de 70,000 dans le premier ordre. Un réseau de mêmes dimensions mais à 150 traits/mm est également prévu. Un petit prémonochromateur à prisme est disposé devant la fente d'entrée afin d'éliminer les ordres indésirables du réseau. Il n'est pas montré sur la figure. L'ensemble du spectromètre est placé dans une enceinte où le vide peut être fait.

L'un des miroirs de l'interféromètre peut être déplacé parallèlement à lui-même avec une grande sensibilité afin d'ajuster la différence de marche entre les deux bras.

La séparatrice S est soit une lame de verre revêtue d'un film de silicium évaporé sous vide et d'épaisseur optique, $1.5/4\ \mu$, soit une lame de fluorine également revêtue de silicium d'épaisseur optique $3.5/4\ \mu$. En utilisant l'une ou l'autre de ces lames, le pouvoir réflecteur de la séparatrice peut être maintenu entre les limites de 30 et 60% sans absorption dans la région de 1 à $7\ \mu$.

La compensatrice est mobile autour d'un axe horizontal parallèle à ses faces et sa rotation est repérée à l'aide d'un miroir de Poggendorf. Ce dispositif permet de modifier la différence de marche et de mesurer les excédents fractionnaires, comme nous le verrons plus loin.

Les cuves à gaz, placées sur chaque bras de l'interféromètre, ont une longueur maximum possible de 100 cm. Elles sont en communication avec un manomètre à mercure et peuvent être remplies avec le gaz étudié. La section utile du faisceau traversant les cuves a un diamètre d'environ 5 cm.

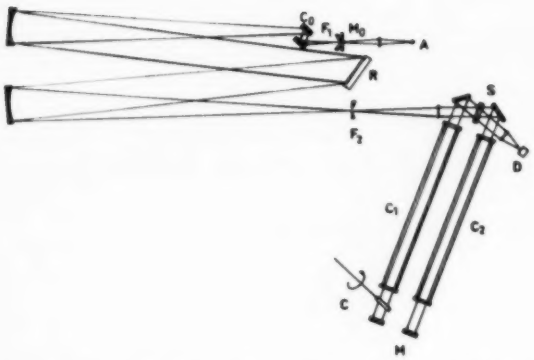

Fig. 1. Schéma du dispositif expérimental de mesure des indices de réfraction. A—source; M_0—modulateur; F_1, F_2—fentes rectilignes d'entrée et de sortie; C_0—système optique d'exploration du spectre; R—réseau; S—séparatrice; C—compensatrice tournante; C_1, C_2—cuves à gaz; M—miroir pouvant être déplacé parallèlement à lui-même; D—détecteur.

Principe des Mesures et Précision

On envisage dans ce paragraphe le cas idéal où les erreurs introduites par la fonction d'appareil du spectromètre sont négligeables.

Cette condition est pratiquement réalisée dans les régions où l'intensité de la source, l'indice de réfraction et l'absorption du gaz varient peu dans le domaine spectral occupé par les fentes. On supposera de plus que l'interféromètre ne présente pas de défaut optique et est éclairé en lumière rigoureusement parallèle.

Dans ces conditions, après traversée de l'interféromètre, l'énergie tombant sur la cellule réceptrice est donnée par

$$i(\nu) = i_0 RT\,[1 + e^{-2x(\nu)} + 2\,e^{-x(\nu)} \cos\varphi(\nu)], \qquad (1)$$

où i_0 est l'énergie lumineuse à l'entrée de l'interféromètre, R et T les coefficients de réflexion et de transmission de la séparatrice.

Les quantités i_0, R et T ne variant généralement que très lentement avec ν, nous les supposerons constantes dans ce qui suit. Le coefficient d'absorption totale de la cuve remplie du gaz à étudier est $X(\nu)$; on suppose qu'il n'y a pas d'absorption dans l'autre cuve. La différence de phase entre les deux faisceaux interférent est $\varphi(\nu)$.

Il est commode d'introduire l'ordre d'interférence:

$$k = \varphi/2\pi. \qquad (2)$$

Plaçons-nous dans les conditions expérimentales suivantes: Le gaz à étudier remplit une des cuves, l'autre est vidée. L'ordre d'interférence s'écrit alors:

$$k(\nu) = 2l[n(\nu) - 1]\nu + \delta(\theta)\nu, \qquad (3)$$

où l est la longueur de la cuve contenant le gaz d'indice n et $\delta(\theta)$ la différence de marche subsistante quand cette cuve est également vidée. Comme nous l'avons vu plus haut, on peut modifier cette différence de marche en tournant la compensatrice C d'un angle θ autour de son axe horizontal.

Préalablement à toute mesure, l'interféromètre est réglé à l'ordre zéro par déplacement du miroir M, les deux cuves étant vidées ($n = 1$) et la compensatrice étant verticale; ce réglage se fait commodément en lumière blanche, et il doit se conserver dans l'infrarouge puisque les traversées dans les milieux susceptibles de dispersion sont parfaitement compensées. On vérifie que cette condition est remplie en faisant varier la longueur d'onde dans un grand intervalle: aucune variation de l'ordre d'interférence ne doit être décelée si l'ordre zéro est maintenu.

Ce réglage que nous avons adopté n'est évidemment pas indispensable, mais il présente les deux avantages suivants:

1° Il permet d'avoir des anneaux d'interférence très peu serrés même quand la cuve est remplie du gaz, étant donné que l'indice d'un gaz est toujours voisin de 1. 2° Il est aisé à faire et permet, si l'interféromètre a été déréglé pour une raison quelconque, de le remettre rapidement et exactement dans les mêmes conditions de fonctionnement.

Deux types de mesures d'indice peuvent être effectuées: 1° À fréquence constante: On fait varier la pression du gaz de zéro à p. L'ordre d'interférence varie de k_0 à k_1 et d'après (1) l'indice à la pression p est donné par

$$n(p,\nu) - 1 = (k_1 - k_0)/2\,l\,\nu.$$

2° À pression constante: On fait varier la fréquence de ν_1 à ν_2. La variation d'indice est donnée d'après (1) par*

$$n(p,\nu_1) - n(p,\nu_2) = \frac{k_1 - k_2}{2\,l\,\nu_1} + \left[n(p,\nu_2) - 1 + \frac{\delta(\theta)}{2\,l}\right]\frac{\nu_2 - \nu_1}{\nu_1}.$$

Il est donc nécessaire de connaître l'indice en ν_2, qui doit être déterminé par la première méthode.

Remarquons cependant que si $\nu_1 - \nu_2$ est petit, une erreur sur $n(p,\nu_2)$ entraîne une erreur sur la différence d'indice beaucoup plus petite. Le terme en $\delta(\theta)$ est généralement négligeable si la rotation de la compensatrice est limitée au voisinage de la position verticale. Cette méthode est particulièrement bien adaptée aux mesures dans les régions de forte dispersion, car elle permet d'obtenir rapidement un grand nombre de points de la courbe de dispersion avec une seule mesure de pression.

Durant une mesure du premier ou du second type, la compensatrice est fixe et un nombre entier de franges plus un excédent fractionnaire sont enregistrés. Celui-ci est déterminé en enregistrant les franges en fonction de

* Cette formule est établie en supposant $\delta(\theta)$ indépendant de ν.

θ, grâce à une rotation régulière de la compensatrice, avant et après la mesure, les autres paramètres étant fixes. Le décalage pour un même angle θ entre les deux systèmes de franges donne l'excédent fractionnaire. Dans une mesure du premier type, à fréquence constante, l'excédent fractionnaire est indépendant de θ. Par contre, dans une mesure du deuxième type, ceci peut ne plus être vrai par suite de la dispersion de l'indice du milieu optique constituant la lame. Mais ce phénomène est négligeable le plus souvent.

Dans les meilleures conditions et en particulier loin des zones d'absorption, il est possible de mesurer les excédents fractionnaires avec une précision d'environ 1/100 de frange. Vers 2 μ et avec des cuves de 100 cm, cette précision entraîne une erreur sur l'indice:

$$\Delta n = \Delta k/2\,l\,\nu = 0.01 \cdot 10^{-6}.$$

Dans les régions d'absorption, cette erreur est évidemment augmentée par suite de la diminution du contraste des franges. Cet effet sera examiné plus loin.

Durant les mesures la dérive de l'interféromètre est contrôlée à intervalles réguliers. Les premières mesures ont montré qu'elle reste toujours inférieure à 0.5 frange visible par heure.

Influence des Dimensions Géométriques de la Fente de Sortie et des Imperfections de l'Optique de l'Interféromètre

Dans ce paragraphe, nous supposerons toujours l'interféromètre éclairé en lumière strictement monochromatique et nous examinerons dans quelle mesure l'étendue géométrique de la fente de sortie F_2 et les imperfections des pièces optiques de l'interféromètre peuvent avoir une influence sur les résultats expérimentaux.

Deux rayons lumineux monochromatiques interférents donnent sur le récepteur une intensité élémentaire de la forme

$$\{1 + e^{-2\chi[l(\tau)]} + 2\,e^{-\chi[l(\tau)]}\cos\varphi\,[\tau, l(\tau)]\}f(\tau)\,d\tau,$$

où τ représente l'ensemble des paramètres fixant les positions dans l'espace des deux rayons lumineux, et $l(\tau)$ la longueur parcourue par l'un des rayons dans le gaz d'indice n. Cette longueur dépend de τ par suite du non parallélisme des faisceaux et des fenêtres de la cuve. La fonction $f(\tau)$ dépend de la répartition de la lumière sur la fente de sortie, des différents diaphragmes limitant les faisceaux, des réflexions et des absorptions des pièces optiques de l'interféromètre.

L'intensité lumineuse totale est donc de la forme

$$i(\nu) = \int \{1 + e^{-2\chi[l(\tau)]} + 2\,e^{-\chi[l(\tau)]}\cos\varphi[\tau, l(\tau)]\}\,f(\tau)\,d\tau, \quad (4)$$

où φ est donné par

$$\varphi = 4\pi l(\tau)\,(n-1)\nu + 2\pi\delta(\tau,\theta)$$

et $\delta(\tau,\theta)$ est une différence de marche comprenant aussi bien celle due à la rotation de la lame compensatrice que celle due aux imperfections, au déréglage de l'interféromètre et au non parallélisme des faisceaux.

Dans tous les cas usuels, $l(\tau)$ ne subit que des variations très faibles dans le domaine d'intégration de l'expression (4). On peut donc dans l'intégrale remplacer $l(\tau)$ par une valeur moyenne $\bar{l}$.

Par contre, le terme $\delta(\tau,\theta)$ peut varier très rapidement avec τ si la fente est assez grande pour que l'ordre d'interférence varie sensiblement d'un point à l'autre de son image sur la surface sensible du récepteur. Ce phénomène est d'autant plus marqué que l'on est loin de l'ordre zéro et que l'interféromètre est plus déréglé. Dans ces conditions l'équation (4) peut s'écrire sous la forme suivante:

$$i(\nu) = \{1 + e^{-2\chi(\bar{l})} + 2a\,e^{-\chi(\bar{l})}\cos[4\chi\bar{l}\,(n-1)\nu + \alpha(\theta)]\}\int f(\tau)d\tau \quad (5)$$

$$\mathrm{tg}\alpha(\theta) = \frac{\int f(\tau)\sin 2\pi\delta(\tau,\theta)d\tau}{\int f(\tau)\cos 2\pi\delta(\tau,\theta)d\tau}$$

et

$$a^2 = \frac{[\int f(\tau)\sin 2\pi\delta(\tau,\theta)d\tau]^2 + [\int f(\tau)\cos 2\pi\delta(\tau,\theta)\,d\tau]^2}{|\int f(\tau)\,d\tau|^2}.$$

Pour des petites variations de δ, $\theta(\tau,\theta)$ peut être considéré comme étant la somme de la différence de marche $\delta_1(\theta)$ due à la lame tournante et pratiquement indépendante de τ, et d'une différence de marche $\delta_2(\tau)$ indépendante de θ due à toutes les autres causes.

$$\delta(\tau,\theta) = \delta_1(\theta) + \delta(\tau)$$

et dans ces conditions a^2 est indépendant de θ, car

$$a^2 = \frac{[\int f(\tau)\sin 2\pi\delta_2(\tau)\,d\tau]^2 + [\int f(\tau)\cos 2\pi\delta_2(\tau)\,d\tau]^2}{|\int f(\tau)d\tau|^2}.$$

Si $\delta_2(\theta)$ est une constante, $a = 1$; dans le cas contraire, $a < 1$.

Les facteurs qui ont été pris en considération dans ce paragraphe ont donc pour effet de diminuer le contraste des franges, mais la substitution de l'équation (5) à l'équation (1) n'entraîne pas de modification dans la méthode de mesure ni dans les résultats. En effet, le facteur a étant indépendant de θ, la méthode de mesure des excédents fractionnaires par rotation de la compensatrice est toujours valable. Si l'amplitude des franges est diminuée, la précision des mesures sera réduite, mais sans introduction d'erreur systématique.

Cependant, le calcul de l'indice de réfraction devrait se faire en toute rigueur avec une longueur de cuve $\bar{l}$ légèrement différente de la longueur moyenne de la cuve l_0. Si les faces des cuves sont parallèles, on peut avoir un ordre de grandeur du rapport $(l_0 - \bar{l})/l_0$, en prenant pour $\bar{l}$ la longueur du trajet dans la cuve d'un rayon faisant un angle avec l'axe égal au quart de l'angle sous lequel est vue la fente de sortie à partir de la lentille d'entrée de l'interféromètre.

Dans le montage décrit ici, la fente de sortie F_2 a une

longueur de 2 cm et la lentille une distance focale de 45 cm; on obtient: $(l_0 - \bar{l})/l_0 = 1/16000$. Pour un gaz $n - 1 \approx 4 \cdot 10^{-4}$ et l'erreur absolue est du même ordre de grandeur que celle due à l'erreur sur k. En pratique pour les mesures de dispersion où l'on ne cherche pas à obtenir une valeur absolue très précise de l'indice, on pourra donc toujours confondre $\bar{l}$ et l_0.

Influence de la Fonction d'Appareil du Spectromètre. Cas d'une Raie Isolée

Au voisinage d'une raie, l'indice de réfraction et le coefficient d'absorption peuvent varier beaucoup dans le domaine spectral occupé par le faisceau éclairant l'interféromètre. Il en résulte une erreur systématique sur la mesure de la courbe de dispersion dans une raie, qui devient très importante quand la largeur spectrale des fentes du spectromètre atteint l'ordre de grandeur de la largeur de la raie.

On sait que l'énergie $e(\nu)$ tombant sur le récepteur est donnée par l'expression

$$e(\nu) = \int_{-\infty}^{+\infty} i(\nu')\, F(\nu' - \nu)\, d\nu', \tag{6}$$

où $F(\nu' - \nu)$ est la fonction d'appareil du spectromètre réglé sur la fréquence ν, et où $i(\nu')$ est une expression du type (1) ou (5). Ces deux expressions ayant la même forme, le calcul de la déformation de la courbe de dispersion conduit au même résultat, que l'on utilise l'une ou l'autre. En substituant l'expression (1) dans l'équation (6), on obtient

$$e(\nu) = i_0 RT \int_{-\infty}^{+\infty} [1 + e^{-2\chi(\nu')}]\, F(\nu' - \nu)\, d\nu' + 2 i_0 RT \int_{-\infty}^{+\infty} F(\nu' - \nu)\, e^{-\chi(\nu')} \cos \varphi(\nu')\, d\nu'. \tag{7}$$

On a supposé que i_0, R et T sont des constantes dans le domaine où $F(\nu' - \nu)$ a une valeur appréciable; $\varphi(\nu')$ est donné par les relations (2) et (3). Dans l'expression (3), le terme $\delta(\theta)\nu'$ ne varie que très peu dans le domaine d'intégration, car la largeur de fente occupe un domaine spectral qui est toujours très petit devant ν. On peut alors développer cos φ dans l'équation (7) et faire sortir de l'intégrale les termes en $\delta(\theta)\nu'$ en remplaçant ν' par ν. On obtient

$$e(\nu) = i_0 RT \int_{-\infty}^{+\infty} [1 + e^{-2\chi(\nu')}]\, F(\nu' - \nu) d\nu' + 2\, i_0 RT b \cos [\alpha + 2\pi\delta(\theta)\nu] \tag{8}$$

avec

$$b^2 = \left| \int_{-\infty}^{+\infty} F(\nu' - \nu)\, e^{-\chi(\nu')} \cos 4\pi l[n(\nu') - 1]\nu'\, d\nu' \right|^2 + \left| \int_{-\infty}^{+\infty} F(\nu' - \nu)\, e^{-\chi(\nu')} \sin 4\pi l[n(\nu') - 1]\nu'\, d\nu' \right|^2,$$

et

$$\operatorname{tg}\alpha = \frac{\int_{-\infty}^{+\infty} F(\nu' - \nu)\, e^{-\chi(\nu')} \sin 4\pi l[n(\nu') - 1]\, \nu' d\nu'}{\int_{-\infty}^{+\infty} F(\nu' - \nu)\, e^{-\chi(\nu')} \cos 4\pi l[n(\nu') - 1]\, \nu' d\nu'}. \tag{9}$$

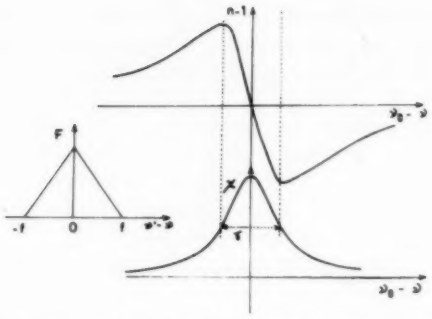

Fig. 2. Indice de réfraction et coefficient d'absorption pour une raie isolée à forme de Lorentz, et fonction d'appareil triangulaire.

L'expression (8) a la même forme que l'équation (1), mais la phase φ est remplacée par une phase apparente $\varphi' = \alpha + 2\pi\delta(\theta)\nu$.

Les mesures permettent de déterminer α et conduisent à calculer l'indice apparent n', en posant

$$\alpha = 4\pi\, l\, (n' - 1)\nu. \tag{10}$$

Le calcul de n à partir de n' dépend donc des formes de la courbe de dispersion, de la courbe d'absorption et de la fonction d'appareil.

Nous avons envisagé le cas suivant qui représente souvent une bonne approximation de la réalité:

On mesure une raie isolée ayant un profil de Lorentz. La dispersion est donnée par

$$n(\nu') - 1 = \frac{S}{4\pi^2 \nu_0} \cdot \frac{\nu_0 - \nu'}{(\nu_0 - \nu')^2 + \gamma^2/4}, \tag{11}$$

où S est l'intensité de la raie (ou force d'oscillateur) exprimée en $\mathrm{cm^{-2}\ atm^{-1}}$. La fréquence au centre de la raie est ν_0 et la largeur de raie à mi-hauteur est γ.

Le coefficient d'absorption est donné par

$$\chi(\nu') = \frac{l\, \gamma\, S}{2\pi} \cdot \frac{1}{(\nu_0 - \nu')^2 + \gamma^2/4}. \tag{12}$$

La fonction d'appareil est une fonction triangulaire:

$$F(\nu' - \nu) = f - |\nu' - \nu| \quad \text{si } 0 < |\nu' - \nu| < f$$
$$= 0 \text{ ailleurs}, \tag{13}$$

où f est la largeur de fente spectrale.

Les trois fonctions $n(\nu') - 1$, $\chi(\nu')$ et $F(\nu' - \nu)$ sont représentées sur la Fig. 2.

Il est commode d'utiliser comme unité de fréquence la demi-largeur de raie $\gamma/2$ et d'introduire les variables réduites:

$$u = 2(\nu_0 - \nu)/\gamma$$

et

$$v = 2(\nu - \nu')/\gamma,$$

ainsi que le paramètre suivant:

$$A = 2lS/\pi\gamma,$$

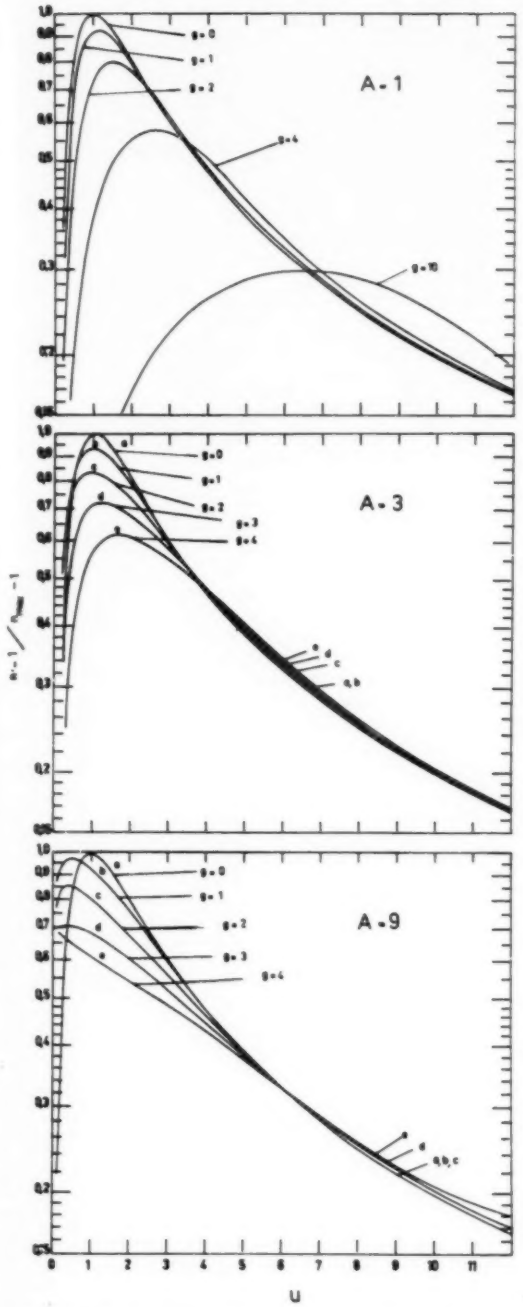

Fig. 3. Courbes de dispersion théoriques déformées par la fonction d'appareil et tracées en variables réduites. Pour $g = 0$ il n'y a pas de déformation quelque soit A.

où A est égal à la variation maximum de phase dans la raie et à la valeur maximum du coefficient d'absorption.

Appelons g la largeur de fente exprimée en demi-largeur de raie,

$$g = 2f/\gamma,$$

et introduisons la valeur maximum de l'indice, obtenue pour $\nu_0 - \nu' = \gamma/2$, soit

$$n_{\max} - 1 = S/4\pi^2\nu_0\gamma.$$

Avec ces nouvelles notations et d'après (9), (10), (11), (12), et (13) on obtient pour l'indice apparent, en confondant ν et ν_0 dans (10),

$$\frac{n'(u) - 1}{n_{\max} - 1} =$$

$$\frac{2}{A}\operatorname{arctg}\frac{\displaystyle\int_{-g}^{+g}(g - |v|)e^{-\frac{A}{(u+v)^2+1}}\sin A\left[\frac{u+v}{(u+v)^2+1}\right]dv}{\displaystyle\int_{-g}^{+g}(g - |v|)e^{-\frac{A}{(u+v)^2+1}}\cos A\left[\frac{u+v}{(u+v)^2+1}\right]dv}.$$

Cette expression ne dépend que des deux paramètres sans dimension A et g.

Les intégrales ne semblent pas pouvoir être ramenées à un type connu. Il est donc nécessaire de les calculer numériquement. Cependant pour les petites valeurs de g on peut effectuer un développement en série des intégrales au voisinage de $g = 0$. Ce calcul, qui ne présente aucune difficulté, conduit à un résultat obtenu ailleurs.[3] Il s'écrit avec les notations utilisées ici:

$$\frac{n' - 1}{n_{\max} - 1} = \frac{2u}{u^2+1}\left[1 - \left(2A\,\frac{u^2-1}{u^2+1} - u^2 + 3\right)\frac{g^2}{6(u^2+1)^2} + \ldots\right].$$

Cette formule donne une bonne approximation tant que g^2/u^4 reste petit.

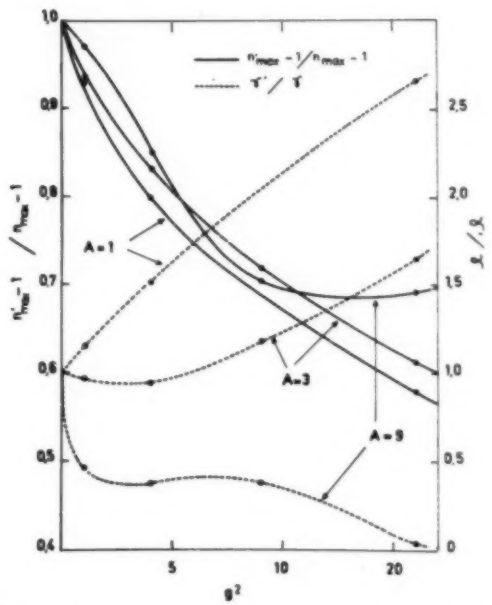

Fig. 4. Variation du maximum de la courbe de dispersion déformée et de la largeur apparente de la raie en fonction d g^2.

Pour g grand, le calcul numérique rigoureux a été effectué pour quelques valeurs de g et de A sur un ordinateur I.B.M. 1620 La détermination convenable de la fonction arctg a été trouvée par continuité à partir des régions où la déformation est faible.

Les résultats sont portés sur la Fig. 3 pour $u > 0$. Les courbes pour $u < 0$ sont symétriques de celles-ci par rapport à l'origine.

Pour $A = 1$, la courbe de dispersion théorique ($g = 0$) subit une déformation régulière, analogue à celle que l'on observe sur la courbe du coefficient d'absorption de la raie. Pour $A = 3$ le maximum de la courbe de dispersion décroît moins vite quand g croît que pour $A = 1$, et au début la largeur apparente de la raie reste presque constante. Pour $A = 9$ le maximum décroît irrégulièrement, et ce qui est assez surprenant, la largeur de la raie décroît fortement et s'annulle presque pour $g = 4$. Sur la Fig. 4 sont montrées les courbes $(n'_{\max} - 1)/(n_{\max} - 1)$ et γ'/γ, largeur apparente de la raie rapportée à la largeur vraie, en fonction de g^2. $(n_{\max} - 1)$ et γ étant deux grandeurs importantes, il est utile de rechercher les meilleures conditions expérimentales pour les déterminer. Au voisinage des extrema de la courbe de dispersion trois conditions doivent être remplies, dans la mesure du possible: 1° correction de largeur de fente faible, 2° bon contraste des franges, 3° grande variation de l'ordre d'interférence d'un extremum à l'autre. Dans le cas d'une raie fine, il faut choisir une largeur de fente aussi réduite que possible, afin d'avoir un facteur g faible. D'autre part, le paramètre A peut être choisi à volonté entre certaines limites puisqu'il est proportionnel à la longueur de cuve, et l'examen des figures 3 et 4 montre que la déformation de la courbe de dispersion est la plus faible pour $A \approx 3$. Les conditions 2 et 3 ne sont pas indépendantes; en effet, on peut admettre raisonnablement que la précision du pointé des franges est proportionnelle à la visibilité* définie par la relation:

$$V = \frac{i_{\max} - i_{\min}}{i_{\max} + i_{\min}}.$$

En supposant pour simplifier que la visibilité n'est pas affectée par la largeur de fente, elle s'écrit d'après (1):

$$V = 2e^{-x}/(1 + e^{-2x}).$$

Aux extrema de la courbe de dispersion on a $\chi = A/2$ et la visibilité est alors en ces points:

$$V = 2e^{-A/2}/(1 + e^{-A}).$$

* On admet que l'erreur sur la position d'une frange est proportionnelle à la moyenne du bruit de fond dans la frange, donc à $i_{\max} + i_{\min}$, et inversement proportionnelle à l'amplitude de la frange: $i_{\max} - i_{\min}$.

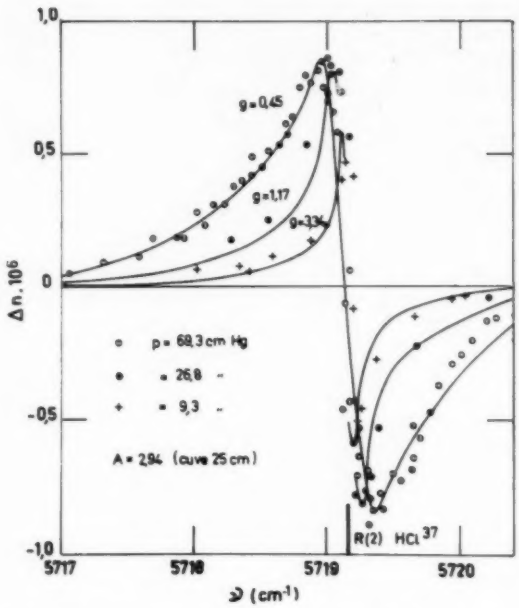

Fig. 5. Résultats expérimentaux dans la raie $R(2)$ de HCl^{37}. Les courbes théoriques déformées ont été déterminées pour $S_0 = 8.93\ 10^{-2}\ cm^{-2}\ (atm\ 300°K)^{-1}$, $\gamma_0 = 0.483\ cm^{-1}\ (atm\ 300°K)^{-1}$, $f = 0.1\ cm^{-1}$, $l = 25$ cm. A la pression de 69.3 cm, les courbes théoriques déformées et non déformées sont presque indiscernables.

La variation maximum d'indice $\Delta n_{\max}$ est proportionnelle à A. L'erreur relative sur $\Delta n_{\max}$ sera donc inversement proportionnelle à A et donc au total inversement proportionnelle à $A\ V$, d'où l'on déduit que le meilleur compromis entre les conditions 2 et 3 correspond au maximum de la fonction $Ae^{-A/2}/(1 + e^{-A})$. Ce maximum est atteint pour $A = 2.4$ et, comme la fonction varie très peu entre 2 et 3, on peut admettre que le meilleur compromis entre les conditions 1 , 2, et 3 se trouve réalisé pour les valeurs de A situées entre 2.5 et 3.

Pour la courbe de dispersion loin de la zone anomale, ces conditions ne sont plus valables , car la déformation devient très faible et peu influencée par A. Il est alors avantageux d'utiliser la plus grande longueur de cuve compatible avec le maintien d'un bon contraste.

Premiers Résultats Expérimentaux

Afin d'éprouver les performances de l'appareillage la dispersion a été mesurée dans les raies $R(2)$ de la première harmonique de HCl . Le résultat pour la raie due à HCl^{37} est montré sur la Fig. 5.

Le spectromètre était équipé du réseau à 600 traits/mm utilisé dans le premier ordre, la largeur de fente était d'environ 0.1 cm^{-1} et la longueur de cuve de 25 cm dans le centre de la raie et 100 cm dans les ailes. Le détecteur était une cellule PbS refroidie et la source un arc concentré au Zr. Les mesures ont été faites

par la deuxième méthode, à trois pressions différentes. En admettant que la courbe de dispersion a une forme de Lorentz et que la largeur et l'intensité de la raie sont proportionnelles à la pression, à chaque valeur de p correspond une valeur de g aisée à déterminer, soit $g = (2f/\gamma_0)(76/p)$. La valeur de A est indépendante de la pression et est donnée par: $A = 2lS_0/\gamma_0$, où S_0 est l'intensité intégrée à la pression atmosphérique.

Les points expérimentaux ont été portés sur le graphique sans correction de largeur de raie et les courbes théoriques ont été calculées en tenant compte de la déformation due à la largeur de raie et déterminées par interpolation entre les courbes de la Fig. 3.* On voit que l'étude théorique des effets de la largeur de fente rend assez bien compte des résultats expérimentaux. La légère différence entre la théorie et l'expérience que l'on observe aux extrema de la courbe de dispersion à faible pression peut s'interpréter en tenant compte de l'élargissement par effet Doppler. Une étude plus complète des résultats obtenus dans le doublet $R(2)$ de HCl est réservée à une publication ultérieure.

* Il a également été tenu compte de l'influence des autres raies de la bande et en particulier de $R(2)$ de HCl^{35}.

Les auteurs experiment leurs remerciements à M. le Professeur Barchewitz pour ses conseils et les facilités qu'il leur a accordées pour la réalisation du montage expérimental. Ils souhaitent également remercier MM. Chauvin et Lévy de la compagnie I.B.M. France grâce auxquels les calculs numériques ont pu être effectués.

Bibliographie

1. J. H. Jaffe, *Advances in Spectroscopy* (Interscience, New York, 1961),Vol. II, p. 263.
2. F. Legay, Thèse, Cahiers phys. **11,** 383 (1957); **12,** 8 (1958).
3. F. Legay, Rev. optique **37,** 11 (1958).
4. Y. Cornet, C. Haeusler, et P. Barchewitz, Compt. rend. **248,** 3290 (1959); C. Haeusler, Y. Cornet, et P. Barchewitz, J. Phys. Radium **21,** 809 (1960).
5. J. N. Shearer et T. A. Wiggins, J. Opt. Soc. Am. **45,** 133 (1955).

Meeting Reports

International Advisory Committee on the Definition of the Meter, Sèvres, France, October 8–10, 1962

Reported by K. M. Baird, NRC Canada

The International Advisory Committee on the Definition of the Meter met at the International Bureau of Weights and Measures at Sèvres, France, in connection with the objectives set out by the Eleventh General Conference of Weights and Measures in 1960, viz: (1) To establish instructions for the practical realization of the new definition of the meter (in terms of the 0.606-μ line of Kr-86), (2) To choose secondary wavelength standards for interferometric length measurement and to establish instructions for their use, and (3) To pursue studies with a view to improving length standards. The meeting was attended by representatives of the major national laboratories and of the I.A.U. and certain other invited specialists.

The meeting marked a departure from the usual procedure of advisory committees of the International Committee of Weights and Measures in that the first two days were devoted to a series of invited talks by specialists, which were followed by discussions; the business of establishing formal recommendations was conducted rapidly on the third day, with the advantage of following the quite thorough treatment of the technical aspects during the first two days. The talks were *The Symmetry of the Spectral Profile*—W. R. C. Rowley, *The Standard Radiation for the Definition of the Meter*—J. Terrien, *Secondary Wavelength Standards*—E. Engelhard, *Wavelength Standards from Atomic Beams and Zeeman Filters*—K. G. Kessler, *Absorption Lines*—R. Lennuier, *Lasers*—P. Connes, and *Interference Comparators*—K. M. Baird. In addition, over twenty reports were submitted by the delegates; these, however, were given by title only.

The meeting passed two resolutions: one recommended specifications for Kr-86, Hg-198, and Cd-114 sources and gave the values of the wavelengths for four radiations (in the visible) for each source; the other concluded that experimental evidence presented confirmed the superiority of the 0.606-μ line Kr-86 as the primary standard and made recommendations concerning research aimed at possible improvement of the primary standard.

A report of the meeting and of the talks and a number of the reports will be published in the Procès Verbaux du Committee International des Poids et Mesures for 1962.

Interdisciplinary Conference on Electromagnetic Scattering, Clarkson College of Technology, Potsdam, N. Y., August 13–15, 1962

Reported by C. C. Grosjean, University of Ghent, and P. Swings, Smithsonian Astrophysical Observatory*

It is commonly assumed that research in modern experimental physics or chemistry requires big and expensive instrumentation. Happily there are still fertile domains which lead to important scientific results with fairly inexpensive laboratory installations. Electromagnetic scattering is one such field. When conducted with great care and guided by solid theoretical considerations, experiments on electromagnetic scattering may still be as rich a source of valuable information as they were at the time of the pioneering endeavors of Peter Debye and others, a few decades ago. Besides their classical applications to chemistry, especially to colloids, the scattering phenomena have become of the utmost significance in many other fields, such as astronomy, aeronomy, meteorology, radar phenomena, solid-state physics, biology, etc.; the variation involved goes from the x rays to the radio waves. Obviously, the interpretation of these applications has required elaborate theoretical investigations which, in most cases, have received considerable impetus from the availability of the modern electronic computers.

* On leave from University of Liège.

It is to the credit of Milton Kerker, chairman of the Chemistry Department at the Clarkson College of Technology, to have realized fully the importance of gathering representatives of the scientific disciplines in which scattering phenomena play a role. To all the participants the conference was a source of inspiration, as it opened vistas into widely different disciplines, often in quite unexpected directions. The volume of Proceedings, which will include the discussions, will be a most valuable source book to many research people in very diverse fields when it is published. The audience was truly international: among the 150 registrants there were scientists from Austria, Belgium, Canada, France, Germany, Israel, Japan, the Netherlands, the United Kingdom, and the U.S.A. The success of ICES is partly due to the participation—and for this Dr. Kerker should be congratulated also—of two senior leaders in the field, Peter Debye and Victor K. La Mer. Of great value also was the presence of a younger specialist, H. C. van de Hulst, whose thorough and encyclopedic knowledge of the problem of scattering is illustrated by his classical book on this topic.

Thirty-five papers were read; they were followed by extremely lively discussions in which Drs. Debye and La Mer played an especially active role. Enthusiastic young research people were quite active too in these discussions. One of them (Richard S. Stein) claimed to be a student of Ziman, who had been a student of La Mer, who had been a student of Debye. Possibly he could have gone on, mentioning Einstein or Smoluchowski or, in the other direction, speaking of his own students at the University of Massachusetts! These 35 papers are discussed below, grouped by session.

The authors of the first nine papers were physicists or chemists, and their work was mainly concerned with the general problem of scattering of visible light by spherical or cylindrical particles, nonhomogeneous spheres, nonuniform objects, cubic or octahedral or irregular particles, including particles larger than the wavelength. One paper discussed the scattering of microwaves by spherical particles. The Mie theory was in the forefront. More than twelve centers have compiled elaborate tables of the Mie functions for real or complex indices of refraction, with the help of electronic computers, and discussion arose—in serious and facetious terms—about the usefulness of all these compilations. Surely they cannot be published in extenso; sometime a small symposium should be devoted to a discussion of the best way to place these tables of Mie functions at the disposal of the users who wish to determine particle sizes and indices, or other characteristics. The Rayleigh-Gans approximation was also discussed, in addition to the exact theories as applied to specific cases.

A second group of seven papers was contributed by astronomers or aeronomists, and the scattering by nonspherical particles was again discussed, including extreme cases such as zinc oxide crystals consisting of four needles originating from a common junction. The astronomers considered mainly the role of small particles in the solar *F*-corona, the zodiacal cloud, the comets, the planets (Venus and Jupiter), and the interstellar space. Pending the launching of comet probes the only way to gather information on the small cometary particles is by measurement of the spectral distribution of the intensity and polarization of the scattered solar continuum of cometary heads or tails. The aeronomists and meteorologists discussed applications to atmospheric problems, including measurements with the help of searchlights. Important considerations on the atmospheric nonabsorbing and partially absorbing suspensions were discussed, with applications to phenomena associated with fog: aureole, rainbow, and counter corona. The role played by the atmospheric aerosols was considered and the interest of observations from high-altitude balloons was clearly demonstrated.

A series of five papers was devoted to light scattering in solutions: dilute solutions of high polymers; non-Gaussian macromolecular coils; electrolyte solutions containing charged colloidal particles; nonideal solutions; biological systems (light and x-ray scattering). The amount of important information which may thus be obtained with fairly simple scattering experiments is truly amazing.

The afternoon session of August 14 was devoted to microwave and radio-wave scattering in the atmosphere. It was considerably shortened because of a ceremony during which the Honorary Degree of Doctor of Science was conferred on Debye, La Mer, and Van De Hulst in recognition of their outstanding contributions to the field of electromagnetic scattering. The first paper presented explained how large spheres of low refractive index can sometimes exhibit an extremely large radar cross section. Clever experimentation with a plexiglass sphere covered by a metal cap at its rear pole has confirmed the importance of the so-called "glory" ray in the phenomenon under consideration. Back scattering cross sections based on simple theoretical calculations were presented. The other two papers were concerned with the exploration of atmospheric structure by means of radio wave scattering. It was shown how the electromagnetic field singly scattered by a medium with irregular dielectric structure is directly related to the three-dimensional Fourier transform of the dielectric space function. The theoretical results, however idealized they might be, were proven to be of fundamental importance in the experimental determination of various structural properties of the troposphere. The authors of the last paper were able to account in a satisfactory way for the ensemble of experimental results obtained in transhorizon, tropospheric propagation. This afternoon session was generally found particularly enjoyable because the authors presented their work with a degree of clarity rarely encountered in highly specialized communications of only 20 minutes duration.

Interactions in solids and liquids was the general topic of a session under the chairmanship of Dr. La Mer. In a clear and very instructive introductory talk on light scattering and molecular forces, Dr. Debye presented a general discussion of work by Smoluchowski, Einstein, Ornstein-Zernike, Brillouin, and others, besides referring to his own contributions. He stressed the significant role played in these studies by the so-called correlation function for scattering in irregular media. The next paper outlined the importance of electromagnetic scattering as a tool for investigating critical phenomena. After a brief review of recent literature, experimental low-angle x-ray measurements were reported for the nitrobenzene-n-heptane system near the critical temperature and at the critical composition. The results do not appear in full agreement with the Ornstein-Zernike theory, but the data suggest that further measurements at small angles are necessary before any definite conclusion about real discrepancies can be drawn. The communication that followed was the only one in the entire conference on which no questions were raised or comments made. Dealing with optical extinction by metal precipitates in semiconductors and insulators it probably fell too far outside the range of subjects of immediate interest to anyone in the audience. The remaining papers of the sessions were concerned with the use of electromagnetic scattering as a means of detecting and measuring heterogeneities and elastic strains in media. It was shown how a multitude of qualitative and quantitative data on crystalline polymeric solids can be obtained from a great variety of well-designed scattering experiments involving polarized as well as unpolarized incident light. Here, the refractive index differences are usually so small that the Rayleigh approximation may be used. Further, the importance of absolute intensity measurements in x-ray small-angle scattering, caused by inhomogeneities of colloidal magnitude in electron densities, was pointed out in

Continued on page 507

A Method of Inferring Single-Path Band Transmission Factors from Double-Path Measurements

M. A. McKiernan and H. W. Wessely

Assuming rectilinear propagation in a linearly stratified medium, a method of estimating single-path band transmission factors from double-path measurements is described. Precise analytical bounds for the uncertainty in the estimates are derived.

I. Introduction

In making transmission measurements over long paths it is frequently desirable to use a double-path rather than a single-path experimental arrangement. The outstanding advantage of the double-path arrangement, of course, is that the source and the spectrometer are in the same location and hence under close control at all times.

The great shortcoming of the double-path type of experiment, however, is that for an inhomogeneous medium there is apparently no way of exactly inferring the single-path transmission from double-path data. Since it is often the single-path transmission which is of interest, the question naturally arises as to whether any reasonably accurate estimate of the single-path transmission can be made from double-path data.

This paper describes a method of making such an estimate based on only two assumptions:

1. The medium is linearly stratified, i.e., it consists of parallel plane layers.
2. The ray paths are essentially straight lines.

II. Basic Formulation

Consider a horizontally stratified medium whose spectral absorption coefficient at any altitude y is described by a function $k(y,\lambda)$, in which λ is the wavelength (see Fig. 1). If a source of uniform spectral intensity I_0 is located at P, then for a path making an angle θ with the vertical, the incremental change in the spectral intensity $\Delta I(y,\lambda)$ at the altitude y for an incremental path Δs is approximately

$$\Delta I(y,\lambda) = -k(y,\lambda)\, I(y,\lambda)\Delta s. \tag{1}$$

Since

$$\Delta y = \Delta s \cos\theta, \tag{2}$$

and

$$I(0,\lambda) = I_0,$$

one easily obtains the well-known result for the spectral intensity at any height h,

$$I(h,\lambda) = I_0 \exp\left[-\sec\theta \int_0^h k(y,\lambda)\ dy\right]. \tag{3}$$

The radiative power in a spectral band $\Delta\lambda$ that would be measured by a spectrometer placed at the height h is simply

$$\int_{\Delta\lambda} I(h,\lambda)\, d\lambda = I_0 \int_{\Delta\lambda} \exp\left[-\sec\theta \int_0^h k(y,\lambda)\, dy\right] d\lambda. \tag{4}$$

The single-path band transmission factor, $T_1(h,\theta,\Delta\lambda)$, for the height h and the angle θ is then

$$T_1(h,\theta,\Delta\lambda) = \frac{1}{\Delta\lambda}\int_{\Delta\lambda} \exp\left[-\sec\theta \int_0^h k(y,\lambda)\, dy\right] d\lambda. \tag{5}$$

Now suppose that the spectrometer at height h is replaced with a retroreflector, and that the spectrometer is moved to P to measure the reflected radiation. It is easy to see that the double-path band transmission factor, $T_2(h,\theta,\Delta\lambda)$, is simply

$$T_2(h,\theta,\Delta\lambda) = \frac{1}{\Delta\lambda}\int_{\Delta\lambda} \exp\left[-2\sec\theta \int_0^h k(y,\lambda)\, dy\right] d\lambda. \tag{6}$$

III. Inferring Double-Path Values from Single-Path Data

If the problem were to infer double-path transmission factors from single-path data, the desired inference

The authors were both at the Laboratories for Applied Sciences, The University of Chicago, Chicago 37, Illinois. H. W. Wessely is now with Aerospace Corporation, El Segundo, California.

Received 7 May 1962.

This work was sponsored by the Air Force Cambridge Research Laboratories with funds from the Advanced Research Projects Agency.

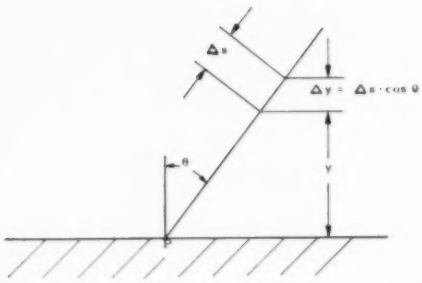

Fig. 1. Slant path transmission in a linearly stratified medium.

could be made directly. Suppose, for example, one wished to know the double-path transmission factor for a vertical path. The desired quantity, therefore, is

$$T_2(h, 0, \Delta\lambda) = \frac{1}{\Delta\lambda}\int_{\Delta\lambda} \exp\left[-2\int_0^h k(y,\lambda)\,dy\right]d\lambda. \quad (7)$$

But this is nothing else than the single-path transmission factor for $\theta = 60°$. Thus, since $\sec 60° = 2$,

$$T_1(h, 60°, \Delta\lambda) = \frac{1}{\Delta\lambda}\int_{\Delta\lambda} \exp\left[-2\int_0^h k(y,\lambda)\,dy\right]d\lambda = T_2(h, 0, \Delta\lambda). \quad (8)$$

Hence, in order to obtain the double-path transmission factor for a vertical path, one simply measures the single-path transmission factor for an inclination angle of 60°.

More generally, if one desires to know the double-path transmission factor for an inclination angle θ_2, one simply measures the single-path transmission factor for an angle θ_1 such that

$$\sec\theta_2 = 2\sec\theta_1. \quad (9)$$

IV. Inferring Single-Path Values from Double-Path Data

It is clear from the preceding section that the single-path transmission factors for slant angles greater than or equal to 60° can be inferred directly from the double-path data. If one simply pairs the double-path slant angles, θ_2, with the single-path slant angles, θ_1, in accord with Eq. (9), then

$$T_1(h, \theta_2, \Delta\lambda) = T_2(h, \theta_1, \Delta\lambda). \quad (10)$$

The problem now reduces to finding the single-path transmission factors for slant angles less than 60°. For these angles there is apparently no way of making direct interferences from the double-path data alone, but remarkably good estimates can be made by using a simple analytical extrapolation procedure.

To illustrate this procedure qualitatively, consider the generalized transmission factor, T, defined by

$$T(h, p, \Delta\lambda) = \frac{1}{\Delta\lambda}\int_{\Delta\lambda} \exp\left[-p\int_0^h k(y,\lambda)\,dy\right]d\lambda. \quad (11)$$

It follows from the definition of the generalized transmission factor that

$$T(h, 0, \Delta\lambda) = 1. \quad (12)$$

Since for double-path measurements,

$$p = 2\sec\theta, \quad (13)$$

it is clear that the values of the generalized transmission factor for $p \geqslant 2$ are given directly by the double-path data. These values are shown as the solid portion of the curve in Fig. 2. Thus, the only unknown portion of the curve is that having the domain

$$0 < p < 2. \quad (14)$$

Now for single-path transmission,

$$p = \sec\theta, \quad (15)$$

for which the domain of T is evidently $p \geqslant 1$. Hence, the only unknown portion of the curve which is of physical interest is that having the domain

$$1 \leqslant p < 2. \quad (16)$$

Since the generalized transmission factor is a smoothly varying function of p, an estimate of its behavior in this interval can be obtained by extrapolating the known curve for $p \geqslant 2$ to the unit point at $p = 0$.

V. Upper and Lower Bounds

The problem now is to put the extrapolation procedure on a firm analytical foundation. Two facets to this problem must be recognized. The first has to do with establishing analytical upper and lower bounds for the desired single-path values in terms of the assumed known double-path values. The second has to do with the inaccuracy of these bounds because of the experimental errors made in measuring the double-path values. Of these two facets it is clear that the establishment of analytical bounds constitutes the real problem, since, once it is solved, a straightforward application of the calculus of errors is all that is needed to determine the inaccuracy of the bounds.

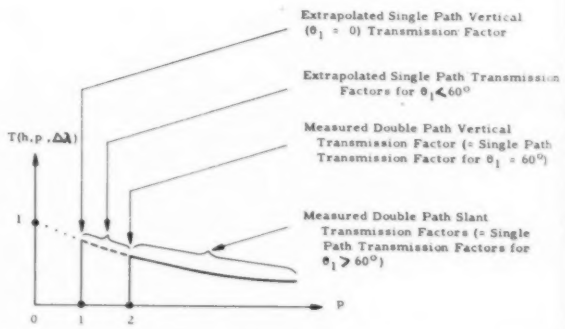

Fig. 2. Graphical representation of the generalized transmi sion factor.

This proves to be a very interesting analytical problem. Although a variety of useful bounds have already been established, the problem of establishing *optimum* bounds, i.e., least upper and greatest lower bounds, still resists a general solution. Nevertheless, the results thus far obtained indicate that from only a few, say, two or three, double-path measurements made at various slant angles, is the uncertainty in the estimated single-path values based on the analytical bounds probably less than the experimental error that would be made if the single-path transmission were measured directly. In fact, for the limiting situation where the double-path transmission is precisely known for an arbitrarily large number of slant angles, it is shown that the single-path values can be predicted with an arbitrarily small error.

In the following only the "better" bounds are presented. It is not claimed that these bounds are optimal, but it is strongly suspected that further analysis will show that this is indeed so.

In the following discussion the altitude, h, and the spectral interval, $\Delta\lambda$, are assumed constant. With this in mind, the somewhat simpler notation of $T(p)$ is henceforth used to denote the generalized transmission factor defined by Eq. (11).

One-Point Bounds

Suppose that the double-path transmission is known only for the vertical direction, i.e., only $T(2)$ is known. What bounds can be placed on the single-path vertical transmission, i.e., $T(1)$?

An upper bound is immediately furnished by the Schwarz inequality, namely

$$T(1) \leq T^{1/2}(2). \tag{17}$$

Since it is clear from Eq. (11) that the generalized transmission factor is a nonincreasing function of p, a lower bound for the single-path transmission is evidently

$$T(1) \geq T(2). \tag{18}$$

Thus, combining these two bounds,

$$T(2) \leq T(1) \leq T^{1/2}(2). \tag{19}$$

At first sight it seems natural to question the equality condition of Ineq. (18), since it hardly seems possible that the double-path and single-path transmission factors could be identical. From an analytical standpoint, however, this possibility must be admitted. Suppose, for example, that for some fraction of the spectral interval $\Delta\lambda$, the medium is perfectly transparent, i.e., the spectral absorption coefficient is zero, and that over the remainder of the interval the medium is perfectly opaque, i.e., the spectral absorption coefficient is infinite. Then $T(p) =$ constant for all $p \neq 0$. This introduces a discontinuity at $p = 0$ where, of course, $T(0) = 1$, but this does not cause any difficulty. Hence, if only $T(2)$ is known, the best possible lower bound for $T(1)$ is $T(2)$ itself. Furthermore, it is not difficult to show that the best possible upper bound for $T(1)$ is $T^{1/2}(2)$. Thus, Ineq. (19) actually gives the optimum bounds for $T(1)$ when only $T(2)$ is known.

It is interesting to note that the maximum uncertainty in $T(1)$ occurs when $T(2) = {}^1/_4$. In this case Ineq. (19) reduced to

$$1/4 \leq T(1) \leq 1/2.$$

Thus, neglecting experimental errors, the maximum uncertainty in $T(1)$ is $\pm {}^1/_8$.

The discussion thus far has been restricted to obtaining bounds for $T(1)$ in terms of $T(2)$. To generalize the discussion suppose now that the generalized transmission factor is known at a single arbitrary point $p_1 \neq 0$. What general bounds can be prescribed for $T(p)$ in terms of the only available knowledge, viz., $T(p_1)$?

There are at least two ways of treating this question: One is based on the Holder inequality,[1] and the other is based on the idea of logarithmic convexity.[2] Since for the specific results to be presented the Holder inequality offers the more direct approach, only that approach is described here.

The Holder inequality states that

$$\left|\int fg\right| \leq \left[\int |f|^\delta\right]^{1/\delta}\left[\int |g|^\beta\right]^{1/\beta} \tag{20}$$

where δ and β are any pair of positive numbers such that ${}^1/_\delta + {}^1/_\beta = 1$, and f and g are any pair of functions for which the integrals in Ineq. (20) exist.

To apply this inequality let

$$f = \exp\left[-p\int_0^h k(y,\lambda)dy\right], \tag{21}$$

and

$$g = 1.$$

With the understanding that the integration in Ineq. (20) covers the interval $\Delta\lambda$, substitution of Eqs. (21) into Ineq. (20) and division by $\Delta\lambda$ yields

$$T(p) \leq T^{1/\delta}(\delta p). \tag{22}$$

Inequality (22) holds for any p and for any $\delta > 1$.

Now suppose that the generalized transmission factor is known at p_1. If in Ineq. (22) p is replaced by p_1, and δp_1 is replaced by p, where now, of course, $p > p_1$, one obtains a lower bound for the generalized transmission for all $p > p_1$. Thus,

$$T^{p/p_1}(p_1) \leq T(p) \qquad (p > p_1). \tag{23}$$

The upper bound for the generalized transmission for $p > p_1$ follows from the nonincreasing character of the generalized transmission. Thus,

$$T(p) \leq T(p_1) \qquad (p > p_1). \tag{24}$$

To obtain bounds for $p < p_1$, let δp in Ineq. (22) be

replaced by p_1. This yields the upper bound

$$T(p) \leq T^{p/p_1}(p_1) \qquad (p < p_1). \tag{25}$$

The lower bound for $p < p_1$ is correspondingly

$$T(p) \geq T(p_1) \qquad (p < p_1). \tag{26}$$

Combining Ineqs. (23) through (26) yields

$$\left.\begin{aligned} &T(p_1) \leq T(p) \leq T^{p/p_1}(p_1) \qquad (p < p_1), \\ &\text{and} \\ &T^{p/p_1}(p_1) \leq T(p) \leq T(p_1) \qquad (p > p_1). \end{aligned}\right\} \tag{27}$$

Two-Point Bounds

Suppose that in addition to knowing the transmission at p_1, the transmission is known at a second point p_2. Because of this additional knowledge, it should be possible to improve the previous bounds which were based upon the knowledge of $T(p_1)$ alone.

To obtain these improved bounds, consider the Holder inequality with

$$\left.\begin{aligned} f &= \exp\left[-u\int_0^h k(y,\lambda)d\lambda\right] \\ &\text{and} \\ g &= \exp\left[-v\int_0^h k(y,\lambda)d\lambda\right] \end{aligned}\right\}, \tag{28}$$

where u and v are any pair of positive numbers. Substituting Eqs. (28) into Ineq. (20) one obtains

$$T(u + v) \leq T^{1/\delta}(\delta u)T^{1/\beta}(\beta v). \tag{29}$$

To apply this inequality, suppose, for example, that $\beta v = 3$, $\delta u = 1$, and $u + v = 2$. For these choices it is clear that $\delta = \beta = 2$ and, hence, Ineq. (29) reduces to

$$T(1) \geq T^{\frac{1}{2}}(2)T^{-1}(3). \tag{30}$$

Since $T(2)T^{-1}(3) \geq 1$, it is clear that Ineq. (30) constitutes a better lower bound for $T(1)$ than that given by Ineq. (18), namely, $T(2)$.

The generalization of this result is straightforward. If the generalized transmission is known at a pair of points p_1 and p_2, where $p_2 > p_1 \neq 0$, say, then it can be shown that

$$\left.\begin{aligned} &T(p) \geq T^{(p_2-p)/(p_2-p_1)}(p_1)T^{(p-p_1)/(p_2-p_1)}(p_2), \\ &\qquad (p < p_1) \text{ or } (p > p_2), \\ &\text{and} \\ &T(p) \leq T^{(p_2-p)/(p_2-p_1)}(p_1)\ T^{(p-p_1)/(p_2-p_1)}(p_2), \\ &\qquad (p_1 < p < p_2). \end{aligned}\right\} \tag{31}$$

Thus, Ineq. (31) furnishes a lower bound for the generalized transmission for values of p outside the interval (p_1, p_2) and an upper bound for values of p inside the interval (p_1, p_2).

The next step in the discussion, obviously, should be the determination of an upper bound when p is outside (p_1, p_2) and a lower bound when p is inside (p_1, p_2). Regrettably, at this writing the general solution to this problem is still unknown. Only a special result has thus far been obtained.

Suppose that the generalized transmission is known at $p = 2$ and at $p = 3$. Consider the Holder inequality with $\delta = \beta = 2$, and with

$$f = \exp\left[-\int_0^h k(y,\lambda)d\lambda\right]\left\{1 - \exp\left[-\int_0^h k(y,\lambda)d\lambda\right]\right\}^{1/2}, \tag{32}$$

and

$$g = \left\{1 - \exp\left[-\int_0^h k(y,\lambda)d\lambda\right]\right\}^{1/2}.$$

Substituting Eqs. (32) into Ineq. (20), one obtains, after a few simple manipulations,

$$[T(1) - T(2)]^2 \leq [T(2) - T(3)]\cdot[1 - T(1)].$$

Solving for $T(1)$, one obtains

$$T(1) \leq \frac{T(2) + T(3) + \sqrt{[T(2) + T(3)]^2 - 4[T^2(2) - T(2) + T(3)}}{2}. \tag{33}$$

An estimate of the accuracy of the estimates of $T(1)$ based on measurements of $T(2)$ and $T(3)$ can now be made. Numerical calculations using Ineqs. (30) and (33) show that the maximum uncertainty in $T(1)$ occurs when $T(2) \approx 0.22$, and $T(3) \approx 0.18$. Using these results, the maximum uncertainty in $T(1)$ is approximately ± 0.05.

Lower Bounds Based on Taylor's Theorem

It is interesting to note that Taylor's theorem furnishes a set of lower bounds which analytically can be made to differ from the true value of the generalized transmission by an arbitrarily small amount.

From Taylor's theorem

$$T(p) - \sum_{n=0}^{N} T^{(n)}(p)\frac{(p-2)^n}{n!} = T^{(n+1)}(p')\frac{(p-2)^{N+1}}{(N+1)!} \tag{34}$$

in which p' lies between p and $p - 2$.

It is clear from Eq. (11) that the derivatives of T with respect to p alternate in sign. When n is odd (even), the nth derivative is negative (positive). The same alternation occurs for $(p-2)^n$ for $p < 2$. Hence, every term in the Taylor expansion for $p < 2$, including in particular the remainder term, is nonnegative. Therefore, for $p < 2$, and for every N,

$$T(p) \geq \sum_{n=0}^{N} T^{(n)}(2)\frac{(p-2)^n}{n!}. \tag{35}$$

Statement of the General *N*-Point Problem

It should be apparent that the preceding analysis represents a beginning, but by no means a complete

treatment of the problem. The real problem is the establishment of *optimum* bounds for *any finite number* of double-path transmission measurements, whereas the bulk of the preceding analysis merely considers bounds based on one and two measurements of the double-path transmission. Moreover, the question of the optimity of the bounds has been almost completely neglected.

In the hope that other analysts may become interested in this problem, a restatement of the general problem in purely analytical terms is given below. The physicist will recognize that no essential features have been lost in this restatement.

Problem: Consider the class of functions $0 \leq f \leq 1$ sectionally continuous on the closed interval $[a, b]$. Given a finite set of pairs of numbers (p_i, A_i), $i = 1, 2, \ldots n$, where $p_i \geq 2$, and

$$A_i = \int_a^b f^{p_i}(x)dx,$$

find the absolute maximum and minimum of

$$\int_a^b f^p(x)dx$$

for $1 \leq p < 2$.

References

1. L. M. Graves, *The Theory of Functions of a Real Variable*, 2nd ed. (McGraw-Hill, New York, 1956), p. 233.
2. R. Courant, *Differential and Integral Calculus* (Interscience, New York, 1948), Vol. II, pp. 325–330.

Meeting Reports *continued from page 502*

connection with the determination of the masses of the geometrical structures constituting the scattering units. Finally, it was also shown, by treating the influence of elastic strains on the components of scattered light of various polarizations with the aid of Fourier transform methods, that the effect of such strains can be separated from the influence of size and shape of the scattering regions. Some possible generalizations of this theory have been discussed.

The final afternoon session of the conference was devoted to multiple scattering, and one of the authors of this report (C.C.G.) presented the introductory talk on recent progress in the development of a new approximate general theory of multiple scattering. After a brief review of his 1956 approximation, he outlined the fundamental ideas and formulas underlying his newest analytical approximate formalism endowed with a set of interesting properties among which the applicability to problems involving any type of nonisotropic single-scattering law with axial symmetry around the direction of incidence deserves attention. This work was followed by an elegant variable-order diffusion-type approximation for treating isotropic multiple scattering in infinite, semi-infinite and finite geometries. An extension to anisotropic multiple scattering, which would be important, was claimed possible. A paper dealing with multiple scattering of waves in dense distributions of large tenuous scatters came next, which was an extension of previously published papers in which propagation through "gas-like" statistical distributions of scatterers was considered for the purpose of discussing the "bulk" electromagnetic properties of such media and their fluctuations, in terms of elementary scattering processes. The generalization consisted in studying multiple scattering in a system whose population is divided between a "gas-like phase" and a "crystal-like phase," both phases contributing to the coherent field whereas only the gas phase contributes to the incoherent scattering. Fourth in line came an excellent contribution on multiple scattering in media with anisotropic scattering, putting greater emphasis on the polarization effects and constituting a substantial generalization of Chandrasekhar's classical treatment. The session closed with a report on some remarkable mathematical studies concerning the uniqueness of solutions to Chandrasekhar's formulation of principles of invariance in the theory of radiative transfer. It was not only shown that, in many cases, certain equations in this formulation have a definite multiplicity of solutions which had so far been only partially explored, but explicit parametric representations of the families of solutions were generally written down.

We cannot end this report without extending special congratulations to Dr. Kerker and his planning committee, for the magnificent job of organization and coordination which they did, a job that was as delicate as the focusing of light and the alignment of lenses in a complicated scattering experiment.

1962 WESCON Meeting, Los Angeles, August 21–24, 1962

Reported by J. Arndt, Space Technology Laboratories

The 1962 WESCON meeting was held August 21–24 in Los Angeles at the Statler Hilton Hotel and the Los Angeles Sports Arena, the latter requiring a canvas-topped annex to accommodate more than 850 exhibitors. Nearly 50,000 attended the show, making it the largest technical exposition of the year. Some 80 papers were presented in 25 technical sessions, and most of these have since been published in the eight-volume *1962 WESCON Convention Record*.* The WESCON convention was obviously influenced, if not dominated, by the vast missiles and space industry along the west coast from Seattle to San Diego. One paper of widespread interest dealt with interstellar communication on a realistic and quantitative level, correlating probability of contact (with an extrasolar civilization) with expenditure of time and money. Laser demonstrations opened the show, with a laser pulse from the Statler Hotel to the Sports Arena triggering an electronic welcome message. Later, a neoprene balloon was sent aloft when its steel restraining wire was severed by a focused laser beam.

Areas of interest were not constrained to electronics, and only a few papers dealt with any one particular field. Most sessions covered complex systems and techniques encompassing several disciplines at a time. Examples of this are the five "special" sessions of general interest, including "Biological Information Transfer on the Molecular Level," "Research in Nuclear Test Detection," and "Lunar Exploration." A few papers dealt with optical devices in the field of pattern recognition including one paper dealing with an optical decision filter capable of classifying pyramids, spheres, cubes, and ellipsoids, regardless of orientation in three-dimensional space. It is worthy of note since the device represents a working machine based on the "perceptron" approach to pattern recognition developed at Cornell University several years ago.

* Write WESCON, 1435 S. La Cienega Blvd., Los Angeles, California, for further information.

There was an impression that a definite fusion is growing between optics and electronics. The entrance of electronics into the optics field was immediately evidenced by the laser demonstrations. Papers dealing with microwaves, including one paper dealing with a ferrite rotation-field phaser (i.e., a half-wave plate for the X-band), indicated that the fusion is two-directional.

American Physical Society, 1962 Winter Meeting in the West, Stanford, California, December 27–29, 1962

Reported by Jurgen R. Meyer-Arendt, Utah State University

The 1962 Winter meeting of the American Physical Society has been held, in part, jointly with the American Geophysical Union. President Sterling of Stanford University dedicated the new $2.5 million Russell H. Varian Laboratory of Physics. The late R. Varian was a unique character. He had much trouble reading and expressing himself in writing and needed some gentle help to write his master's thesis; but he was an inventive genius, most famous for the klystron, developed in a basement room in the old physics building. The royalties from this invention ($1 million) partly financed the new building.

About 1200 people attended the multiple sessions during which more than 200 papers were presented. Topics ranged from progress reports on the Stanford two-mile linear accelerator to the radioactivity (induced by the van Allen belt) of steel fragments, recovered in Wisconsin while still very hot and believed to be from Sputnik 4. Readers of this journal will be primarily interested in two sessions.

In the session on optical spectroscopy and masers, H. L. Welsh *Toronto*, the teacher of A. L. Schawlow who presided at the session, spoke on "Molecular Interactions in the Raman Spectrum of Hydrogen". The essential point of the lengthy theoretical considerations was that frequency shifts are not due to differences in density alone, but that they depend on the distribution function of the molecules and vibrational perturbations as well. W. L. Faust *Bell Telephone Laboratories* reported on maser spectroscopy in the infrared. The gas laser used has the window end plate inclined at Brewster's angle so that the output beam is partially linearly polarized. The detectors were thermocouples. In xenon, a number of new lines in the infrared were found, some of them described previously in Appl. Phys. Letters **1**, 85–88 (1962), others, such as the 11.3 and 18.5 μ lines, reported here for the first time. The 3.5080 and 5.5754 μ oscillations have a particularly high gain. Some transitions, 2.6276 and 2.6608 μ, in xenon were found to oscillate only with dielectric mirrors as the end plates, not with silver mirrors. Other new lines found were 2.5241 μ in krypton and $\approx$5.40 μ in neon. A xenon line at 47 μ, not yet observed, can be predicted from the energy levels. Xenon has one of the narrowest laser lines which is explained by the fact that the fractional Doppler width $\Delta\nu/\nu$ is inversely proportional to the atomic mass number (xenon = 131). R. W. Hellwarth *Hughes Research Laboratories* discussed giant optical pulses and stimulated Raman scattering. Very high-power, so-called "giant", laser pulses were produced by first pumping up a large population excess in the laser ruby while laser action is quenched by preventing regeneration. This is called Q-spoiling. By suddenly supplying high regeneration (Q-switching), the energy stored in the laser material is converted into coherent light. The convertible amount of energy is $^1/_2\ Nh\nu$, where N is the pumped population excess, h Planck's constant, and ν the laser frequency. The output, in theory, should be 12 joules/cm^3 of pumped ruby. In practice it is less, probably because some of the ruby may not be active. Peak powers of several MW/cm^2, pulse durations of 3 . . . 30 nanosec, and bandwidths of less than $^3/_{10}$ Å were obtained. Giant pulses of this kind have been used for the study of Raman shifts in a number of liquids, some aromatic compounds showing particularly pronounced shifts.

Here may be mentioned a report on laser reflection for the analysis of lunar topography by Ch. H. Wilcox and A. D. Jacobson, given at the concurrent meeting of the AGU in which the use of a giant pulse laser is described for the determination of surface structures on the moon. Height measurements, it was said, could be made to an accuracy of 1.5 m while the areal resolution is about 1.6 km.

N. Bloembergen *Harvard* presented an excellent survey on wave propagation in nonlinear optical media. The problem of coherent induced polarization is usually treated by quantum mechanics but can be reduced to a classical-mechanical problem involving induced dipole moments. The gist of the matter is that light passing through the crystal (actually, only through the last superficial layer of the crystal) consists essentially only of its second harmonic, that is, the light emerging has been doubled in frequency (red to UV), with an efficiency claimed to be as high as 30%. The theoretical aspects of this conversion are quite involved; they are based on the inhomogeneous wave equation, an extension of Maxwell's equations, and certain boundary conditions.

In a second session on light and masers, a total of 15 papers was presented, some of which are reported here. J. L. Emmett and R. W. Hellwarth discussed double pulse excitation of a ruby laser where regular and reproductive pulsations of large amplitude have been obtained from a ruby laser. The ruby is initially pumped in the usual manner by a flash lamp in an elliptical cavity. Shortly after threshold is reached, the same flash lamp is pulsed with 6.5 kV for 15 μsec, producing a peak power output of up to 50 kW. H. P. Broida and G. L. Pollack have studied the spectroscopic absorption of NO in crystalline and liquid krypton. The liquid and crystalline states of rare gases are essentially transparent from the ultraviolet to the infrared. This offers the possibility of obtaining absorption spectra of suitable molecules trapped in the melt or crystal. Absorption spectra, between 2000 and 4100 Å, were shown of krypton +1% NO at temperatures near the krypton triple point (116°K). P. Kisliuk, A. L. Schawlow, and M. D. Sturge, in a talk on energy levels in concentrated ruby, related sign and magnitude of exchange coupling and total spin at different energy levels of chromium-doped ruby. W. N. Hansen has recorded absorption spectra by means of multiple-attenuated total reflection. The instrument, somewhat similar to that by Karrer and Orr [J. Opt. Soc. Am. **36**, 42 (1946)], consists of a solid glass rod, bent into a loop and surrounded by a hollow cylinder filled with the test liquid. The light is projected into the rod where it undergoes, as it passes along, multiple total reflections. The net absorption, as shown on highly absorbing $KMnO_4$ solutions, depends on the absorptance index K of the liquid and is comparable to, but easier to obtain than, that in a very thin cell. J. R. Meyer-Arendt, J. O. Porteus, and H. E. Bennett have determined the transfer characteristics of reflecting surfaces and found that even fairly rough reflectors give distinct images up to high spatial frequencies although the over-all contrast, naturally, is reduced.

In his talk at the joint APS–AGU banquet, E. U. Condon referred to the fact that about 100 articles on physics are published *a day* and that, if we could extrapolate from the growth in the past, the number of physics *journals* in the year 2000 would reach *one million*. Obviously, we still have to find a solution; more precise, nonrepetitive writing of scientific articles and more emphasis in graduate schools on teaching the techniques of preparing written reports are needed.

An Analysis of Radiation Transfer By Means of Elliptical Cylinder Reflectors

S. B. Schuldt and R. L. Aagard

Expressions are derived giving the relative amount of pumping radiation transferred from a cylindrical source to a cylindrical laser by means of a reflector in the shape of an elliptical cylinder. The general expression depends upon the radii of the source and laser, the eccentricity of the ellipse and the length of its semimajor axis, and an arbitrary angular distribution of source radiation. The effect of radiation reflected back into the source itself (source-blocking) is also considered. A very considerable simplification in the calculation results when the source distribution is invariant under a rotation of the source about its axis, i.e., when the distribution depends only on the direction of the radiation with respect to the local normal, thus corresponding to virtually all practical cases. Moreover, the special case of a Lambertian source distribution yields efficiencies which may be evaluated directly. Especially simple and illustrative is the Lambertian source which is sufficiently small compared to the reflector that source-blocking can be ignored.

Introduction

Elliptical reflectors have often been employed to transfer pumping radiation from a cylindrical source to the active medium in an infrared or optical maser. This type of reflector can be constructed with reasonable ease,[1] and it has served equally well for ruby,[2–4] metal vapor,[5,6] and rare-earth doped laser materials.[7–10] However, there is little or no information in the literature concerning the focusing properties of an elliptical reflector. In order to become more familiar with the elliptical reflector, we have studied the subject analytically within the framework of the following three considerations.

Considering an elliptical cylinder in cross section, we will observe that an object at one focus is imaged at the other focus with the least magnification when the foci are closest together. If the image of a light source falls within the circular cross section of the laser rod, all of the rays leaving the source, except those blocked by the source itself, are considered to be transferred to the laser. We speak of an efficiency, then, which represents the relative percentage of rays leaving the source which enter the laser circle. Generally, the efficiency is greatest when the source and laser are close together and the reflector is nearly circular. It is easy to see that this may lead to enormous reflectors, and one would like to know how much the efficiency is compromised by reducing the dimensions of the ellipse.

The effect of the relative size of the source and receiver leads to a second important consideration. We would also expect the efficiency to be greatest when the diameter of the source is small and the laser large. Just the opposite condition pertains to the elements alone. That is, the laser material requires a high flux density implying small diameter, while the power available from the pumping lamp increases with the diameter. Therefore, the designer would like to know if the additional power obtained by increasing the lamp diameter more than makes up for the loss in efficiency.

Rays leaving normal to the surface of the source in the cross-sectional plane will, of course, reach the laser, but rays leaving at an angle will be imperfectly focused. In this consideration, we must satisfy ourselves that the problem reduces to one of studying the distribution of rays in the two dimensions of a cross section. If we assume an infinitely long cylindrical source and reflector and a finite laser, it is obvious that the distribution of light rays entering the laser is, except for end effects, the same for any cross section through the laser. Furthermore, the geometry of the focusing does not depend on the angle that a ray makes with the plane of the cross section, since the surfaces of the source, reflector, and laser are generated by parallel lines (perpendicular to the cross section). The condition of infinitely long source and reflector can be effectively met in practice by enclosing the ends of the elliptical cylinder with plane reflectors of very high specular quality, located flush

The authors are with the Honeywell Research Center, Hopkins, Minnesota.

Received 21 November 1962.

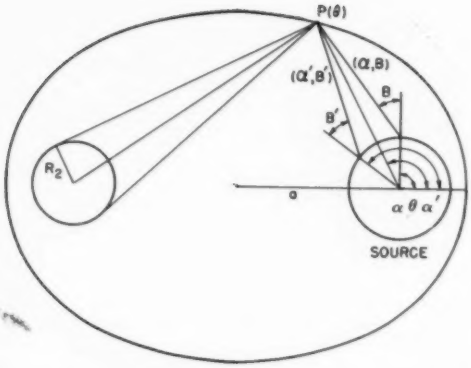

Fig. 1. The construction used to derive Eqs. (2)–(6), specifying part of the boundary of the region in which $G(\alpha, \beta) = 0$.

with the silvered ends of the laser. This arrangement also eliminates end effects. Therefore, the efficiency of the system depends upon the cross-sectional dimensions of the source, laser, and reflector, and on the angular distribution of rays from the source projected onto the plane of the ellipse.

The method of analytical ray tracing is employed to obtain an expression for the system efficiency in terms of the dimensions of the elements and the angular distribution of rays from the source. Only single reflections are considered. The expression will accommodate any angular distribution of rays, but we have made calculations only for the case of a Lambertian distribution, primarily because the efficiency can then be reduced to a relatively simple formula.

Definition of Efficiency

With the foregoing considerations in mind, we define an efficiency as the relative amount of energy transferred from the linear source to the laser rod. In two dimensions, a particular ray having its origin on the circumference of the source is specified by (α,β), where α gives the angular position of the point of origin on the source circumference, and ρ is the direction of the projected ray relative to the normal, as shown in Fig. 1. Under the conditions stated above, the efficiency η may be expressed

$$\eta = \int_{-\pi}^{+\pi} d\alpha \int_{-\pi/2}^{+\pi/2} I(\alpha,\beta)\, G(\alpha,\beta)\, d\beta, \qquad (1)$$

where

$$\int_{-\pi}^{+\pi} d\alpha \int_{-\pi/2}^{+\pi/2} I(\alpha,\beta)\, d\beta = 1.$$

In this equation the function $I(\alpha,\beta)$ gives the normalized density of the plane-projected rays per unit position angle α and per unit direction angle β. This function has an obvious simple relation to the luminance, a term we choose to avoid in the present two-dimensional calculation. Also the function is assumed to be independent of the wavelength of the light over the useful spectral range of the source. The weight function $G(\alpha,\beta)$ is defined equal to unity if the ray (α,β) passes into the laser circle before the ray either (1) undergoes two reflections by the ellipse, or (2) re-enters the source circle. Otherwise the weight function is equal to zero. Any ray, which re-enters the source circle after only one reflection by the ellipse and has not passed into the laser circle, is said to be source-blocked.

Specification of $G(\alpha,\beta)$

In the α,β diagram, the boundaries of the regions in which $G(\alpha,\beta) = 1$ are curves which cannot be designated $\alpha = \alpha(\beta)$ or $\beta = \beta(\alpha)$, but can be described parametrically:

$$\alpha = \alpha(\theta),$$
$$\beta = \beta(\theta).$$

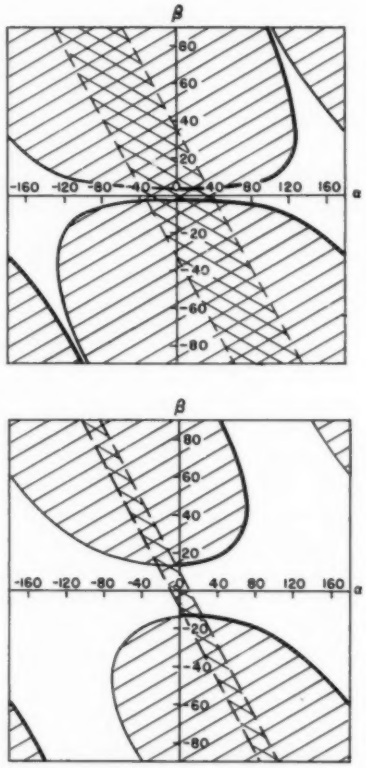

Fig. 2. Specification of $G(\alpha, \beta)$. The solid curves represent source rays which, after a single reflection by the ellipse, pass just tangent to the laser. These curves are the loci of the solutions of Eqs. (2)–(5). The dashed curves represent the limiting source-blocked rays. The total shaded area corresponds to $G(\alpha, \beta) = 0$, while the open areas correspond to $G(\alpha, \beta) = 1$. The parameters for the calculations illustrated here are: for (a)—$\epsilon = 0.6$, $R_1/a = 0.2$, and $R_2/R_1 = 0.25$; for (b)—$\epsilon = 0.6$, $R_1/a = 0.05$, $R_2/R_1 = 1$.

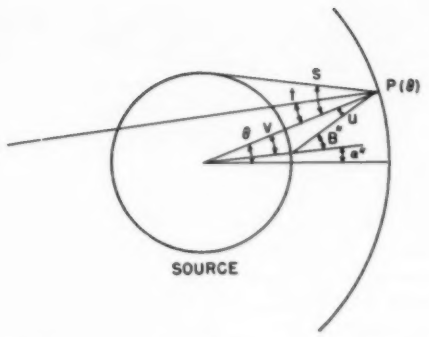

Fig. 3. The construction used to derive Eqs. (7)–(8) for the limiting source-blocked rays, which complete the boundary of the region $G(\alpha, \beta) = 0$.

This parametrization follows from the simple construction illustrated in Fig. 1 and described below.

We denote the source and effective receiver radii by R_1 and R_2, respectively, and the semimajor axis and eccentricity of the ellipse by a and ϵ, respectively. A line is drawn from the source focus at an arbitrary positive angle θ toward the elliptical boundary, where it is reflected at $P(\theta)$ into the laser focus. The two rays are then constructed from $P(\theta)$ tangent to the laser circle. Reflecting these rays backward gives their points of origin on the source circle, providing the implied intersections occur. With some trigonometric manipulating, these limiting rays are found to be (α,B) and (α',B') with

$$B = \sin^{-1}\left[\frac{R_2}{R_1}\cdot\frac{1-\epsilon^2}{1+\epsilon^2+2\epsilon\cos\theta}\right], \tag{2}$$

$$B' = -B \tag{3}$$

$$\alpha = \theta + \sin^{-1}\left[\frac{R_2}{a}\cdot\frac{1+\epsilon\cos\theta}{1+\epsilon^2+2\epsilon\cos\theta}\right] - B, \tag{4}$$

$$\alpha' = 2\theta - \alpha. \tag{5}$$

If, for a particular θ, the rays tangent to the laser are not reflected backward into the source, it turns out that no real solution B can be found from Eq. (2), that is the argument if the sine is greater than 1. The range of θ over which corresponding values of α and B can be calculated is given by $0 \le \theta \le T$, with

$$T = \begin{cases} 0, & \dfrac{R_2}{R_1} > \dfrac{1+\epsilon}{1-\epsilon}, \\ \cos^{-1}\left[\dfrac{(R_2/R_1)(1-\epsilon^2)-(1+\epsilon^2)}{2\epsilon}\right], & \dfrac{1-\epsilon}{1+\epsilon} \le \dfrac{R_2}{R_1} \le \dfrac{1+\epsilon}{1-\epsilon}, \\ \pi, & \dfrac{R_2}{R_1} < \dfrac{1-\epsilon}{1+\epsilon}. \end{cases} \tag{6}$$

If Eq. (2) has no solution for a particular θ, this means that all source rays reflected through $P(\theta)$ will strike the laser.

By allowing θ to vary over the range $0 \le \theta \le T$, the corresponding (α,B) and $(\alpha',-B)$ may be calculated and plotted as shown in Figs. 2(a) and 2(b) (heavy curves). The reflections of these curves through the origin (light curves) are also seen to represent limiting rays because of the symmetry of the problem. It is fairly obvious that the shaded areas between the upper curve and $\beta = \pi/2$ and between the lower curve and $\beta = -\pi/2$ represent sets of rays which are not reflected into the laser. In these areas the weight function $G(\alpha,\beta)$ must be set equal to zero.

To complete the specification of $G(\alpha,\beta)$ it is necessary to consider (1) source-blocked rays and (2) rays which illuminate the laser directly, i.e., pass into the laser before any reflection occurs. The former determine a region in the α,β diagram in which $G(\alpha,\beta)$ must be set equal to zero, while the latter determine a region in which $G(\alpha,\beta)$ must be set equal to unity. An exact analysis giving the limiting source-blocked rays is performed via the construction illustrated in Fig. 3. A ray from the source focus in the direction θ determines a reflection point $P(\theta)$. If there is a ray from the source which is reflected at $P(\theta)$ and then passes tangent to the source, its designation (α'',B'') is derived from a few trigonometric relations, as follows:

$$\sin s = \frac{R_1}{a}\left(\frac{1+\epsilon\cos\theta}{1-\epsilon^2}\right),$$

$$\sin t = \frac{2\epsilon\sin\theta\,(1+\epsilon\cos\theta)}{\epsilon^2+1+2\epsilon\cos\theta},$$

$$u = s - t,$$

$$\sin B'' = \frac{a}{R_1}\frac{\sin u\,(1-\epsilon^2)}{1+\epsilon\cos\epsilon}; \tag{7}$$

$$v = B'' - u,$$

$$\alpha'' = \theta - v. \tag{8}$$

If $P(\theta)$ is near the right-hand vertex of the ellipse, i.e., if θ is small, solutions to Eqs. (7) can be found. Geometrically, this means that source-blocked rays reflected at $P(\theta)$ do exist when θ is small. However, $a\Theta_+$ and $a\Theta_-$ can be found

$$0 < \Theta_+ < \pi,$$

$$-\pi < \Theta_- < 0,$$

such that no real solutions of Eqs. (7) exist if $\theta > \Theta_+$ or if $\theta < \Theta_-$. Hence no source-blocked rays are reflected through $P(\theta)$ if $P(\theta)$ is far enough away from the right-hand vertex of the ellipse. By applying Eqs. (7) and (8) throughout the range $\Theta_- \le \theta \le \Theta_+$, one obtains the set of limiting (α'',B'') represented by dashed curves in Figs. 2(a) and 2(b). (These new curves have the appearance of parallel lines but are actually slightly curved and are not equidistant as measured parallel to the α-axis.) The shaded areas in which $G(\alpha,\beta)$ is equal to zero are extended to include all of the source-blocked rays (the areas between the dashed curves).

Regarding direct illumination of the laser, it may be seen that practically all of the direct rays are already in the regions $G(\alpha,\beta) = 1$ of Figs. 2(a) and 2(b) since all or most of the rays which intersect the laser circle directly, intersect it also a second time after reflection by the ellipse. There may be some unique contributions by direct rays if the source is large compared to the laser, but these rays leave the source nearly tangentially (β nearly $\pi/2$) where the luminance is relatively low. Figures 2(a) and 2(b), as they stand, therefore, illustrate a virtually exact specification of $G(\alpha,\beta)$.

A More Convenient Formulation of η

Equation (1) cannot yet be integrated in closed form because the boundaries of the regions where $G(\alpha,\beta) = 1$ are not expressed in terms of α and β alone. However, if source-blocking is neglected for the moment, and if the distribution $I(\alpha,\beta)$ is independent of α, i.e.,

$$I(\alpha,\beta) = I(\beta),$$

it is possible to avoid most of the numerical computations. To show this we recall that the curves of Figs. 2(a) and 2(b) marking the boundaries of the region $G(\alpha,\beta) = 1$, are the loci of the points $[\alpha(\theta),B(\theta)]$ and $[\alpha'(\theta),-B(\theta)]$ calculated from Eqs. (2)–(5), together with the reflections of these curves through the origin. If we were to proceed with a numerical computation of η, we could begin with a Riemann sum such as the following, which makes use of the symmetry properties just mentioned:

$$\begin{aligned}\eta = &\sum_{i=0}^{N-1} [\alpha(\theta_{i+1}) - \alpha(\theta_i)] \cdot \int_{-B(\theta_i)}^{+B(\theta_i)} I(\beta)\, d\beta \\ &+ [\pi - \alpha(\theta_N)] \int_{-\pi/2}^{+\pi/2} I(\beta)\, d\beta \\ &+ \sum_{i=0}^{N-1} [\alpha'(\theta_{i+1}) - \alpha'(\theta_i)] \cdot \int_{-B(\theta_i)}^{+B(\theta_i)} I(\beta)\, d\beta \\ &+ [\pi - \alpha'(\theta_N)] \int_{-\pi/2}^{+\pi/2} I(\beta)\, d\beta, \end{aligned} \tag{9}$$

where $\theta_{k+1} - \theta_k = \Delta\theta = T/N$, and $B(\theta)$, $\alpha(\theta)$, $\alpha'(\theta)$, and T are the solutions of Eqs. (2), (4), (5), and (6). However, by Eq. (5) we have

$$\alpha'(\theta) + \alpha(\theta) = 2\theta,$$

and Eq. (9) therefore reduces to

$$\begin{aligned}\eta = &\sum_{i=0}^{N-1} 2(\theta_{i+1} - \theta_i) \int_{-B(\theta_i)}^{+B(\theta_i)} I(\beta)\, d\beta \\ &+ 2(\pi - \theta_N) \int_{-\pi/2}^{+\pi/2} I(\beta)\, d\beta \\ = &\ 2\Delta\theta \sum_{i=0}^{N-1} \int_{-B(\theta_i)}^{+B(\theta_i)} I(\beta)\, d\beta \\ &+ \left(1 - \frac{\theta_N}{\pi}\right). \end{aligned} \tag{10}$$

The last term in Eq. (10) follows from the normalization of $I(\beta)$. Next, letting $N \to \infty$ and noting that $\theta_N = T$, we obtain

$$\eta = 2\int_0^T d\theta \int_{-B(\theta)}^{+B(\theta)} I(\beta)\, d\beta + \left(1 - \frac{T}{\pi}\right), \tag{11}$$

for the efficiency neglecting source-blocked rays.

To account for the source-blocked rays, we find it expedient to make the following approximation. We introduce the quantity S equal to one-half the width (along the α-axis) of the source-blocked zone, and find this to be given by

$$S = \cos^{-1}\left\{\frac{(1-\epsilon^2)^2\sqrt{4\epsilon^2 - (R_1/2)^2} - (R_1/a)^2(1+\epsilon^2)}{2\epsilon[(1-\epsilon^2)^2 + (R_1/a)^2]}\right\}. \tag{12}$$

We assert that the efficiency is given to very close approximation by

$$\eta = \begin{cases} 2\displaystyle\int_S^T d\theta \int_{-B(\theta)}^{+B(\theta)} I(\beta)\, d\beta & S < T \\ 1 - \dfrac{S}{\pi} & S \geq T. \end{cases} \tag{13}$$

This approximation would be represented graphically by substituting two pairs of vertical lines for the diagonal curves illustrated in Figs. 2(a) and 2(b). A severe test of the approximation would be in a case where the source-blocking zone is nearly as wide as the maximum width of the curve obtained from Eqs. (2)–(5), in other words where S is approximately equal to T. Several of these cases have been checked carefully by numerical integration according to Eq. (1), and the efficiencies obtained agreed with those obtained from Eq. (13) to within a fraction of a percent.

Finally, we observe that $I(\beta)$ is always integrable if we are able to fit the measured distribution by a partial Fourier series, and the double integral of Eq. (13) is consequently reduced to a single integral, and this integration is easily performed in the special case of a Lambertian distribution. It is worth noting that η is determined by the three parameters ϵ, R_2/R_1, and R_1/a, which are numerics. The only occurrence of R_1/a in Eq. (13) is in S, which is associated with the source-blocked rays. One would therefore expect an asymptotic efficiency depending only upon ϵ and R_2/R_1 as the ratio R_1/a approaches zero, i.e., as source-blocking becomes negligible.

Results for the Lambertian Source Distribution

For the Lambertian distribution,

$$I(\beta) = \frac{1}{4\pi}\cos\beta, \tag{14}$$

Eq. (13) reduces to

Table I. Efficiencies Corresponding to a Lambertian Source With and Without Source-Blocking $R_1/a \neq 0$ and $R_1/a = 0$, Respectively, Calculated from Eq. (15)

$\epsilon = 0.2$							$\epsilon = 0.4$						
$\frac{R_2/R_1}{R_1/a}$	0.20	0.16	0.12	0.08	0.04	0	$\frac{R_2/R_1}{R_1/a}$	0.40	0.32	0.24	0.16	0.08	0
3	—	—	—	0.9042	0.9522	1.000	3	—	—	—	0.9258	0.9628	1.000
2	—	—	0.8558	0.9042	0.9522	1.000	2	—	—	0.8755	0.9095	0.9415	0.9733
1	0.7051	0.7408	0.7748	0.8077	0.8399	0.8718	1	0.6575	0.6739	0.6900	0.7061	0.7220	0.7380
1/2	0.4167	0.4345	0.4515	0.4679	0.4841	0.5000	1/2	0.4464	0.4546	0.4627	0.4707	0.4787	0.4866
1/3	0.2750	0.2868	0.2980	0.3089	0.3195	0.3300	1/3	0.3035	0.3088	0.3142	0.3195	0.3247	0.3300
$\epsilon = 0.6$							$\epsilon = 0.8$						
$\frac{R_2/R_1}{R_1/a}$	0.40	0.32	0.24	0.16	0.08	0.00	$\frac{R_2/R_1}{R_1/a}$	0.20	0.16	0.12	0.08	0.04	0.00
3	—	—	—	—	0.9084	0.9403	3	—	—	—	—	0.6655	0.6894
2	—	—	—	0.7688	0.7900	0.8112	2	—	—	—	0.5414	0.5573	0.5733
1	0.5370	0.5477	0.5584	0.5690	0.5797	0.5903	1	0.3697	0.3777	0.3851	0.3937	0.4017	0.4096
1/2	0.3789	0.3843	0.3896	0.3950	0.4003	0.4056	1/2	0.2667	0.2707	0.2747	0.2786	0.2826	0.2866
1/3	0.2936	0.2971	0.3007	0.3042	0.3077	0.3112	1/3	0.2153	0.2179	0.2206	0.2232	0.2258	0.2285

$$\eta = \begin{cases} 1 - \dfrac{T}{\pi} + \dfrac{2}{\pi}\left(\dfrac{R_2}{R_1}\right)\left[\tan^{-1}\dfrac{(1-\epsilon^2)\tan\left(\dfrac{T}{2}\right)}{(1+\epsilon)^2} - \tan^{-1}\dfrac{(1-\epsilon^2)\tan\left(\dfrac{S}{2}\right)}{(1+\epsilon)^2}\right] & S < T \\ 1 - \dfrac{S}{\pi}, & S \geq T. \end{cases} \quad (15)$$

This expression for η has been evaluated for various combinations of values of the parameters ϵ, R_2/R_1, and R_1/a, and the results are given in Table I. Certain constraints on the parameters, which are necessary in order to keep the source and receiver inside the reflector and to keep them from overlapping, account for the blank spaces in the table. Examining the tabulated figures, we see that the efficiency is most sensitive to ϵ and R_2/R_1, and least sensitive to R_1/a. We confine the subsequent discussion, therefore, to negligible source-blocking ($R_1/a \sim 0$) and examine briefly the dependence of η on ϵ and R_2/R_1.

We note that our intuitive introductory observations are borne out by the calculations. Namely, the efficiency increases as the reflector is made more circular and also as the ratio of the laser and source radii (R_2/R_1) increases. If $R_1/a = 0$, it follows from Eq. (15) that the efficiency reduces to $\eta = R_2/R_1$ whenever $R_2/R_1 < (1-\epsilon/1+\epsilon)$, and $\eta = 1$ whenever $R_2/R_1 > (1+\epsilon/1-\epsilon)$. This behavior is evident from the curves of Fig. 4.

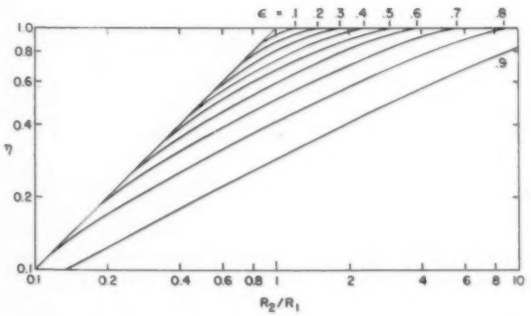

Fig. 4. Efficiencies calculated for a Lambertian source distribution and negligible source-blocking ($R_1/a = 0$).

References

1. R. H. Hornick, R. C. Jones, and C. J. Broneo, Rev. Sci. Instr. **33,** 776 (1962).
2. J. L. Wentz, Proc. Inst. Radio Engrs. **50,** 1528 (1962).
3. M. Ciftan, C. F. Luck, C. G. Shafer, and H. Statz, Proc. Inst. Radio Engrs. **49,** 960 (1961).
4. C. Bowness, D. Missio, and T. Rogola, Proc. Inst. Radio Engrs. **50,** 1704 (1962).
5. S. Jacobs, G. Gould, and P. Rabinowitz, Phys. Rev. Letters **7,** 415 (1962).
6. P. Rabinowitz, S. Jacobs, and G. Gould, Appl. Opt. **1,** 513 (1962).
7. G. D. Boyd, R. J. Collins, S. P. S. Porto, A. Yariv, and W. A. Hargreaves, Phys. Rev. Letters **8,** 269 (1962).
8. L. F. Johnson, G. D. Boyd, K. Nassar, and R. R. Soden, Phys. Rev. **126,** 1406 (1962).
9. L. F. Johnson, Proc. Inst. Radio Engrs. **50,** 1691 (1962).
10. A. Yariv, Proc. Inst. Radio Engrs. **50,** 1699 (1962).

The Optical Society of America

Officers of the Society

President STANLEY S. BALLARD, Department of Physics, University of Florida, Gainesville, Fla.
President-Elect RICHARD C. LORD, Spectroscopy Laboratory, MIT, Cambridge 39, Mass.
Past President DAVID L. MACADAM, Research Laboratories, Eastman Kodak Company, Rochester 4, N.Y.
Executive Secretary MARY E. WARGA, OSA, 1155 16th Street N.W., Washington 6, D.C.
Treasurer ARCHIE I. MAHAN, Applied Physics Laboratory, 8621 Georgia Avenue, Silver Spring, Md.
Editor of the Journal of the Optical Society of America DEANE B. JUDD, National Bureau of Standards, Washington 25, D.C.
Editor of Applied Optics JOHN N. HOWARD, AFCRL, Bedford, Mass.

Directors-at-Large

** Term expires December 31 of the indicated year.*

RUDOLF KINGSLAKE (63)* Eastman Kodak Company, Rochester 4, N.Y.
EARLE K. PLYLER (63)* Department of Chemistry, Florida State University, Tallahassee, Fla.
DAVID RICHARDSON (63)* Bausch & Lomb, Inc., Rochester 2, N.Y.
GEORG H. HASS (64)* ERDL, Fort Belvoir, Va.
R. CLARK JONES (64)* Polaroid Corp., Cambridge, Mass.
E. D. MCALISTER (64)* Scripps Institution of Oceanography, La Jolla, Calif.
W. LEWIS HYDE (65)* J. W. Fecker, Inc., 4709 Baum Boulevard, Pittsburgh, Pa.
JOHN A. SANDERSON (65)* Naval Research Laboratory, Washington 25, D.C.
GEORGE WALD (65)* Biological Laboratories, Harvard University, Cambridge 38, Mass.

Local Sections

Rochester
JOHN L. TUPPER *President*
JOSEPH L. ROOD *President-Elect*
SHELDON PHILLIPS *Secretary*
Eastman Kodak Co.
Rochester 4, N.Y.
MANUEL KINER *Treasurer*

Detroit
RICHARD MAJKOWSKI *President*
CARL LEISTNER *President-Elect*
DANIEL L. HARMON *Secretary*
16152 Parkside, Detroit 21, Mich.
SAMUEL COHEN *Treasurer*

Niagara Frontier
E. SCHUSTIK *President*
THOMAS FROST *President-Elect*
CALVIN W. YOUNG *Secretary*
Carborundum Metals Co.
Box 32, Akron, N.Y.
RAY ANNINO *Treasurer*

New England
DAVID S. GRAY *President*
CHARLES KOESTER *Vice-President*
GEOFFREY HARVEY *Secretary*
Itek Corporation
10 Maguire Rd.
Lexington, Mass.
WILLIAM J. DAVIS *Treasurer*

Texas
CHARLES S. WILLIAMS *President*
P. O'B. MONTGOMERY *Vice-President*
HARRY J. AUVERMANN *Secretary-Treasurer*
LTV Research Center
P.O. Box 5003
Dallas 22, Tex.

Delaware Valley
F. J. WARZAK *President*
J. E. TUDOR *Secretary*
General Electric Company MSVD
3316 Spring Garden Street
Philadelphia, Pa.
M. CONSHERRY *Treasurer*

Chicago
FRED CLARKE *President*
DONALD PONTARELLI *Vice-President*
RICHARD STECK *Secretary*
4556 North Oakview
Chicago 31, Ill.
HOWARD PADGITT *Treasurer*

Southwestern Connecticut
LEONARD EISNER *President*
ROBERT C. GORE *Vice-President*
MARTIN ROME *Secretary*
Machlett Laboratories, Inc.
1063 Hope Street
Springdale, Connecticut
EDWARD SPEYER *Treasurer*

Southern California
R. HENRY FRELS *President*
ERNEST DAVIDSON *Vice-President*
CLIFFORD O. THOMAS *Secretary*
10 Miramonte Drive
Fullerton, Calif.
W. S. GALLAWAY *Treasurer*

Northern California
ANDREW L. JORGENSEN *President*
CLYDE C. SHAW *Vice-President*
HARVEY MORTON *Secretary-Treasurer*
Tinsley Laboratories
2448 Sixth Street
Berkeley, Calif.

National Capital
RICHARD TOUSEY *President*
FREDERICK W. PAUL *First Vice-President*
HARRY K. HAMMOND, III *Secretary*
National Bureau of Standards
Washington 25, D.C.
RICHARD S. HUNTER *Treasurer*

San Diego
JOHN E. TYLER *President*
JOHN H. TAYLOR *Vice-President*
JOHN M. HOOD *Secretary-Treasurer*
Bldg. 4, U.S. Navy Electronics Laboratory
San Diego 52, Calif.

The Optical Society of America was organized in 1916 **"to increase and diffuse the knowledge of optics in all its branches, pure and applied, to promote the mutual interests of investigators of optical problems, of designers, manufacturers and users of optical instruments and apparatus of all kinds and to encourage cooperation among them."** The Society invites to membership all who are interested in any branch of optics, either in research, in instruction, in optical or illuminating engineering, in the manufacture and distribution of optical goods of all kinds, or in physiological and medical optics. Further information may be obtained from the Executive Secretary of the Society. **Annual Dues:** Regular members and Fellows, $17.00; Associate members, $13.00; Corporate members, $125.00. These dues include subscription to the Society's official journal, the **Journal of the Optical Society of America,** but not to its other publications.

Spectral Band Absorptance for Atmospheric Slant Paths

Gilbert N. Plass

A number of equations are derived for the absorptance along a slant path. The absorptances of slant and homogeneous paths are compared. Various combinations of assumptions are made in the derivation of these equations as to the variation of the temperature and absorber concentration along the path, the extent and nature of the overlapping of the spectral lines, the variation of the intensity and half-width from line to line, the shape of the spectral lines, and the extent of the frequency interval considered. The particular assumptions applicable to each result are clearly stated. A general method is developed for obtaining slant path absorptances from homogeneous path data when either the weak or strong line approximation is valid. A combination of the weak and strong line results gives new general expressions for the relationship of slant and homogeneous path absorptance. These results are correct in both of the weak and strong line limits and in addition provide a good approximation for all values of the parameters.

I. Introduction

The first article[1] of this series discussed various useful representations for the absorptance of a spectral band along a homogeneous path. It is shown there that under almost all conditions at least one of the following approximations can be used to represent the variation of the absorptance with path length and pressure: strong line approximation; weak line approximation; nonoverlapping line approximation. The regions of validity for these approximations are derived when the actual spectral band can be represented by the Elsasser[2] or statistical[3,4] models of a band, but have not as yet been given in detail for more complicated models such as the random Elsasser[5] or the quasi-random[6] model.

In general there is a continuous variation of the pressure, temperature, and fractional concentration of the absorbing gas along a slant path in the atmosphere. It is almost impossible to simulate such a path in the laboratory within a reasonable space since at most it is feasible to use only a few cells in parallel which are at different pressures and contain different gas concentrations. Thus, it is important to be able to calculate the absorptance over a slant path from absorption data measured or calculated for homogeneous paths along which the pressure and temperature are constant.

In Section II general methods are developed for the calculation of slant path absorptance from homogeneous path absorptance data. These methods are valid when either the weak line or the strong line approximation may be used. The conditions of validity for each equation are carefully stated. In Section III exact analytical expressions are presented for the slant path absorptance when both the temperature and fractional concentration of the absorbing gas are constant along the path. Similar but necessarily more complicated expressions for the slant path absorptance are given in Section IV when the temperature and fractional concentration of the absorbing gas as well as the pressure vary along the path.

In Section V a procedure is developed for the approximate calculation of slant path absorptance. The input data can be any experimental measurement, theoretical expression, or table which represents the absorptance over a homogeneous path. The pressure and amount of absorbing gas for the homogeneous path are obtained from equations which necessarily give the correct value for the slant path absorptance in both the weak line and strong line regions. In addition this same expression provides a good approximation for the absorptance in the intermediate range of the parameters.

II. Slant Path Absorptance

General methods for the conversion of homogeneous path absorptance data to slant path absorptance are developed in this section. These methods are valid

The author is with the Research Laboratory, Aeronutronic Division, Ford Motor Company, Newport Beach, California.

Received 20 September 1962.

This work was supported by the Space Systems Division, Air Force Systems Command, Los Angeles, California. A preliminary report of this work was presented at the March 1962, Washington meeting of the Optical Society of America, J. Opt. Soc. Am. **52**, 606 (1962).

when either the weak line or strong line approximation may be used. A generalization of these methods is given in Section V which is valid in both limits and provides an interpolation for the results in the intermediate region.

The mass of the absorbing gas per unit area along a slant path is

$$u = \int_0^l \rho_a dl, \tag{1}$$

where ρ_a is the density of the absorbing gas and l is the length measured along the direction of the path. The absorptance A over a finite wavenumber interval $\Delta\nu$ of radiation which traverses a slant path is

$$A\Delta\nu = \int_{\Delta\nu} \left\{1 - \exp\left[-\int_0^u k_\nu [p(u'), T(u')]du'\right]\right\} d\nu, \tag{2}$$

where u is the mass of the absorbing gas per unit area for the entire slant path and $k_\nu[p(u'), T(u')]$ is the absorption coefficient at the frequency ν and at the spatial location along the slant path where the mass per unit area has the particular value u'. The pressure p and temperature T are taken to be functions of u'.

The absorption coefficient may be written as

$$k_\nu(u) = \sum_{i=1}^{N} S_i b_i[\nu, \alpha_i(u)], \tag{3}$$

where the summation is over the N spectral lines which contribute to the absorption in the frequency interval $\Delta\nu$, S_i is the intensity of the ith spectral line, and b_i is the line shape factor for the ith spectral line which is a function of the frequency ν and half-width α_i. The integral of b_i over all frequencies is normalized to have the value unity. The pressure broadened half-width is proportional to an effective pressure[7] p (defined to give extra weight to the greater effect of self-broadening compared to foreign gas broadening) and inversely to the square root of the absolute temperature T, so that

$$\alpha = \alpha_0(p/p_0)(T_0/T)^{1/2}, \tag{4}$$

where α_0, p_0, T_0 refer to the values of these quantities measured under one particular set of conditions. Since carbon dioxide and water vapor occur in the atmosphere only in relatively small amounts, the total pressure and the effective pressure are not greatly different for atmospheric absorption problems.

For the Lorentz pressure broadened line shape, the line shape factor is

$$b_i(\nu, \nu_{0i}, \alpha_i) = \alpha_i / \{\pi[(\nu - \nu_{0i})^2 + \alpha_i^2]\}, \tag{5}$$

where ν_{0i} is the center of the ith line. On the other hand, the Doppler line shape factor is

$$b_i(\nu, \nu_{0i}, \alpha_D) = \frac{1}{\alpha_D}\left(\frac{\ln 2}{\pi}\right)^{1/2} \exp\left[-\frac{(\nu - \nu_{0i})^2 \ln 2}{\alpha_D^2}\right], \tag{6}$$

where α_D is the Doppler half-width.

Most of this report is concerned with spectral lines which have the Lorentz line shape. In this case it is found from Eqs. (2), (3), and (5) that the absorptance for a slant path is given by the expression

$$A\Delta\nu = \int_{\Delta\nu} \left\{1 - \exp\left[-\frac{1}{\pi}\sum_{i=1}^{N} \int_0^u \frac{S_i\alpha_i du'}{(\nu - \nu_{0i})^2 + \alpha_i^2}\right]\right\} d\nu. \tag{7}$$

This expression is compared frequently in this article with the absorptance A_h over a homogeneous path at constant pressure and temperature

$$A_h\Delta\nu = \int_{\Delta\nu} \left\{1 - \exp\left[-\frac{1}{\pi}\sum_{i=1}^{N} \frac{S_{ih}\alpha_{ih}u_h}{(\nu - \nu_{0i})^2 + \alpha_{ih}^2}\right]\right\} d\nu, \tag{8}$$

where the subscript h refers to the appropriate values for quantities measured along the homogeneous path.

A. Weak Line Approximation

The weak line approximation is valid when the absorption of each spectral line considered individually is small even near the line center. A special case of the weak line approximation is called the linear approximation. In this case the absorptivity increases linearly with the path length and line strength when all of the absorption from the spectral lines whose centers are within the frequency interval also occurs within $\Delta\nu$. The linear approximation is valid when the *total* absorption due to all of the spectral lines is small at every frequency within the interval. In this case the exponential in Eq. (2) may be replaced by the first two terms of its series expansion. If the line shape factor b_i is introduced from Eq. (3) and the frequency limits for the interval $\Delta\nu$ are ν_1 and ν_2, then the absorptance along a slant path becomes

$$A\Delta\nu = \sum_{i=1}^{N} \int_{\nu_1}^{\nu_2} d\nu \int_0^u S_i(u')\, b_i[\nu, \nu_{0i}, \alpha_i(u')]du'. \tag{9}$$

When the order of integration is interchanged, it is found that

$$\begin{aligned} A\Delta\nu &= \sum_{i=1}^{N} \int_0^u S_i(u')du' \int_{\nu_1}^{\nu_2} b_i[\nu, \nu_{0i}, \alpha_i(u')]d\nu \\ &= \sum_{i=1}^{N} \int_0^u S_i(u') I_{\nu_1}^{\nu_2}[\nu_{0i}, \alpha_i(u')]du', \end{aligned} \tag{10}$$

where

$$I_{\nu_1}^{\nu_2}[\nu_{0i}, \alpha_i(u')] = \int_{\nu_1}^{\nu_2} b_i[\nu, \nu_{0i}, \alpha_i(u')]d\nu \tag{11}$$

is the integral of the line shape factor over the finite frequency interval and is a function of the positions of the line centers, ν_{0i}, and the half-width, α_i. When the frequency interval becomes infinitely large, $I_{\nu_1}^{\nu_2}[\nu_{0i}, \alpha_i(u')]$ approaches the value unity because of the normalization of b_i.

The corresponding result for a homogeneous path is

$$A_h \Delta\nu = u_h \sum_{i=1}^{N} S_{ih} I_{\nu_1}^{\nu_2}(\nu_{0i}, \alpha_{ih}), \tag{12}$$

where $S_{ih} = S_i(T_h)$, $\alpha_{ih} = \alpha_i(p_h, T_h)$, and p_h and T_h are the pressure and temperature along the homogeneous path.

Thus the absorptance over the homogeneous and slant paths as given by Eqs. (12) and (10) is the same when the path length u_h is chosen to satisfy the equation

$$u_h \sum_{i=1}^{N} S_{ih} I_{\nu_1}^{\nu_2}(\nu_{0i}, u_h) = \sum_{i=1}^{N} \int_0^u S_i(u') I_{\nu_1}^{\nu_2}(\nu_{0i}, u') du'. \tag{13}$$

When the linear approximation is valid, Eq. (13) gives the most general expression for correlating slant path and homogeneous path absorptances. This equation states that the absorptance along the slant path is equal to that of a homogeneous path which has an absorber concentration u_h and is at a particular temperature T_h at which the line intensities are S_{ih}. This result is valid for any line shape regardless of whether the line is pressure broadened or not. It is also valid for any distribution of spectral line intensities and for any variation in the spacing between adjacent spectral lines. The temperature and absorber concentration may vary in any prescribed manner along the slant path.

When virtually all of the absorption from the spectral lines occurs within the frequency interval $\Delta\nu$, then the factors $I_{\nu_1}^{\nu_2}(\nu_{0i}, u_h)$ which occur in Eq. (13) are identically equal to unity. In this case the absorptance has the same value for the homogeneous and slant paths when the optical thickness u_h satisfies the equation

$$u_h \sum_{i=1}^{N} S_{ih} = \sum_{i=1}^{N} \int_0^u S_i(u') du'. \tag{14}$$

Thus the optical thickness u_h is the optical thickness of the slant path weighted by the line intensity along the path. This is probably the most useful general result for the correlation of the absorptance along slant and homogeneous paths.

If in addition the temperature along the slant path is constant and equal to that along the homogeneous path, then it follows from Eq. (14) that

$$u_h = u. \tag{15}$$

Equations (14) and (15) have only been derived when the linear approximation is valid. When the spectral lines begin to overlap strongly, this approximation is no longer valid. However, the weak line approximation may still be applicable provided the absorption is still small for each line considered individually. Equations (14) and (15) may be used whenever the weak line approximation is valid, even when the spectral lines overlap strongly. Since the weak line approximation is valid, the amount of radiation absorbed by each line is always a small fraction of the incident flux. However, when many such weak lines overlap in an interval, almost all of the radiation may be absorbed in a given frequency band. In this case the absorption coefficient no longer is a rapidly varying function of frequency and is almost constant. It no longer matters whether the lines are arranged in a regular or random pattern.

Under these conditions it is easiest to compute the absorptance along a slant path for the Elsasser model from the exact expression for the absorption coefficient summed over the contributions of all the individual lines.[2] For a slant path Elsasser's derivation can be generalized to give

$$Ad = \int_{\nu^{(0)}}^{\nu^{(0)}+d} \left\{ 1 - \exp\left[- \int_0^u \frac{S}{d} \frac{\sinh\beta}{\cosh\beta - \cos(2\pi\nu/d)} du' \right] \right\} d\nu,$$

where $\nu^{(0)}$ is some arbitrary frequency within the band and $\beta = 2\pi\alpha/d$. The case considered here corresponds to $\beta >> 1$, so that the integrand reduces to S/d to a good approximation. Thus

$$A = 1 - \exp\left(-d^{-1} \int_0^u S du' \right). \tag{16}$$

When this result is compared with the corresponding result for a homogeneous path,

$$A_h = 1 - \exp(-S_h u_h / d),$$

it is seen that Eq. (14) still represents the correlation between slant and homogeneous paths. The same result can also be derived for the statistical model. The arrangement of the spectral lines cannot matter in this region where the absorption coefficient is only a slowly varying function of frequency. Thus, when the weak line approximation is valid, Eqs. (14) and (15) represent the correlation between slant path and homogeneous path absorptivities regardless of how much the spectral lines overlap. Further examples of the use and derivation of weak line approximations to the absorptance are given in Sections III and IV.

B. Strong Line Approximation

The strong line approximation is valid when the absorption of the incident radiation is virtually complete over frequency intervals at least several half-widths wide around the centers of the strongest lines in the band and when these lines are largely responsible for the absorption over the given frequency interval. When this is the case, the factor α_i^2 may be neglected[1,8] compared to $(\nu - \nu_{0i})^2$ in the expression for the Lorentz line shape, Eq. (5), in calculations of the amount of radiation which is absorbed. The line shape factor is then proportional to the pressure since α_i occurs only in the numerator in this approximation. The line shape factor can be written as

$$b_i(\nu, \nu_{0i}, \alpha_i) = \alpha_i g_i(\nu, \nu_{0i}), \quad (17)$$

where g_i is a function only of the frequencies of the line centers, ν_{0i}, and the frequency under consideration, ν. This equation is actually valid not only for the Lorentz line shape, but also for any pressure broadened line shape which has been proposed including those with asymmetric wings.[9]

From Eqs. (2), (3), and (17), the absorptance over a slant path when the strong line approximation is valid is found to be

$$A\Delta\nu = \int_{\Delta\nu} \left\{1 - \exp\left[-\sum_{i=1}^{N} g_i(\nu, \nu_{0i}) \int_0^u S_i \alpha_i du'\right]\right\} d\nu. \quad (18)$$

The corresponding expression for the absorptance over a homogeneous path is

$$A_h\Delta\nu = \int_{\Delta\nu} \left\{1 - \exp\left[-\sum_{i=1}^{N} g_i(\nu, \nu_{0i}) S_{ih}\alpha_{ih} u_h\right]\right\} d\nu, \quad (19)$$

where S_{ih}, α_{ih}, and u_h are the line intensities, half-widths, and mass of absorbing gas per unit area for the temperature, T_h, and pressure, P_h, along the homogeneous path.

These two expressions are equal when the arguments of the exponentials are equal. Thus the absorptance along the slant path and the homogeneous path are equal when

$$u_h(\nu) \sum_{i=1}^{N} g_i(\nu, \nu_{0i}) S_{ih}\alpha_{ih} = \sum_{i=1}^{N} g_i(\nu, \nu_{0i}) \int_0^u S_i \alpha_i du'. \quad (20)$$

An equivalent amount of absorbing gas, u_h, can be calculated at each frequency from Eq. (20) such that the absorptances are equal over these slant and homogeneous paths. Since the value of u_h which is calculated in this manner might be a rapidly varying function of frequency, this equation does not appear to be of practical interest. However, it can be shown that u_h is independent of the frequency ν in several different cases.

First, assume that all of the spectral lines in the frequency interval $\Delta\nu$ have the same intensity and that their half-widths are equal, so that

$$S_i(T) = S(T) \quad (21)$$

and

$$\alpha_i(p, T) = \alpha(p, T). \quad (22)$$

In this case Eq. (20) becomes

$$S_h\alpha_h u_h = \int_0^u S\alpha du', \quad (23)$$

since the summation over the factors g_i now cancels on both sides of the equation. The only assumptions made in deriving Eq. (23) are that the strong line approximation is valid, the spectral lines in the interval $\Delta\nu$ all have the same intensity and half-width, and that they have a pressure broadened line shape. Note that this result is valid for a band of equally intense lines which do not have to be equally spaced. This result is valid in particular for a single spectral line. Equation (23) is valid for any arbitrary variation of the pressure and temperature along the slant path and for *any* arbitrary variation in the spacing between adjacent spectral lines. Under these conditions the slant and homogeneous paths have the same value of the absorptance for an equivalent amount of absorbing gas, u_h, and an equivalent half-width, α_h, for the homogeneous path as calculated from Eq. (23).

A slightly more general equation which does not assume that the half-widths of the different spectral lines are equal may be derived from Eq. (4) which may be rewritten as

$$\alpha_i = \alpha_{ih}(p/p_h)(T_h/T)^{1/2}. \quad (24)$$

From Eqs. (20), (21), and (24) it follows that

$$S_h p_h T_h^{-1/2} u_h = \int_0^u S p T^{-1/2} du'. \quad (25)$$

Equation (25) is valid under the same conditions as Eq. (23) except that it is no longer necessary to assume that all the half-widths α_i are equal. Equation (25) can be reduced to the same form as Eq. (23) by the use of Eq. (24).

Another solution of Eq. (20) can be obtained if it is assumed that the temperature variation of all the spectral lines is given by the same function of temperature, so that

$$S_i = S_{ih} s(T) \quad (26)$$

where $s(T)$ is a function which can be calculated from the theory of molecular spectra. Of course, this assumption is not valid when large temperature differences occur along the slant path and the spectral lines have quite different intensities. However, along many slant paths of interest the temperature variations are relatively small, and this may be an excellent approximation. In this case Eq. (20) can be solved for any distribution of line intensities and half-widths.

It follows for Eqs. (20), (24), and (26) that

$$p_h T_h^{-1/2} u_h = \int_0^u s(T) p T^{-1/2} du' \quad (27)$$

or

$$S_{ih}\alpha_{ih} u_h = \int_0^u S_i \alpha_i du',$$

which is independent of i because of Eqs. (24) and (26). Equation (27) assumes only that the strong line approximation and a pressure broadened half-width are valid and that the temperature variation of the line intensities can be represented by Eq. (26). Equation (27) is valid for any variation of the line intensities, half-widths, and spacing between the lines in the spectral interval $\Delta\nu$.

If in addition the temperature along the slant path can be considered to be constant and equal to that along the homogeneous path, then $s(T)$ as defined by Eq. (26) is unity. In this case Eq. (27) simplifies to the expression

$$p_h u_h = \int_0^u p\,du'$$

or (28)

$$\alpha_h u_h = \int_0^u \alpha\,du'.$$

This very simple and useful result determines the amount of absorbing gas for a homogeneous path so that it has the same absorptance as a prescribed slant path. This result does not depend on the variation of the spacing between spectral lines in the band or on the variation of line intensity or half-width from line to line. It assumes a pressure broadened half-width, that the strong line approximation is valid, and that the temperature along the slant path is constant.

Another form of Eq. (28) can be obtained by defining the fractional concentration c of an absorbing gas as the ratio of the density of the absorbing gas to the total density. Then

$$g\,du = -c\,dp \sec\theta,$$

where g is the acceleration of gravity and θ is the angle which the slant path makes with the vertical. Thus, Eq. (28) can be written

$$p_h u_h = \sec\theta \int_{p_0}^{p_1} c g^{-1} p\,dp, \tag{29}$$

where p_0 and p_1 are the pressures at the ends of the slant path.

The above results, Eqs. (28) and (29), for a constant temperature slant path were first derived by Plass.[10] They were used as the basis for a numerical treatment of the slant path problem by Carpenter.[11]

Some infrared absorbing gases such as CO_2 are to a good approximation dispersed uniformly throughout the atmosphere. In this case c is a constant. If in addition the variation of the acceleration of gravity with height can be neglected, then Eq. (29) simplifies to

$$p_h u_h = {}^1/_2(p_0 + p_1)u. \tag{30}$$

If the amount of absorbing gas is chosen to be the same over the two paths ($u = u_h$), then the pressure for the homogeneous path is required to be the mean of the pressures at the two ends of the slant path.

The variation with height of the fractional concentration of H_2O can often be adequately represented as a power of the pressure, so that

$$c = c_0(p/p_0)^l, \tag{31}$$

where c_0 and p_0 are particular values of the fractional concentration and the pressure. In this case it follows from Eqs. (28), (29), and (31) that

$$p_h u_h = \left(\frac{l+1}{l+2}\right)\left(\frac{p_1^{\,l+2} - p_0^{\,l+2}}{p_1^{\,l+1} - p_0^{\,l+1}}\right) u. \tag{32}$$

A number of equations [Eqs. (23), (25), (27), (28), (29), (30), (32)] have been derived here which determine the amount of absorbing gas and pressure along a homogeneous path so that its absorptance is the same as a prescribed slant path. These equations can be used to convert laboratory measurements or calculated absorptance tables into slant path absorptance values. Any equation which has been derived for a homogeneous path can be changed into one valid for a slant path by these same procedures. A number of examples of the use of these equations are given in the following sections.

III. Exact Expressions for the Transmission When the Temperature and Fractional Concentration Can Be Considered Constant

In this section a number of expressions are given for the slant path absorptance when the temperature and fractional concentration of the absorbing gas as measured along the path can be considered constant. These expressions are compared with the results derived in Section II where appropriate.

A. Nonoverlapping Line Approximation

The nonoverlapping line approximation assumes that there are N spectral lines in the frequency interval $\Delta\gamma$ which do not overlap to an appreciable extent. Thus, the total absorptance due to the N lines is obtained by merely totaling the contribution from each of the lines individually.

When the spectral lines have the Lorentz line shape, the absorptance is given by the expression[12]

$$A\Delta\nu = 2\pi N\gamma\alpha_1\left(\frac{p_0}{p_1}\right)^{\gamma}\left[P_\gamma\left(\frac{p_0^2 + p_1^2}{2p_0p_1}\right) - \left(\frac{p_0}{p_1}\right)P_{\gamma-1}\left(\frac{p_0^2 + p_1^2}{2p_0p_1}\right)\right], \tag{33}$$

where

$$\gamma = \frac{Sc_0p_s\sec\theta}{2\pi g\alpha_s} = \frac{Su}{[2\pi(\alpha_1 - \alpha_0)]}, \tag{34}$$

α_0 and α_1 are the values of the half-width at the two ends of the slant path where the pressures are p_0 and p_1, P_γ is the Legendre function of order γ (P_γ is the Legendre polynomial when γ is an integer), the quantity which appears in the parenthesis after P_γ is the argument of the Legendre function, c_0 is the constant value of the fractional concentration of the absorbing gas defined as the ratio of its density to the total density, g is the acceleration of gravity, α_s is the value of the half-width at some standard pressure p_s, and u is defined for the path by Eq. (1). For simplicity the above

expression is written as though each of the spectral lines had the same intensity and half-width. When this is not the case, an expression of the form of Eq. (33) can be computed for each of the spectral lines individually and the separate results totaled. It should be mentioned that in the derivation of this result it is necessary to assume that the frequency interval $\Delta\nu$ is infinite. In practice this requires that the interval $\Delta\nu$ include all of the absorption from the wings of the spectral lines whose centers are within the given interval.

As an example of the use of Eq. (33), if the nondimensional parameter $\gamma = 1$, then with the help of Eq. (34) it follows that

$$\begin{aligned} A\Delta\nu &= \pi N\alpha_1[1 - (p_0^2/p_1^2)] \\ &= {}^1/_2 NSu[1 + (\alpha_0/\alpha_1)], \end{aligned} \tag{35}$$

Equation (33) simplifies considerably when one end of the slant path is essentially outside of the atmosphere as would be the case for observations from a satellite. In this case $p_0 = 0$ and it can be shown either by direct integration, or from Eq. (33) and the limiting expression for the Legendre function as the argument becomes large, that

$$A\Delta\nu = \frac{2\pi N\alpha_1\gamma\Gamma(\gamma + {}^1/_2)}{\pi^{1/2}\Gamma(\gamma + 1)}, \tag{36}$$

where

$$\Gamma(x) = \int_0^\infty y^{x-1}e^{-y}dy, \tag{37}$$

α_1 is the value of the half-width at the lower end of the slant path, and the other end of the path is assumed to be essentially outside of the atmosphere. Equation (36) was first derived by Pedersen[13] and Strong and Plass.[14]

When the weak line approximation is valid, Eq. (33) reduces to

$$A\Delta\nu = 2\pi N\gamma(\alpha_1 - \alpha_0) = NSu. \tag{38}$$

This is the same result as is obtained for a homogeneous path with the same amount of absorbing gas, in agreement with the previously derived result, Eq. (15).

Equation (33) can be expanded in the form[12]

$$A\Delta\nu = 2\pi^{1/2}\gamma^{1/2}N(\alpha_1^2 - \alpha_0^2)^{1/2}\left[1 - \frac{p_0^2 + p_1^2}{8\gamma(p_1^2 - p_0^2)} + \cdots\right]. \tag{39}$$

The leading term of this expression is the strong line approximation. This term may be rewritten with the aid of Eq. (34) as

$$A\Delta\nu = N[2Su(\alpha_0 + \alpha_1)]^{1/2}. \tag{40}$$

The corresponding expression for the absorptance along a homogeneous path is[5]

$$A_h\Delta\nu = N(4S_h\alpha_h u_h)^{1/2}. \tag{41}$$

These last two expressions are in agreement with Eq. (30) which correlates the absorption along slant and homogeneous paths when the strong line approximation is valid.

When the Doppler line shape, Eq. (6), is the most important cause of line broadening the slant path absorptance is[15]

$$A\Delta\nu = NSu\sum_{n=0}^{\infty}\frac{(-1)^n k_0^n u^n}{(n+1)!(n+1)^{1/2}}, \tag{42}$$

where

$$k_0 = \frac{S}{\alpha_D}\left(\frac{\ln 2}{\pi}\right)^{1/2}. \tag{43}$$

The first term of this expansion is the weak line approximation for the absorptance; the equation is most useful in this limit. Another expansion for the absorptance is[15]

$$A\Delta\nu = 2N\alpha_D(\ln 2)^{-1/2}[\ln(k_0u)]^{1/2}\{1 + [C/2\ln(k_0u)] - \ldots\}, \tag{44}$$

where C is Euler's constant. The first term of this expansion is Euler's constant.

When the line shape is determined by both collision broadening and Doppler processes, the absorptance is given by[15]

$$A\Delta\nu = 2\pi^{1/2}\gamma^{1/2}N(\alpha_1^2 - \alpha_0^2)^{1/2}(1 + {}^1/_4 f + \ldots), \tag{45}$$

where

$$f = \frac{1}{2\gamma(\alpha_1^2 - \alpha_0^2)}\left(\frac{3\alpha_D^2}{\ln 2} - \alpha_1^2 - \alpha_0^2\right). \tag{46}$$

Higher order terms in the expansion may be found in ref. 15. Because the wings of the Lorentz line shape decrease much less rapidly than those of the Doppler line shape, the latter is usually not important for a strong line until the Doppler half-width is many times larger than the Lorentz half-width.[15]

Any of the results of this section can be generalized to the case where the line strengths and half-widths of the spectral lines are different. The absorptance is first calculated for each of the spectral lines individually. Since the spectral lines do not overlap, the total absorptance is merely the sum of these individual results.

B. Elsasser Model

When the concentration of the absorbing gas and temperature are constant along a slant path, the following exact expression for the absorptance[12] can be obtained for the Elsasser model:

$$A = \gamma\sinh^\gamma\beta_0\int_{\beta_0}^{\beta_1}\frac{1}{\sinh^\gamma\beta}P_\gamma\left(\frac{\cosh\beta_0\cosh\beta - 1}{\sinh\beta_0\sinh\beta}\right)d\beta, \tag{47}$$

where

$$\beta = 2\pi\alpha/d, \tag{48}$$

d is the mean line spacing, γ is defined by Eq. (34), β_0 and β_1 are the values of the parameter β at the two ends of the slant path, and P_γ is the Legendre function. By differentiation of Eq. (47), the alternative expression

$$\frac{\partial A}{\partial \beta_1} = \gamma \frac{\sinh^\gamma \beta_0}{\sinh^\gamma \beta_1} P_\gamma \left(\frac{\cosh\beta_0 \cosh\beta_1 - 1}{\sinh\beta_0 \sinh\beta_1} \right) \tag{49}$$

is obtained.

When γ is an integer, the absorptance can always be written in closed form.[12] For example, when $\gamma = 1$

$$A = (\cosh\beta_1 - \cosh\beta_0)/\sinh\beta_1. \tag{50}$$

The limiting forms of Eq. (47) for the weak and strong line approximations together with some interpolation equations are given in Sections IV and V.

C. Statistical Model

Whenever an expression for the absorptance of a single line can be derived, then a corresponding expression can be obtained for the absorptance of a group of overlapping lines which obey the statistical model. A general derivation of this result is given first which is valid for any arbitrary variation of the temperature and absorber concentration along the slant path. This derivation is similar to the one for homogeneous paths and is only outlined here. The absorptance at the center of the frequency interval from ν_1 to $\nu_1 + D$ due to a random distribution of N lines whose centers lie within that interval is[5]

$$A = 1 - \left\{ 1 - D^{-1} \int_0^\infty P(S)dS \int_{\nu_1}^{\nu_1+D} \left[1 - \exp\left(- \int_0^u S\alpha g du' \right) \right] d\nu \right\}^N, \tag{51}$$

where $P(S)dS$ is the normalized probability of finding a spectral line in the intensity interval between S and $S + dS$, and g is the line shape factor defined by Eq. (17).

Define in agreement with Eq. (2) the absorptance $A_{s.l.,D}$ of a single line over the frequency interval D by

$$A_{s.l.,D} = D^{-1} \int_{\nu_1}^{\nu_1+D} \left[1 - \exp\left(- \int_0^u S\alpha g du' \right) \right] d\nu \tag{52}$$

and the absorptance averaged over the intensity distribution by

$$\bar{A}_{s.l.,D} = \int_0^\infty A_{s.l.,D} P(S)dS. \tag{53}$$

Thus, the absorptance for the random distribution of these spectral lines is found to be

$$A = 1 - (1 - \bar{A}_{s.l.,D})^N \tag{54}$$

or in the limit when there are a very large number of lines in the interval

$$A = 1 - \exp(-N\bar{A}_{s.l.,D}). \tag{55}$$

In the derivation of these equations it has been assumed that the half-widths of all the spectral lines are equal. The equations can be generalized if desired by the introduction of a probability distribution function for the half-widths.

Equations (54) and (55) are of great generality and are valid for any line shape, regardless of how the temperature and absorber concentration vary along the slant path. Whenever the absorptance by a single line is known, then the absorptance by a band of randomly arranged lines can be obtained immediately from these results.

Any of the results of Section III can be substituted into Eqs. (53) and (54) or (55) to obtain the absorptance along a slant path. In particular the results given in Eqs. (33), (35), (36), (42), (44), and (45) could be used for this purpose.

As a simple example, when $\gamma = 1$ the single line absorptance is given by Eq. (35). If there is an exponential distribution of line intensities, then

$$P(S) = S_0^{-1} \exp(-S/S_0). \tag{56}$$

It follows from Eqs. (35), (53), (54), and (56) that

$$\bar{A}_{s.l.,D} = {}^1/_2 u S_0 [1 + (\alpha_0/\alpha_1)], \qquad \gamma = 1,$$

so that

$$A = 1 - \{1 - (uS_0/2D)[1 + (\alpha_0/\alpha_1)]\}^N, \qquad \gamma = 1. \tag{57}$$

The expression for the absorptance given by Eq. (35) is calculated over an infinite frequency interval and thus increases indefinitely as u increases. However, this value can be used for the finite interval D until there is appreciable wing absorption outside the interval from spectral lines with their centers within the interval. In cases where this additional factor must be considered a more complicated expression for the equivalent width of a single line over a finite frequency interval,[16] Eq. (88), must be used. This equation can be changed into an expression for slant path absorptance by the method discussed in Section V.

For the statistical model the weak and strong line expressions for the absorptance are obtained from Eqs. (38), (40), (53), (54), or (55). These results are all in agreement with the general correlation procedure given by Eqs. (15) and (30).

IV. Exact Expressions for the Transmission When the Temperature and Fractional Concentration Vary Along the Path

Exact expressions are given in this section for the absorptance when the temperature and fractional concentration of the absorbing gas vary along the slant path. Results are derived for both the statistical and Elsasser band models and for the nonoverlapping line approximation.

A. Nonoverlapping Line Approximation

When there are N spectral lines in the frequency

interval which do not overlap to an appreciable extent, the absorptance due to these lines is given by the expression[17]

$$A\Delta\nu = N \sum_{n=0}^{\infty} \frac{\lambda_n \Gamma(n + 1/2,\ \gamma_s\mu_{-1})}{2^{n-1} n!\ \mu_0^{2n-1/2}\ \gamma_s^{n-1/2}}, \tag{58}$$

where

$$\mu_l = \int_{\alpha_0}^{\alpha_1} \alpha^{2l} G(\alpha) d\alpha,$$

$$\gamma_s = S(\alpha_s)c(\alpha_s)p_s \sec\theta/2\pi\alpha_s g,$$

$$G(\alpha) = \frac{2S(\alpha)c(\alpha)T^{1/2}(\alpha)}{S(\alpha_s)c(\alpha_s)T^{1/2}(\alpha_s)} \left(1 + \frac{\alpha}{2T}\frac{dT}{d\alpha}\right)\alpha,$$

$$\lambda_0 = 1,$$
$$\lambda_1 = -\mu_1,$$
$$\lambda_2 = 4\mu_2\mu_0 - 5\mu_1^2,$$
$$\cdot$$
$$\cdot$$
$$\cdot$$

In these expressions the line intensity, fraction concentration, and temperature are considered to be functions of the half-width of the spectral lines as this factor varies along the slant path. The subscript s refers to some standard set of conditions. The incomplete gamma function is defined as

$$\Gamma(a, b) = \int_a^b x^{a-1} e^{-x} dx. \tag{59}$$

The values of the half-width at the two ends of the slant path are α_0 and α_1. For simplicity it has been assumed that the N nonoverlapping spectral lines have the same half-width and intensity. When this is not the case, the contribution to the absorptance from each of the individual spectral lines as given by Eq. (58) is summed in order to obtain the absorptance of the entire frequency interval. The Lorentz line shape has been assumed in deriving Eq. (58).

Although Eq. (58) appears complicated at first glance, the series usually converges very rapidly so that only a few terms need be used. The limiting forms for the strong and weak line approximations are given by Plass and Fivel.[17]

As an example, assume that the actual pressure and temperature variation along the slant path is such the $G(\alpha)$ can be represented by an expression of the form

$$G(\alpha) = 2\alpha^m \alpha_s^{1-m}, \tag{60}$$

where m can be any constant. In this case the strong line approximation for the absorptance is found from Eq. (58) to be[17]

$$A\Delta\nu = 2\gamma_s^{1/2} \left(\frac{2}{m+1}\right)^{1/2} \left(\frac{\alpha_1^{m+1} - \alpha_0^{m+1}}{\alpha_s^{m-1}}\right)^{1/2}. \tag{61}$$

When the strong line approximation is valid, the absorptance still varies as $\gamma_s^{1/2}$ even though the temperature and fractional concentration vary along the slant path.

B. Elsasser Model

A general expression for the transmittance along a slant path has not been derived for the case when the Elsasser model is applicable. However, several limiting expressions can be derived from the results given in Section II. The absorptance of an Elsasser band along a homogeneous path is given by the expression[1]

$$A_h = 1 - \exp(-S_h u_h/d), \tag{62}$$

when the weak line approximation is valid, and by

$$A_h = \phi[d^{-1}(\pi S_h \alpha_h u_h)^{1/2}], \tag{63}$$

where

$$\phi(z) = 2\pi^{-1/2} \int_0^z e^{-y^2} dy,$$

when the strong line approximation is valid.

It follows from Eqs. (14) and (62) that the absorptance for an Elsasser band over a slant path is

$$A = 1 - \exp\left[-d^{-1} \int_0^u S(u')du'\right], \tag{64}$$

when the weak line approximation is valid.

Similarly the absorptance, when the strong line approximation is valid, as derived from Eqs. (23) and (63) is

$$A = \phi\left[d^{-1}\left(\pi \int_0^u S(u')\alpha(u')du'\right)^{1/2}\right]. \tag{65}$$

C. Statistical Model

The absorptance along a slant path when the statistical model is valid can be obtained directly from previously derived equations. Equation (54) is valid even when the temperature and fractional concentration of the absorbing gas vary along the slant path. The expression for the equivalent width given by Eq. (58) can be used whenever the interval $\Delta\nu$ is sufficiently wide so that most of the absorption is within this interval from lines whose centers are also within this interval. Under these conditions the absorptance due to N randomly arranged spectral lines is

$$A = 1 - \left[1 - \frac{1}{Nd} \sum_{n=0}^{\infty} \int_0^{\infty} \frac{P(S)\lambda_n \Gamma(n + 1/2,\ \gamma_s\mu_{-1})}{2^{n-1} n! \mu_0^{2n-1/2} \gamma_s^{n-1/2}} dS\right]^N, \tag{66}$$

where the symbols which appear here are explained after Eq. (58). The integral over the intensity distribution $P(S)$ can be eliminated if all the spectral lines in the group under consideration have nearly the same intensity.[6]

Considerably simpler expressions for the absorptance can be written when the strong or weak line approximations are valid. The results for the absorptance of a single spectral line in these limits as given by Plass and Fivel[17] can be substituted directly into Eq. (54) to obtain the absorptance for a band. For example, when the weak line approximation is valid, it

follows from Eq. (31) of ref. 17 that the absorptance of N lines randomly arranged in frequency is given by

$$A = 1 - [1 - \pi(\alpha_1 - \alpha_0)\gamma_s\bar{G}(\alpha_0)/Nd\alpha_0]^N, \quad (67)$$

where α_0 and α_1 are the half-widths at the beginning and end of the path, γ_s is defined after Eq. (58), and $\bar{G}(\alpha_0)$ is the value of $G(\alpha)$ as defined after Eq. (58) with $\alpha = \alpha_0$ and also with the factor $S(\alpha_0)$ in the numerator averaged over the intensity distribution function of the spectral lines, $P(S)$.

Similarly when the strong line approximation is valid, it follows from Eq. (33) of ref. 17 that the absorptance of N lines randomly arranged in frequency is given by

$$A = 1 - \left\{1 - (2\pi^{1/2}\gamma_s^{1/2}/Nd)\left\langle\left[\int_{\alpha_0}^{\alpha_1} G(\alpha)d\alpha\right]^{1/2}\right\rangle_{Av}\right\}^N, \quad (68)$$

where the average is to be performed over the intensity distribution function $P(S)$. When the number of lines N in the interval is large, the product over N lines in Eqs. (66), (67), and (68) can be replaced by an exponential as in Eq. (55).

V. Approximate Expressions for Slant Path Absorptance Valid over a Wide Range of Pressures and Path Lengths

General results are derived in Section II for the correlation of the absorptance of slant and homogeneous paths when either the weak or strong line approximations are valid. The results for the weak line approximations, Eqs. (13), (14), and (15), determine the amount of absorbing gas, u_h, along the homogeneous path, but are independent of the pressure along this path. On the other hand, the results for the strong line approximation, Eqs. (23), (25), (27), (28), (29), (30), and (32), determine the product $u_h\alpha_h$ (which is proportional at constant temperature to $u_h p_h$).

It is possible to satisfy simultaneously any pair of these weak and strong line equations since the weak line equation determines the value of u_h and the strong line equation can then be solved to find α_h or p_h. These results can then be substituted into any equation or used in conjunction with any table which has been derived or set of experimental measurements for the absorptance of a homogeneous path. The slant path absorptance calculated in this manner necessarily agrees with the correct result in both the weak and strong line limits. In the intermediate region where both the weak and strong line approximations may be somewhat in error, the result derived in this manner provides a smooth interpolation between the absorptance curves which are valid in the weak and strong line limits. This procedure for obtaining slant path absorptance values is called the interpolation method. In general, the value obtained from this method is very close to the actual slant path absorptance.

There follow three examples of some of the most useful combinations of the strong and weak line equations:

1. Assume all the line strengths and half-widths are equal. Then it follows from Eq. (14) that

$$S_h u_h = \int_0^u S du' \quad (69)$$

When this result is combined with Eq. (23), it is found that

$$\alpha_h = \frac{\int_0^u S\alpha du'}{\int_0^u S du'} \quad (70)$$

The absorptance equation for a homogeneous path is most conveniently expressed in terms of the parameters $\beta_h = 2\pi\alpha_h/d$,

$$x_h = \frac{S_h u_h}{2\pi\alpha_h}, \quad (71)$$

and, for the Elsasser band, the parameter

$$y_h = \frac{S_h u_h}{d \sinh\beta_h}. \quad (72)$$

These quantities which occur in the homogeneous path equations are related to the quantities along a slant path by the expressions

$$x_h = \frac{\left[\int_0^u S du'\right]^2}{2\pi \int_0^u S\alpha du'} \quad (73)$$

and

$$y_h = \frac{\int_0^u S du'}{d \sinh\left[\int_0^u S\alpha du'/2\pi \int_0^u S du'\right]}. \quad (74)$$

These equations are valid in particular both for a single spectral line and for the Elsasser model. Equations (69) and (70) are still valid if the half-width α_i varies from line to line provided the subscript i is added to the half-widths which occur in Eq. (70). All of these equations are valid for any arbitrary variation of the spacing between lines in the spectrum.

2. Assume the line intensities S_i are different but satisfy Eq. (26) and that the half-widths α_i may vary from line to line, then it follows from Eqs. (14) and (27) that

$$S_{ih} u_h = \int_0^u S_i du' \quad (75)$$

and

$$\alpha_{ih} = \frac{\int_0^u S_i \alpha_i du'}{\int_0^u S_i du'}. \quad (76)$$

Because of the assumptions which have been made,

the quantity u_h in Eq. (75) is independent of i as is the ratio α_{ih}/α_i.

3. Assume that the temperature is constant along the path. Then it follows that $u_h = u$, Eq. (15), and from Eq. (28) that

$$\alpha_h = u^{-1}\int_0^u \alpha du', \tag{77}$$

$$x_h = S_h u^2/2\pi\int_0^u \alpha du'. \tag{78}$$

These equations are valid even when the intensity varies from line to line, in which case the quantity S_h in Eq. (78) is a suitably defined mean intensity.

Examples of the use of these relations are given in the following sections. Any combination of weak and strong line equations which relate homogeneous and slant path absorptance can be used to determine u_h and α_h. These values can then be substituted in any expression for homogeneous absorption. The result is an interpolation equation which is correct in both the weak and strong line limits and which usually provides a good approximation to the slant path absorptance over the entire range of parameters.

The method given here is a generalization of the interpolation procedure developed by Curtis,[18] Godson,[19] and Kaplan.[20] In these papers the interpolation equations are derived only for a single spectral line and then are applied to the statistical band model when the number N of spectral lines in the interval is large. The present treatment in terms of the weak and strong line approximations shows directly how the interpolation equations can be derived for other than random arrangements of spectral lines in a band. Results are derived here which are also valid for the Elsasser and random Elsasser models.

A. Elsasser Model

The absorptance over a homogeneous path according to the Elsasser model is[8]

$$A_h = 1 - \sinh\beta_h \int_{y_h}^{\infty} \exp(-z\cosh\beta_h) I_0(z) dz, \tag{79}$$

where I_0 is the Bessel function of imaginary argument. Since Eqs. (69)–(74) are valid for the Elsasser model, it follows that a good approximation to the slant path absorptance is given by Eq. (79) with y_h replaced by its value from Eq. (74) and $\beta_h = 2\pi\alpha_h/d$ replaced by the value obtained from Eq. (70). The corresponding result for the random Elsasser model is[5]

$$A = 1 - \prod_{i=1}^{n} (1 - A_{Ei}), \tag{80}$$

where n Elsasser bands are randomly superposed and A_{Ei} is the absorptance of the ith Elsasser band, which can be obtained from Eq. (79) with the substitutions already described.

A very simple and interesting interpolation equation which is valid when $\beta_h < 0.3$ is

$$A = \phi[{}^1/_2\pi^{1/2}\beta_h f(x_h)], \tag{81}$$

where

$$f(x) = xe^{-x}[I_0(x) + I_1(x)], \tag{82}$$

ϕ is the error function integral defined after Eq. (63), I_0 and I_1 are the Bessel functions of imaginary argument of order 0 and 1, and β_h and x_h are obtained from Eqs. (70) and (73).

When the strong line approximation is valid,[5] $f(x) = (2x/\pi)^{1/2}$ and Eq. (81) becomes identical with Eq. (65). On the other hand, when the weak line approximation is valid,[5] $f(x) = x$. From the series expansion for the error function integral, it then follows from Eq. (81) that

$$A = d^{-1}\int_0^u S(u')du', \tag{83}$$

which is the correct expression for the absorptance in the linear region of the weak line approximation. Thus, Eq. (81) reduces to the correct value in the linear region of the weak line approximation and in the region of validity of the strong line approximation. It also provides a reasonable approximation to the absorptance at intermediate values of the argument. The restriction $\beta_h < 0.3$ must be made since Eq. (81) cannot reproduce the exponential dependence of the absorptance given by Eq. (64) which occurs when $\beta_h > 3$ or the behavior for intermediate values of β_h.

Equation (63) is the generalization to slant paths of an expression for the absorptance over a homogeneous path given by Goody[21] and originally suggested by Godson.

B. Statistical Model

The statistical model expressions for the absorptance along a slant path, Eqs. (54) and (55), depend on the equations for the absorptance of a single spectral line. The absorptance over a homogeneous path of a single spectral line is given by[1,5,22]

$$A_h\Delta\nu = 2\pi\alpha_h f(x_h), \tag{84}$$

where $f(x_h)$ is defined by Eq. (82). It is assumed in the derivation of Eq. (84) that there is no absorption from the spectral line outside of the frequency interval $\Delta\nu$.

When the statistical model is valid, the slant path absorptance obtained from Eqs. (54) and (84) is

$$A = 1 - [1 - 2\pi\alpha_h f(x_h)(\Delta\nu)^{-1}]^N, \tag{85}$$

when all the spectral lines have the same intensity and where α_h and x_h are given by Eqs. (70) and (73), respectively. For the exponential intensity distribution, Eq. (56), the slant path absorptance is[5]

$$A = 1 - [1 - 2\pi\alpha_h x_{0h}(1 - 2x_{0h})^{-1/2}(\Delta\nu)^{-1}]^N, \tag{86}$$

Table I. Conditions for Validity of Slant Path Equations[a]

Eq.	(1) Limiting approximation	(2) Overlap of spectral lines?	(3) Temperature varies along path?	(4) Fractional concentration varies along path?	(5) S_i different?	(6) α_i different?	(7) Finite $\Delta\nu$?	(8) Line spacing	(9) Special assumptions
(13)	W	Yes	Yes	Yes	Yes	Yes	Yes	A	(a)
(14)	W	Yes	Yes	Yes	Yes	Yes	No	A	—
(15)	W	Yes	No	Yes	Yes	Yes	No	A	—
(23)	S	Yes	Yes	Yes	No	No	Yes	A	—
(25)	S	Yes	Yes	Yes	No	Yes	Yes	A	—
(27)	S	Yes	Yes	Yes	Yes	Yes	Yes	A	(b)
(28–29)	S	Yes	No	Yes	Yes	Yes	Yes	A	—
(30)	S	Yes	No	No	Yes	Yes	Yes	A	—
(32)	S	Yes	No	Yes	Yes	Yes	Yes	A	(c)
(33)	N	No	No	No	Yes	Yes	No	A	—
(36)	N	No	No	No	Yes	Yes	No	A	(d)
(42)	N	No	No	No	Yes	Yes	No	A	—
(44)	N	No	No	No	Yes	Yes	No	A	—
(45)	N	No	No	No	Yes	Yes	No	A	—
(47;49)	None	Yes	No	No	No	No	Yes	Reg	—
(54)	None	Yes	Yes	Yes	Yes	No	Yes	Ran	—
(55)	None	Yes	Yes	Yes	Yes	No	Yes	Ran	(e)
(58)	N	No	Yes	Yes	Yes	No	No	A	—
(64)	W	Yes	Yes	Yes	No	No	Yes	Reg	—
(65)	S	Yes	Yes	Yes	No	No	Yes	Reg	—
(66)	None	Yes	Yes	Yes	Yes	No	No	Ran	—
(67)	W	Yes	Yes	Yes	Yes	No	No	Ran	—
(68)	S	Yes	Yes	Yes	Yes	No	No	Ran	—
(69–74)	I	Yes	Yes	Yes	No	No	No	A	—
(75–76)	I	Yes	Yes	Yes	Yes	Yes	No	A	(b)
(77–78)	I	Yes	No	Yes	Yes	Yes	No	A	—
(79)	I	Yes	Yes	Yes	No	No	No	Reg	—
(80)	I	Yes	Yes	Yes	No	No	No	RE	—
(81–82)	I	Yes	Yes	Yes	No	No	No	Reg	(f)
(85–87)	I	Yes	Yes	Yes	Yes	No	No	Ran	—
(88)	I	Yes	Yes	Yes	Yes	No	Yes	Ran	—

[a] The equation given in the first column is valid when the appropriate conditions specified in the following columns are satisfied: (1) the following limiting approximations are valid: W, weak line approximation; S, strong line approximation; N, nonoverlapping approximation; I, interpolation procedure described in Section V; (2) may the spectral lines overlap?; (3) may the temperature vary along the slant path?; (4) may the fractional concentration of the absorbing gas vary along the slant path?; (5) may the line intensities S_i vary from line to line?; (6) may the half-widths α_i vary from line to line?; (7) may the interval $\Delta\nu$ be finite (so that appreciable absorption can occur outside of the interval due to spectral lines whose centers are within the interval)? (8) the following assumptions about the spacing between lines in the band are made: A, may be anything; Reg, regular spacing as required by Elsasser model; Ran, random spacing as required by statistical model; RE, equal spacing of subbands which are randomly superposed as required by random Elsasser model; (9) special assumptions: (a) valid in linear region only; (b) line intensities satisfy Eq. (26); (c) fractional concentration satisfies Eq. (31); (d) $p_0 = 0$; (e) large number of lines within the interval; (f) $\beta_h < 0.3$.

where $x_{0h} = S_{0h}w_h/2\pi\alpha_h$. For any distribution of line intensities it follows from Eqs. (53), (54), and (84) that the slant path absorptance is

$$A = 1 - [1 - 2\pi\alpha_h(\Delta\nu)^{-1}\langle f(x_h)\rangle_{\Delta\nu}]^N, \qquad (87)$$

where the average value of $f(x_h)$ over the intensity distribution is used. These expressions for slant path absorptance are correct in both the weak and strong line limits and usually provide a very good approximation at intermediate values.

The expressions given by Eqs. (85)–(87) do not apply when there is appreciable absorption from the spectral lines outside of the frequency interval $\Delta\nu$. In this case a more complicated expression for the absorptance of a single line over a finite frequency interval must be used,[16]

$$A_h = \exp[-2x_h\zeta_h^2/(1+\zeta_h^2)] - \zeta_h x_h \exp(-x_h)[I_0(x_h) + I_1(x_h)](\pi - \psi) + 2\zeta_h \exp(-x_h)\sum_{n=1}^{\infty} I_n(x_h)\sin n\psi + \exp(-x_h)\sum_{n=1}^{\infty}[I_n(x_h) + I_{n+1}(x_h)]n^{-1}\sin n\psi, \qquad (88)$$

where $\psi = 2\tan^{-1}\zeta_h$ and $\zeta_h = 2\alpha_h/\Delta\nu$. The corresponding expression for slant path transmittance is obtained by substituting for α_h and x_h from Eqs. (70) and (73) and, if necessary, averaging over the

intensity distribution. If the temperature is constant along the path, then the simpler expressions for α_h and x_h given by Eqs. (77) and (78) may be used.

A number of the results derived in this report depend on the existence of a region where the strong line approximation is valid. This region may not be as extensive as suggested by simple considerations[1] when there are numerous weak lines present in the spectrum. This has been demonstrated by both experimental measurements[23] and theoretical calculations.[6,24] However, in actual spectra there always seems to be a strong line region for sufficiently large values of u and small values of p.

VI. Conclusions

A number of equations have been developed in this article which allow the computation of the absorptance for a slant path from data for homogeneous paths. Since the assumptions made in the derivation of these equations vary considerably, the more important results are listed in Table I together with the conditions for the validity of each of these equations.

Some of these results are in the form of theoretical equations for the absorptance of a slant path. Other results are obtained by substitution in the more familiar theoretical representations for the absorptance along a homogeneous path. Still other results are in such a form that they can be conveniently used to calculate the absorptance of a slant path directly from experimental measurements or from theoretically calculated tables of homogeneous path absorption. Approximate equations for slant path absorptance have been derived in Section V which are necessarily valid in both the weak and strong line limits and provide good representations of the absorptance for all values of the parameters.

References

1. G. N. Plass, J. Opt. Soc. Am. **50,** 868 (1960).
2. W. M. Elsasser, Phys. Rev. **54,** 126 (1938).
3. H. Mayer, "Methods of Opacity Calculations," Los Alamos, LA-647 (October 31, 1947).
4. R. M. Goody, Quart. J. Roy. Meteorol. Soc. **78,** 165 (1952).
5. G. N. Plass, J. Opt. Soc. Am. **48,** 690 (1958).
6. P. J. Wyatt, V. R. Stull, and G. N. Plass, J. Opt. Soc. Am. **52,** 1209 (1962).
7. D. E. Burch, E. B. Singleton, and D. Williams, Appl. Opt. **1,** 359 (1962).
8. W. M. Elsasser, *Heat Transfer by Infrared Radiation in the Atmosphere, Harvard Meteor. Studies No. 6* (Harvard University Press, Cambridge, Massachusetts, 1942).
9. G. N. Plass, J. Meteorol. **9,** 333 (1952).
10. G. N. Plass, J. Opt. Soc. Am. **42,** 677 (1952), see Eq. (15).
11. R. O'B. Carpenter, J. A. Wight, A. Quesda, and R. E. Swing, *Predicting Infrared Molecular Attenuation for Long Slant Paths in the Upper Atmosphere,* AFCRC-TN-58-253 (November 1957); J. Opt. Soc. Am. **48,** 285 (1958).
12. G. N. Plass, J. Meteorol. **12,** 191 (1955).
13. F. Pedersen, Meteorol. Ann. **1,** 115 (1942).
14. J. Strong and G. N. Plass, Astrophys. J. **112,** 365 (1950).
15. G. N. Plass and D. I. Fivel, Astrophys. J. **117,** 225 (1953).
16. P. J. Wyatt, V. R. Stull, and G. N. Plass, J. Opt. Soc. Am. **52,** 1209 (1962).
17. G. N. Plass and D. I. Fivel, Quart. J. Roy. Meteorol. Soc. **81,** 48 (1955).
18. A. R. Curtis, Quart. J. Roy. Meteorol. Soc. **78,** 638 (1952).
19. W. L. Godson, J. Meteorol. **12,** 272 (1955).
20. L. D. Kaplan, *The Rossby Memorial Volume* (Rockefeller Institute Press, New York, 1959), pp. 170–177.
21. R. M. Goody, Quart. J. Roy. Meteorol. Soc. **87,** 428 (1961).
22. R. Landenberg and F. Reiche, Ann. Physik **42,** 181 (1913).
23. D. E. Burch and D. Williams, Appl. Opt. **1,** 473 (1962).
24. G. N. Plass, Appl. Opt. (in press).

photo Standard Photo Service Co.

Herbert S. Friedman *Naval Research Laboratory.*

Thomas B. Dowd *ONR,* Chairman IRIS

photo Standard Photo Service Co.

The Use of Polarized Infrared Radiation in Magneto-Optical Studies of Semiconductors

E. D. Palik

Infrared magneto-optical studies of semiconductors often necessitate the use and measurement of various types of polarized radiation. Several magneto-optical experiments such as cyclotron resonance, Faraday effect, Voigt effect, and magneto-plasma effects are briefly described with emphasis on the types of polarized radiation involved. The design and use of several polarizing devices which have been made to facilitate these studies are discussed.

I. Introduction

During the past seven years a number of magneto-optical experiments have been developed to study the band structure of semiconductors. Many of these may be performed in the infrared spectral region. In most of these experiments, it is necessary to produce and measure various types of polarized radiation. Polarizing devices for the infrared can usually be extensions of devices well established for the visible such as pile-of-plates polarizers and quarter wave plates. The difficulty is in finding optical materials transparent in the infrared. In this paper we describe several magneto-optical experiments, the pertinent formulas and information obtained, and the experimental arrangements, with the types of polarized radiation needed. The design of the polarizing devices is discussed. All formulas in this paper are in unrationalized cgs units.

II. Magneto-Optical Experiments

A. Cyclotron Resonance

In the presence of an external magnetic field H, free carriers such as electrons in the conduction band or holes in the valence band execute cyclotron orbits. This motion alters the index of refraction n and extinction coefficient k of the semiconductor making it possible to observe several types of magneto-optical effects. The cyclotron frequency ω_c is given by

$$\omega_c = \frac{eH}{m^* c}, \tag{1}$$

where e is the absolute value of the charge, c is the speed of light, and m^* is the effective mass of the free carriers.

The author is in the U.S. Naval Research Laboratory, Washington 25, D.C.

Received 4 May 1962.

To observe a distinct absorption line, it is necessary that $\omega_c\tau > 1$ where τ is the relaxation time of the carriers. The effective mass is determined from the measurement of the cyclotron frequency and magnetic field. The relaxation time may be estimated from the width of the absorption line. For a simple conduction or valence band for radiation propagating along the magnetic field (orientation I, longitudinal), electrons absorb left circular polarized radiation; holes absorb right circular polarization. The reverse is true if propagation direction is antiparallel to field. Consequently, the use of circular polarization can distinguish between hole and electron absorption. Left circular polarization designated + is defined as electric vector rotating counterclockwise when viewed against the direction of propagation. Linearly polarized or unpolarized radiation would show both types of absorption. When H lies in the sample plane and the direction of propagation is perpendicular to H (orientation II, transverse), the electric vector parallel to H does not couple with the electron motion and, consequently, there is no cyclotron resonance absorption. The free carrier absorption present in zero field is still present. For electric vector perpendicular to H, cyclotron absorption is observed. Orientations I and II are shown in Fig. 1.

Cyclotron resonance may also be observed in reflection as a change in reflectivity due to dispersion associated with the absorption. Cyclotron resonance has been measured in various portions of the infrared region 12–150 μ for several semiconductors such as InSb, InAs, InP, and GaAs.[1–8]

B. Faraday Effect

For this experiment plane polarized radiation propagates parallel to H (orientation I). This radiation can

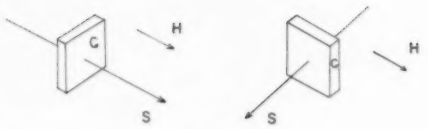

(I) (II)

Fig. 1. Sample orientations I (longitudinal) and II (transverse) showing directions of magnetic field H and propagation of radiation S and electron cyclotron orbit.

be considered as being made up of equal components of left and right circular polarizations. The indexes of refraction are different for the two polarizations producing a relative phase shift and a rotation of the plane of polarization. Working at a frequency much higher than the cyclotron frequency, so that the condition $(\omega - \omega_c)\tau \gg 1$ holds, the rotation θ for electrons is given by

$$\theta = \frac{\pi d}{\lambda}(n_- - n_+) = \frac{e^3 N d \lambda^2 H}{2\pi c^4 n m^{*2}}, \tag{2}$$

where N is the carrier concentration, d is the sample thickness, λ is the wavelength, n is the index of refraction in the absence of the magnetic field, and n_+ and n_- are the indices for left and right circular polarization. For electrons in the approximation above, $n_- > n_+$ so the sense of the rotation is positive or counterclockwise looking against the direction of propagation and magnetic field. Reversing the magnetic field or changing the carriers from electrons to holes reverses the sense of the rotation since the roles of n_- and n_+ are interchanged. This experiment allows a determination of m^*. In the approximation valid for Eq. (2) $\omega_c\tau$ need not necessarily be larger than unity. The rotation in this experiment is independent of τ provided $(\omega - \omega_c)\tau \gg 1$. This type of free carrier Faraday rotation has been measured in several semiconductors including InSb, InAs, InP, GaAs, and Bi_2Te_3.[9-17] If there is a small differential absorption between left and right circular polarized radiation due to absorption in the wing of the cyclotron resonance line, there is a slight ellipticity of the radiation along with the rotation. Measurement of this ellipticity allows a determination of τ.[18] Faraday rotation experiments are usually performed in the spectral region 5–30 μ.

Faraday rotation may also be observed in the region of the cyclotron frequency giving a rotation curve similar to the usual dispersion curve associated with an absorption line. The expression for rotation is complicated and dependent on τ near ω_c. For electrons in the case $(\omega_c - \omega)\tau \gg 1$, i.e., at a frequency much lower than ω_c, the rotation is given by

$$\theta = -\frac{2\pi e N d}{nH}. \tag{3}$$

This rotation is independent of τ and m^*. The sense of the rotation is the opposite of the rotation discussed above.

Near the band gap of a semiconductor, there is an additional Faraday rotation due to the dispersion associated with the across-the-gap absorption discussed in Section II,F, the interband magneto-optical effect.[19,20]

C. Voigt Effect

In orientation II plane polarized radiation oriented at 45° with respect to H may be considered as equal components of $E_\perp$ and $E_\parallel$, electric vectors perpendicular and parallel to the magnetic field. The indices $n_\perp$ and $n_\parallel$ are different so, consequently, a relative phase shift occurs, and the resultant radiation emerges elliptically polarized. Measurement of the ellipticity gives the phase shift δ as

$$\delta = \frac{2\pi d}{\lambda}(n_\parallel - n_\perp) = \frac{e^4 N d \lambda^3 H^2}{4\pi^2 c^6 n m^{*3}}, \tag{4}$$

when $\omega \gg \omega_c, \omega_p, 1/\tau$. Here $\omega_p = (4\pi N e^2/\epsilon_0 m^*)^{1/2}$, the usual plasma frequency, and ϵ_0 is the lattice dielectric constant. In this case the sense of the phase shift is always positive since $n_\parallel > n_\perp$ regardless of the direction of H or whether the free carriers are electrons or holes. Any differential absorption due to cyclotron resonance produces a rotation of the ellipse which complicates the measurement. The ellipticity or phase shift may be measured with a quarter wave plate and plane polarizer. The free carrier Voigt effect is usually measured in the same spectral region as the free carrier Faraday effect.

Dividing Eq. (3) by Eq. (4) gives $\delta/\theta = \omega_c/\omega$. Thus, doing both experiments allows a determination of m^* and N optically without recourse to an electrical measurement to determine the free carrier concentration N.[7,21,22] In practice, a small correction term to Eq. (4) requires that an interactive procedure be followed to obtain N and m^* from Eqs. (2) and (4).[22]

D. Interference Fringes

The interference fringes produced by a thin, plane parallel sample in orientation I using left and right circularly polarized radiation are shifted in a magnetic field. For electrons the fringes observed with left circular polarization shift to higher frequency while those observed with right circular polarization shift a different amount to lower frequency. This shift for $\omega \gg \omega_c$ for the minima of reflection fringes is given by

$$\Delta\lambda_\pm = \frac{2d}{M}(n_\pm - n) \approx \frac{2d}{M}(\epsilon_\infty)^{1/2}\left\{\left[1 - \frac{\omega_p^2}{\omega(\omega \mp \omega_c)}\right]^{1/2} - \left[1 - \frac{\omega_p^2}{\omega^2}\right]^{1/2}\right\}, \tag{5}$$

where M is the fringe order and n is the index in zero

magnetic field. The expressions for $n_\pm$ and n in Eq. (5) are obtained from ref. 22. Reversing the direction of the magnetic field reverses the sense of the fringe shift, as does changing the carriers from electrons to holes. Fringe shifts in orientation II are also possible with $E_\perp$ but will not be as large and will not depend on magnetic field direction or the sign of the free carrier.

E. Magneto-Plasma Effects

In the vicinity of the plasma frequency ω_p for orientation I, the reflectivity minimum shifts in a magnetic field. For n-type material containing electrons as free carriers with left circular polarization, the shift is to higher frequency while for right circular polarization the shift is to lower frequency. These shifts in the reflection minimum (essentially the plasma frequency) are given by

$$\omega \approx \omega_p \pm {}^1/_2\,\omega_c + {}^1/_8\,\frac{\omega_c^2}{\omega_p} \qquad (6)$$

for $\omega_p >> \omega_c$. Measurement of either shift gives ω_c and thus m^*. Reversing the magnetic field direction or changing the sign of the free carrier reverses the sense of this shift.

The same measurements in orientation II using $\parallel$ and $\perp$ radiation give somewhat similar results from which ω_c may also be obtained.[23–28] For most semiconductors the plasma frequency occurs at a wavelength longer than 10 μ.

The magneto-optical Kerr effect naturally follows the previous experiment.[26,29] In this case plane polarized radiation is incident upon a sample in orientation I. Upon reflection, the plane of polarization rotates and the radiation is elliptically polarized. The rotation is due to a relative phase shift in the left and right circular components upon reflection. The ellipticity is due to the differential reflectivity in the two circular components. The phase shift for each circular component $\Delta_\pm$ is given by $\tan \Delta_\pm = 2k_\pm/(1 - n_\pm{}^2 - k_\pm{}^2)$, and the rotation is $\theta = (\Delta_- - \Delta_+)/2$. Here $k_\pm$ are the extinction coefficients for left and right circular polarization, respectively. The rotation reverses when the magnetic field direction is reversed or if the free carriers are changed from electrons to holes.

In orientation II with radiation plane polarized at 45° with respect to the magnetic field, interesting rotation and ellipticity effects are observed. In this case rotation is due primarily to differential reflectivity in $E_\parallel$ and $E_\perp$ components while ellipticity is due primarily to a relative phase shift in the components on reflection.

F. Interband Magneto-Optical Effect

The cases discussed above have been primarily free carrier effects except for the interband Faraday effect. In a magnetic field the valence and conduction bands form Landau levels. Transitions of electrons from valence to conduction band across the forbidden energy gap between various levels can occur giving distinct absorption lines. Using a very thin section ($\sim$5 μ thick) with $\omega_c\tau > 1$ the continuous sample absorption just inside the band gap changes to discrete absorption lines. The selection rules for these transitions depend on both the polarization and orientation of the incident radiation with respect to the magnetic field. Observations with the sample in orientation I are especially definitive using left and right circular polarizations, while for orientation II, plane polarized radiation parallel and perpendicular to the magnetic field is desirable to give simpler spectra.[30–40] The experiment yields information about the electron and hole effective masses and the magnitude of the band gap. Also, interband effects may be studied in reflection.[41]

III. Results for Various Experiments

Typical experimental results are presented in this section emphasizing the information obtained about the band structure of semiconductors.

Results from cyclotron resonance experiments done at NRL are discussed in refs. 5–8.

The Faraday effect has been measured in n-type lead sulfide PbS at room temperature. Results are shown in Fig. 2. The two plots show θ vs. H and θ vs. λ^2. The pertinent data are $N = 1.5 \times 10^{17}$ cm^{-3}, $d = 0.060$

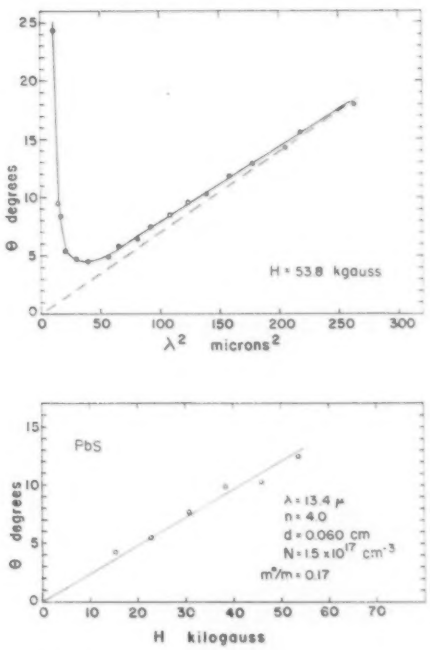

Fig. 2. Faraday effect in n-type PbS at room temperature.

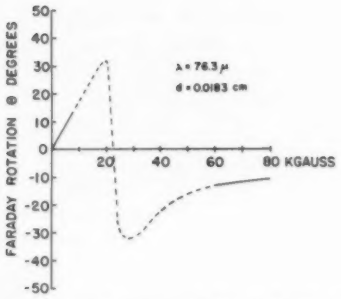

Fig. 3. Faraday effect in n-type InSb at liquid nitrogen temperature near the cyclotron resonance frequency.

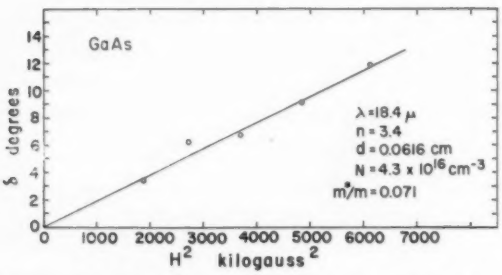

Fig. 4. Voigt effect in n-type GaAs at room temperature.

cm, and $n = 4.0$. The upturn in rotation at short wavelengths is the contribution of the intrinsic gap. Measurements on a purer sample which showed no free carrier rotation gave an interband rotation which, when subtracted from the solid curve, gave roughly the dotted straight line for θ vs. λ^2. The effective mass ratio obtained was 0.17 ± 0.02.

Faraday rotation has been measured in n-type InSb near 80°K where the cyclotron resonance frequency ω_c has been varied from 0 to about 450 cm^{-1} while ω was fixed at 132 cm^{-1}. At the low magnetic fields when $\omega \gg \omega_c$ Eq. (2) holds while at the highest fields where $\omega \ll \omega_c$, the rotation is given by Eq. (3). The rotation is shown in Fig. 3. Experimental points were obtained throughout the magnetic field range shown but the extremes are shown as solid lines for emphasis. Combining the result of the rotation at both extremes yielded an effective mass ratio $m^*/m = 0.015$ and carrier concentration $N = 1.0 \times 10^{15}$ cm^{-3}.

The Voigt effect for n-type GaAs at room temperature is shown in Fig. 4 where δ vs. H^2 is plotted at $\lambda = 18.4\ \mu$. Hall measurements gave $N = 4.3 \times 10^{16}$ cm^{-3}, $d = 0.061$ cm, and $n = 3.4$. The effective mass ratio was found to be 0.071 ± 0.005. Also, data not shown for n-type InSb give a straight line for δ vs. λ^3 verifying the wavelength dependence in Eq. (4).

The shift in interference fringes with magnetic field has been observed in n-type InSb at room temperature. The sample was a plane parallel plate 30 μ thick. The sample was intrinsic with 2×10^{16} carriers/cm^3. Fringes were observed in transmission and reflection using circularly polarized radiation in the spectral region 25–43 μ. To improve the contrast of the reflection fringes, the back surface of the sample was aluminized. The high reflectivity tends to counteract the effect of the free carrier absorption, thus enhancing the contrast.[42] This does not change the wavelength position of the reflection minima which are of interest. The results for reflection are shown in Fig. 5. The fringes shift to lower frequency for right circular polarization and to higher frequency for left circular polarization by a larger amount. Using Eq. (5) the fringe shifts were calculated for the fringe orders shown. The agreement is reasonable. An effective mass ratio of 0.018 was assumed for intrinsic InSb which is reasonable from other experiments of Faraday and Voigt effects. In principle, the fringe experiment would be another method of determining effective mass in semiconductors, although, in practice, the shifts are too small to observe easily in any but the lightest mass materials.

The magneto-plasma measurements were carried out on n-type InSb with $N = 1.0 \times 10^{18}$ cm^{-3} in the spectral range 18–32 μ. The results are shown in Fig. 6 for orientation I. The reflectivity is plotted as a function of frequency with magnetic fields of zero and 25.4 kG for circularly polarized radiation. The shifts in the plasma reflectivity edge are observed to be slightly different for the two circular polarizations. The shifts of the reflection minima (or steep part of the edge) are given by Eq. (6). The cyclotron frequency is found to be 68 cm^{-1} giving $m^*/m = 0.035$. The small term $(1/8)\ \omega_c^2/\omega_p$ accounts for the difference in the shifts to high and low frequency.

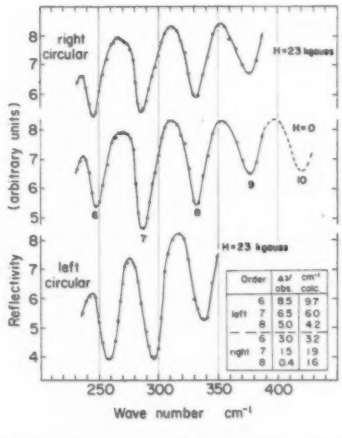

Fig. 5. Reflection interference fringes observed with intrinsic InSb.

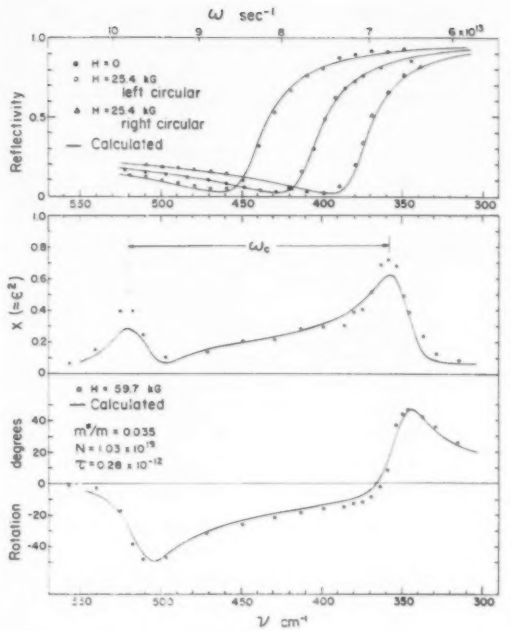

Fig. 6. Magneto-plasma reflection and Kerr rotation and ellipticity in n-type InSb at room temperature for the longitudinal orientation I.

The magneto-optical Kerr effect measurements on the same sample using larger magnetic field are also shown in Fig. 6. The rotation in degrees and a quantity X, closely related to the square of the ellipticity, are shown as a function of frequency. Generally, the extrema in the Kerr rotation and the ellipticity are separated by about the cyclotron frequency ω_c for orientation I. The reflection, rotation and ellipticity data of Fig. 6 can be fitted using complete equations.[10,29] In this way N, m^*, and τ may be determined. For the sample used $N = 1.03 \times 10^{18}$ cm^{-3}, $m^*/m = 0.035$, and $\tau = 2.8 \times 10^{-13}$ sec gave a good quantitative fit to the observed data.

IV. Optical Arrangements

The experiments of Section II, A–F, discussed above have been performed at NRL using the optical arrangements shown in Fig. 7. The optical systems are built around an air core, solenoidal magnet with a 10-cm cylindrical aperture. At the center of the magnet, a vertical field of 80 kG is produced at an expenditure of 2.5 MW of power. The sample orientations I and II are shown in Fig. 7(c). The basic systems shown in solid lines in Fig. 7(a) and 7(b) are used to observe cyclotron resonance. Prism, grating, and reststrahlen monochromators are used in various spectral regions. The radiation is usually partially plane polarized by the optical components.

For cyclotron resonance measurements, the sample may be in the vertical or horizontal position when no special polarizing devices are used, although the horizontal orientation I is preferable to minimize depolarizing effects[3] which will not be discussed here. To detect circular polarization, a quarter-wave plate in the form of a Fresnel rhomb and a linear polarizer are inserted as shown in Fig. 7(a) by dotted lines at B and C near focal points with the subsequent deviation of the beam. The sample is horizontal in orientation I when circular radiation is detected.

For the Faraday effect with orientation I, a rotating linear polarizer is placed into the fore optics near focal point A, and a fixed linear polarizer is set near the slit of the monchromator in Fig. 7(a). Of course, no quarter-wave plate is included.

For the Voigt effect, a rotating, linear polarizer and a quarter-wave plate are inserted at A and a linear polarizer at C. Orientation II is used.

The magneto-plasma Kerr effect is studied by inserting a rotating polarizer at A and a fixed polarizer at C just in the Faraday effect. However, a split spherical mirror replaces mirror M, and the sample is placed in a horizontal position as shown in Fig. 7(c).

Various reflection and transmission filters are placed near focal points as needed in different spectral regions. To reduce the heating of the sample which may be at 4.2°K or lower, it is sometimes necessary to arrange the optics with the monochromator in the fore optics before

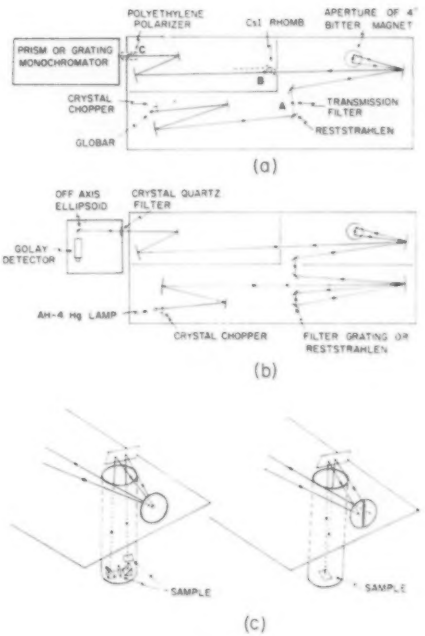

Fig. 7. Optical systems used with 4-in. (10.2-cm) air core solenoidal magnet.

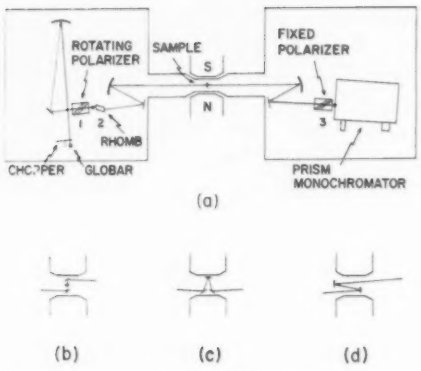

Fig. 8. Optical systems used with iron core magnet showing sample orientations.

the sample, so that only the wavelength interval of immediate interest is focused on the sample.

It may be noted that, frequently, the polarizing components are in the reverse of the usual order one finds described in optics books. Usually, for the Faraday effect the polarizer is fixed before the sample and the analyzer is rotated after the sample. In the present experiment the second polarizer is fixed at the slit of the monochromator to minimize the polarization due to the prism, and the first polarizer is rotated. In the Voigt effect, if one mentally reverses the beam direction in the present arrangement the usual order is obtained. These reverse arrangements may be shown mathematically to give the same results as the usual ones.[43] The reflections from the aluminum mirrors do not produce sufficient ellipticity to cause trouble.

An iron core Arthur D. Little magnet has been used for some of the measurements as shown in Fig. 8. The air gap was 5 cm wide producing a maximum field of 25 kG. The necessary polarizing components are shown for the Voigt effect in positions 1, 2, and 3. By appropriate deletion and change in sample orientation, all the experiments of Section II, A–F, have been performed. Other sample orientations are shown in Figs. 8(b), (c), and (d). The sample is located at a focal point indicated by a large dot. In Table I, the polarizing components are labeled RL, FL, and Q signifying rotating linear polarizer, fixed linear polarizer, and quarter wave plate, respectively. Sample orientations are labeled a, b, c, d. Table I summarizes the optical systems which have been used. In some cases the samples were located in nonmagnetic stainless steel dewars equipped with suitable windows. To reduce the effect of water vapor absorption, the entire optical paths in the solenoid and iron core optical systems are covered with vinyl plastic tents 125 μ thick, and the air is circulated through a commercial molecular sieve to reduce the relative humidity to less than 0.1%. Commercial Perkin-Elmer breaker and amplifier systems are used with display of the data on a Brown Elektronic recorder. In some cases photoconducting detectors are used with subsequent faster chopping and appropriate amplification and rectification.

Recently, experimental techniques involved in several types of solid-state optical experiments have been reviewed with some emphasis on polarization.[44]

V. Polarizing Components

The two basic polarizing components for these magneto-optical experiments are the linear polarizer producing plane or partially plane polarized radiation and the quarter wave plate. These two components may be used to produce or measure any degree of linear polarization or elliptical polarization including, of course, circular polarization. Various optics books discuss the analyzing of different types of visible light.[45–47]

A. Linear Polarizers

In the magneto-optical experiments, various linear polarizers are used including the Polaroid HR filter,[48,49] the silver chloride[50–53] and polyethylene[11,54] pile-of-plates polarizers, and a reflection polarizer using germanium crystals.[55,56] Pile-of-plates polarizers have been discussed by several workers.[57–59] Polaroid HR is a convenient sheet polarizer which may be inserted into the beam at a focal point or elsewhere without beam deviation. The commercial material may be used to 2.7 μ where a strong absorption begins. It is slightly transparent to 5.5 μ but does not polarize well at wavelengths longer than 2.7 μ. At 2 μ it passes 76% of a plane polarized beam and produces more than 97% polarization.

In the present experiments, the polarizers are usually placed near a focal point to limit the size. The beam

Table I. Summary of Optical Systems Used for Various Magneto-optical Experiments in an Iron Core Magnet[a]

Experiment	Polarizing components 1	2	3	Sample orientation
Cyclotron resonance			FL	a
	FL	Q		b
Faraday effect	RL		FL	b
Voigt effect	RL	Q	FL	a
Interference fringes	FL	Q		b
	FL	Q		c
Magneto-plasma reflection	FL	Q		c
			FL	d
Magneto Kerr effect	RL		FL	c
	RL		FL	d
Interband absorption			FL	a
	FL	Q		b

[a] RL, FL, and Q represent rotating linear polarizer, fixed linear polarizer, and quarter-wave plate, respectively. The letters a, b, c, d refer to the sample orientations shown in Fig. 8.

is not collimated. The AgCl polarizer contains four plates of average index 1.95 inclined at the Brewster angle of 63°. Actually the index varies from 2.00 at 2 μ to 1.90 to 20.0 μ. The Brewster angle ϕ is found from the relation $\tan \phi = n$. This polarizer is useful from 2 to 22 μ with a calculated 99% polarization. In practice in the present equipment it is about 97% polarizing at 15 μ and passes 77% of a plane polarized beam. To eliminate beam deviation, especially for use as a rotating polarizer, two sets of plates may be inclined in opposite directions.[53]

The polyethylene polarizer consists of twelve sheets of polyethylene each about 11 μ thick, stretched at the Brewster angle $\phi = 55° 30'$ for $n = 1.46$. Each sheet is separated by a polyethylene spacer about $^3/_4$ mm thick. The thin polyethylene may be obtained from dry cleaning bags. Each sheet is stretched over an embroidery hoop apparatus and separated by a spacer. The assembly is done at a temperature slightly above ambient by using a heat lamp. When the stack cools to ambient, it stretches tightly. Use of nonuniformly thick spacers is desirable to reduce the effects of multiple reflections of the unwanted components.[58,59] The percent polarization of this polarizer was measured by first obtaining an essentially plane polarized beam with an eight-sheet AgCl polarizer at about 15 μ and then measuring the intensity passed at each position of the polyethylene polarizer. The measurements were made in a converging beam of an $f/4$ system. The percent polarization P is obtained from I_{min} and I_{max} as

$$P = \frac{I_{max} - I_{min}}{I_{max} + I_{min}} \times 100. \quad (7)$$

Generally, the polarizer measures about 94% polarizing. Roughly $I_{max} = 32\ I_{min}$. This measured value may be compared with the calculated value obtained from

$$P = \frac{1 - [2n/(n^2+1)]^{4m}}{1 + [2n/(n^2+1)]^{4m}}, \quad (8)$$

where m is the number of sheets. This expression holds if no unwanted multiply reflected rays reach the detector.[58,59] For $m = 12$, $P = 94\%$. This percent polarization is adequate for many uses. The addition of more sheets improves the performance of the polarizer but reduces the transmitted energy. One usually must compromise between energy and percent polarization. The 12-sheet polarizers tested passed about 65% of a plane polarized beam at 15 μ. The polarizer may be rotated continuously with no detrimental beam deviation. Twelve sheets 11 μ thick deviate the beam about 60 μ. The polarizer is usable from 14 μ into the far infrared. There are windows where the polarizer is usable from 2 to 14 μ.[11] This type of polarizer can show interference effects which cause a drop in percent polarization at certain wavelengths.[54] These effects

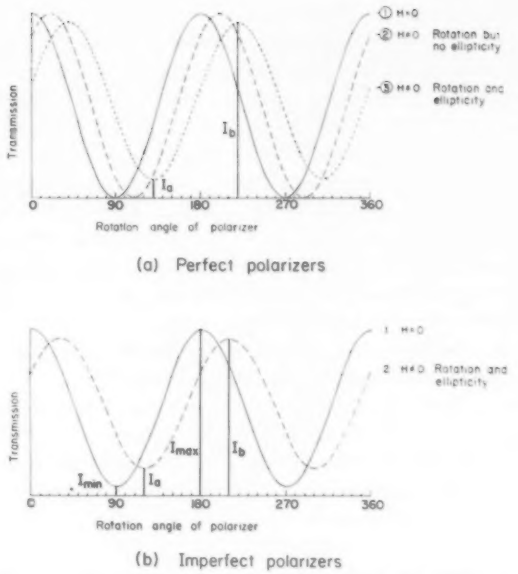

Fig. 9. Transmission of two plane polarizers, one fixed and one rotating illustrating Faraday rotation.

are reduced if the sheets are not uniformly thick. Slight changes in percent polarization were noted as a function of wavelength, but the polarization was never less than 92% from 14 to 40 μ. Calculations indicated that a minimum in percent polarization might be observable at 27 μ where the first-order interference should occur and one at 13.5 μ corresponding to a second-order interference.

In Faraday rotation experiments, the transmission of the fixed and rotation polarizers gives the usual type of sinusoidal trace as shown in Fig. 9(a). With magnetic field the sample also rotates the beam producing the dashed curve 2 shown. The shift in the minima are taken as the rotation angle θ. Usually, the minima occur at 90° and 270°, but the maxima are distorted slightly from 180° and 360° because of the effect of the additional polarizing element in the monochromator.[60] The rotating polarizer is adjustable about vertical and horizontal axes to make the two minima the same height and the two maxima the same height.

When two identical imperfect polarizers are used to produce the transmission curve 1 in Fig. 9(b), the minima do not become zero. The percent polarization of either polarizer may be measured in terms of the ratio $R = I_{max}/I_{min}$. If $I_{max} \gg I_{min}$, then $P = (2R - 1)/(2R + 1)$. The use of imperfect polarizers for experiments which, in principle, require perfect polarizers is becoming of more interest in regions of the infrared where no "perfect" polarizer is available.[61]

Reflection from two surfaces of germanium at the Brewster angle 74° produces over 97% polarization at 13 μ. The polarizer passes about 65% of a plane

polarized beam. The polarizer is usable throughout the infrared since germanium has a nearly constant high reflectivity of 37%. A polarizer utilizing just two surfaces of germanium could not be rotated without producing beam deviation. However, reflecting from germanium to a mirror to a germanium surface, a polarizer can be made so that rotation about the axis of the system will not produce beam deviation.[55] In the far infrared, because of the large angle of incidence and the fact that the extinct coefficient is increasing, there is the possibility of producing elliptically polarized radiation thus decreasing the efficiency of the polarizer. Several reflection polarizers using germanium or selenium have been discussed.[55,56,62–64]

It is known that at the reststrahlen band of an alkali halide like KBr, for an angle of incidence $\neq 0$, the s (perpendicular to the plane of incidence) and p (parallel) components are reflected with different intensities.[54] In the reststrahlen monochromator shown in Fig. 7(b), three crystals with angle of incidence 45° produce about 53% polarization, which is sufficient to measure Faraday rotation when a rotating polyethylene polarizer is placed near the focal point at the crystal quartz filter.

In the near infrared, the prism in a prism monochromator produces enough polarization to give an intensity ratio of about 0.7 between radiation polarized parallel and perpendicular to the slit.[65] In the magneto-optical experiments, a fixed polarizer is usually placed before the entrance slit to pass the component of largest intensity or after the exit slit depending on whether the monochromator is in the fore optics before the sample or in the after optics.

The polarizing effects of the usual reflection echellete grating used as a dispersion element have been discussed.[54,66–68] Generally, at angles less than the blaze angle the p component is more intense while for angles larger than the blaze angle, the s component is more intense.[54]

Echellete gratings used as reflection filters polarize the reflected radiation preferentially. At wavelengths much larger than the grating space where the grating acts as a mirror, there are no significant polarizing effects, but in the transition region where the wavelength is comparable, there can be appreciable differences between the s and p components.[54]

The polarizing effects of wire grids for wavelengths larger than the wire spacing are well known.[69–71] Difficulties in the fabrication of grids with sufficiently narrow spacing has limited the range of these polarizers to the far infrared and microwave regions of the spectrum.[69,70] Recent work has extended this range to the near infrared by developing a technique for evaporation of metal strips on a transparent, rigid base.[71] Other techniques are now available for the construction of grids useful at wavelengths longer than 40 μ. Buckle-

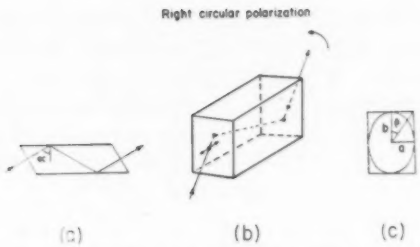

Fig. 10. Fresnel rhomb. (a) Top view showing internal angle of incidence α. (b) Perspective view showing incident plane polarized radiation and emerging right circular polarized radiation. (c) View normal to entrance face showing incident plane polarized radiation oriented at arbitrary angle β.

Meers Company, Minneapolis, Minnesota, has made metal grids on suitable backings[72] for use as far infrared polarizers. Wire polarizers are desirable for infrared applications since they may be designed to produce virtually perfect polarization for all wavelengths longer than some minimum wavelength set by the wire spacing, they are practically lossless, and do not deviate the beam on rotation.

B. Quarter-Wave Plates

Along with the linear polarizer, the quarter-wave plate is also a necessary element for producing and analyzing polarized radiation. The most useful device has been the Fresnel rhomb as shown in Fig. 10. Its use was suggested by M. Hass of this Laboratory. The rhomb is based on the principle that at a particular angle of incidence α, E_p and E_s suffer a relative phase shift of 90° after two total internal reflections. For the region of total reflection, these phase shifts are given by

$$\tan\frac{\delta_s}{2} = \frac{(n^2\sin^2\alpha - 1)^{1/2}}{n\cos\alpha}, \qquad (9)$$

$$\tan\frac{\delta_p}{2} = \frac{n(n^2\sin^2\alpha - 1)^{1/2}}{\cos\alpha}.$$

For NaCl with $n = 1.50$ at 9.0 μ there are two angles α for which $\delta_p - \delta_s = 45°$ for one reflection, namely, 50° 25′ and 53° 20′. The relative phase shift curve peaks at $\delta_p - \delta_s = 45°\ 15'$ for $\alpha = 51°\ 30'$. The rhomb may be made with either angle to produce a 90° phase shift after two internal reflections. The larger angle is preferable because the rate of change of $\delta_p - \delta_s$ with α is less. For practical purposes for NaCl the angle of the rhomb may be anywhere from 50° 25′ to 53° 20′. For a CsI rhomb with $n = 1.70$ at 32 μ $\delta_p - \delta_s = 45°$ at $\alpha = 38°\ 30'$ and 60° 30′, the latter angle being preferable. The phase shift curves for NaCl and CsI are shown in Fig. 11. The rhomb is used at a focal point to minimize its size. Consequently, not all rays are incident at the exact angle to produce a 45° phase shift. For a CsI rhomb with

$\alpha = 60° 30'$, if the central ray of an $f/4$ beam is incident at $60° 30'$, then $\delta_p - \delta_s = 45°$. The extreme rays are incident at about 57° and 64° making $\delta_p - \delta_s$ about 50° and 40°, respectively. The Fresnel rhomb has the advantage that it is usable over a wide wavelength range. A disadvantage is that it deviates the beam.

As shown in Fig. 10(b), plane polarized radiation inclined at an angle $\beta = 45°$ with respect to the vertical emerges from the rhomb as left or right circular polarized radiation. Left circular polarization is defined as electric vector rotating counterclockwise when viewed against the direction of propagation.[45–47] It should be noted that while the plane polarizer and quarter-wave plate produce a sense of left or right circular polarization, which can be deduced, at every reflection after this, the sense changes because of the reversal in direction of propagation; starting with right, one reflection produces left, the next produces right, etc. Therefore, it is important to check the number of pertinent mirror reflections involved. If the angle β is not 45°, elliptically polarized radiation emerges. The angle β determines the ellipticity ϵ. If a and b are the minor and major axes of the amplitude ellipse, $\epsilon^2 = a^2/b^2 = \tan^2\beta$ as shown in Fig. 10(c). The Fresnel rhomb is discussed in several optics books.[45–47]

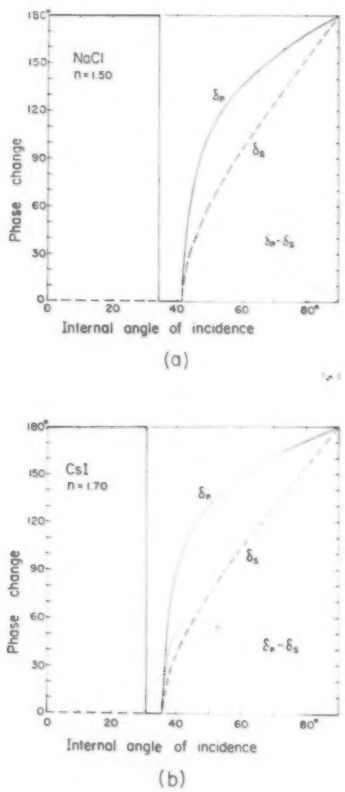

Fig. 11. Phase change of the electric vector for plane polarized radiation internally reflected in NaCl and CsI.

A possible rhomb for the far infrared beyond 40 μ could be made of polyethylene. The path length would be about 4 cm. Polyethylene this thick might be wasteful of energy. Attempts were made to construct a rhomb from paraffin but, again, 4 cm of paraffin was not transparent enough to make a useful rhomb.

The index of crystal quartz is 2.2 in the far infrared where it is transparent. Calculations indicate that the maximum phase shift for one internal reflection is 83° for an internal angle of incidence of 37°. An isosceles prism with angles 37°, 106°, 37° utilizing one internal reflection has been constructed. Radiation normally incident on one surface suffers an internal reflection at an incident angle of 37° and emerges normally through the other face of the prism. The path length through quartz is about 1.2 cm. While not a perfect quarter-wave plate, this device may be useful for some kinds of work. The usual rhomb can be made also, since the larger angle at which a 45° relative phase shift occurs is 69°. The path length of crystal quartz is fairly long, however.

Some thought has been given to using reflection of a plane polarized beam from the surface of a semiconductor like indium antimonide to give circular or elliptically polarized radiation. Since the free carrier and lattice absorption are well known, the index and extinction coefficients may be calculated. The proper angle of incidence and azimuth angle of the plane polarized beam to produce circular polarized radiation at a given wavelength may be calculated from equations given in ref. 46, p. 572. Sample calculations were made for n-type InSb with parameters $N = 1.0 \times 10^{18}$ cm^{-3}, $m^*/m = 0.035$, and $\tau = 3 \times 10^{-13}$ sec. The index of refraction n and extinction coefficient k were calculated from these parameters using equations which take into consideration both free carrier and lattice vibration effects.[74] For normal incidence the sample is over 95% reflecting at wavelengths longer than about 34 μ, except in the region of the lattice absorption near 58 μ. At $\lambda = 72.5\ \mu$ (138 cm^{-1}), $n = 0.819$ and $k = 10.51$. Then $\bar{\psi} = 42° 17'$ and $\bar{\phi} = 83° 28'$, where $\bar{\psi}$ is the principal azimuth angle and $\bar{\phi}$ is the principal angle of incidence. For $\lambda = 82.7\ \mu$ (121 cm^{-1}) $\bar{\psi} = 42° 41'$ and $\bar{\phi} = 85° 30'$. For an incident plane polarized beam making an angle of 45° with respect to the s direction, the electric vectors E_s and E_p are equal. At the principal angle of incidence ϕ, the reflected electric vectors R_s and R_p suffer a 90° phase shift. The resulting amplitude ellipse has its major axis oriented at the principal azimuthal angle $\bar{\psi}$ measured with respect to the s direction. Then $\tan\bar{\psi} = R_p/R_s$. If the incident plane polarized beam is now oriented at an angle $90° - \bar{\psi}$ with respect to the s direction, the reflection amplitudes are equal and the

radiation is circularly polarized. Both ϕ and ψ vary with wavelength since n and k vary with wavelength. Therefore, such a device requires that these angles could be changed readily if it is used over a long wavelength interval.

The usual quarter-wave plate is a thin, plane-parallel plate of naturally double refracting material with the optic axis in the plane of the plate. The ordinary and extraordinary electric vectors parallel and perpendicular to this axis shift phase by an amount given by

$$\delta = \frac{2\pi d}{\lambda}(n_O - n_E). \tag{10}$$

The thickness of the plate may be made any number of quarter waves, although $\delta = \pi/2$ is the usual case. The advantage of plates is that they may be inserted at a focal point easily. The disadvantage is that each plate is good for one particular wavelength or small wavelength region.

Mica is about 70% transparent from the visible to 5 μ with strong absorption at 3.5 μ. The material cuts off gradually to 7 μ. Using the indexes of refraction determined from the sodium D line, we made quarter-wave plates for the near infrared. These did not act as quarter-wave plates for the designed wavelengths but were suitable for other wavelengths indicating that the indexes are different in the infrared. Also, the indexes may vary from sample to sample as the samples were not all the same color. We used the quarter-wave plates to measure the difference in indexes precisely. The plates have the disadvantage that they show interference fringes. This presents no problem in work at a fixed wavelength, however.

Cadmium sulfide CdS is double refracting and commercially available from Eagle Picher Company, Cincinnati, Ohio. In its pure state, grown from the vapor phase, it is 70% transparent out to 15 μ and then rapidly becomes opaque. We have made a quarter-wave plate for use in the 2–15 μ region. It is 2070 μ thick. The difference in index was determined by measuring the wavelengths at which the plate produced circular polarization. The plate was oriented at 45° with respect to the horizontal and placed before an AgCl polarizer fixed to pass the horizontal component into the monochromator. A polarizer before the plate was rotated through 360° to measure the ellipticity of the radiation. The ellipticity plotted against wave number showed oscillations between 0.9 and 0.2 which were roughly evenly spaced. For $n_E - n_O$ a constant, the spacing would be uniform. From the measured wavenumbers at which circular polarized radiation was produced, the difference in index $|n_E - n_O| = \Delta n$ was determined. This difference is plotted in Fig. 12 as a function of wavelength. The difference varies from 0.0050 at 2 μ, to 0.0040 at 11.5 μ. The quarter-wave plate did not produce strictly circular polarization

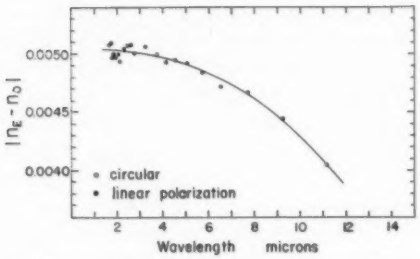

Fig. 12. Difference of the ordinary and extraordinary indexes of refraction for pure CdS in the infrared.

because no great effort was expended to make the surfaces plane parallel and optically flat, and the plate was inserted at a focal point rather than in a collimated beam. For a constant Δn circular polarization would be produced at frequencies ν given by $\nu = (2m - 1)/4d\,\Delta n$ where $m = 1, 2, 3, \ldots$ is an index indicating the "order" of the circular polarization. The first wave number at which circular polarization would be produced for a fixed $\Delta n = 0.0050$ is $\nu = 242$ cm^{-1}, the next at 726 cm^{-1}, the next 1210 cm^{-1}, next 1694 cm^{-1}, etc. Consequently, the above plate could be used at several different wavelengths. By changing d, another plate can be made which is usable at a different set of wavelengths. The changing value of Δn must be taken into consideration in designing an actual plate.

We measured the wavelengths at which linearly polarized radiation was produced by inserting the quarter-wave plate oriented at 45° between crossed linear polarizers. A phase shift of π, 3π, 5π, etc. produced linear polarized radiation rotated by 90° and consequently passed by the second polarizer, while a phase shift of 2π, 4π, 6π, etc. produced linearly polarized radiation in the same plane as the original polarized beam, and consequently was not passed by the second polarizer. The transmission of the system as a function of wavenumber produced oscillations roughly uniformly spaced from which Δn was determined confirming the previous results. Two linear polarizers and several quarter-wave plates may be combined to produce narrow band Lyot filters for the infrared, although they may be wasteful of energy. (See ref. 46, p. 537, for example.) If Soliel compensators are used instead, it is possible to produce a variable wavelength narrow band pass filter.

Tin selenide, SnSe, may be prepared in sufficient purity to achieve about 30% transmission out to 30 μ. It is doubly refracting with a difference of indexes of about 0.5 in the 10 μ region,[74] the two indexes being 4.7 and 4.2. The indexes and difference in indexes probably decrease somewhat out to 30 μ. This material is not yet commercially available.

Sapphire has been found to be transparent and double refracting at wavelengths longer than 150 μ[75] and from the visible to 6 μ. The design of a quarter-

wave plate for the long wavelength region is straightforward. We have made such a plate, but have not tested it yet in the far infrared, but have tested it in the region 2–6 μ.

Since crystal quartz is double refracting in the visible, the possibility exists for its use as a quarter-wave plate at wavelengths longer than 40 μ. The indexes for the ordinary and extraordinary rays at long wavelengths have been determined.[76] On the basis of the difference of indexes $\Delta n = 0.065$ we made a quarter-wave plate of crystal quartz 3.67 mm thick. To test it in the region 100–200 cm^{-1} two polyethylene polarizers were placed in the uncrossed position with the plate oriented at 45° between them at a focal point. For phase shifts of odd multiples of π, the system did not transmit, while for even multiples of π there was considerable transmission. The minima occurred at $\nu = (2m - 1)\pi/2d\,\Delta n$ from which Δn was determined to be 0.070.

The disadvantage that each quarter-wave plate is good at only one wavelength or series of wavelengths may be overcome by constructing a Soliel compensator which is adjusted by a micrometer movement. We are making such a device using CdS. It may be adjusted to be a quarter-wave plate at any wavelength from 2 to 15 μ. It consists of two wedges which slide over each other forming a plane-parallel block with a maximum thickness of 4.75 mm and another block 4.75 mm thick. The optical axes in the two blocks lie in the planes of the blocks and are normal to each other. The appropriate phase shift is obtained by moving one wedge, thus varying the optical paths.

Some of the magneto-optical experiments discussed here could, in principle, be used to produce circularly polarized radiation. For example, in the Voigt effect, the sample becomes doubly refracting, and so could be used as a quarter-wave plate, the magnetic field determining at what wavelengths it acts as a quarter-wave plate. The Voigt effect in n-type indium antimonide is fairly large. In a sample with $N = 2 \times 10^{17}$ carriers/cm^3, $d = 0.5$ mm, $m^*m = 0.023$, and $\lambda = 20$ μ, a phase shift of $\pi/2$ is obtained with 16 kG. There are materials now being made[28] with effective masses an order of magnitude smaller than in InSb which might make feasible such polarizing devices with magnetic fields as small as 1 kG. However, these particular materials are not very transparent.

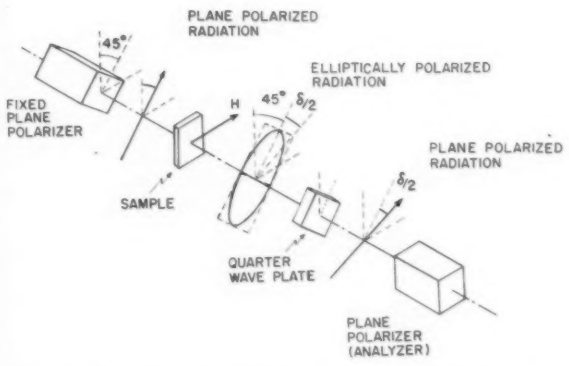

Fig. 13. Measurement of elliptically polarized radiation in the Voigt effect.

In the magneto-plasma reflection experiment, using unpolarized radiation, at $\omega_p - (1/2)\,\omega_c$, the radiation is reflected strongly left circularly polarized as can be seen in Fig. 6. This wavelength position can be varied with the magnetic field.

V. Measurement of Elliptically Polarized Radiation

The need to measure ellipticity arose in the measurements of the Faraday and Voigt effects. In the former, as shown by curve 1 in Fig. 9(a), for perfect polarizers the intensity is zero at the crossed positions of the polarizers. When plane-polarized radiation becomes elliptical, the major axis shrinks and the minor axis grows. As shown by curve 3, the maxima become smaller and the minima become larger. Of course, the major axis of the ellipse rotates by the usual angle θ. The ellipticity is then given by $\epsilon^2 = a^2/b^2 = I_a/I_b = \tan^2 \delta/2$, where a and b are the minor and major axes of the amplitude ellipse. The more complex case occurs when the two identical polarizers are not perfect and the minima are not negligible in zero field[18] as shown in Fig. 9(b). Then $\epsilon^2 = (M - X)/(MX - 1)$, where M is the ratio of minimum to maximum for zero field and X is the same ratio with magnetic field. If $X \gg M$, then $X \approx \epsilon^2$. This is the case for the results shown in Fig. 6 for the magneto-optical Kerr effect.

In the Voigt effect, the ellipse, oriented at 45° with respect to the magnetic field, was measured, at first, in the manner described above; by measuring the intensities with polarizers in crossed and uncrossed positions. Because of the signal-to-noise ratio the limit on determining the phase shift δ was about 20°. A better method utilizes a Fresnel rhomb and a linear polarizer. As shown in Fig. 13, the plane polarized radiation emerges from the sample as elliptical. A quarter-wave plate aligned along the major axis introduces another 90° phase shift thus producing a plane polarized beam making an angle $\delta/2$ with respect to the original 45° position. The plane polarized beam is analyzed with a linear polarizer to measure $\delta/2$. Generally, $\delta/2$ could be measured to within ±1°.

In Voigt effect measurements, if H is not exactly perpendicular to propagation direction S in the sample, the Faraday effect due to the component of H along S will add to the effective rotation measured due to ellipticity giving an error. The sample is generally adjusted to eliminate Faraday rotation. In Fig. 8(a), by moving the polarizer at position 1 to the opposite

side of the rhomb, the rhomb becomes unimportant and the usual Faraday rotation due to sample skewness can be measured and minimized by adjusting the sample.

Various techniques for measuring ellipticity have been discussed by several workers.[77–82]

The author wishes to thank M. Hass, B. W. Henvis, D. L. Mitchell, J. R. Stevenson, S. Teitler, and R. F. Wallis who have assisted in various aspects of this work.

References

1. E. Burstein, G. S. Picus, and H. A. Gebbie, Phys. Rev. **103,** 825 (1956).
2. R. J. Keyes, S. Zwerdling, S. Foner, H. H. Kolm, and B. Lax, Phys. Rev. **104,** 1804 (1956).
3. B. Lax and J. G. Mavroides, Solid State Phys. **11,** 261 (1960).
4. B. Lax, J. G. Mavroides, H. J. Zeiger, and R. J. Keyes, Phys. Rev. **122,** 31 (1961).
5. E. D. Palik, G. S. Picus, S. Teitler, and R. F. Wallis, Phys. Rev. **122,** 475 (1961).
6. E. D. Palik and R. F. Wallis, Phys. Rev. **123,** 131 (1961).
7. E. D. Palik, S. Teitler, and R. F. Wallis, J. Appl. Phys. Suppl. **32,** 2132 (1961).
8. E. D. Palik, J. R. Stevenson, and R. F. Wallis, Phys. Rev. **124,** 701 (1961).
9. E. W. J. Mitchell, Proc. Phys. Soc. (London) **A68,** 973 (1955).
10. M. J. Stephen and A. B. Lidiard, J. Phys. Chem. Solids **9,** 43 (1959).
11. S. D. Smith, T. S. Moss, and K. W. Taylor, J. Phys. Chem. Solids **11,** 131 (1959).
12. A. K. Walton and T. S. Moss, J. Appl. Phys. **30,** 951 (1959).
13. T. S. Moss and A. K. Walton, Proc. Phys. Soc. (London) **74,** 131 (1959).
14. T. S. Moss and A. K. Walton, Physica **25,** 1142 (1959).
15. I. G. Austin, J. Electronics and Control **8,** 167 (1960).
16. I. G. Austin, Proc. Phys. Soc. (London) **76,** 169 (1960).
17. M. Cardona, Phys. Rev. **121,** 752 (1961).
18. S. D. Smith and C. R. Pidgeon, Proceedings International Conference on Semiconductor Physics, Prague 1960, p. 342.
19. B. Lax and Y. Nishina, Phys. Rev. Letters **6,** 464 (1961).
20. B. Lax and Y. Nishina, J. Appl. Phys. Suppl. **32,** 2128 (1961).
21. S. Teitler and E. D. Palik, Phys. Rev. Letters **5,** 1546 (1960).
22. S. Teitler, E. D. Palik, and R. F. Wallis, Phys. Rev. **123,** 1631 (1961).
23. W. S. Boyle, A. D. Brailsford, and J. K. Galt, Phys. Rev. **109,** 1396 (1958).
24. B. Lax and G. B. Wright, Phys. Rev. Letters **4,** 16 (1960).
25. W. S. Boyle and A. D. Brailsford, Phys. Rev. **120,** 1943 (1960).
26. B. Lax and S. Zwerdling, *Progress in Semiconductors* (Wiley, New York, 1960), Vol. 5.
27. G. B. Wright and B. Lax, J. Appl. Phys. Suppl. **32,** 2113 (1961).
28. T. C. Harmon, A. J. Strauss, D. H. Dickey, M. S. Dresselhaus, G. B. Wright, and J. G. Mavroides, Phys. Rev. Letters **7,** 403 (1961).
29. E. D. Palik, B. W. Henvis, and S. Teitler, Bull. Am. Phys. Soc. **7,** 184 (1962).
30. E. Burstein, G. S. Picus, H. A. Gebbie, and F. Blatt, Phys. Rev. **103,** 826, (1956).
31. S. Zwerdling, R. J. Keyes, S. Foner, H. H. Kolm, and B Lax, Phys. Rev. **104,** 1805 (1956).
32. E. Burstein and G. S. Picus, Phys. Rev. **105,** 1123 (1957).
33. S. Zwerdling and B. Lax, Phys. Rev. **106,** 51 (1957).
34. S. Zwerdling, B. Lax, and L. M. Roth, Phys. Rev. **108,** 1402 (1957).
35. S. Zwerdling, L. M. Roth, and B. Lax, Phys. Rev. **109,** 2207 (1958).
36. S. Zwerdling, B. Lax, K. J. Button, and L. M. Roth, J. Phys. Chem. Solids **9,** 320 (1959).
37. S. Zwerdling, B. Lax, L. M. Roth, and K. J. Button, Phys. Rev. **114,** 80 (1959).
38. D. F. Edwards and V. J. Lazazzera, Phys. Rev. **120,** 420 (1960).
39. E. Burstein, G. S. Picus, R. F. Wallis, and F. Blatt, Phys. Rev. **113,** 15 (1959).
40. S. Zwerdling, W. H. Kleiner, and J. P. Theriault, J. Appl. Phys. Suppl. **32,** 2118 (1961).
41. R. N. Brown, J. G. Mavroides, M. S. Dresselhaus, and B. Lax, Phys. Rev. Letters **5,** 243 (1960).
42. W. G. Spitzer and M. Tannenbaum, J. Appl. Phys. **32,** 744 (1961).
43. G. K. T. Conn and G. K. Eaton, J. Opt. Soc. Am. **44,** 484 (1954).
44. H. Y. Fan, *Methods of Experimental Physics* (Academic Press, New York, 1959), Vol. 6, Part B, p. 249.
45. R. W. Wood, *Physical Optics* (Macmillan, New York, 1934).
46. F. A. Jenkins and H. E. White, *Fundamentals of Optics* (McGraw-Hill, New York, 1950).
47. J. Strong, *Concepts of Classical Optics* (Freeman, San Francisco, 1958).
48. R. P. Blake, A. S. Makas, and C. D. West, J. Opt. Soc. Am. **39,** 1054 (1949).
49. Polaroid Corp. literature, Cambridge 29, Massachusetts.
50. N. Wright, J. Opt. Soc. Am. **38,** 69 (1948).
51. R. Newman and R. S. Halford, Rev. Sci. Instr. **19,** 270 (1948).
52. E. Charney, J. Opt. Soc. Am. **45,** 980 (1955).
53. A. S. Makas and W. A. Shurcliff, J. Opt. Soc. Am. **45,** 998 (1955).
54. A. Mitsuishi, Y. Yamada, S. Fujita, and H. Yoshinaga, J. Opt. Soc. Am. **50,** 433 (1960).
55. R. N. Brown, T. F. Deutsch, and S. Zwerdling, Lincoln Laboratory Quarterly Progress Report, Nov. 1957, p. 40.
56. D. F. Edwards and M. J. Bruemmer, J. Opt. Soc. Am. **49,** 860 (1959).
57. A. Elliot, E. J. Ambrose, and R. Temple, J. Opt. Soc. Am. **38,** 212 (1948).
58. G. K. T. Conn and G. K. Eaton, J. Opt. Soc. Am. **44,** 553 (1954).
59. G. R. Bird and W. A. Shurcliff, J. Opt. Soc. Am. **49,** 235 (1959).
60. E. Charney, J. Opt. Soc. Am. **51,** 912 (1961).
61. G. Heilmann, Optik **18,** 440 (1961).
62. A. H. Pfund, J. Opt. Soc. Am. **37,** 558 (1947).
63. N. J. Harrick, J. Opt. Soc. Am. **49,** 376, 379 (1959).
64. S. Takahashi, J. Opt. Soc. Am. **51,** 441 (1961).
65. I. Simon, J. Opt. Soc. Am. **41,** 336 (1951).
66. J. H. Rohrbaugh and R. D. Hatcher, J. Opt. Soc. Am. **46,** 104 (1956); **48,** 704 (1958).
67. A. Hadni, E. Decamps, D. Grandjean, and C. Janot, Compt. rend. **250,** 2007 (1960).
68. S. Mizushima, T. Shimanouchi, I. Ichishima, M. Tsuboi, I. Nakagawa, M. Hyashi, A. Yamaguchi, K. Fukushima, H. Kamayama, S. Tsuchiya, S. Takeda, J. Seto, I. Suzuki, and H. Takahashi, "A report on the Perkin-Elmer grating spec-

trometer model 112-G." English translation published by the Perkin-Elmer Corporation, Norwalk, Connecticut (1959).
69. H. du Bois and H. Rubens, Phil. Mag. **22,** 322 (1911); Ann. Physik **35,** 243 (1911).
70. C. W. Peters and W. K. Pursley, J. Opt. Soc. Am. **42,** 877(A) (1954); W. K. Pursley, Ph.D. dissertation, University of Michigan 1956.
71. G. R. Bird and M. Parrish, J. Opt. Soc. Am. **50,** 886 (1960).
72. D. L. Mitchell, private communication.
73. M. Hass and B. W. Henvis, private communication.
74. D. L. Mitchell, Ph.D. dissertation, Syracuse University 1959.
75. E. Loewenstein, J. Opt. Soc. Am. **51,** 108 (1961).
76. H. Rubens, Berlin Ber., p. 1280 (1916).
77. J. R. Beattie and G. K. T. Conn, Phil. Mag. **46,** 222 (1955).
78. J. R. Beattie, Phil. Mag. **46,** 235 (1955).
79. G. K. T. Conn and G. K. Eaton, J. Opt. Soc. Am. **44,** 477, 546 (1954).
80. R. C. Plumb, J. Opt. Soc. Am. **50,** 892 (1960).
81. H. G. Gerrard, J. Opt. Soc. Am. **38,** 35 (1948).
82. M. Richartz and H. Hsii, J. Opt. Soc. Am. **39,** 136 (1949).

Applied Optics

Letters to the Editor

Letters to the Editor should be addressed to the Editor, APPLIED OPTICS, 1155 16th St., N.W., Washington 6, D.C.

Improved Silver Films for Multiple-Beam Interferometry

D. J. Bradley

Royal Holloway College, London, England (now at Imperial College, London, England).
Received 2 August 1962.

In multiple-beam interferometry, high reflecting powers with minimum absorption are necessary to obtain high finesse with reasonable spectral transmittance. At wavelengths greater than about 5300 Å, freshly prepared silver films with reflectances varying from 0.97 to 0.96 have been found to compete favorably in transmittance with multilayer films of the same reflectance,[1] without suffering from the selectivity in wavelength-working region of the latter. Moreover, they are much easier to prepare and can be easily removed without damaging the interferometer optical finish. The difficulty with silver films has been that they deteriorate even under controlled laboratory conditions.

Recently, the author had to use the same interferometer plates over the range 4900–6200 Å in a spectral determination of isotope abundance.[2] High finesse was necessary to resolve isotope spectral components without overlap of orders, and, at the same time, maximum transmittance was required for a good signal-to-noise ratio from the photomultiplier detector.

From the results of Sennet and Scott[3] on silver and Hass *et al.*[4] on aluminum, it was apparent that rapid evaporation is essential for the production of the best quality reflecting metal films for interferometry. A difficulty here, as distinct from the preparation of totally reflecting mirrors, is the control of the film thickness, since the usual monitoring systems are too slow; so reliance on evaporation of a weighed amount was necessary. The films were evaporated, at a distance of 30 cm from a molybdenum boat, in a 46-cm bell jar evacuated by a three-stage oil-diffusion pump with a speed of 1000 liter/sec^{-1} backed by a 15-cm rotary pump. Before evaporation, the interferometer plates were degreased by washing in dilute H_2O_2, then detergent, and a final rinse in distilled water, followed by discharge cleaning, the discharge being run at 3000 V for 3 min. Any slight variations in the optical properties of the films over their area were found to be due to variation in thickness, as measured by Tolansky fringes, and, hence, not to variation in substrate cleanliness.

Merely using the inverse square law to calculate the mass of silver needed is not sufficient, a geometrical factor being introduced by the focusing properties of the boat filament, and 5 preliminary calibration is necessary. On passing a current of 15a A through the filament, most of the silver goes off in less than 0 sec at a pressure $< 5 \times 10^{-5}$ mm Hg.

This evaporation procedure gives very good quality reflect'ng films, $R = 0.95$, $T = 0.034$ being typical at λ 5300, corresponding to a reflecting finesse of 61 and an interferometer transmittance of 0.46, which compare favorably with the best results published for silver. The results are quite reproducible.

Films of different thicknesses were also prepared and tested. Thinner films were found to age more rapidly. A film with $T = 0.20$ initially, decreased to $T = 0.14$ after 16 hr, while an initial $T = 0.10$ decreased to 0.08 over the same period. On the other hand, there was very little change in the transmittance of thicker films. Over 34 days, two films with $R = 0.95$ had transmittance changes from 0.032 and 0.034 to 0.029 and 0.032, respectively. During these periods, the films were kept under conditions of normal use in a spectroscopy laboratory. Even after six months, no difference could be discerned in the interferometer fringe patterns. A typical aging for good quality films evaporated in 5 min, giving $R = 0.95$ is from $T = 0.03$ to 0.02 after 22 days.[5]

Thus, it seems that rapid evaporation produces a high quality silver film with excellent keeping properties. The rapid aging of the thinner films is to be expected from their more aggregated structure. A continuous film having a smaller exposed surface area is less liable to contamination. Similarly, the more rapid aging of slowly evaporated films is explicable in terms of their more aggregated structure.[3] A similar reduced aging in electrical conductivity of silver films produced in a vacuum chamber previously flushed with helium has been reported by Srivastava and Scott.[6]

References

1. D. A. Jackson and K. Kuhn, Nature **170,** 455 (1952).
2. D. J. Bradley, Proc. Roy. Soc. (London) **A262,** 529 (1961).
3. R. S. Sennet and G. D. Scott, J. Opt. Soc. Am. **40,** 203 (1950).
4. G. Hass, W. R. Hunter, and R. Tousey, J. Opt. Soc. Am. **46,** 1009 (1956).
5. H. Kuhn and B. A. Wilson, Proc. Phys. Soc. (London) **43,** 745 (1950).
6. G. N. Srivastava and G. D. Scott, Brit. J. Appl. Phys. **12,** 255 (1961).

Angular Distribution of Light Rays from a Gas Discharge Source

R. L. Aagard, R. A. Dufault, and S. B. Schuldt

Honeywell Research Center, Hopkins, Minnesota
Received 21 November 1962.

The angular distribution of rays about the normal to a point on the surface of a gas discharge source is important to the calculation of the efficiency with which an elliptical reflector transfers pumping radiation from a cylindrical source to a cylindrical laser.[1] Let us denote this distribution by a function $I(\beta)$, where β is the angle with respect to a normal to the surface of the source measured in a plane of cross section. At the present time the quantity $I(\beta)$ is not generally known, but it seems likely that it will eventually be made available as a part of the technical information accompanying a particular discharge source. In anticipation of this, we wish to present some measurements of the angular distribution of rays from a gas discharge source, and discuss how they are related to the efficiency of an elliptical reflector.

A linear 6.3-mm diam Ne discharge lamp with 1-mm wall thickness was operated at 60 cps for these measurements. A narrow slit 1 mm wide and 25 mm long was made along the surface of the discharge tube by shaving off a layer of black paint which had been applied in the neighborhood of the slit. The remainder of the light was shielded by a blackened absorber which surrounded the tube, except for a wide slit over the opening in the paint strip. The relative output intensity was measured as a function of position angle β using a photomultiplier and an improvised goniometer. The photomultiplier signal was displayed on an oscilloscope and the relative amplitude of this signal is shown as a function of β in Fig. 1.

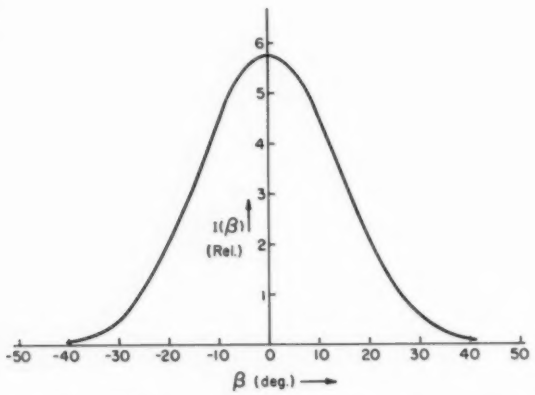

Fig. 1. Angular distribution of rays from a gas discharge source, where β is the angle with respect to a normal to the surface of the source measured in a plane of cross section.

We note that the distribution is sharply sloped about the normal $\beta = 0$ and drops to zero near $\beta = \pm 30°$. In terms of the transfer efficiency of an elliptical reflector, this means that the rays appear to come from points very near the source focus. Therefore, the output from the lamp will be reasonably well focused at the laser. This accounts for the fact that in practice elliptical reflectors are relatively insensitive to eccentricity.

The concentration of rays about the normal is due primarily to the curvature of the tube envelope, so that we would expect the distribution to broaden as the ratio of wall thickness to envelope diameter decreases. Hence, the past success of elliptical reflectors can be explained in these rather simple terms. However, as systems are made larger, we expect a thorough analysis will be required to optimize the reflector transfer efficiency.

Reference

1. S. B. Schuldt and R. L. Aagard, Appl. Opt. **2**, 509 (1963).

Dichroic Multiple Beam Interferometer Microscope

M. J. Irland and E. B. Schermer

Scientific Laboratory, Ford Motor Company, Dearborn, Michigan.
Received 12 June 1962.

For precise measurement of thicknesses of thin films in the range 0.1–0.01 μ or less, the advantages of multiple-beam interferometry with the microscope over two-beam interferometry are well known.[1] Gains in transparency and potential resolution result from the use of a nonabsorbing multilayer film stack in place of a metallic film.[2,3] The small air space permissible with multiple-beam interferometry makes contact between the specimen and the reference flat almost inevitable. When a microscope is provided with a special objective having a built-in reference flat, contact with specimens is likely to damage the coating on the flat, requiring renewal more frequently than is convenient. In an effort to avoid excessive frequency of film renewal, the authors replaced the glass reference flat with one of fused silica coated with a multilayer stack composed of titanium dioxide (rutile) and silicon monoxide, materials known for their good adhesion and abrasion resistance.[4,5]

Since multilayers can be made to yield widely different reflectances at relatively nearby wavelengths, it was decided to design the multilayer for high reflectance at the green line of mercury and high transparency in blue light. Figure 1 shows the calculated and measured reflectances for a three-layer film combination, HLH on fused silica. Refractive indices at the mercury green line are taken as 2.66 for TiO_2 and 1.87 for SiO in agreement with values measured for single films on glass. The films are one-quarter wavelength thick at 6250 Å. Dispersions of the films are taken into account, but that of silica was neglected as insignificant.

The reflectance curve was measured with an attachment for a Beckman DU Spectrophotometer built at this laboratory which permits measurement of absolute reflectance at angles of incidence from 5° to nearly 90°.

The TiO_2 films were formed by evaporation of the metal in a vacuum of 10^{-5} Torr at a rate of ±25 Å/sec to an optical transmission of 4.8% at 5461 Å, followed by heating in air at 500°C for 8 hr. Silicon monoxide was vacuum evaporated at ±150 Å/min to an optical thickness of $\lambda/4$ at 6250 Å. This optical thickness was substantially unchanged by subsequent heating after the third (titanium) layer had been deposited.

In use, the film has proved substantially more satisfactory than any metal or dielectric film previously used. It is unmarred after approximately 100 applications, whereas other metal and dielectric films have shown significant damage after this much use. The reflection coefficient matches approximately that of polished steel, giving good fringe contrast on metallographic specimens. The fringe width when sharpened by photography permits measurement of the thickness of thin films with an accuracy of ±10 Å (see Fig. 2). Further accuracy can be attained by adding more layers, at some sacrifice. In principle, each additional pair of nonabsorbing layers having the refractive

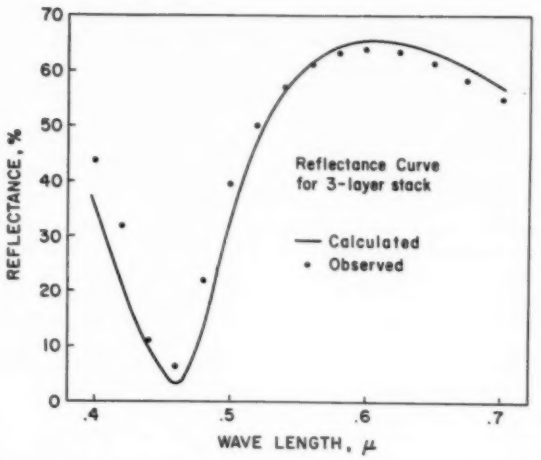

Fig. 1. Calculated and observed reflectance curves for three-layer dielectric stack.

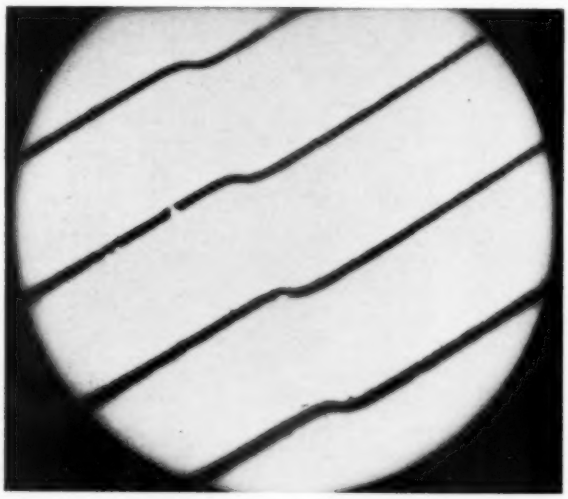

Fig. 2. Multiple-beam fringes between three-layer stack and Ge-coated surface.

indices of the materials used here will approximately halve the fringe width. In practice, the widths are greater because of absorption in the film and the difficulty of controlling the thickness of TiO_2 layers with the necessary precison. Moreover, increasing the number of layers decreases the abrasion resistance.

References

1. S. Tolansky, *Multiple Beam Interferometry* (Clarendon, Oxford, 1948), p. 45 ff.
2. J. A. Belk, S. Tolansky, and D. Turnbull, J. Opt. Soc. Am. **44,** 5 (1954).
3. O. S. Heavens, *Optical Properties of Thin Solid Films* (Butterworths, London, 1955), pp. 215, 224.
4. G. Hass, Vacuum **II,** 331 (1952).
5. G. Hass and N. W. Scott, J. Opt. Soc. Am. **39,** 179 (1949).

An Alignment Interferometer

James B. Saunders

National Bureau of Standards, Washington, D.C.

Received 5 January 1963.

An alignment interferometer that permits very accurate alignment of points along a straight line several miles long, is illustrated in Fig. 1. The annulus or perforated mirrors, M_1 and M_2, are approximately spherical. The semireflecting mirror, B, is plane (a beam divider). The two Kösters double-image prisms, P_1 and P_2, are similar and have their dividing planes perpendicular and parallel, respectively, to the plane of the figure. Interference fringes are formed by rays of light from a small circular-shaped light source near the axis and at a distance, D, to the right of the figure. Interference is formed by combining pairs of rays 2–2′, 3–3′, 4–4′, and 5–5′ at the dividing planes of the two prisms.

The high degree of compensation attainable in this system permits the use of white light without filtering. The fringes produced by this system have the highest contrast ever observed by this author. This permits settings, without an eyepiece for magnification, to better than one-twentieth of a fringe spacing, or to one-thousandth, electronically.

The reflecting surfaces, M_1 and M_2, are not critical. They should, however, approximate spheres. The convex surface of the prism has similar characteristics but the other optical surfaces of the prisms should be quite plane if straight fringes are to be obtained. Assuming plane surfaces on prisms made from good optical glass, the only remaining requirement for straight fringes is that all curved surfaces be surfaces of axial symmetry. A homogenous atmosphere is assumed for this discussion.

Contrast in the fringes begins to deteriorate with an increase in diameter of the source beyond $\lambda D/(4A)$, where λ is the wavelength of the light and A the diameter of M_1. Ample illumination is obtainable with zirconium arc lamps.

In order for fringes to be observable, it has been found experimentally that some polarization means must be introduced, such as polarizers or quarter-wave plates, shown as C_1 and C_2 in Fig. 1. When a plane polarizer (such as a sheet of Polaroid) is inserted as indicated and is rotated, the fringe pattern is seen to alternate between two states that are out of phase, so that the resultant of both states (seen with no polarizer, or seen with equal intensities of s and p polarization) is uniform illumination over the field. The fringe pattern can best be observed with quarter-wave plates at positions C_1 and C_2, and oriented to superimpose the fringe

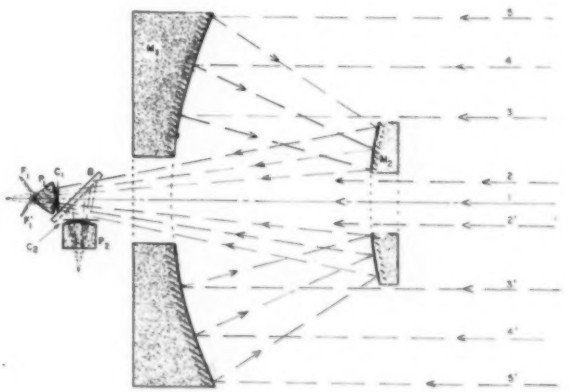

Fig. 1. An alignment interferometer. Rays 2 and 2′ are incomplete because of crowding.

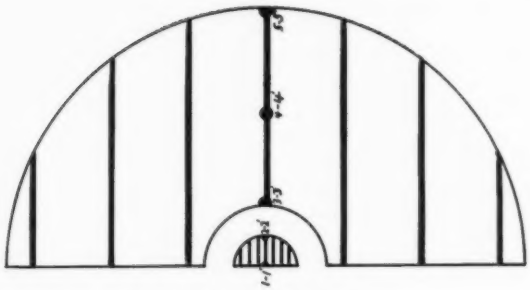

Fig. 2. Fringes of interference.

patterns of the two states of polarization. In this way the transmission efficiency of the alignment interferometer is maximized.

Two sets of fringes (shown in Fig. 2) are formed, one by pairs of rays between 1–1′ to 2–2′, which enter the prisms directly, and another set formed by pairs of rays 3–3′ to 5–5′, which are reflected from M_1 to M_2 before entering the prisms. Each of these sets may be seen by an observer located at any one of four points, from F_1 and F_1' through prism P_1 and from two other similar points, F_2 and F_2', (outside of the plane of Fig. 1 above and below P_2) through prism P_2. The inner sets of fringes are used for aligning points near the instrument and the outer sets are for aligning more distant points. The fringes seen at F_1 and F_1' are for alignment in the plane of Fig. 1 and those seen at F_2 and F_2' are for alignment in a plane perpendicular to that of Fig. 1.

An error of one-tenth of a fringe spacing corresponds (for $\lambda = 5.6 \times 10^{-5}$ cm and $A = 25$ cm) to $2.2\ D \times 10^{-7}$ cm, or less than 0.4 mm for $D = 1.6$ km and less than 4 mm for $D = 16$ km. This same error (one-tenth fringe) in the inner set for which the aperture (of the prisms) would normally be 2.5 cm, would be ten times larger. However, this set would only be used for smal, values of D. The corresponding error in it, for $D = 16$ ml would be approximately 0.04 mm.

Electronic Chopper for Spectral Lamps

R. C. Mackey and S. A. Pollack

R. C. Mackey is in the Engineering Department, University of California, Los Angeles, California. S. A. Pollack is with the Space Technology Laboratories, Redondo Beach, California.
Received 6 January 1963.

In the spectroscopic study of luminescent materials it is frequently of interest to know the decay time from an excited state to the terminal state. The usual measurement techniques require one-shot determinations with a flash source or a periodic presentation using a mechanically chopped light source. Mechanical choppers are not particularly fast for diffuse sources or easily varied in chopping rate. For measuring the mean lifetime of luminescence of very short duration, less than 10^{-6} sec, the so-called phase shift technique is usually used.[1,2] Two techniques which are known as "electronic switching"[3] and "stroboscopic sampling,"[4] to which references are often made, deal with the method of detection and recording of the decay of luminescence rather than with the method of excitation.

Here we describe an electronic chopping technique which has proved successful with several types of spectral sources and has materially reduced the labor of data recording. Availability of the moderately priced Osram discharge lamps makes it possible to cover almost continuously the range of excitation between 3000 Å and 9000 Å as indicated in Fig. 1. An early attempt at electrically chopping the source with a mechanical vibrator[5] suffered from current limitation, contact bounce, and fixed frequency operation.

Figure 2 is a block diagram of the system used to display repetitively the decay characteristics of luminescent materials. A square-wave generator of variable frequency causes the chopper circuit to switch the spectral source on and off with essentially equal periods. During the on period, the sample is illuminated and an excited steady state is achieved. When the lamp is switched off the decay characteristic is sensed by the photomultiplier and displayed repetitively by the oscilloscope. The monochromator permits resolution and detailed examination of the emission spectra. The variable frequency of the square-wave generator enables the on and off time to be made compatible with the decay time of the particular material under study. Figure 3 shows the decay characteristic of the emission of ruby ($Al_2O_3:Cr^{3+}$) and $CaF_2:Er^{3+}$ when excited by a Pen-Ray mercury lamp.

The decay characteristic of a spectral lamp determines its suitability for electronic chopping as it is necessary that the de-ionization time be short compared to the decay time of the emission line under study. Because it is time ratio that is of importance even spectral sources with long de-ionization times may be useful with some materials. Table I presents the extinction time for several spectral lamps. The extinction time is

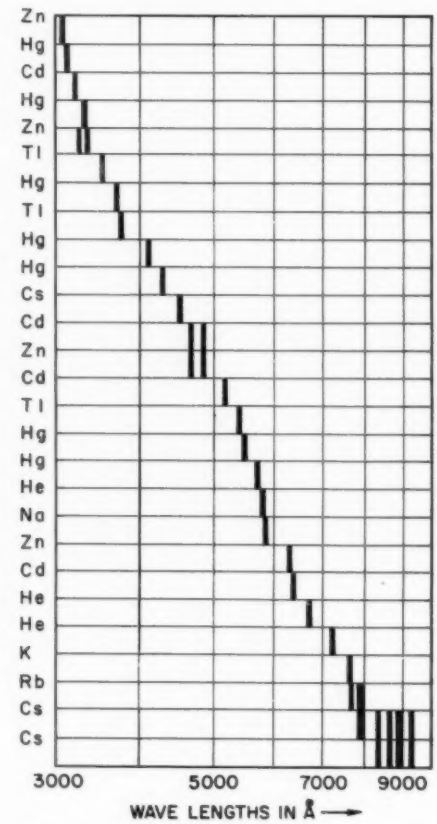

Fig. 1. Spectral lines of Osram lamps in combination with suitable filters.

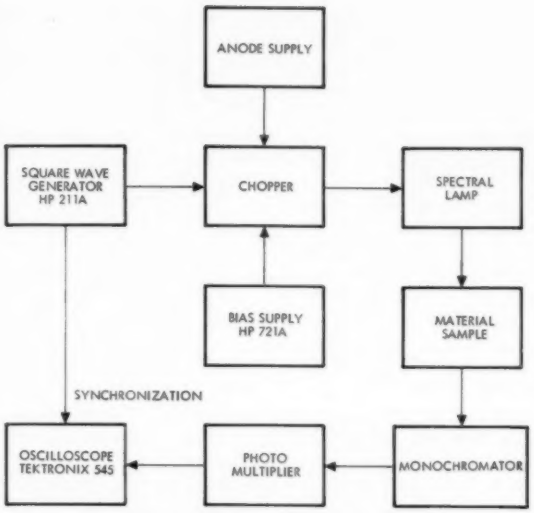

Fig. 2. Chopper system block diagram.

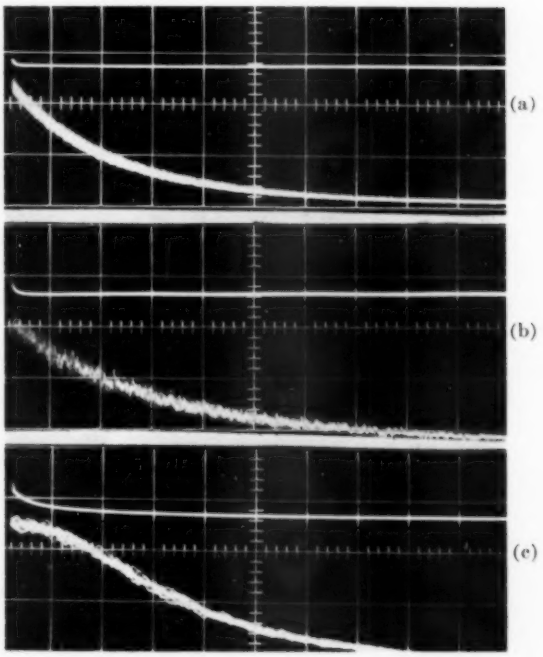

Fig. 3. Decay of luminescence for: (a) 6943-Å emission of ruby $Al_2O_3(Cr^{3+})$ excited with Pen-Ray mercury lamp (time 2 msec/cm); (b) 9600-Å emission from $CaF_2:Er^{3+}$ excited at 2537 Å (time 5 msec/cm); and (c) same as (b) but 6600-Å emission (time 200 μsec/cm). Upper trace represents lamp intensity.

the time required for the light intensity to drop from 90 to 10% of the full "on" intensity. This is a more meaningful time than the $1/e$ time constant as many of the lamps do not exhibit an exponential decay of intensity with time. Figure 4 shows the chopped characteristics of the Beckman hydrogen arc, Nestor type, lamp. Figure 4(a) shows the complete on-off cycle for a chopping frequency of approximately 150 cps; the top trace monitors the lamp current. Figure 4(b) shows the extinction characteristic on a scale of 5 μsec/cm; the top trace is again lamp current.

In general, the extinction time is shortened for cooler operation of the lamp as indicated in Table I for the Hanovia lamp. For many lamps the extinction time is also shortened as the on current is decreased. However, the stability, intensity, and spectral distribution is adversely affected if the lamp current is greatly decreased below the continuous rating of the manufacturer.

Figure 5 is a schematic diagram of the chopper circuit for the high current lamps (0.5–2.5 A). Six type 6CD6GA tubes are paralleled to provide the required current capacity. These tubes were chosen for their extremely high perveance, high plate current at low plate and screen voltages and their high ratio of plate-to-screen current. The magnitude of the on current is controlled by the setting of the bias supply voltage. The square wave

Table I. Lamp Extinction Time

Lamp	Extinction time (μsec)	On current
UV products		
Pen-Ray	52	20 mA
Hanovia type		
SH (uncooled)	240	2.0 A
(Blower cooled)	160	2.0 A
Hydrogen arc Nestor type		
(Beckman)	10.5	400 mA
Osram		
Sodium	42.5	2.0 A
Thallium	15	2.0 A
Mercury	600	2.0 A
Mercury sulfide	110	2.0 A
Rubidium	100	2.0 A
Cadmium	47	1.5 A
Zinc	20	1.5 A
Mercury cadmium	200	2.0 A
Potassium	66	1.5 A
Neon	200	1.5 A

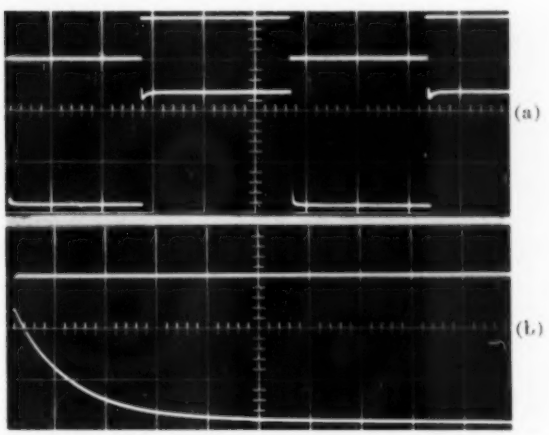

Fig. 4. Extinction characteristic of hydrogen arc lamp. The upper and the lower traces represent the lamp current and intensity, respectively. (a) Time scale: 1 msec/cm; (b) time scale: 5 μsec/cm.

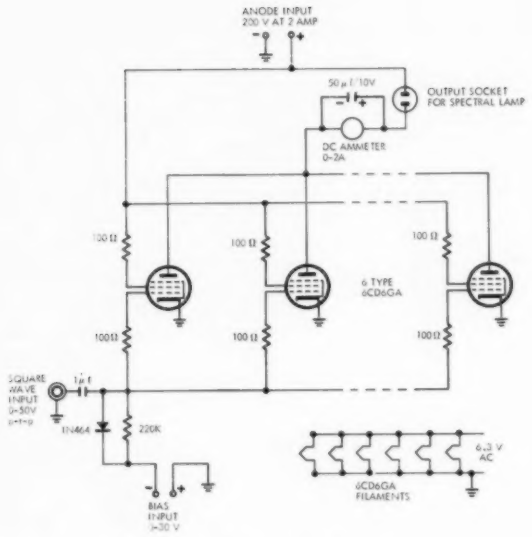

Fig. 5. High current chopper.

must have sufficient amplitude to drive the tubes to cutoff under the condition of highest "on" current.

A similar circuit is used to chop the high voltage-low current lamps such as the Pen-Ray and the Beckman Hydrogen lamp. For these lamps one to three type 6AV5 pentodes are paralleled to supply the required current and the screen grids are supplied a fixed 150 V.

References

1. P. M. Lord and A. L. G. Rees, Proc. Phys. Soc. (London) **58,** 280 (1946).
2. L. A. Tumerman, J. Phys. U.S.S.R. **4,** 151 (1951).
3. D. W. Steinhaus, H. M. Crosswhite, and G. H. Dieke, Spectrochim. Acta **5,** 436 (1953).
4. C. F. Hendee and W. B. Brown, Phillips Tech. Rev. **19,** 50 (1958).
5. P. M. Lord and A. L. G. Rees, Proc. Phys. Soc. (London) **58,** 289 (1946).

On Diffraction Losses in Laser Interferometers

A. G. Fox, Tingye Li, and S. P. Morgan

Bell Telephone Laboratories, Incorporated, Holmdel and Murray Hill, New Jersey.

Received 28 December 1962.

In a recent communication[1] Tang has calculated, using a variational principle, the diffraction losses of the modes in an optical maser interferometer. Similar computations have also been carried out by Culshaw.[2] We wish to comment briefly on the paper by Tang.

One of us[3] has pointed out elsewhere that certain mathematical misconceptions seem to be prevalent concerning integral equations with complex symmetric kernels. These misconceptions probably stem from the fact that the treatment of homogeneous linear integral equations of the second kind in most standard textbooks relates to equations with Hermitian kernels, including real symmetric kernels as a special case. Some texts (e.g., Tang's ref. 5) treat only real symmetric kernels. Unfortunately the kernel of the integral equation in question is complex symmetric. So far as we know, no mathematical theorem has ever been published which relates specifically to the existence of eigenvalues of integral equations with complex symmetric kernels. The question whether such a kernel has any eigenvalues must be settled on a more or less individual basis. In the present case the existence of eigenvalues has been demonstrated numerically by the iterative computations of Fox and Li.[4]

Similarly, the treatment of the extremal properties of eigenfunctions in most standard textbooks relates only to integral equations with Hermitian kernels. We know of no published mathematical theorem which guarantees the extremal property of the variational quotient used by Tang to estimate the eigenvalues of the integral equation in question. Therefore, there is no basis for Tang's presumption that his variational values of the moduli of the reciprocal eigenvalues are more accurate than those of Fox and Li,[4] simply because they are larger than the latter values. In fact, examples can be found[3] for which the variational quotient associated with a complex symmetric kernel can assume values from zero to infinity. Of course, one is always free to guess an approximate eigenfunction of a complex symmetric kernel and to call the variational quotient an approximate eigenvalue, but there is no way of knowing *a priori* how close the result is to the actual eigenvalue or in what direction the error lies. Furthermore, it appears impossible to use any of the well-known procedures, such as the Rayleigh–Ritz method, to refine the eigenvalue, since in the absence of an extremal principle, what criterion can be used to adjust the parameters of a trial function to get closer to the exact eigenvalue?

Tang's idea of introducing a geometrical factor G, based on the concept of length of diffracting edge per unit area, to obtain the diffraction loss of a finite mirror from that of a strip is plausible but vague. The ratio of perimeter to area for any given geometrical shape will depend on some linear dimension of the diffracting object. For example, the ratio is $4/D$ for a circular disk of diameter D, and $2/W$ for an infinite strip of width W. Tang has obtained a factor of 2 between the disk and the strip by setting $D = W$, but he has given no *a priori* justification for doing this. Furthermore, it is not clear how "the idea of introducing the geometrical factor, G, to obtain the diffraction loss for a circular disk from that of a strip can be generalized to other shapes of mirrors . . . ." In the case of an elliptical mirror, for example, one would not know whether to equate the major or the minor axis to the width of the infinite strip.

The vagueness of the geometrical factor concept can also be seen by applying it to two shapes which have the same ratio of perimeter to area, such as a disk of diameter D and a square of side D with slightly rounded corners. By the geometrical factor argument, both of these shapes would have the same diffraction loss, namely twice the diffraction loss of the infinite strip of width D. But Fox and Li[4] have shown numerically that the loss for the circular mirror is greater than that for the square mirror. In fact, it is the square mirror whose loss is more nearly equal to twice the infinite-strip loss, since the eigenvalue for the square mirror is the square of the infinite-strip eigenvalue.

Finally, we wish to make it clear that iterative methods of solving the integral equation for the maser interferometer are capable of yielding more than the dominant eigenvalue and its eigenfunction for each symmetry. Bodewig[5] gives methods by which eigenvalues of the higher-order modes can be extracted from successive iterations. His methods have been applied with success in a study of modes in tilted mirror interferometers.[6]

References

1. C. L. Tang, Appl. Opt. **1**, 768 (1962).
2. W. Culshaw, IRE Trans. Microwave Theory Tech. **10**, 331 (1962).
3. S. P. Morgan, IEEE Trans. Microwave Theory Tech. **11**, (1963), to be published.
4. A. G. Fox and T. Li, Bell System Tech. J. **40**, 453 (1961).
5. E. Bodewig, *Matrix Calculus* (North-Holland, Amsterdam, 1959), 2nd ed., p. 292.
6. A. G. Fox and T. Li, Proc. IEEE **51**, 80 (1963).

Author's Reply

C. L. Tang

Research Division, Raytheon Company, Waltham 54, Mass.

Received 4 February 1963.

Two points raised in the preceding letter call for comments. First, I am now convinced also that the existence of eigenvalues of integral equations with complex kernels does not seem to follow directly from the symmetry property of the kernel alone. Second, the argument which I offered following my remark, "This could be an indication that the former results (variational) are more accurate than the latter (iterative results of Fox and Li) . . .," appears incomplete. However, although Dr. Morgan gives in his paper an example showing that the magnitude of the variational quotient with some other complex kernel, which is not related to our problem, is not bounded, it would perhaps be more useful to show that the magnitude of the variational quotient in our problem is not bounded. Answers to their other criticisms are contained in the text and the numerical results given in my original note.

In conclusion, I should like to point out that one should not forget the extreme convenience in using the variational principle and its inherent accuracy. With negligible amount of effort, one obtains analytical and numerical results which seem to me quite satisfactory in that, in all the cases compared by myself and others, they are in fairly close agreement with the numerical results obtained by the cumbersome iterative method. In those cases where such minor discrepancies are considered important, one may well have to worry about how accurate is the original integral equation in describing the laser interferometer. In the solid-state case, one knows it is very far from reality. In the gaseous laser case, the situation is a little better. In any case, can one know *a priori* how good is such an approximate mathematical model?

Practical Aspects of Aerial Photographic Targets

Milton D. Rosenau, Jr.

The Perkin-Elmer Corporation, Norwalk, Connecticut.

Received 29 October 1962.

The use of modulation transfer functions (MTF) to specify, design, and test optical systems during fabrication and laboratory development is now quite practical. In fact, this is common practice at the Perkin-Elmer Corporation as well as others, and the basis for this has been established by many authors.[1] While the application of MTF technology is not required for routine optical system manufacture, it has proved to be extremely helpful for diagnosis and evaluation in the development of optical systems with performance beyond present practice. It is therefore desirable to extend the technology to field testing and diagnosis.

Recently, the approximate MTF of an aerial camera was measured in actual use.[2] In this case, variable-area sine-wave reflectance targets were used as the test objects. In other work, it might be more appropriate to use other types of targets. In this letter, three types of target are discussed, and the practical factors governing a choice are compared.

1. The MTF is the Fourier transform of the line-spread function,[3] so a line target can be employed. The spatial variation of the transmission in the processed negative is then related to the spatial variation of the exposure by a knowledge of the film characteristic curve, and the Fourier transform is obtained by curve fitting a known transform or by using a suitable computer program.

2. The MTF is approximated by graphically connecting several points where each point is determined by the modulation reduction of a single-frequency sine-wave reflectance target. The transmission modulation[4] can be related to the exposure modulation, and this, in turn, gives the MTF factor at the spatial frequency of the target.[2,5]

3. USAF 1951 targets with each spatial frequency k repeated at several contrasts may be used.[6] In this case, the contrast of each of the highest resolved frequencies, $C_r(k)$, is converted to a modulation value[7] $M_r(k)$, and this is converted to an MTF factor $T(k)$ by

$$T(k) = \frac{R(k)}{M_r(k)},$$

where $R(k)$ is that value of image modulation required for limiting detection, 0.04 being a suggested single value. However, granularity is significant, and $R(k)$ also is a function of spatial frequency, which must be determined for each emulsion.

The number of targets of each type required to evaluate a single camera at one altitude is 1 long line, 4 or 5 sine-wave targets at equally spaced spatial frequencies in the range of the camera, and 40 USAF tri-bars assuming 10 contrasts at each of 4 frequencies. If the MTF is not likely to be monotonic (e.g., a camera system with a very bad focus or a large amount of image motion, or a catadioptric lens with a large central obscuration), more frequencies of sinewave and USAF tri-bars may be needed; for an unrestricted testing capability, some larger number of each target type is required. If the area available for targets is limited, long lines are preferred.

In data reduction, sensitometric data are needed, and for long lines, a microdensitometer and a computer to obtain the Fourier transform of the line-spread function (unless an approximation by curve fitting to known transforms is acceptable), for the sine-wave targets, a microdensitometer and some numerical manipulation; and for USAF targets a means of visual inspection (e.g., microscope) and some numerical manipulation. If one is unwilling to undertake the determination of spatial frequency dependence of $R(k)$ or to accept the personal judgment required with USAF targets, the choice between long lines and sine-wave targets is dictated by data reduction equipment availability or by the working knowledge of Fourier transforms on the part of the analyst.

Sometimes, a single "figure of merit" may be quickly desired; for a long line, this could be the distance on the negative for a specified density change; for the sine-wave target, it could be the highest frequency visually resolved; and for the USAF target, it could be the highest frequency visually resolved at a specified contrast.

References

1. See R. M. Scott, Phot. Sci. Eng. **3**, 201–209 (1959) for a thorough introduction; and F. H. Perrin, J. Soc. Motion Picture Television Engrs. **69**, 151, 239 (1960) for a general survey and extensive list of references.
2. M. D. Rosenau, F. Scott, and W. F. Thiessen, Phot. Sci. Eng., to be published.
3. R. C. Jones, J. Opt. Soc. Am. **48**, 934 (1958).

4. F. Scott and M. D. Rosenau, Phot. Sci. Eng. **5**, 266 (1961).
5. M. D. Rosenau, Phot. Sci. Eng. **6**, 265 (1962).
6. Mil. Std. 150-A, 12 May 1959, Photographic Lenses.
7. R. M. Scott, ref. 1.

Observation of Ionization of Gases by a Ruby Laser

E. K. Damon and R. G. Tomlinson

Antenna Laboratory, Department of Electrical Engineering, The Ohio State University, Columbus, Ohio.
Received 26 December 1962.

Apparent photoionization due to 6943-Å laser radiation has been observed in recent experiments. By focusing coherent radiation from a pulsed ruby laser into an evacuated chamber, ionization has been produced in argon, helium, and a neutral air mixture. This effect is a function of peak input power and is strongly nonlinear. No detectable ionization was produced by input pulses with peaks below 50 kW.

The experimental arrangement is shown in Fig. 1. Two gold probes separated by 1 cm are placed in the focal plane of the primary lens in such a way as to avoid illuminating them with direct radiation. A 3-V dc potential is maintained between the probes to sweep out ionization products. The chamber was evacuated to 20 μ to prevent the recombination of ionization products before they could be swept out.

A typical recording is shown in Fig. 2. The upper trace is

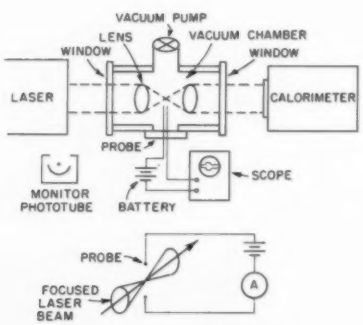

Fig. 1. Experimental apparatus.

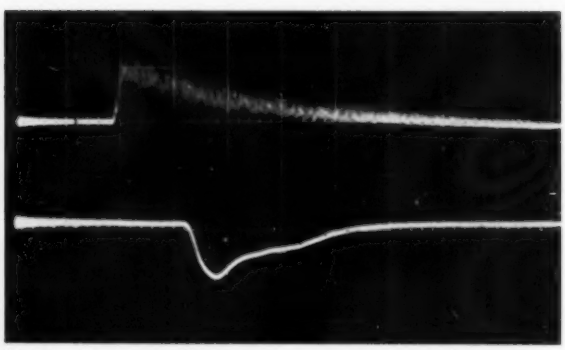

Fig. 2. Typical oscilloscope traces. Upper trace: laser output, 200 μsec/division; lower trace: ionization, 200 μsec/division, 0.01 V/division.

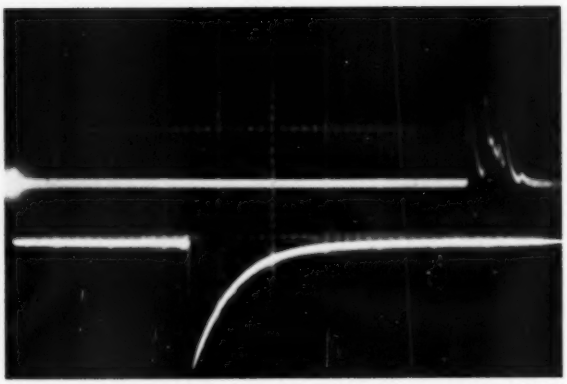

Fig. 3. Typical oscilloscope traces. Upper trace: Q-switched laser output, 2 μsec/division (delayed); lower trace: ionization current, 200 μsec/division, 0.005 V/division.

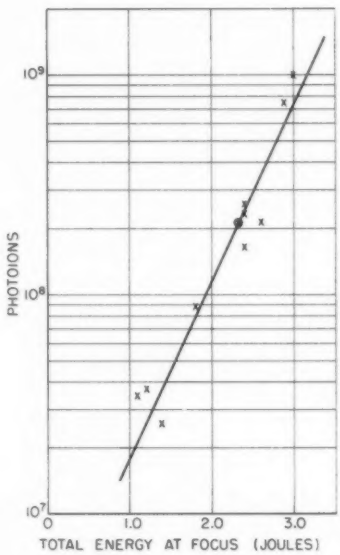

Fig. 4. Photoions observed vs laser energy.

that of the input laser pulse as monitored by a photodiode, and the lower trace is the current due to the induced ionization in air. Structure in the lower trace due to the larger relaxation spikes in the laser pulse (which are not resolved in this photograph) gives the first indication that the effect is dependent on peak power. The calorimeter measurement for this pulse indicates an energy of 0.9 J at the focal region and the integrated probe current is equivalent to the production of 1.5×10^7 photoions.

By using a rotating partially reflecting dielectric window as one end wall of an external cavity, the ruby laser can be Q-switched to produce pulses of much higher peak power with much lower total energy. This gives results such as that shown in Fig. 3. Here the total laser energy at the focal region is only 0.12 J but 1.35×10^7 photoions are produced in air. The largest spike in this pulse has a peak power of 210 kW.

The number of photoions produced in air vs the total laser energy in joules at the focus is shown in Fig. 4. In this region

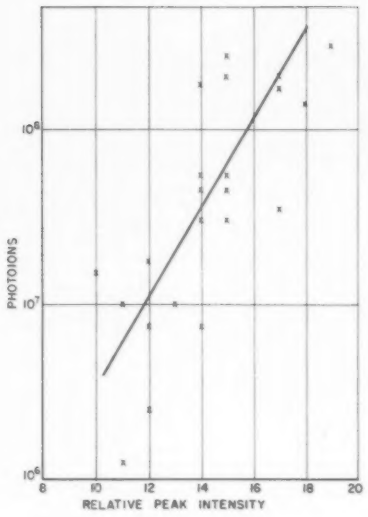

Fig. 5. Photoions observed vs peak laser intensity.

the curve appears to be exponential and is proportional to $e^{1.9P}$, where P is the input power in joules.

Figure 5 is a plot of the number of photoions produced in commercial purity argon vs the peak pulse power for the Q-switched pulse. These data show considerable experimental scatter which is believed to be primarily due to the complex structure of the Q-switched pulses used, as seen in Fig. 3, and the difficulty in completely resolving some of the laser spikes which are of the order of 100-nsec duration. However, Fig. 5 does show a correlation between the highest peak in the Q-switched pulse and the resulting photoionization. Here ionization seems to be proportional to e^{aI}, where I is the peak power of the laser pulse. Data taken in air and in commercial purity argon and helium were similar.

Upon consideration of the small (1.79 eV) energy per laser photon, the small (order of 10^{-9} cm) amplitude with which any free electrons present would be induced to oscillate by the electric fields involved, and the exponential form of the dependence on peak power, it appears that ionization is being produced by a nonlinear field effect rather than by electron impact, by thermal effects where the interaction would be proportional to energy, or by conventional photoionization which requires significantly higher photon energies for the gases involved.

The research described in this paper was supported by a U.S. Air Force contract.

Applied Optics Patents

Reviewing panel

C. Shepard (Chairman) *Rochester*
R. Anwyl *Rochester*
G. L. Clark, *Illinois*
G. W. Cleek *National Bureau of Standards*
A. Danti *Texas A & M*
J. Fitzmaurice *Baird-Atomic*
F. F. Hall, Jr. *ITT Federal Labs*
R. S. Hunter *Hunter Assocs.*
W. L. Hyde *Fecker*
S. F. Jacobs *TRG*
R. Kingslake *Eastman Kodak*
D. J. Lovell *University of Michigan*
D. L. MacAdam *Eastman Kodak*
A. Mann *Spectrolab*
T. K. McCubbin *Penn. State University*
R. K. McDonald *Boeing*
J. R. Meyer-Arendt *Utah State University*
G. W. Stroke *MIT*
D. E. Williamson *Cordis*

The patents reviewed below have been issued by the U.S. Patent Office on the dates quoted except where otherwise mentioned. The patent number, date of issuance, and classification number are quoted in the first line. The filing date is that of the earliest patent application. The opinions stated in the reviews are those of the reviewers and are not meant to express the thinking either of the organizations with which members of the panel are associated, of the Optical Society of America, or of this journal. Normally, statements of fact are based upon the patents and not independently verified. Printed copies of American patents may be ordered from the Commissioner of Patents, Washington 25, D.C., for 25¢ each. A weekly subscription service to any selected subclass is also available from the Patent Office.

3,043,685 July 10, 1962 (Cl. 96–1)
Xerographic and magnetic image recording and producing.
J. F. Rosenthal. Assigned to the Xerox Corp. Filed July 18, 1957.

The relatively permanent part, e.g., a business form, of a combination image consists of powder attracted by magnetism. The other part, which may be changed by the usual xerographic procedure, is held by electrostatic change. Each image may be erased or modified independently of the other. The images may be separately developed, with different colors as desired. The magnetic image is formed by passing a magnetically coated surface under a line of magnetic recording heads which are fed suitably coded pulses in parallel, or by a sweep circuit. The usual photoconductive xerographic layer is formed on top of the magnetic coating. D.L.M.

3,043,686 July 10, 1962 (Cl. 96–1)
Xerographic color masking.
J. T. Bickmore. Assigned to Xerox Corp. Filed July 8, 1958.

For preparation, by xerography, of the magenta component of a three-colorant subtractive print, a positively charged plate is discharged, imagewise, by light from a green separation positive. A transparent electrode placed over the plate is then connected to a negative potential sufficient to reverse the electric field in the selenium layer, but without discharging the plate. The plate is then discharged by exposure, in register with the first (green) image, to a red separation positive. After removal of the transparent electrode the remaining positive charge is said to be a red-masked magenta printer, corrected for the green absorption of the powder with which the cyan component is printed. D.L.M.

3,043,702 July 10, 1962 (Cl. 106–47)
Optical glass.
H. Brömer and N. Meiner. Assigned to Ernst Leitz G.m.b.H. Filed Sept. 17, 1959 (in Germany Sept. 20, 1958).

Optical glasses are described that have refractive index values above the range of conventional optical glasses, medium values of dispersion, and abnormal partial dispersions. The glasses are composed primarily of lead-borate or lead-phosphate, boric oxide, tantalum oxide, aluminum oxide, zinc oxide, cadmium oxide, zirconium oxide, alkaline earth oxides, and rare earth oxides. The glasses are said to possess excellent chemical stability. The refractive index values for the helium E line (5876 Å) range from 1.697 to 1.747 with Abbe values from 37.8 to 33.9. G.W.C.

3,044,343 July 17, 1962 (Cl. 88–2.3)
Optical instrument of the reflection type.
M. P. P. de Fontguyon. Filed Apr. 16, 1959 (in France Apr. 17, 1958).

A sighting instrument having one plane reflecting surface oriented by gravity or a gyro is described. Applications suggested are leveling, artificial horizons, and so on. D.E.W.

3,044,344 July 17, 1962 (Cl. 88–2.4)
Range finding device.
J. T. Hartmeister. Filed Apr. 15, 1960.

An afocal adapter to go over the front of a rifle sight to bring two views of the object into the pupil. One enters the center of the objective; the other the periphery. Range is determined by bringing the images into coincidence. W.L.H.

3,044,355 July 17, 1962 (Cl. 88–57)
Zoom lenses.
A. Cox and W. J. Johnson. Assigned to Bell and Howell Co., Chicago. Filed May 25, 1961.

A 4:1 *f*/1.8 mechanically compensated zoom lens is described comprising an afocal zoom portion followed by a 4-element fixed rear member. The front component of the zoom portion consists of a positive cemented doublet followed by a positive single lens, which is cam driven to hold focus and is also adjustable for object distance; the second component which slides linearly comprises a negative meniscus element followed by a biconcave doublet; and the third component is a biconvex element in front of the stop. In one of the embodiments shown, there is a beam-splitter inserted between the zoom portion and the stop to divert light to a viewfinder. One example ranges from 8.2 to 32.4 mm and the other from 9.1 to 35.6 mm. R.K.

3,044,356 July 17, 1962 (Cl. 88–57)
Zoom lens.
A. Cox and W. J. Johnson Assigned to Bell and Howell Co., Chicago. Filed May 26, 1961.

A 2:1 mechanically compensated zoom lens is described comprising an afocal zoom portion followed by a 4-element fixed rear member. The front component of the zoom portion is a positive flint-in-front doublet, which is cam driven to hold focus and is also adjustable for object distance; the second component which slides linearly comprises a negative meniscus followed by a biconcave cemented doublet; and the third component is a positive cemented doublet situated immediately behind the stop. In the example given, the focal length ranges from 10 to 20 mm at *f*/1.9. R.K.

3,044,357 July 17, 1962 (Cl. 88–57)
Catadioptric objective.
W. R. Linke. Assigned to Bell and Howell Co., Chicago. Filed Mar. 2, 1959.

A biconvex element is closely followed by a plano-concave element silvered on its plane side to form an imaging system of aperture *f*/4 and angular field 25°. Only one half of the field is used to avoid obstruction of the entering light by the receiving surface. The film plane is slightly tilted to match the inward-curving field. The system is well suited for use as a table projector. R.K.

3,044,358 July 17, 1962 (Cl. 88–61)
Color projection system.
W. E. Glenn, Jr. Assigned to General Electric Company. Filed Dec. 24, 1958.

In a color projection system, employing an electrostatically deformable refracting or reflecting medium with which three primary colors are produced, imagewise, by diffraction gratings of suitable spacings, the spectrum mask apertures are made wider for the red primary than for the green and blue primaries by forming the edges of those apertures out of clear red filter material. This arrangement is said to yield a purer and more intense red primary than is otherwise possible. D.L.M.

3,044,888 July 17, 1962 (Cl. 106–50)
Glass fiber.
J. D. Provance. Assigned to Houze Glass Corp. Filed July 5, 1960.

Glass compositions are described from which can be made glass fibers that have high strength, high modulus of elasticity, and high durability at temperatures in the vicinity of 1093°C. The fibers are used as laminates in structural materials where high strength, high modulus of elasticity, and high temperature resistance are important. The compositions given are said to have good working characteristics and to produce long stable glass fibers that are resistant to devitrification. G.W.C.

3,045,117 July 17, 1962 (Cl. 250–49.5)
Image intensifying photosensitive film.
J. W. Beatty. Assigned to U.S.A. as represented by the Secretary of the Air Force. Filed Nov. 20, 1957.

Describes a scheme for intensifying light in a series of layers on a photographic film base. Photoelectrons are emitted from the first layer and multiplied at subsequent layer until a phosphor is reached. This has been done in a vacuum, but the inventor claims it can be done in a solid. One claim. W.L.H.

3,045,124 July 17, 1962 (Cl. 250–226)
Light responsive means.
H. de L. McKinlay, Jr. Assigned to Bell and Howell Co. Filed Feb. 21, 1958.

A method for constructing a photoelectric exposure control for a camera which automatically compensates for differences in film such as Kodachrome daylight type and type "A." A filter is employed that excludes from daylight those wavelengths that are absent from tungsten light. D.E.W.

3,045,530 July 24, 1962 (Cl. 88–14)
Optical system having aberration-correcting plate member with ring-shaped phase-retarding layers.
J. Tsujiuchi. Assigned to Agency of Industrial Science and Technology, Ministry of Trade and Industry, Japan. Filed July 14, 1960.

A correcting plate is described for use in conjunction with a telescope objective, the plate carrying concentric ring zones of evaporated material that can alter either the intensity of the zone (by absorption) or the phase of the zone (by reason of the thickness of the layer) or both. This corrector plate is intended primarily for use in an alignment telescope since by its aid, two or three distinct foci can be obtained at different distances along the optical axis. R.K.

3,045,545 July 24, 1962 (Cl. 88–57)
Optical system for sighting instruments.
H. D. Korones and H. E. Rosenberger. Assigned to Bausch & Lomb, Inc. Filed Nov. 10, 1960.

A pancratic telescope for sighting instruments is described having a 4:1 range of magnifying power, the positions of the image and the exit pupil remaining substantially fixed while the power is being changed. The objective is of the telephoto type followed by a positive field lens; this is followed by a pair of movable cemented doublets which constitute the zoom erector, after which comes the field stop and eyepiece. The focal lengths of the various components are related by a series of specific inequalities. R.K.

3,045,546 July 24, 1962 (Cl. 88–57)
Optical objectives of variable focal length.
G. H. Cook. Assigned to Taylor, Taylor and Hobson Ltd., Leicester. Filed Sept. 29, 1958 (in Great Britain Oct. 2, 1957).

A complex 13-element mechanically compensated zoom lens covering a focal-length range of $3^1/_2$ to 1 is described. The lens is intended primarily for television purposes, and the actual focal length and relative aperture can be altered by interchanging the fixed rear positive member. Thus the focal length can be varied from 2.2 to 8.0 cm at *f*/1.8, or alternatively from 2.2 to 8.0 inches at *f*/4.5. R.K.

3,045,547 July 24, 1962 (Cl. 88–57)
High-speed photographic or cinematographic objective with wide image angle.
W. Albrecht. Assigned to J. Schneider & Co., Kreuznach. Filed Sept. 30, 1958 (in Germany Oct. 11, 1957).

A rather long reversed telephoto lens is described having an aperture of *f*/1.8, a semifield of 30°, a back focus of 1.9*f* and a length of 7*f*. The front component contains a positive doublet followed by a strong negative doublet; the rear component contains two positive doublets with a single positive lens between them. R.K.

3,045,548 July 24, 1962 (Cl. 88–57)
Telephoto optical design.
J. G. Baker. Assigned to the U.S. Air Force. Filed April 10, 1959.

A highly corrected *f*/4 telephoto lens covering ±6° is described, the total length being 77% of the focal length. The front component contains a single lens and a thick deeply curved meniscus triplet. There is a weak cemented triplet behind the stop, and a positive field flattener close to the focal plane. Two numerical examples are given. R.K.

3,045,549 July 24, 1962 (Cl. 88–57)
Telephoto optical design.
J. G. Baker. Assigned to the U.S. Air Force. Filed April 10, 1959.

A highly corrected *f*/4.5 telephoto lens covering ±8° is described, the total length being 78% of the focal length. The front portion contains a thick meniscus-shaped component having a negative Petzval sum, which is neutralized by a positive field lens close to the focal plane. There is one picture claim. R.K.

3,046,399 July 24, 1962 (Cl. 250–51.5)
X-ray spectrograph.
J. Ladell. Assigned to North American Philips, Inc. Filed Nov. 3, 1958.

This x-ray diffractometer is built similar to a quantometer used for light optical spectrography. It contains a series of detectors positioned in such a way with respect to the diffracting crystal that the presence of several elements, e.g., Cu, Ni, Cr, Sn, Mo, in order of decreasing Brass angles, can be directly assessed. J.R.MA

3,046,838 July 31, 1962 (Cl. 88–57)
Six-component lens.
M. Reiss. Assigned to Eastman Kodak Company. Filed Nov. 21, 1960.

A highly corrected *f*/3.5 lens is described, intended to cover a narrow field ($\pm 7^1/_2°$) for use in aerial photography. It consists of a triplet design, each component of which has been split into two to minimize the aberration residuals. The narrow parallel airspace in the rear greatly reduces zonal aberration and sphero-chromatism. The rear element contains a buried surface for chromatic correction. The design is controlled by sixteen inequalities. R.K.

3,046,839 July 31, 1962 (Cl. 88–65)

Processes for preparing light-polarizing materials.

G. R. Bird and M. Parrish, Jr. Assigned to Polaroid Corp. Filed Jan. 12, 1959.

Methods of making metallized-grid structures capable of polarizing light throughout a wide range of wavelengths are described. Light polarizers of this type are said to have high efficiency and marked stability. They are said to operate in the near and far infrared and the visible portions of the spectrum, although no wavelength limits are given. G.W.C.

3,049,054 Aug. 14, 1962 (Cl. 88–57)

Astronomical cameras and optical systems therefor.

R. L. Waland. Filed Nov. 24, 1958 (in Great Britain Nov. 26, 1957).

A catadioptric Cassegrain system is described of the Maksutov type with a "buried" achromatizing interface within the correcting lens, and a secondary convex spherical mirror to reflect the image through a hole in the center of the primary concave spherical mirror. As the second mirror is stronger than the primary mirror, a negative field flattener is used to eliminate the Petzval sum, and also correct the small lateral color caused by the internal achromatizing surface. The system is intended to be constructed in a very large size, e.g., 5.8-m diameter and 25-m focal length. R.K.

3,049,975 Aug. 21, 1962 (Cl. 88–57)

Four-component wide-angle objective lens of Gaussian type.

A. W. Tronnier. Assigned to Farrand Optical Company. Filed Oct. 20, 1958.

An objective of the double Gauss type is described, comprising a positive doublet, a negative single element, the diaphragm, a negative doublet, and a single positive rear element, in that order. Three examples are given, of aperture about $f/2.8$ and covering a wide field ($\pm 30°$). The claims contain a list of the powers of the successive lens surfaces. R.K.

3,051,048 Aug. 28, 1962 (Cl. 88–57)

Mechanism for relatively displacing the components of optical objectives.

H. Mahn. Assigned to J. Schneider and Co., Kreuznach. Filed Mar. 24, 1960 (in Germany Apr. 22, 1959).

A number of linkage mechanisms are described by means of which the various components of a zoom lens can be moved through the correct relative distances without the use of cams. R.K.

3,051,049 Aug. 28, 1962 (Cl. 88–57)

Catadioptric objective.

W. R. Linke. Assigned to Bell and Howell Co., Chicago. Filed Mar. 2, 1959.

Four examples are given of a monocentric lens having a plane mirror serving as the effective stop of a symmetrical system. The image, which lies wholly to one side of the optical axis, is spherical and concentric with the refracting surfaces. R.K.

3,051,050 Aug. 28, 1962 (Cl. 88–57)

Binocular lens system.

H. Kohler. Assigned to C. Zeiss, Heidenheim. Filed Apr. 30, 1959 (in Germany May 2, 1958).

The Erfle-type eyepieces used in prismatic binoculars often exhibit a residual of lateral chromatism, which is ordinarily corrected by the prisms used in the binocular. However, if mirrors are used instead of prisms, this lateral chromatism becomes visible. It may be corrected by the use of an airspaced objective having the flint element in front. R.K.

3,051,051 Aug. 28, 1962 (Cl. 88–57)

Optical justifying means.

J. H. Jeffree. Assigned to CAPS Ltd., London. Filed July 7, 1959 (in Great Britain July 11, 1958).

A line of type is imaged on film by two sets of cylindrical lenses, one set giving 1:1 imagery for the line height, and the second set giving 1:1 imagery for the line length. Two of the lenses in the second set may be moved longitudinally to produce a small variation in the line length magnification for the purpose of line justification. R.K.

3,051,052 Aug. 28, 1962 (Cl. 88–57)

Varifocal lens system with four points of exact image shift compensation.

L. Bergstein. Filed Aug. 31, 1959.

The author describes a 4-component optically compensated zoom system in which lenses 1 and 3 are of one sign while lenses 2 and 4 are of the opposite sign. Lenses 2 and 4 are coupled together and move as a unit to vary the focal length of the system. A fixed rear lens may be added if desired to alter the actual focal lengths of the system. Formulas are given relating the powers and separations of the lenses by means of which the image-position errors between the four exact points may be minimized. R.K.

3,051,053 Aug. 28, 1962 (Cl. 85–57)

Photographic objective.

G. J. Berger. Assigned to C. Zeiss, Heidenheim. Filed Oct. 5, 1959 (in Germany Oct. 10, 1958).

A highly corrected seven-element double Gauss objective is described, having a weakly negative additional cemented doublet situated in the central diaphragm space. In the example given, the front negative component is a single element, and two lenses in the rear negative component may be cemented or spaced with a narrow airgap. R.K.

3,053,672 September 11, 1962 (Cl. 106–50)

Glass composition.

D. Labino. Assigned to Johns-Manville Corp. Filed Dec. 19, 1960.

Glass compositions are given that are said to be improved compositions for the production of glass fibers. The improvements are in such properties or characteristics of the glasses as viscosity, low softening point, broad temperature working range, low liquidus temperature, and high degree of durability and resistance to moisture of the resulting fibers. G.W.C.

3,054,326 Sept. 18, 1962 (Cl. 88–57)

Projecting device for photolithography.

H. Giesecke. Assigned to C. P. Goerz, Inwood, N.Y. Filed Aug. 23, 1959.

A "straight-line reverser" is described, containing a central lens with a roof prism on one side of it and a plane mirror on the other side. For compactness, the deviation produced by the prism is somewhat less than a right angle, e.g., between 60° and 80°. The lens covers an angular field of approximately $\pm 22°$. The axes of entering and emerging beams are parallel to each other, but not in one continuous line. R.K.

3,054,327 Sept. 18, 1962 (Cl. 88–57)

Afocal front attachment for photographic or cinematographic objectives.

W. Albrecht and W. Wagner. Assigned to J. Schneider, Kreuznach. Filed Aug. 13, 1959 (in Germany Sept. 16, 1958).

An afocal telephoto attachment is described having a magnifying power of 3×, intended for use in front of the lens of an 8-mm motion-picture camera. The system is complex, embodying four elements in the front positive member, and two elements in the rear negative member. Two examples are given. R.K.

3,054,686 September 28, 1962 (Cl. 106–54)

Glass composition having high chemical durability.

E. C. Hagedorn. Assigned to Owens-Illinois Glass Co. Filed May 18, 1960.

The composition range for glasses is given that are said to possess higher chemical durability than normal soda-lime glasses and that are particularly suitable for the production of small glass containers for packaging pharmaceuticals, drugs, and solutions. The chemical durability is determined by the U.S.P. XVI Type I test which describes a standard test for resistance to water attack of newly formed glass containers. G.W.C.

3,056,330 October 2, 1962 (Cl. 88–14)

Spectroscopic apparatus.

J. L. Saunderson and G. Altman. Assigned to Baird-Atomic, Inc. Filed Feb. 18, 1960.

A servo system is described which automatically keeps a direct reading multiple-exit-slit photoelectric-spectrometer in adjustment. A servo-motor-driven screw acts upon a long lever arm that turns the grating and a concave monitoring mirror. Modulated light from a monitoring entrance slit reaches the slightly offset double-exit-slits after reflection from the monitoring mirror. Balance occurs when the monitoring exit-slits receive equal illumination. (See patent 3,064,520 to be reviewed in a later issue.) T.K.M.

3,057,257 Oct. 9, 1962 (Cl. 88–57)

High-speed photographic or cinematographic varifocal objective.

G. Klemt and K. Macher. Assigned to J. Schneider, Kreuznach. Filed Feb. 11, 1960 (in Germany Feb. 17, 1959).

A novel 4:1 afocal zoom attachment is described, in which the front and rear positive members are fixed and two internal sliding negative components are moved simultaneously to vary the focal length. By a suitable choice of lens powers and spacings, the motions of these negative components can be made substantially linear without any significant movement of the image position. R.K.

3,057,259 Oct. 9, 1962 (Cl. 88–57)

Variable magnification optical systems.

R. F. Schuma. Assigned to Bausch & Lomb, Inc. Filed Apr. 21, 1958.

A mechanically compensated zoom system is described for use between the objective and eyepiece of a variable-power Greenough binocular microscope. A negative doublet is moved approximately linearly above the objective lens and a rear positive doublet is moved by a cam to hold the image in focus. R.K.

3,057,260 Oct. 9, 1962 (Cl. 88–57)
Triplet lens.
F. E. Altman and L. W. VonHalla. Assigned to Eastman Kodak Company. Filed Aug. 1, 1961.

A high-quality $f/3.9$ triplet objective using high-index glasses is described, covering an angular field of $\pm 28°$. A single picture claim is included. R.K.

3,059,532 Oct. 23, 1962 (Cl. 88–57)
Optical system.
T. I. Harris and I. C. Sandback. Assigned to Bell and Howell Co. Filed Jan. 12, 1959.

A compact 2× afocal telescopic attachment is described, for use in front of a camera lens. By means of a complex type of construction, distortion has been corrected, and the other aberrations are drastically reduced. Two examples are given, which are covered by 7 inequalities. R.K.

3,059,533 Oct. 23, 1962 (Cl. 88–57)
Zoom lens.
F. W. Mellberg. Assigned to Bell and Howell Company. Filed Nov. 23, 1959.

A pin-and-slot mounting for a mechanically compensated zoom camera lens is described, in which the zoom sleeve may be slid from a front position in which the focusing movement is locked in its hyperfocal position, to a rear position in which the focusing motion of the front component is freely operable. R.K.

3,059,534 Oct. 23, 1962 (Cl. 88–57)
Adjusting device for an objective.
E. Keznickl. Assigned to A. Handler and K. Vockenhuber, Vienna. Filed Dec. 1, 1959 (in Austria, Jan. 8, 1959).

A link mechanism is described for operating the lenses in a mechanically compensated zoom lens. Rotation of a crank drives the internal lens directly, while a disk cam attached to the crank shaft moves the fulcrum of a lever. The upper end of this lever drives the front element in such a way as to hold the image in focus, and the lower end of the lever is moved by the focusing knob on the camera. R.K.

3,059,535 Oct. 23, 1962 (Cl. 88–57)
Zoom lens system.
A. Cox and W. J. Johnson. Assigned to Bell and Howell Company. Filed May 26, 1961.

An $f/1.9$ zoom lens covering a 2 1/2:1 range of focal lengths is described. The 3-element front component is moved by a cam to maintain focus, while the 3-element middle negative component is moved linearly. A single picture claim is given. R.K.

3,059,536 Oct. 23, 1962 (Cl. 88–57)
Zoom lens system.
A. Cox and W. J. Johnson. Assigned to Bell and Howell Company. Filed May 26, 1961.

An $f/1.8$ zoom lens covering a 3.25:1 range of focal lengths is described. The 3-element front component is moved by a cam to maintain focus, while the 3-element middle negative component is moved linearly. A single picture claim is given. R.K.

3,060,805 October 30, 1962 (Cl. 88–57)
Image-forming element.
C. H. Brumley. Assigned to Bausch & Lomb, Inc. Filed May 4, 1959.

An optical device is described for copying a flat document on a sheet of photosensitive paper. A stack of thin glass plates, optically separated from each other by opaque reflecting interfaces, gives "fiber-optics" imagery in one meridian, and each plate is cut with circular interfaces and arranged as a solid cemented cylindrical lens in the other meridian. The resulting image of a document formed on the opposite side of the stack of plates is therefore inverted and left-handed, ready to be received on photographic paper pressed against the stack. R.K.

3,060,806 October 30, 1962 (Cl. 88–57)
Image-forming element.
R. E. Lewis and R. J. Meltzer. Assigned to Bausch & Lomb, Inc. Filed May 4, 1959.

This device is similar to that described by Brumley in U.S. Pat. 3,060,805, except that curved cylindrical mirrors are used in place of cylindrical lenses to effect the desired imagery in one meridian. R.K.

3,062,100 November 6, 1962 (Cl. 88–57)
Focusing telescope objective.
M. Ludewig and F. Stumpf. Assigned to E. Leitz, Wetzlar. Filed Apr. 23, 1957 (in Germany Aug. 24, 1953).

A 3-element telescope objective is described which may be focused by varying the airspace between a single positive element and the remaining cemented doublet. The fixed and movable components have approximately equal power. The rear fixed component may be sealed into the tube to prevent the entry of moisture into the rest of the system. R.K.

3,062,101 November 6, 1962 (Cl. 88–57)
Anastigmatic catoptric systems.
E. L. McCarthy. Assigned to Perkin-Elmer Corp. Filed May 29, 1959.

An all-mirror objective is described comprising a magnifying afocal system followed by a Schwarzschild-type imaging system. The afocal portion contains two concave parabolic mirrors having a common internal focus, a diagonal plane mirror at this image position serving to bend the beam through a right angle. The imaging system contains a small convex spherical mirror and a much larger concave spherical mirror mounted about a common center of curvature, the radii being so chosen as to make the over-all Petzval sum zero. R.K.

3,062,102 November 6, 1962 (Cl. 88–57)
Mechanism for operation of zoom lens.
W. A. Martin. Assigned to Eastman Kodak Co. Filed Nov. 25, 1959.

The 2 movable components of a mechanically compensated zoom lens are mounted so as to slide along 3 fixed rods. A knurled wheel mounted on an axle perpendicular to the optical axis of the lens carries a crank mechanism to drive the front movable lens of the zoom system, and a flat cam to move the rear zoom component by the correct amount to keep the image in focus. R.K.

3,063,341 November 13, 1962 (Cl. 88–57)
Zoom lens.
J. C. Beck. Assigned to Encino Engineering Co. Filed Sept. 12, 1961.

An optically compensated zoom lens is described, having a focal-length range of 95 to 205 mm (2.15:1) at $f/6.3$, for use on a single-lens reflex camera. The two coupled moving components are positive flint-in-front doublets, and the intermediate fixed component is a negative crown-in-front doublet. There is a narrow airspace in the front and middle components. The fixed rear lens behind the diaphragm is a single positive meniscus element. R.K.

3,064,532 November 20, 1962 (Cl. 88–57)
High-aperture optical system for telescopes.
E. J. Lescher and A. W. Tronnier. Assigned to Farrand Optical Co. Filed Mar. 2, 1960.

A compact system for a prismatic binocular is described, having a three-element objective of high relative aperture ($f/2$ to $f/3$) and a simplified Erfle eyepiece covering a $\pm 30°$ field. The objective is a telephoto lens comprising two positive elements followed by a negative element, the second positive element being of meniscus form. A single numerical example is given, bound by several inequalities. R.K.

3,064,533 November 20, 1962 (Cl. 88–57)
Photographic objective.
L. M. Hudson. Assigned to Bausch & Lomb, Inc. Filed May 16, 1960.

A highly corrected reversed telephoto lens is described, covering a field of $\pm 32°$ at an aperture of $f/1.8$ or $f/2$. The front negative member comprises a negative doublet followed by a single negative lens, while the rear positive member is a 6-element double Gauss lens. The back focus is at least 1.3 times the focal length. R.K.

3,065,670 November 27, 1962 (Cl. 88–57)
Optical imaging system.
J. Becker. Assigned to Optische Industrie De Oude Delft. Filed Jan. 13, 1958 (in The Netherlands Jan. 12, 1957).

A high-aperture concentric catadioptric system of the Bouwers type is described, having two concentric correcting elements—the first being traversed by the incoming parallel light and the second being traversed by the light in the space between the concave mirror and the image. Three embodiments are shown, the second correcting element being either mounted in a hole in the first corrector or cemented to the back of it or following a plane mirror in the rear of the system. R.K.

3,065,671 November 27, 1962 (Cl. 88–57)
Optical objective.
W. J. Johnson and I. C. Sandback. Assigned to Bell and Howell Co. Filed Mar. 20, 1959.

A high-aperture ($f/1.9$) highly corrected four-component objective is described, of the plus-plus-minus-plus type, the second component being a cemented doublet of meniscus form. The first three components are compactly mounted, but there is a wide airspace between components 3 and 4. Five examples are given and are covered by a large number of specified inequalities. R.K.

RUSSIAN MASERS

Typical examples of Russian masers papers published in recent issues of OPTICS AND SPECTROSCOPY, OSA's monthly translation journal:

Transmission and Reflection of a Plane-Parallel Layer in the Conditions of Amplification and Generation Stepanov and Khapalyuk

Detection of the Isotope K^{40} by Means of Optical Pumping Alexandrov and Chodovoy

Deformation Splitting of Lines in the Spectra of Alkali Fluoride Crystals Activated by Sm and Eu Divalent Ions Kaplyanskii and Przhevuskii

Zeeman Effect in the Absorption and Luminescence Spectrum of CaF_2-Sm^{++} and SrF_2-Sm^{++} Zakharchenya and Ryskin

Microwave Spectrum of the HDNCN and D_2NCN Molecules Shipulo

Spectroscopic Sum Rules Taking into Account the Induced Emission Rebane and Sild

Determination of the Mean Lifetime of Excited States by a Polarimetric Method Agarbiceanu, Kukurezianu, Popesku, and Vasilu

Some Problems of the Nonlinear Theory of the Optical Properties of Plane-Parallel Layers Samson and Stepanov

Calculation of the Maser Power of a System of Particles with Three Energy Levels Stepanov and Samson

Amplification Properties of a Dielectric Filament Prokhurov

Emission Pulsations from a Ruby Laser Galanin, Leontovich, Sviridenkov, Smorchkov, and Chizhikova

Absorption, Luminescence and Stimulated Emission of Neodymium in SrF_2 Crystals Kariss and Feofilov

Order your subscription to the 1963 issues now (Feb. '63 issue published in English translation in May)

OPTICS AND SPECTROSCOPY
ROOM 101, OSA
1155 16th St. N.W.
Washington 6, D.C.

ORDER FORM

Please enter my/our subscription to the 1963 issues of OPTICS AND SPECTROSCOPY (Vols. XIV and XV):

- ☐ OSA member rate $7.50 monthly
- ☐ OiS club member rate $11.00 monthly
- ☐ Nonmember rate $15.00 monthly

Name _____ OSA Membership No. _____

OiS Club Cooperating Society _____

Address _____

_____

_____

_____ **cash with order preferred**

Papers to appear in subsequent issues

Overhauser and Jeffries-Abragam Effect in a Four-Level System —*Narchal and Barker*

Spurious Harmonic Generation in Optical Heterodyning—*Cummins, Knable, and Yeh*

Interferometric Measurement of Vibration Amplitudes—*Bowie*

Infrared Transmission through the Atmosphere—*Green and Griggs*

Infrared Transmission through Fogged Salt Windows—*Morrow and Turk*

Total Absorptance of Water Vapor in the Near Infrared—*Burch et al.*

A Simple Grating Calibrator for the Visible and Vacuum Ultraviolet—*Hammer, Arakawa, and Birkhoff*

Photorefractometer II. Measurement of N and K—*Kapany and Pontarelli*

Lighting Parameters and Generalized Characteristics of Xenon Lamps—*Marshak*

Design of Superachromatic Lenses—*Herzberger and McClure*

Reflection and Transmission of Infrared Materials—*McCarthy*

The Use of Polarized Infrared Radiation in Magneto-optical Studies of Semiconductors—*Palik*

A Multicolor Photoelectric Photometer for Artificial Satellite Observations—*Moore and Elliott*

An 8–14 μ IR Astronomical Photometer—*Westphal and Murray*

An Optical Null Double-Beam Double-Pass IR Spectrophotometer—*Minami*

A Photomultiplier Circuit for Precision Spectrophotometry—*Budde*

Large-Scale Photoelectric Planimeter for Leaves—*Carman*

A New Method for High-Speed Motion Picture Photography of Transparent Drops—*Pfeiffer*

Photometric Accuracy of Infrared Spectrophotometers—*Stewart*

Absorption by Ozone in the 4.75-μ Region of the Solar Spectrum—*McCaa and Shaw*

The 15–26 μ Sky Emission Spectrum at Jungfraujoch (3570 m) —*Bolle*

Infrared Dispersion of Some Oxide Glasses—*Malitson et al.*

Study of the Fabrication of Aspherical Surface—*Sakurai and Shishido*

Transmission of Isotropic Radiation Across An Interface Between Two Dielectrics—*Stern*

Helium Continuum Light Source for Photoelectric Scanning in the 600–1100 Å Region—*Huffman, Tanaka, and Larrabee*

Asymmetry of an Integrating Sphere—*Olson and Pontarelli*

Isosceles Total Internal Reflectors as Optical Elements—*Rothstein*

Direct Recording of Integrated Band Intensities from a Linear Wavelength Spectrometer—*Schurin, Williamson, and Clough*

Jet Controlled Arc I—Excitation of Second Spectra—*Thygesen and Moore*

Men and Milestones in Optics II—Thomas Young—*Barr*

Test of Theoretical Absorption Band Model Approximations—*Burch and Williams*

Brighter Spectrographic Images by the Use of Anamorphic Optics—*Eisner*

Optics in Norway—*Hisdal and Omholt*

Empirical Methods for Computing the Integrated Absorptances of Infrared Bands of Atmospheric Gases at Nonuniform Pressures—*Shaw*

Use of an Analog Computer in Side-on Arc Spectroscopy—*Shumaker and Yokley*

The Evaporation Rate of Filament Material from Alternating Current Heated Filaments—*Wilson*

A New Condenser for a Sun-Powered Continuous Laser—*Keck, Redmann, White, and DeKinder*

Performance of a cw Neodymium Laser—*Keck et al.*

Attenuation by Ozone and the Earth's Albedo in the Middle Ultraviolet—*Green*

Tilted Plate Interferometry with Large Plate Separations—*Moos et al.*

Double Monochromator System—*Christensen and Potter*

Experiments with the Optical Excitation of Mercury Vapor for the Production of Isolated Fluorescence—*Zito and Schraeder*

Application of the Senarmont Polariscope to Analysis of Optical Light—*Hellerstein*

Hole Burning Model of Oscillation of Ruby Laser—*DeMaria and Gagosz*

Electro-Optic Light Modulation with Cubic Crystals—*Buhrer, Bloom, and Baird*

Observations of Near Infrared Radiation from the Solar Atmosphere—*Taylor and MacQueen*

Simple Method for Photographic Photometry—*MacAdam and Altman*

Irradiance on a Flat Object Underwater—*Tyler and Shaules*

The Detectivity of Cryogenic Bolometers—*Low and Hoffman*

Kirchhoff Diffraction Pattern Calculations—*Moore*

Electro-Optic Effect of Gallium Arsenide—*Ho and Buhrer*

Interference Rings in Ruby Maser Beams—*Stoicheff and Szabo*

Electronic Flash Illumination of a Large Wilson Cloud Chamber —*Edgerton*

Interference Filter Spectrometer for Low Intensity Extended Sources—*Carter, MacRae, Nelson, Birkhoff, and Arakawa*

A Universal Spectrophotometer—*Kaye*

The Atomic Spectra of the Rare Earths: Their Presence in the Sun—*Moore*

The Observation of Extraphotographic Infrared Atomic Emission Spectra—*Humphreys and Paul*

The Review of Reviews of Atomic Spectroscopy—*Meggers*

Recent Work on the Second Spectra of Some Iron Group Elements—*Velasco, Iglesias, Gullon, and Diago*

An Image Inverter for Spectral Projector Comparator—*Hodge and Horey*

The Spectra of the Doubly and Triply Ionized Rare Earths—*Dieke and Crosswhite*

Spectroscopic Line Profile Studies of Long, Magnetically Confined, High-Current, Steady-State Vacuum Arcs—*McNally and Skidmore*

Infrared Transmission of the Atmosphere to Solar Radiation—*Gates and Harrop*

The Stressed-Plate Shutter: A New Moderate-Speed Electro-Optical Light Modulator—*Hauser, Smith, and Marlowe*

A Method for Measuring the Distortion of Photographic Objectives—*Zimmerman*

A Vacuum Ultraviolet Photoionization Detector—*Stober, Scolnik, and Hennes*

Analysis of Stimulated Raman Scattering of a Giant Laser Pulse —*Hellwarth*

Measurement of Energy Flux Density Distribution in the Focus of an Arc Image Furnace—*Beyer, McCulley, and Evans*

Irradiance Linearity Corrections for Multiplier Phototubes—*Baker and Wyatt*

An Interferometer for Precision Angle Measurements—*Rohlin*

ANNUAL SUBSCRIPTIONS

OSA members	$ 6.00
Other AIP societies' members	$ 8.00
Non-members and libraries	$10.00
Single copies	$ 2.00

Subscriptions should be addressed to APPLIED OPTICS Subscription Handling, American Institute of Physics, 335 East Forty-Fifth Street, New York 17, New York. **Eight weeks should be allowed for order processing.**

ADVERTISING

Advertising inquiries, orders, plates, and correspondence should be addressed to the APPLIED OPTICS Advertising Office, 1155 Sixteenth Street, N.W., Washington 6, D.C. 202-DI 7-4131. Mrs. Boraks.

42 MODELS of INTERFEROMETER-SPECTROMETERS for the UV, VISIBLE and IR

used *successfully* in:

- SATELLITES
- BALLOONS
- ROCKETS
- AIRCRAFT
- LABORATORIES
- ASTRONOMY
- INDUSTRY

(including such advanced techniques as monochromatic reference controlled servo drive)

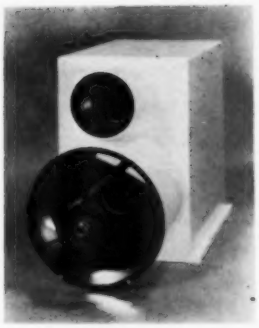

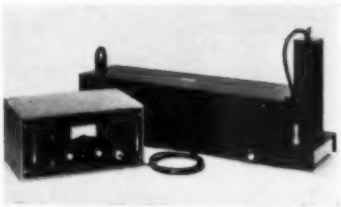

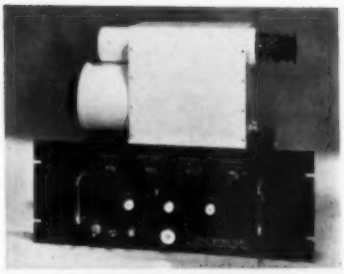

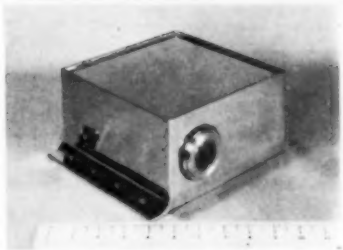

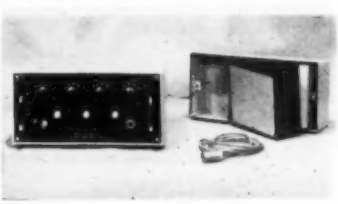

Special developments supported in part by the Geophysics Research Directorate of AFCRL under ARPA sponsorship and by Jet Propulsion Laboratory under NASA sponsorship.

Block Engineering, Inc.

Cambridge, Mass.

LIGHT BEAM SPLITTERS

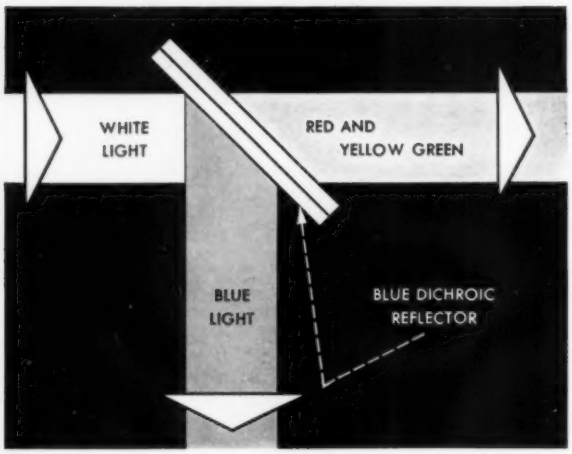

Dichroic reflectors can put light and heat to work as you specify

What do you want to do with a light beam? In millimicrons, what wave lengths do you want reflected? Where do you want spectrophotometric reflection to peak?

Liberty Mirror offers a standard line of dichroic coatings that reflect 90% or more of incident light in wave lengths from as low as 350 millimicrons up to 1,000 millimicrons. If a Hi-Efficiency dichroic coating hasn't already been pinpointed to meet your specifications, Liberty Mirror will develop one that does.

Vacuum-deposited coatings of various metals are used to make front-surface mirrors, neutral filters, transparent mirrors, high-efficiency beam splitters, beam-splitting dichroic mirrors and filters. Metallic and transparent electrically conducting coatings are available for resistance heating. Static-dissipating and high-frequency shielding coatings are also available.

Applied to all types of glass, metal or plastic, the coatings are used in such varied products as scientific and optical instruments, cameras, toys, pin setters, wheel-aligning equipment, aircraft and missiles. Free data sheets are available on all coatings.

Write L·O·F, Liberty Mirror Division, 5553 Libbey·Owens·Ford Building, Toledo 2, Ohio.

LIBERTY MIRROR DIVISION
LIBBEY·OWENS·FORD

MADE IN U.S.A.
LOF GLASS

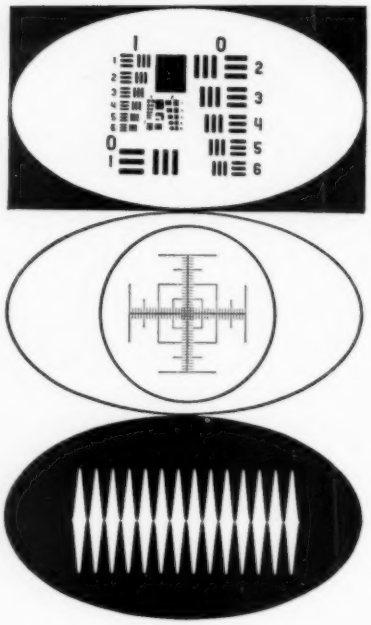

PRECISION TEST PATTERNS

- . . Standard Resolving Power Targets on film or glass to 228 lines/mm, Mil Std 150A pattern
- . . Target Strips on 35mm or 70mm film spaced 1½" apart on centers
- . . Custom Targets on film or glass to 600 lines/mm or higher
- . . Line widths to 1 micron
- . . Supplied as negative or positive; high, medium or low contrast; film or glass
- . . 13-Pattern Arrays on special widths, to order

MICRO IMAGES

Special targets, reticles, micro-images, precision masks and micro-etchings can be supplied to customer specifications.

For further information, write Department AO-120

Itek

Itek Corporation
10 Maguire Road
Lexington 73, Massachusetts

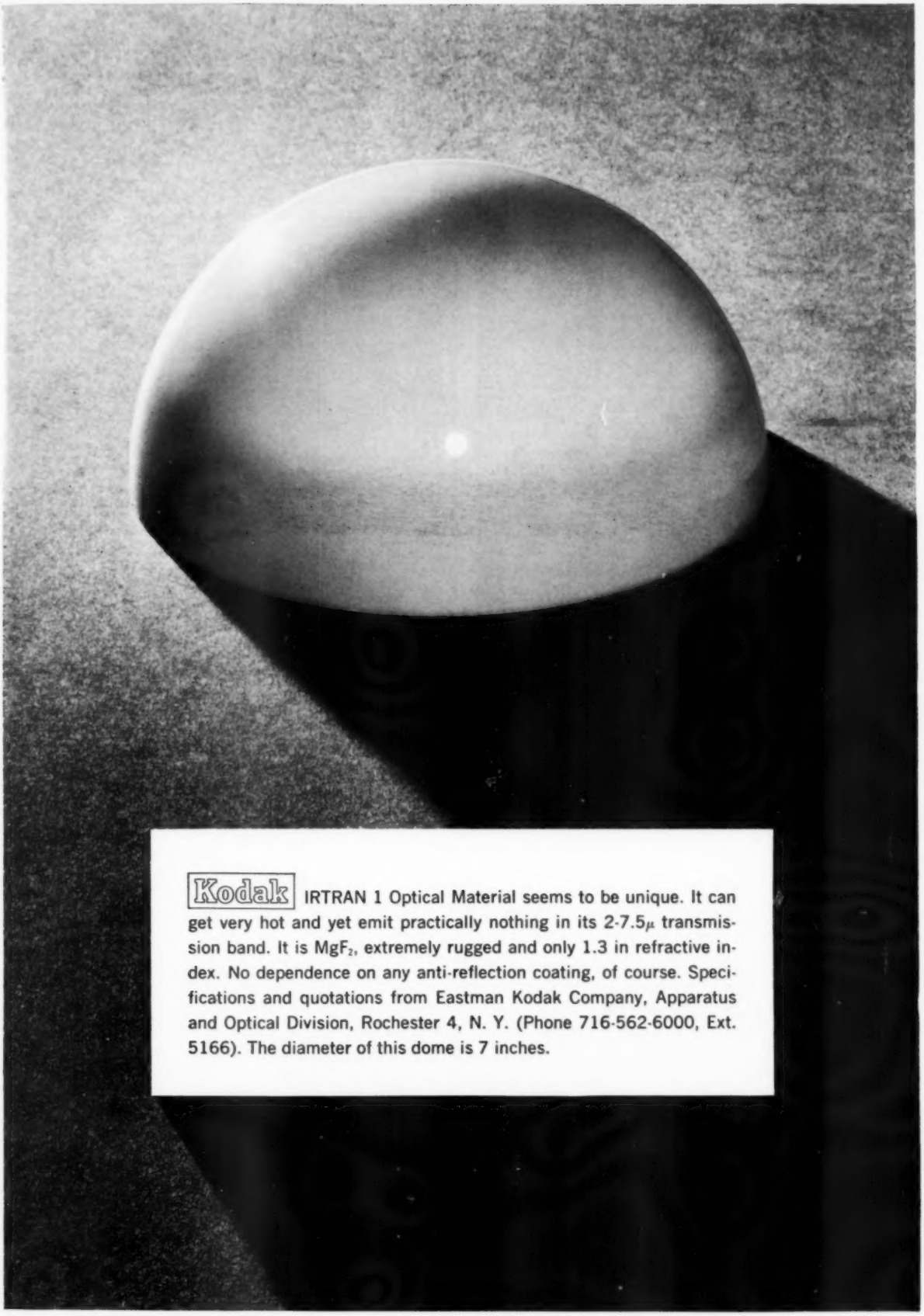

Kodak IRTRAN 1 Optical Material seems to be unique. It can get very hot and yet emit practically nothing in its 2-7.5μ transmission band. It is MgF_2, extremely rugged and only 1.3 in refractive index. No dependence on any anti-reflection coating, of course. Specifications and quotations from Eastman Kodak Company, Apparatus and Optical Division, Rochester 4, N. Y. (Phone 716-562-6000, Ext. 5166). The diameter of this dome is 7 inches.

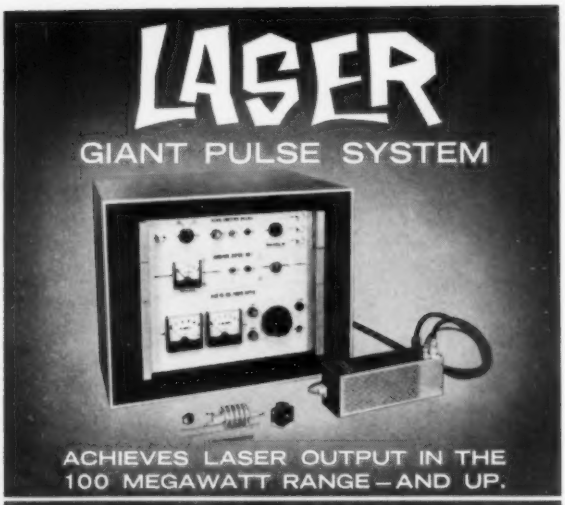

Kappa Scientific's Kerr Cell LASER Control System is a precision apparatus for controlling the pulse shape, timing and amplitude of a LASER to achieve a single intense pulse output in the multi-megawatt range.

This system is part of a growing line of LASER products and accessories covered in our new catalog. Write for your copy today.

KAPPA SCIENTIFIC CORPORATION

49 South Baldwin Ave. / Sierra Madre, Calif. / EL 6-1614

FUTURE FEATURES

Each issue will specially feature one area of applied optics in addition to the usual contributed papers, shop and technical notes, reports of meetings, Letters to the Editor, book reviews, Meetings Calendar, and special columns. The feature subject of each issue is the responsibility of the named editor.

1963		
July	**Atomic Spectroscopy**	M. E. Warga
August	**Masers**	—
September	**Spectroscopic Instrumentation**	—
October	**Bubble Chamber Optics**	S. Rosin
November	**Coblentz Commemoration**	E. K. Plyler
December	**Lens Design and Computers**	D. P. Feder
1964		
January	**Optics of the Photographic System**	G. C. Higgins
February	**Atmospheric Optics**	D. Q. Wark
March	**Chemical Optics**	M. K. Wilson
April	**Visibility**	S. Q. Duntley
May	**Microscopy**	J. R. Benford
June	**Fiber Optics**	C. W. Peters
July	**Optics in Japan**	R. A. Oetjen
November	**High-Speed Photography**	—
December	**Solar Optics**	G. Newkirk, Jr.
1965		
February	**Plasma Radiation**	L. M. Branscomb
April	**Optical Processing of Information**	G. W. King
May	**Optics and Microwaves**	G. Stroke
June	**Detectors**	—

Information for Contributors

Scope: Papers are welcomed in the broad areas of applied optics, in disciplines related to optics and employing optical techniques. Papers should be sent to *The Editor, APPLIED OPTICS, 1155 Sixteenth St., N.W., Washington 6, D.C.* Manuscripts may be submitted in English, French, German, or Russian, and the presentation should be as succinct as comprehension will permit. In general, the metric system of units is preferred. One original and one carbon copy of the manuscript, with two sets of all illustrations, must be sent in. Manuscripts should be typed double or triple spaced on one side of 22 × 28 cm (8½ × 11 in.) paper, leaving a 3.8 cm (1½ in.) margin all around. Equations must be typed not hand written wherever possible. Papers on the more fundamental aspects of experimental and theoretical optics should be sent to *The Editor, JOURNAL OF THE OPTICAL SOCIETY OF AMERICA, National Bureau of Standards, Washington 25, D.C.*

An **abstract,** adequate as an index and a summary, of not more than 100 words should appear at the beginning of the paper after the *title, author's name, affiliation, and address.* In the case of papers in a non-English language, they must be accompanied by an abstract in English as well as an abstract in the language of the paper. It should be borne in mind that this abstract may be used in toto by the abstracting journals, therefore it should be self-contained.

Figures suitable for printer's use should be sent. Bear in mind that illustrations will normally be reduced to column width (8.4 cm—3⅜ in.—20 picas). *Halftones:* two sets of glossy prints are needed, which should be mailed flat, with any proportion or framing indicated on a working copy. *Line drawings* should be suitable for reproduction and be not larger than 22 × 28 cm (8½ × 11 in.). *Captions* should be listed on a separate sheet in addition to each caption appearing on each illustration.

Tables should be typed on separate sheets and the data therein be intelligible, by title, without reference to the text. Tables should include a minimum of vertical ruling.

References must be typed on a separate sheet, be numbered consecutively in the order of their appearance in the text, and follow this form:

1. F. C. Brown, Phys. Rev. **12,** 345 (1821).
2. J. Culpeper, *Space Optics* (Georgetown Institute of Technology Press, Washington, D.C., 1861), pp. 12, 345.

A list of abbreviations for the names of journals is published in *Chem. Abstr. List of Periodicals 1961.* To make for uniformity of presentation generally, the American Institute of Physics *Style Manual,* second edition, should be used. In general, *APPLIED OPTICS* differs from the *Style Manual* only inasmuch as footnotes appear at the bottom of the page of text, while references are listed numerically at the end of the paper.

There will be no **page charge** for publishing in *APPLIED OPTICS* for the time being.

Letters to the Editor should follow the above suggestions, but no abstract is required.

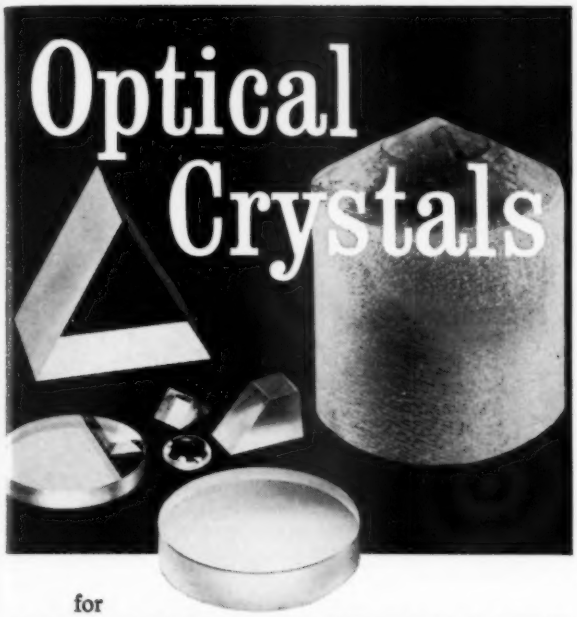

for

INFRARED-ULTRAVIOLET

ISOMET exercises the utmost care and control in growing high resolution, low strain crystals that are impurity-free. Crystal growth, fabrication and precision finishing are all handled within ISOMET's own plant. The most ideal conditions are precisely maintained to assure you of the finest in crystals.

Polished Windows • Lenses • Prisms
Cleaved or sawed blanks
available for prompt delivery

Sodium Chloride	**Thallium Bromide-Iodide**
Potassium Bromide	**Silver Chloride**
Potassium Chloride	**Calcium Fluoride**
Potassium Iodide	**Barium Fluoride**
Cesium Bromide	**Lithium Fluoride**
Cesium Iodide	**Fused Quartz**

KBR Pellet Powder

Quick Repair Service for all makes of fogged, scratched or damaged windows and infrared cells.

Infrared Cells
Sealed Liquid, Micro, Variable space and gas cells for all standard spectrometers.

FREE BROCHURE
Ask for Technical Bulletin #AO-1100

ISOMET
CORPORATION
PALISADES PARK, NEW JERSEY

FS TM REG

MULTI-LAYER INTERFERENCE FILMS

Made in our own New Rochelle coating laboratory.

For dichroic and achromatic beam splitters and filters . . . High efficiency . . . Relatively wide band.

Our coatings were used in the first TELSTAR color TV transmission

•

New Developments

A series of multi-layer thin films with reflectivities of about 99.6% at any desired wave length.

A cold mirror for operating lamps as used in closed circuit color TV systems.

•

Thin Glass Substrate Material

Ground and polished: .020–.030″ thick
Machine drawn: .010–.020″ thick

SCHOTT

Solid Colored Optical Glass Filters
Jena Glass

Processed in our New Rochelle optical shop in about 100 types for the ultraviolet, visible, and infrared spectral regions.

SCHOTT

Narrow Band Interference Filters
Jena Glass

For the spectral region from 300 to 2000 mμ with transmission up to 60% and half-widths down to 5 mμ, depending on filter type.

Available as line and band filters, line and band double filters, broad band filters, spectral band filters, and wedge filters.

FISH-SCHURMAN CORPORATION
90 Portman Road, New Rochelle, N. Y.

Crystals of all types and sizes, guaranteed to laser!

In stock, hundreds of single crystals. All configurations (plain flat and parallel ends, TIR configuration, Brewster's angle). Optically corrected for lowest threshold, narrowest beam divergence. Extra slow grown and annealed for minimum strain. **Guaranteed to laser!**

- NEW glass crystals w/neodymium^{3+} 2.0% — finest quality, no bubbles, straie, strains.
- New NPS1 super-uniform ruby crystals.
- Ruby rods up to 12"
- Calcium tungstate crystals w/neodymium^{3+} 0.5% up to 5" long.
- Strontium fluoride crystals w/samarium^{2+} 0.1%, neodymium^{3+} 0.5%.
- Barium fluoride crystals w/neodymium^{3+} 0.5%, uranium^{3+} 0.1%.
- Calcium fluoride crystals w/neodymium^{3+} 0.5%, samarium^{2+} 0.1% dysprosium^{2+} .05%, or uranium^{3+} 0.1%.

For full specifications and prices, write or call Adolf Meller Company, Box 6001, Providence 1, R. I. Telephone: DExter 1-3717 (Area Code 401).

MELLER SAPPHIRE PRODUCTS

Synthetic Sapphires • Ruby Lasers & Masers
Alumina Powder

Physical Optics

TECH/OPS is a medium-sized research company. Our work in physics is in plasma and upper atmosphere physics, high energy systems, gamma-ray scattering, hyper-velocity experimentation and physical optics. Programs in physical optics are in modern optics with particular emphasis on spatial filtering techniques, propagation phenomena and laser applications.

EXPERIMENTAL OPTICS

- In this area we are looking for a senior physicist with training on the graduate level and with a background in such fields as modern optics, interferometric techniques, spatial filtering, phase-contrast microscopy, electro-optical imagining systems, photographic processing or diffraction of partially coherent light. A position is also available for a physicist with lesser experience.

THEORETICAL OPTICS

- Here we need a senior physicist who is interested in doing theoretical work. Training should be on the graduate level with a general background in electromagnetic theory with emphasis in such fields as diffraction theory, modern image theory, theory of partial equations and Fourier analysis. A position is also available for a theoretical physicist with lesser experience.

LASERS

- At present we have a position available for a senior physicist with training or experience in quantum electronics and solid states physics who would like to work in the laser and maser field. A position is also available for a man with lesser training and experience for work in the same field.

TECH/OPS has several intangibles that are worth thinking about if you are seeking a new position. We have a somewhat informal atmosphere that encourages an individual to do his best work. We operate with a minimum of red tape and spend our efforts solving research problems. A staff member's progress is tied to scientific achievement and not length of service or position in the organization. Staff members are encouraged to publish and participate in activities of their professional society. Lastly, our research programs provide an opportunity for creative individuals to make full use of their technical ability.

tech/ops

ROBERT L. KOLLER
TECHNICAL OPERATIONS RESEARCH
Burlington, Massachusetts
An equal opportunity employer

SHARP FOCUS?

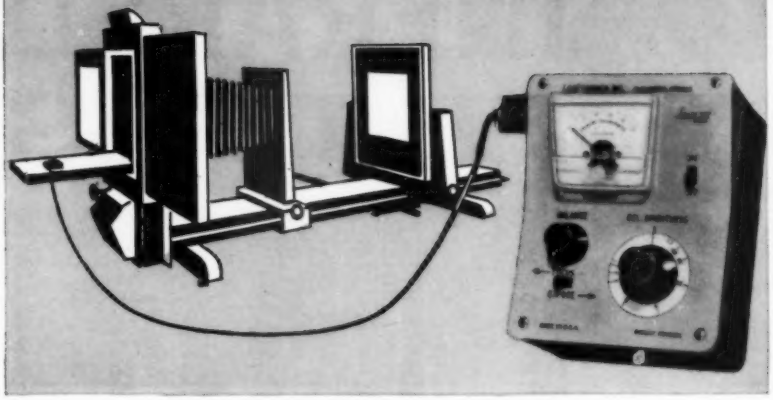

THE HUMAN EYE has up to now been the only practical instrument for finding sharp focus. No matter how experienced, though, you could never really be sure you had it right.

THE NEW FOCATRON METER today positively indicates maximum image sharpness—many times more accurately and consistently than the average eye. The Focatron Image Sharpness Meter is simple, rugged, comparatively low-cost. The Model C (shown) includes a meter case and sensor probe and uses a half-tone target. It also measures image brightness.

Send now for the LogEtronics four-page technical bulletin on the Focatron Image Sharpness Meters.

LogE Focatron BY LogEtronics Inc.

Box L30, 500 E. Monroe Ave., Alexandria, Va. TE 6-5180

MODEL L-35

INTERFEROMETER

for
PRECISE EVALUATION OF
LASER CRYSTALS
PRISMS & FLATS
LENS SYSTEMS

A General Purpose Twyman-Green Interferometer
Vibration Isolated, Versatile, & Compact.

Specifications: 3.5cm Aperture, Pinhole Turret,
with Prefocused Reflex Camera—$1950.00

Cadmium Source, Housing & Power Supply— $160.00

TROPEL, INC., 52 WEST AVE., FAIRPORT, N.Y.

CONSULTANTS AND DESIGNERS OF OPTICAL SYSTEMS
MANUFACTURERS OF PROTOTYPE LENSES AND INSTRUMENTS

New Catalog . . .

OPTICAL BENCHES

- ☐ triangular benches
- ☐ lathe bed benches
- ☐ research benches
- ☐ non-magnetic and student-teaching benches

Free catalog . . . just ask

THE Ealing CORPORATION

2239 Massachusetts Avenue
Cambridge 40, Massachusetts

DIFFRACTION GRATINGS

INTERFEROMETRICALLY RULED

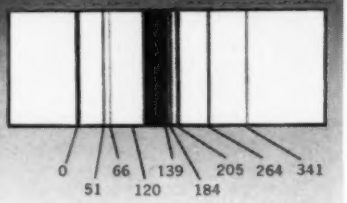

Hg 4358 A from a Jarrell-Ash replica of MIT master (14th order), 11-Meter Spectrograph. Res. better than 750,000.

Jarrell-Ash offers exceptionally high quality replicas (up to 190 x 80 mm, ruled area) from masters ruled interferometrically at MIT, and, by a new Jarrell-Ash engine.

GHOST INTENSITY
1st Order (Less Than):
.003% on 15,000 g.p.i.
.010% on 30,000 g.p.i.
.001% on 7,500 g.p.i.

RESOLUTION (Better Than):
85-90% of theoretical, high orders

EFFICIENCY At Blaze (Better Than):
70%, 15,000 g.p.i.
60%, 30,000 g.p.i.
85%, 7,500 g.p.i.

CONVENTIONAL GRATINGS, INTERFEROMETRICALLY CONTROLLED

Jarrell-Ash also manufactures mechanically ruled gratings featuring ghost intensities of less than 0.1% (15,000 g.p.i.), resolutions of 75-90% of theoretical, efficiencies of 40-85% at the blaze. All are inspected interferometrically.

GRATINGS FOR INFRARED AND METROLOGY

Jarrell-Ash also offers a complete selection of high quality special purpose, and educational gratings.

Jarrell—Ash

Dedicated to excellence in research, development and manufacture of precision analytical instrumentation.

For further information . . . clip the coupon, attach to your company letterhead and mail.

JARRELL-ASH COMPANY
26 Farwell Street
Newtonville 60, Mass.

NAME _____

GR

OCLI SQUARE BAND INFRARED FILTERS

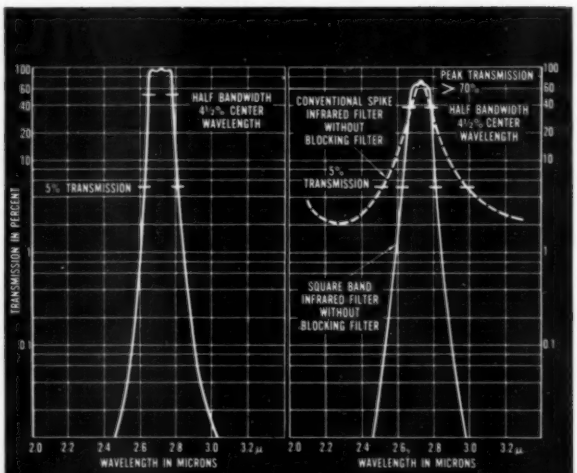

THEORETICAL
Transmittance of an unattenuated Square Band Filter

MEASURED
Transmittance of two unattenuated Bandpass Filters

- **When the ratio of transmission to rejection must be high —**
- **When closely spaced energy bands must be resolved —**
- **When maximum integrated energy in the bandpass is necessary —**
- **When wavelength shift due to angle must be minimized — Or**
- **When filter characteristics must remain unchanged in a hostile atmosphere —**

SPECIFY AN OCLI SQUARE BAND INFRARED FILTER

For detailed information about OCLI square band infrared filters — or any infrared or ultraviolet filters — contact:

OPTICAL COATING LABORATORY, INC.
2789 GIFFEN AVENUE, SANTA ROSA, CALIFORNIA, U.S.A.
Teletype 707-546-4959 Telephone 707 Liberty 5-6440

ELECTRODELESS DISCHARGE LAMPS

for Interferometry & Metrology

Hg 198 Kr 86

WATER-COOLED OR AIR-COOLED

RECOMMENDED SECONDARY WAVELENGTH STANDARDS

LOW OPERATING PRESSURE

NARROW LINE-WIDTH

OPHTHOS INSTRUMENT CO.

9600 Overlea Drive Rockville, Maryland

PEN-RAY®

MINIATURIZED QUARTZ LAMPS

- Monochromatic light sources for optical systems
- Reference standard for calibrating wavelength of spectrophotometers

Specialized designs...

- Any size or shape with special gases and windows to your specifications

For more details...

Write to Dept AO-5

Pioneers in Ultraviolet since 1932

MINERALIGHT® BLAK-RAY® PEN-RAX®
CHROMATO-VUE® STERILAIRE®

ULTRA-VIOLET PRODUCTS, INC.

San Gabriel, Calif.

OPTICAL CRYSTALS

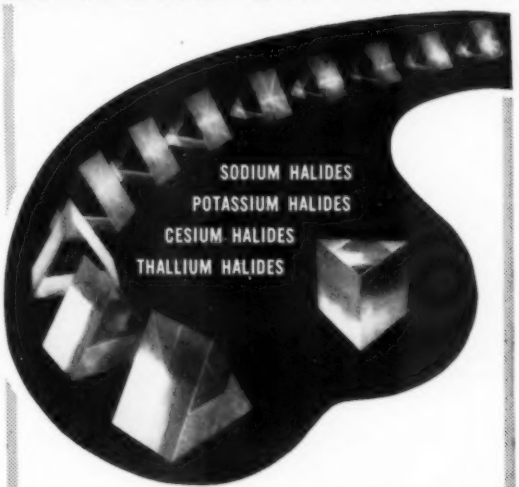

Special crystals grown to order, optical blanks cut to specifications, finish polishing as required.

123 WOODLAND AVENUE WESTWOOD NEW JERSEY

CRYSTALS DIVISION
ISOTOPES, INC.

A FLY'S EYE—150X MAGNIFICATION

like to hire a new kind of private eye?

Looking for a new kind of eye? Impressed by the long distance vision of TIROS and NIMBUS? Those were ELGEET lens systems specifically engineered to prove that "pie-in-the-sky" could become actual "eye-in-the-sky" concepts. At ELGEET we have the optical know-how and the design imagination you may be seeking for your own project. We'll send our Design Section to meet with you in your office and take that optical problem off your desk. We feed it into experienced minds and high-speed computers to break-through to your possible solutions. Let ELGEET be your Private Eye. Take your choice of a deep look, a quick look, a dim look, a bright look, a wide look, a forward look, a top-side look or an underbelly look. But first: *write to* ELGEET OPTICAL COMPANY, *838 Smith Street, Rochester 6, New York for a fully illustrated information file on our optical capabilities and performance.*

CREATIVE OPTICS
Elgeet
FOR EARTH AND SPACE

When you think of

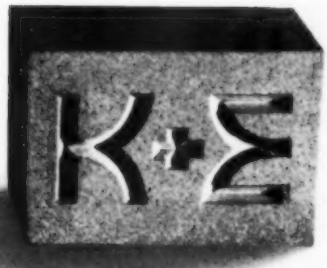

Undoubtedly you think of slide rules . . . transits . . . tracing paper. Correct? But to round out the picture, please enter K&E in your file for these highly advanced space-age instruments . . .

SPACE AND MISSILES SYSTEMS

Solar and Star Simulators • Cine and Special Theodolites • Antenna Contour Checking Instruments • Contour Probing Instruments • Polaris Guidance and Fire Control Instruments • Collimation Test Instruments • Deviators • Borescopes — Electronic and Visual

R&D AND LABORATORY INSTRUMENTS

Auto-Collimators — Electronic and Visual • Electronic Levels • Gravity Reference Instrument • Jig Theodolite • Angle Index Tables and Read-out Devices • Gratings • Targets and Special Scales

INSTRUMENTS FOR MANUFACTURING, INSPECTION, QUALITY CONTROL

A complete line of alignment instruments and accessories

Want specific product information? Write K&E today. Our O&M Division can assist you with R&D.

OPTICS AND METROLOGY DIVISION

KEUFFEL & ESSER CO.

HOBOKEN, NEW JERSEY

3704

HIGH RESOLVING POWER APPARATUS

HILGER & WATTS

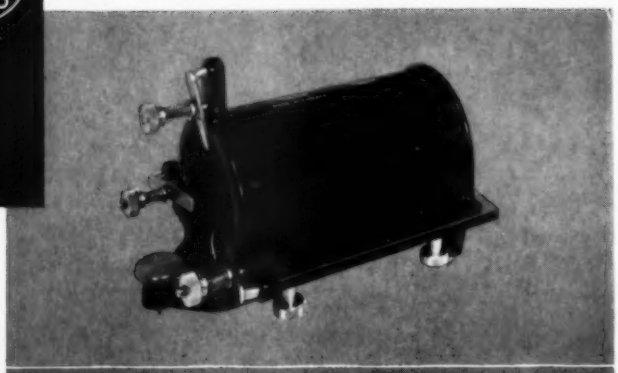

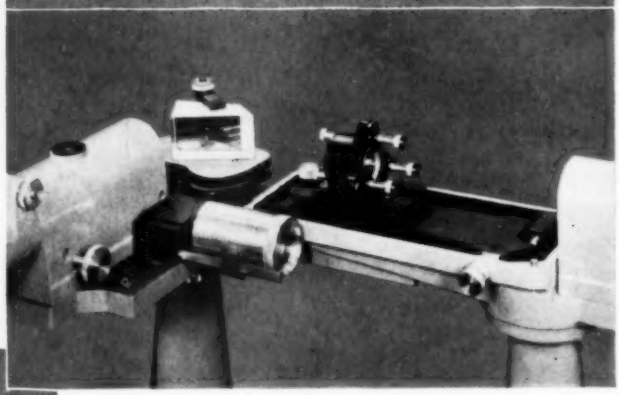

The development of the maser and laser has substantially broadened the use of high resolving power apparatus. Hilger & Watts now provide a comprehensive selection of equipment to meet the increased requirements.

Among the more important are etalon and interferometer plates — ranging from 20 mm. aperture to 100 mm. aperture; with flatnesses to 1/200 of a wavelength. Mounts for these plates, as well as wave length spectrometers designed to accommodate etalons within the instrument, are standard stock items.

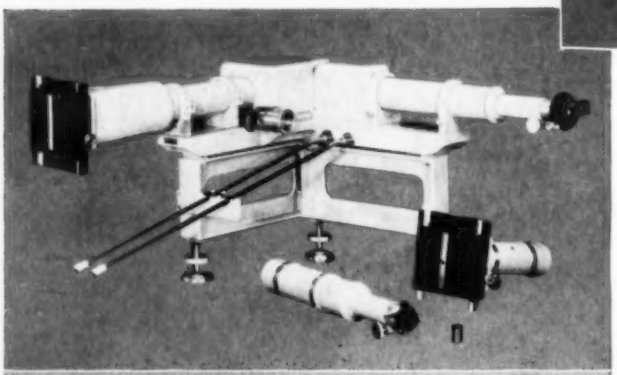

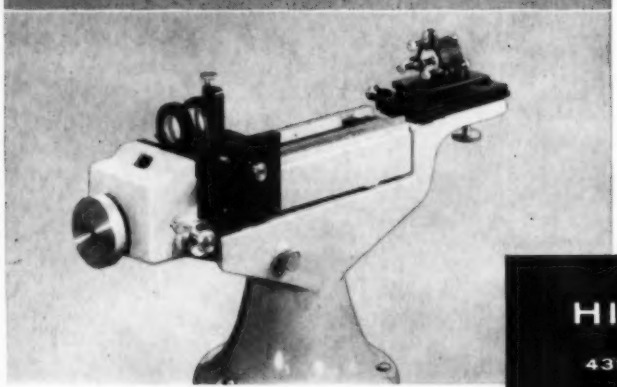

Other new developments include: motor driven Fabry-Perot and Michelson interferometers with fringe counting and amplitude measuring equipment; dielectric coatings for all plates. Lummer-Gehrcke plates and transmission echelon gratings are also available.

Illustrated Top Right—
B345 100 mm. Aperture Etalon

Illustrated Center Right—
D186 Spectrometer with Etalon mounted

Illustrated Center Left—
D260 Large Aperture Spectrometer with Etalon

Illustrated Bottom Left—
N34 Interferometer with Etalon

• *Ask for individual catalog sheets and for complete instrument listing.*

HILGER & WATTS, INC.

431 SOUTH DEARBORN ST. CHICAGO 5, ILL.

Sales, Service, Parts by

ENGIS EQUIPMENT COMPANY

CHICAGO 5, ILL.